Inhibition of macrophage metabolism by oxLDL

A thesis submitted in partial fulfillment of the requirements for the

Degree of Doctor of Philosophy in Biochemistry

By

Hanadi Ahmed Katouah

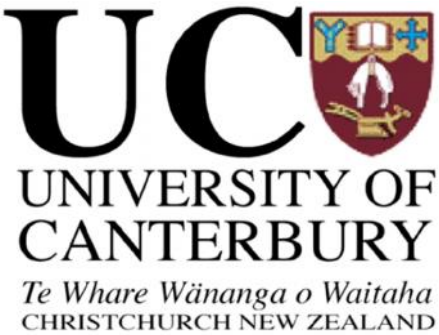

School of Biological Sciences

University of Canterbury

Christchurch, New Zealand

2012

CONTENTS

List of Figures

List of Tables

Acknowledgements

I would like to thank my supervisor, Associate Professor Steven Gieseg, for all the guidance, advice, assistance and patience he has provided throughout my PhD. This thesis would not have been completed without his extensive experience in science research. I am also grateful for the support provided by my co-supervisor, Professor Bill Davison.

I wish to express my gratitude to the ministry of high education, in particular Umm Al-Qura University for the scholarship and financing my PhD studies. Also, I am grateful for the support from the Saudi cultural office in Auckland and Australia that insure a very good educational environment during the period of study.

I would also like to thank Associate Professor Mark Hampton and Dr. Sarah Cuddihy, of the free radical research laboratory of the Christchurch School of Medicine of Otago University, for giving me guidance in the experiment of measuring sensitivity GAPDH thiol and scan SDS-PAGE gel; also for their gift of protease inhibitors and 5-IAF to the free radical biochemistry laboratory. Also, I thank the Hematology research laboratory of the Christchurch School of Medicine of Otago University for gifting the U937 cell line to the free radical biochemistry Laboratory. In addition, thanks to Dr. Barry Hock of the Department of Hematology for his gift of GM-CSF to the Free Radical Biochemistry Laboratory. Special thanks to Associate Professor Malcolm Forster, of the physiology research laboratory of Canterbury University, for using his laboratory and his valuable advice in oxygen consumption experiment. Thank you to Dr. Leonard Forgan for being patient while teaching me in the physiology laboratory.

Thanks to all the secretaries and technical staff in the School of Biological Sciences, in particular Maggie Tisch for her help with keeping the laboratory running smoothly and for her warm care, Jackie Healy for assistance with the ultracentrifuge and Matt Walters for photography work.

Thank you to the haemochromatosis patients for donating blood and to the New Zealand Blood Service (Riccarton branch) for collecting the haemochromatosis blood. Thanks also to blood donors at the University of Canterbury. Special thanks to Canterbury Health Center for blood-letting of the university blood donors.

A big thank you to all the members of the Free Radical Biochemistry Laboratory for the warm encouragement, help and support through all the good and bad times and listening to my complaints and whining throughout my PhD and keeping me accompanied during late night experiments, in particular Zunika, Tina, Nick, Lucy, Raj, Anastasia, Laura, Alpha, Hannah, Rebecca, Izani, Waffaa and Elizabeth. Special thanks to Zunika and Tina for teaching me at the laboratory. I have shared with those wonderful researchers the stressful time during the earthquakes, moving from the building and extensions. I will treasure our friendship. I really appreciate Lucy, Hannah and Zunika for proof-reading my thesis. I also want to express my thanks towards my other friends in Christchurch.

I would like to dedicate this thesis to my beloved husband Dr. Anas Sedayo for being patient with me, providing entertainment, caring of me and teaching me the newest computer programs. My PhD would not have been possible without his support. I also want to give my deepest love and thanks to my beloved children Eyad Sedayo, Lamer Sedayo and Obai Sedayo for giving me inspiration, making me happy, and accompanying

me when I was under tremendous pressure and crying. I would like to express my deepest gratitude to my mum Lutfeah Kinsarah, my dad Ahmed Katouah and my brothers Ayman Katouah, Ehab Katouah and Hattan Katouah for always embracing me and believing that I could do it. I also express love and thanks to my family in low for encouraging me and giving me a moral support through my PhD. Lastly, I have been incredibly fortunate to be surrounded with such an amazing family.

Abbreviations

Abbreviation	Glossary
%	Percentage
ΔPO_2	Change in PO_2
αO_2	Oxygen solubility of the ringer based on the osmolarity
γ-GCS	γ-Glutamylcysteine synthetase
°C	Degree centegree
µg	Microgram
µg/µl	Microgram per microlitre
µg/ml	Microgram per millilitre
µl	Microlitre
µl O_2. $10^6 cells^{-1}$ $.hr^{-1}$	Microlitre of oxygen per million of cells per hour
µm	Micrometre
µM	Micromolar
µmol	Micromole
µmol/10^6 cells	Micromole per million of cells
µmol/min	Micromole per minute
1, 3-PGA	1, 3-Diphospho-glycerate
3HAA	3-Hydroxyanthranilic acid
5-IAF	5-Iodoacetamidofluorescein
673 genes	Stem-loop sequence mmu-mir-673
7,8-NP	7,8-Dihydroneopterin
7-KC	7-Ketocholesterol
AA	L-Ascorbic acid
AAPH	2,2'-Azobis (2-amidinopropane) hydrochloride
ABCA1	ATP-binding cassette transporter sub-family ABCA member 1
ABCG1	ATP-binding cassette sub-family ABCG member 1

Abbreviation	Glossary
ACAT	Acyl coenzyme A: cholesterol acyltransferase
acLDL	Acetylated LDL
Acn	Acetonitrile
ADP	Adenosine diphosphate
aggoxLDL	Aggregated oxidised low density lipoprotein
agLDL	Aggregated low density lipoprotein
ALCK	Acetylleucine chloromethyl ketone
AMP	Adenosine monophosphate
AMPK	AMP-activated protein kinase
apoA1	Apolipoprotein A1
apoB100	Apolipoprotein B100
ATP	Adenosine triphosphate
B cells	B lymphocytes (originate from bone marrow)
BCA	Bicinchoninic acid
BE	Biomechanical efficiency
BHT	Butylated hydroxytoluene
BSA	Bovine serum albumin
BSO	Buthionine sulfoximine
$C_{16}H_{37}NO_4S$	Tetrabutylammonium bisulpfate
$C_2H_5NO_2$	Glycine
C_2H_5OH	Ethanol
C_2H_6OS	β-Mercaptoethanol
$C_3H_4O_3$	Pyruvate
$C_3H_8O_3$	Glycerol
Ca^{+2}	Calcium ion
CD36	Cluster of differentiation36
$CD4^+$ T cells	T helper cells express the surface protein $CD4^+$
CD68	Cluster of differentiation 68

Abbreviation	Glossary
cells/ml	Cells per millilitre
$CH_3(CH_2)_4CH_3$	Hexane
$CH_3CHOHCH_3$	Isopropanol
CH_3COCH_3	Acetone
CH_3COOH	Acetic acid
CH_3OH	Methanol
CHAPS	3-[(3-Cholamidopropyl)dimethylammonio]-1-propanesulfonate
CHF	Chronic heart failure
CHOL	Cholesterol
Cm	Centimetre
cm^2	Centimetre square
CO_2	Carbon dioxide
CoQ10	Coenzyme Q10
CPDA-1	Citrate-phosphate-dextrose-adenine
CPP32	Putative cysteine protease
CSF-1	Colony stimulating factor-1
$CuCl_2$	Copper chloride
$CuSO_4.5H_2O$	Copper sulfate pentahydrate
Cys	Cysteine
Cys^{149}	Cysteine at residue 149
Cys^{150}	Cysteine at residue 150
Cys^{153}	Cysteine at residue 153
Cys^{34}	Cysteine at residue 34
DCs	Dendritic cells
DHAA	Dehydro-L-ascorbic acid
DHE	Dihydroethidium
DiI	1,1'-Dioctadecyl-3,3,3',3'-tetramethylindocarbocyanine perchlorate

Abbreviation	Glossary
DMSO	Dimethyl sulfoxide
DNA	Deoxyribonucleic acid
DTT	Dithiothreitol
ECs	Endothelial cells
EDTA	Ethylene diamine tetraacetic acid
EGTA	Ethlyleneglycol-bis(2-aminoethylether)-N,N,N',N'-tetracetic acid
ETC	Electron transport chain
G	Gauge
G	Gram
G	Gravity acceleration
g/L	Gram per litre
g/ml	Gram per millilitre
g/mol	Gram per mole
GAP	Glyceraldehyde-3-phosphate
GAPDH	Glyceraldehydes-3-phosphate dehydrogenase
GM-CSF	Granulocyte macrophage colony stimulating factor
GSH	Glutathione
GSSG	Oxidised GSH
GTP	Guanosine triphosphate
H_2O	Water
H_2O_2	Hydrogen peroxide
H_3PO_4	Phosphoric acid
HASMCs	Human aortic smooth muscle cells
HBDH	α-Hydroxybutirate dehydrogenase
HCAECs	Human coronary artery endothelial cells
HCl	Hydrochloric acid
HDL	High density lipoprotein

Abbreviation	Glossary
HeLa cells	Human cell line derived from cervical cancer cells taken from Henrietta Lacks
HEPES	Hydroxy ethyl prazine ethane sulfonic acid
HHE	4-Hydroxy-2-hexenal
HI-FCS	Heat-inactivated foetal calf serum
HIHS	Heat-inactivated human serum
HMDM	Human monocyte-derived macrophage
HNE	4-Hydroxy-2-nonenal
$HO^{\bullet}$	Hydroxyl radical
HOCl	Hypochlorite
HOCl-oxLDL	Hypochlorite oxidised low density lipoprotein
HPLC	High performance liquid chromatography
hr	Hour
HUASMCs	Human umbilical artery smooth muscle cells
HUVECs	Human umbilical vein endothelial cells
HVSMCs	Human vascular smooth muscle cells
Hz	Hertz
IDO	Indoleamine2,3-dioxygenase
$I_{K(ATP)}$	Pinacidil-primed
IL-1	Interleukin-1
IL-1 β	Interleukin-1beta
IL-10	Interleukin-10
IL-23	Interleukin-23
IL-6	Interleukin-6
IL-8	Interleukin-8
J774	Murine macrophage-like cell line
K_2CO_3	Potassium carbonate
KBr	Potassium bromide
kDa	Kilo Dalton

Abbreviation	Glossary
L	Litre
$L^{\bullet}$	Carbon-centered lipid radical
L6 cells	Myogenic cell line
LDH	Lactate dehydrogenase
LDL	Low-density lipoprotein
LH	Lipid containing polyunsaturated fatty acids
$LOO^{\bullet}$	Lipid peroxyl radical
LOOH	Protein hydroperoxides
LPS	Lipopolysaccharide
LXR−RXR	Liver X receptor-retinoic acid receptor heterodimers
M	Molar
M	Number of the cells in the respirometers
$M^{-1}cm^{-1}$	Reciprocal molar x reciprocal centimetre
MBB	Monobromobimane
M-CSF	Macrophage-colony stimulating factor
MDA	Malondialdehyde
Met	Methionine
MFI	Mean fluorescence intensity
mg	Milligram
mg protein/ml	Milligram protein per millilitre
mg/ml	Milligram per millilitre
min	Minute
MitoSox	Red mitochondrial superoxide indicator
ml	Millilitre
ml/min	Millilitre per minute
mLDL	Minimally oxidised low density lipoprotein
mm	Millimetre
mM	Millimolar

Abbreviation	Glossary
mmHg	Millimetre of mercury
$mmHg.time^{-1}$(sec)	Millimetre of mercury per time in second
mmol $O_2.L^{-1}.mmHg^{-1}$	Millimole of oxygen per liter per millimetre of mercury
mmol/L	Millimole per liter
MMPs	Metalloproteinases
mod-LDL	Moderately oxidised low density lipoprotein
mol/molLDL	Mole per mole of LDL
MOPS	4-Morpholine-propanesulfonic acid
MPO	Myeloperoxidase
mtROS	Mitochondrial reactive oxygen species
MTT	Thiazolyl blue tetrazolium bromide
mV	Millivolt
MVSMCs	Mouse vascular smooth muscle cells
MW	Molecular weight
$Na_2C_4H_4O_6$	Sodium tartrate
Na_2CO_3	Sodium carbonate
$Na_2H_2AsO_4.7H_2O$	Sodium arsenate
NAC	N-Acetylcysteine
NaCl	Sodium chloride
NAD(P)H-dehydrogenases	Nicotinamide adenine dinucleotide phosphate dehydrogenases
NAD^+	Nicotinamide adenine dinucleotide (oxidised form)
NADH	Nicotinamide adenine dinucleotide (reduced form)
$NADP^+$	Nicotinamide adenine dinucleotide phosphate (oxidised form)
NADPH	Nicotinamide adenine dinucleotide phosphate (reduced form)
$NaH_2PO_4H_2O$	Sodium dihydrogen orthophosphate
$NaHCO_3$	Sodium hydrogen carbonate

Abbreviation	Glossary
NaOH	Sodium hydroxide
NF-kB	Nuclear factor kappa-light-chain-enhancer of activated B cells
nLDL	Native LDL
nm	Nanometre
nM	Nanomolar
nmol	Nanomole
nmol/mg	Nanomole per milligram
NO	Nitric oxide
$NO_2^{\bullet}$	Nitric dioxide
NOC18	1-hydroxy-2-oxo-3,3-bis(2-aminoethyl)-1-triazene
NOR3	(E)-4-ethyl-2-[(E)-hydroxyimino]-5-nitro-3-hexenamide
NOX	NADPH-oxidase
NVTi-65	Near Vertical Beckman NVT65 Rotor
º	Degree
O_2	Oxygen
$O_2^{\bullet-}$	Superoxide
$ONOO^-$	Peroxynitrite
oxLDL	Heavily oxidised low density lipoprotein
oxLDL	Oxidised low density lipoprotein
P	Statistical significance value
p17	Active subunit in CPP32
P388D1	Murine macrophage-like cell line
PBS	Phosphate buffered saline
PCA	Perchloric acid
pen/strep	Penicillin per streptomycin
pH	Potential hydrogen
PO_2	Partial pressure of oxygen

Abbreviation	Glossary
PPAR-γ	Peroxisome proliferator activated receptor-γ
PS	Phosphatidylserine
Psi	Pounds per square inch
PUFAs	Polyunsaturated fatty acids
pVO_2	Peak the rate of oxygen consumption
$R^{\bullet}$	Reactive free radical
RASMCs	Rabbit aortic smooth muscle cells
REM	Relative electrophoretic mobility
RNA	Ribonucleic acid
$RO^{\bullet}$	Alkoxyl radical
RO-H_2O	Reverse osmosis-water
$ROO^{\bullet}$	Peroxyl radical
ROS	Reactive oxygen species
rpm	Revolutions per minute
RPMI-1640	Roswell Park Memorial Institute-1640
R-S-S-R	Disulfides
$-S^-$	Thiolate anion
SDS	Sodium dodecyl sulfate
SDS-PAGE	Sodium dodecyl sulfate polyacrylamide gel electrophoresis
sec	Second
SEM	Standard error of the mean
-SH	Sulfydryl group
SMCs	Smooth muscle cells
SNAP	S-Nitroso-N-acetyl-DL-penicillamine
-SNO	S-Nitrosothiols group
SOD	Superoxide dismutase
SNP	Sodium nitroprusside
$-SO_2H$	Sulfinic group

Abbreviation	Glossary
$-SO_3H$	Sulfonic group
-SOH	Sulfenic group
SR-A	Scavenger receptor A
SR-B1	Scavenger receptor B1
SW41- Ti	Beckman Swing out Bucket Rotor
T	Time
T cells	T lymphocytes (thymocytes)
TBA	2-Thiobarbituric acid
TBARS	Thiobarbituric acid reactive substances
TCA	Trichloroacetic acid
TGF-β	Transforming growth factor-β
Th-1 cells	T helper cells class 1
THP-1	Human acute monocytic leukemia cell line
TLR4	Toll-like receptor 4
TMP	1,1,3,3-Tetramethoxypropane
TNF-α	Tumour necrosis factor-α
Tris	Tris(hydroxymethyl)aminomethane
Trolox	6-Hydroxy-2,5,7,8-tetramethylchroman-2-carboxylic acid
Trp	Tryptophan
Tyr	Tyrosine
U/ml	Unit per millilitre
U937	Human histiocytic lymphoma cell line
UV	Ultraviolet
V	Volt
V	Volume
v/v	Volume per volume
VO_2	Rate of oxygen consumption
w/v	Weight per volume

Abbreviation	Glossary
x	Multiplied

Abstract

Intracellular oxidative stress is induced by oxidised low density lipoprotein (oxLDL) in macrophages. In the atherosclerotic lesions, this oxLDL dependent oxidative stress appears to cause macrophage cell death, a key process in the development of the necrotic core within the complex plaque. Macrophages are activated by γ-interferon to synthesise and release a potent antioxidant, 7,8-dihydroneopterin (7,8-NP), which has been previously shown to protect human monocyte-like U937 cells and human monocyte-derived macrophage (HMDM) cells from oxLDL cytotoxicity. This study examined whether oxLDL causes the loss of cellular metabolic function and whether 7,8-dihydroneopterin can prevent this loss of metabolic activity in U937 cells and HMDM cells.

OxLDL prepared by copper oxidation caused cell death in both U937 and HMDM cells at concentrations of 0.5 and 2.0 mg/ml, respectively. Cell morphology showed the oxLDL caused a necrotic like death in both cells as indicated by cell swelling and lysis. The decrease in cell viability was only observed after the loss of intracellular glutathione (GSH) which occurred in the first 3 hours in U937 cells following oxLDL addition. The loss of GSH appeared to be due to the production of intracellular oxidants generated in response to the presence of the oxLDL.

Within 3 hours of oxLDL addition to both cell types, there was a rapid and progressive shutdown of cell metabolism indicated by a significant decrease in the enzymatic activity of the glycolytic enzyme glyceraldehyde-3-phosphate dehydrogenase (GAPDH) and a fall in lactate production and intracellular ATP levels. GAPDH activity was found to be

inactivated rather than being lost from the cell. Gel electrophoresis with specific staining for oxidised proteins showed that the GAPDH had been oxidatively inactivated in the cells when oxLDL was present. Unlike GAPDH, lactate dehydrogenase (LDH) was not inactivated by the oxidation but was lost from the cells due to cell lysis. The observed rate of glycolysis failure was similar in both cell types except the HMDM cells did not lose lactate, LDH activity and cell viability until 6 hours compared to 3 hours with the U937 cells.

The rate of oxygen consumption (VO_2) was measured in U937 cells by taking cells at set time points and placing them in the respirometers to measure the VO_2. U937 cells were found to increase their VO_2 with incubation but this increase was inhibited in the presence of oxLDL within 3 hours.

The addition of the 7,8-dihydroneopterin above 100 μM to both the U937 and HMDM cells significantly inhibited the oxLDL-induced loss of cell viability. GAPDH activity loss was also inhibited while lactate production was maintained. The 7,8-dihydroneopterin also prevented the decrease in the VO_2 in oxLDL-treated U937 cells.

OxLDL was labelled with fluorescent DiI to measure the uptake of oxLDL by HMDM cells. The incorporation of DiI into oxLDL was found to make it non-cytotoxic, possibly due to DiI's antioxidant properties. Studies were therefore conducted using either a mixture of oxLDL and DiI labelled oxLDL (DiI-oxLDL) at non-protective concentrations or low concentration of DiI-oxLDL alone. These studies showed that 7,8-dihydroneopterin downregulated the oxLDL uptake in oxLDL-treated HMDM cells. Surprisingly the uptake rates also suggested that there was no relationship between

oxLDL uptake and cell death assuming oxLDL and DiI-oxLDL are taken up by the same mechanism.

This research showed that oxLDL-induced oxidative stress in macrophage cells causes a rapid oxidative loss of GAPDH activity which leads to the loss of glycolytic activity and a fall in ATP levels. The failure of cell metabolism appears to be a key event in the death mechanism triggered by the oxLDL. The radical scavenging activity of 7,8-dihydroneopterin appears to prevent the oxidative stress as indicated by the protection of the GSH pool. Without the oxidative stress, GAPDH remains functioning, glycolytic activity is maintained and both the U937 cells and HMDM cells did not die. This suggests that within the atherosclerotic plaque, 7,8-dihydroneopterin may act to stabilise the metabolism of macrophage cells in the presence of oxLDL and downregulate the oxLDL uptake.

1 Introduction

1.1 Atherosclerosis

Atherosclerosis is a chronic inflammatory disease, often linked to high plasma concentrations of cholesterol, in particular low-density lipoprotein (LDL) cholesterol (Carpenter *et al.*, 1991, Blasi, 2008). High concentrations of plasma LDL appear to be linked to the accumulation of cholesterol filled macrophages in the artery wall. The macrophage is the predominant cell type in the atherosclerotic plaque making up 66% of the inner plaque region, but is also elevated in concentration in the media region of a carotid plaques where 13% of the cells are monocyte/macrophage with endothelial cells making up 20%, smooth muscle (44.0%) and T cells (14%) (Rekhter & Gordon, 1995). This high percentage of immune/inflammatory cells clearly shows atherosclerotic plaques are a site of inflammation. The macrophage cells generate significant amounts of oxidants as part of the inflammatory process as well as absorbing lipids, mainly cholesterol, from the oxidatively modified lipoproteins, within the artery wall. The resulting high intracellular content of cholesterol lipid transforms these lipid-loaded macrophages into foam cells, which then remain stuck in the artery wall. It is the collection of these foam cells in the artery wall that causes the narrowing of the artery and is called an atherosclerotic plaque (Figure 1.1). In extreme cases these plaques can eventually block the artery stopping the flow of blood. The death of the macrophage foam cells leads to plaque rupture, resulting in thrombosis (Takahashi *et al.*, 2002).

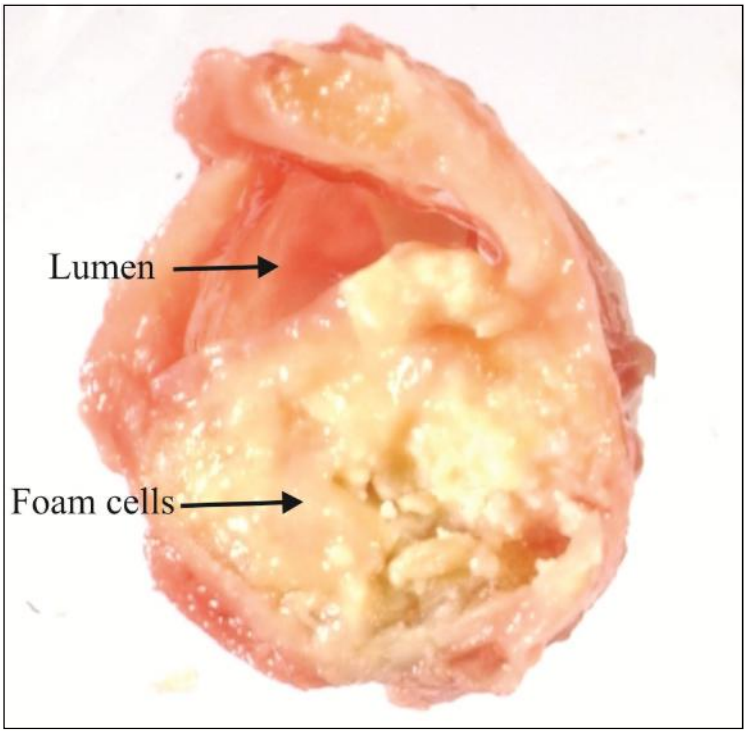

Figure 1.1 A cross section of atherosclerotic plaque.
Cross section of a plaque (4.0mm diameter) removed from the left common carotid artery of an 84 year old non-smoking patient who presented with transient ischemic attacks. Ultrasound analysis showed 85% stenosis (narrowing) of the vessel. This is the classic type of advanced, lipid-filled plaque with a large necrotic core region and significant levels of calcification. Adapted from (Gieseg *et al.*, 2009a).

In humans, oxidised low density lipoprotein (oxLDL) within atherosclerotic lesions is strongly associated with coronary artery disease, acute coronary syndromes, and vulnerable plaques (Tsimikas *et al.*, 2005). The death of the foam cells and resulting plaque instability, is thought to be driven in part by the cytotoxicity of oxLDL. The mechanism of oxLDL cytotoxicity is not clear with membrane/cellular instability, kinase activation, metabolic failure and oxidative mechanisms being proposed (Asmis *et al.*, 2005). OxLDL has been shown to cause the shutdown of endothelial cells metabolism through oxidative modification of key metabolic enzymes (Chisolm & Chai, 2000). Whether this happens in the more oxidant resistant macrophage and whether the macrophages own antioxidant can count the oxidative stress of oxLDL will be explored in the research described in this thesis.

1.1.1 Development of atherosclerosis

Atherosclerotic plaque development is a progressive process usually taking many years. It is characterised by the acquirement and differentiation of a variety of inflammatory cells, mainly monocytes and T-cells. Smooth muscle cells (SMCs) become a major component in advanced plaques. The developing plaque also contains significant amounts of extracellular matrix and lipoprotein. Cholesterol and cholesterol crystal deposition has also been described (Libby *et al.*, 2002, Lusis, 2000). The process of formation plaque and growth is summarised in the following sections and in Figure 1.2. The figure outlines the events leading to the earliest stages of atherosclerosis, with foam cells differentiation and the fatty streak lesion formation (Steinberg, 1997).

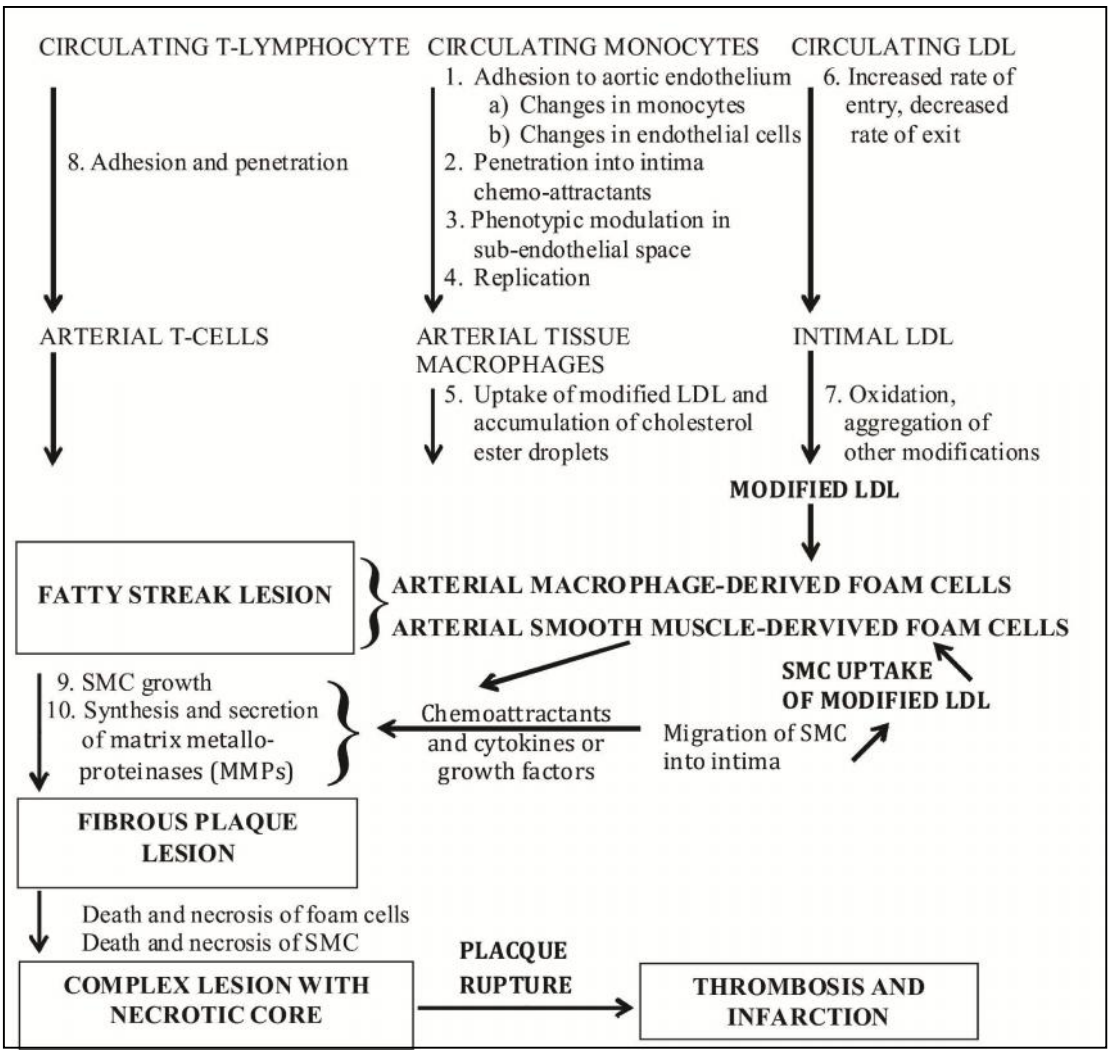

Figure 1.2 The sequence of events in atherosclerosis.
Adapted from (Steinberg, 1997).

This progresses to advanced plaques through cell growth, matrix deposition, cell migration, cell death and necrosis (Ross, 1993).

1.1.2 Foam cell formation

Modifications of LDL (discussed in section 1.2.2) appear to release inflammatory lipids that induce endothelial cells to express leukocyte adhesion molecules. It has also been proposed that mechanical stress on the artery wall (Hansson *et al.*, 2006) also contributes to the expression of inflammatory cell surface markers which cause the requirement of monocytes/macrophages into the artery walls intima layer. The oxLDL particles are taken up by specific scavenger receptors (section 1.2.4) on macrophages, resulting in the formation of foam cells (Figure 1.3) (Hansson, 2005). Foam cells are characterised as macrophage cells loaded with cholesterol esters (Steinberg *et al.*, 1989). OxLDL taken up by macrophages consists of free cholesterol and cholesterol esters that are hydrolysed in lysosomes. The free cholesterol undergoes esterification which is catalysed by acyl coenzyme A:cholesterol acyltransferase (ACAT). The free cholesterol is also stored in the lipid droplets that characterise foam cells (Ouimet & Marcel, 2011). Endothelial cells (ECs) and SMCs in lesions also accumulate lipid droplets, but monocyte-derived macrophage foam cells predominate (Steinberg, 2009). Cholesterol esters within these lipid droplets can in turn be hydrolysed by cholesteryl ester hydrolase (acid lipase) and proteases generating free cholesterol and fatty acids, for incorporation into membranes and transport out of the cells (Ouimet & Marcel, 2011).

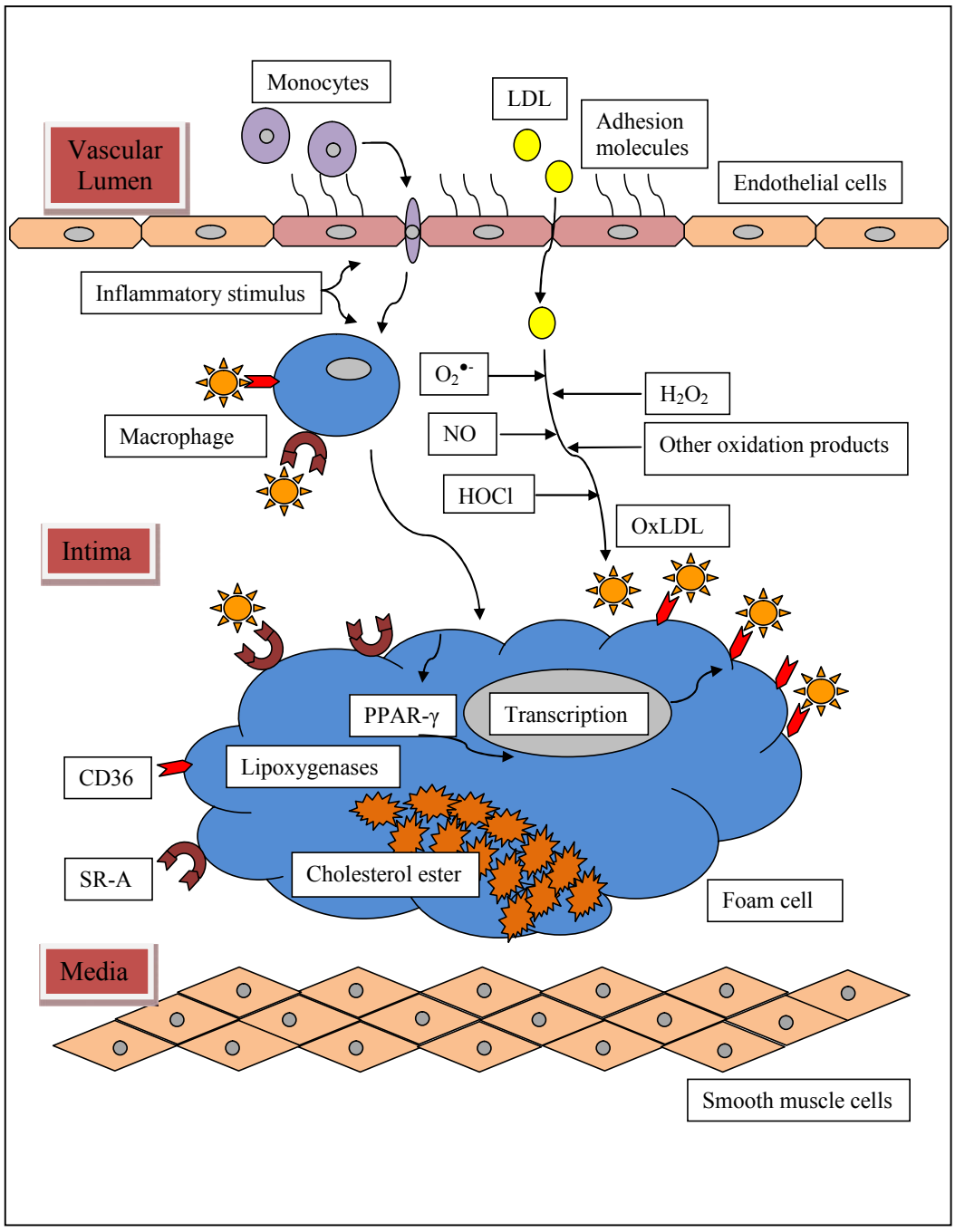

Figure 1.3 Scavenger receptors-mediated macrophage foam cell formation. Inflammatory stimuli of ECs and macrophage cause the secretion of oxidative enzymes (lipoxygenases) and reactive oxygen species including NO, $O_2^{\bullet-}$, H_2O_2, and HOCl. These oxidants cause LDL oxidation generating oxLDL in the artery wall. The uptake of oxLDL by ECs, SMCs and macrophages cells via scavenger receptors CD36, SR-A and other oxLDL receptors is not downregulated in response to increasing intracellular cholesterol levels causing the macrophage cells to form large lipid loaded foam cells.

Mechanisms mediating excess cholesterol efflux are critical for the maintenance of cholesterol homeostasis in macrophages since the build-up of excess cholesterol is cytotoxic to the cells (Warner *et al.*, 1995). Therefore, in the presence of an appropriate extracellular acceptor, mainly high density lipoprotein (HDL), and in particular the apolipoprotein A1 containing lipoproteins (apoA1), excess cholesterol can be exported from the cell via the plasma membrane ABCA1 and ABCG1 transports (Moore & Tabas, 2011). This process appears to be partially impaired in foam cells by oxysterols within oxLDL (Kritharides *et al.*, 1995, Maor & Aviram, 1994). In the absence of extracellular acceptors, excess free cholesterol in the cytosol undergoes re-esterification to detoxify the excess cholesterol before storage as cholesterol ester in the cytosol (Van Reyk & Jessup, 1999). OxLDL also inhibit normal processing of lipids through the endosomes and lysosomes. The oxysterols and oxLDL appear to resist processing by the lysosomal esterase and proteases (Maor & Aviram, 1994, Van Reyk & Jessup, 1999). This leads to intra-cytoplasmic accumulation of cholesterol ester as membrane-free lipid droplets and transformation of macrophages into foam cell (Maor & Aviram, 1994). The formation of foam cells has been cited as a key process in plaque development (Steinberg *et al.*, 1989). It is the clustering of the foam cells that leads to the development of the fatty streak. Thereafter, continued cell influx and proliferation leads to more advanced lesions, distinguished by their complex structures, fibrous character with areas of lipid deposition and often calcification (Mendis *et al.*, 2005).

1.1.3 Cell death mechanisms

Cell death occurs either by necrosis or apoptosis or both together (Halliwell & Gutteridge, 2007). Necrotic cell death is characterised by swelling of the cell and internal organelles, rupture of the plasma membrane, loss of integrity of mitochondrial, peroxisomal and lysosomal membranes. The cells content is released as a result of this lysis to the surrounding environment and so will affect the nearby cells. This cellular content can contain pro-oxidants such as copper iron, antioxidants such as glutathione (GSH) and degradative molecules such as activated calpains (Halliwell, 2003). Collectively the internal cellular contents can trigger cellular inflammation. In contrast apoptotic cell death is characterised by cell shrinkage and bleb formation on the surface of the cell membrane without the membrane losing its integrity. Internal organelles retain their structure, but chromatin condensation and nuclear fragmentation occur (Yuan *et al.*, 2000). The cell breaks into small membrane-surrounded fragments (called apoptotic bodies), without rupture of organelle membranes (Haunstetter & Izumo, 1998). The apoptotic bodies are then cleared by phagocytosis without inciting an inflammatory response. The redistribution of phosphatidylserine (PS) to the outer surface of plasma membrane is also a hallmark of apoptosis, which enables the recognition of apoptotic bodies by phagocytic cells (Van Engeland *et al.*, 1998). If the apoptotic bodies are not phagocytosed, a process known as secondary necrosis will occur, in which the membranes of apoptotic bodies lyse and the contents of the bodies are released (Tabas, 2005).

1.1.4 Lesion progression, immunological response and inflammation

Macrophages, T cells, mast cells, ECs and SMCs play a key role in the formation and progression of atherosclerotic lesions (Hansson, 2005). All stages of atherosclerosis, from initiation to progression, have an involvement of the immune system (including both innate immunity and adaptive immunity). In atherosclerotic plaques there is an accumulation of immune cells, such as monocytes/macrophages, dendritic cells (DCs), and numerous lymphocytes, which include different subpopulations of leukocytes (Shimada, 2009). In the sub-endothelial space, there are complexes of antibodies and antigens also present (Prohaszka & Fust, 2004, Binder *et al.*, 2007).

In response to inflammatory signals, circulating monocytes near the artery wall attach to endothelial cells of the artery wall by cell adhesion molecules. Monocytes migrate through the endothelial layer into the intima (Li & Glass, 2002). In the sub-endothelial space, the activation of monocytes, ECs and mast cells together with mononuclear cells, such as $CD4^+$ T cells occurs (Prohaszka & Fust, 2004, Mandal *et al.*, 2004). Endothelium activation is induced by a chemoattractants and cytokines or growth factor (macrophage-colony stimulating factor, M-CSF) released in the intima. This causes the stimulation of monocytes to enter the artery wall and undergo differentiation into macrophages. These inflammatory markers also cause the proliferation and migration of SMCs, net matrix deposition, and fibrous cap formation in advanced lesions (Newby & Zaltsman, 1999).

Circulating LDL can diffuse through the endothelial layer into the intima where they can become trapped by proteoglycans at the artery wall. In the intima LDL appears to be modified to various forms of oxLDL including the laboratory defined minimally oxidised LDL (mLDL) and heavily oxidised oxLDL (section 1.2.2). It has been proposed that the oxidation of LDL in the arterial wall is catalysed by transition metal ions through the release of iron from transferrin, due to low pH environment of the intima (Lamb & Leake, 1994). There is also evidence that the oxidation also occurs by oxidative enzymes including lipoxygenases and oxidative products produced by specific enzymes such as nitric oxide synthase generating nitric oxide (NO), NADPH-oxidase (NOX) generating superoxide ($O_2^{\bullet -}$), and hydrogen peroxide (H_2O_2), and myeloperoxidase (MPO) generating hypochlorite (HOCl). These oxidants are secreted from ECs and macrophages during inflammatory stimuli and are thought to generate oxLDL in the artery wall. Superoxide production from both the plasma membrane and cytoplasm has been reported in macrophage, ECs and SMCs. Some of this oxidant production appears to be due to the release of cytochrome c from the mitochondria as a result of cell death and lysis (Harada-Shiba *et al.*, 1998, Kinscherf *et al.*, 1998, Zmijewski *et al.*, 2005, Sukhanov *et al.*, 2006).

The resulting oxLDL can be taken up by macrophages via scavenger receptors CD36, SR-A and other oxLDL scavenger receptors (section 1.2.4) which results in the accumulation of cholesterol ester in the macrophages, leading to the formation of foam cells (section1.1.2). At the same time SMCs migration from the media region into the intima causes irregular thickening of arterial intima and migration along

endothelial layer. SMCs synthesise extracellular matrix leading to formation of fibrous plaque lesion (Newby & Zaltsman, 1999).

The interaction oxLDL and other oxidative products with the various cells within the artery wall leads to release of additional inflammatory cytokines (e.g., γ-interferon and tumour necrosis factor-α, TNF-α), chemokines, oxygen and nitrogen radicals, and other inflammatory molecules (Hansson, 2005). Antigens presented by macrophages and DCs (antigen-presenting cells) also may trigger the activation of antigen-specific T cells in the artery. Most of the activated T cells produce Th-1 cytokines (e.g. γ-interferon), which activate macrophages and vascular cells, leading to inflammation (Hansson, 2005). Interferon-γ improves the efficiency of antigen presentation and augments synthesis of the inflammatory cytokines such as TNF-α and interleukin-1(IL-1) (Szabo *et al.*, 2003). Regulatory T cells modulate the process by secreting anti-inflammatory cytokines, such as interleukin-10 (IL-10) and transforming growth factor-β (TGF-β). The balance between inflammatory and anti-inflammatory activity controls the progression of atherosclerosis. Metabolic factors may affect this process in several ways, by contributing to lipid deposition in the artery and initiating new rounds of immune-cell involvement (Hansson, 2005).

In early and advanced lesions oxLDL appears to induce foam cells death by apoptosis/necrosis. As a result of prolonged inflammation, foam cells and SMCs have been shown to undergo apoptosis and secondary necrosis leading to the formation of the necrotic core. This necrotic core region contains cell debris from necrotic cells plus insoluble protein, free cholesterol and cholesterol ester deposits (Seimon &

Tabas, 2009). This necrotic core region can become unstable if the overlying fibrous cap is produced forming vulnerable plaque which is prone to rupture. The release of matrix metalloproteinases (MMPs) by macrophages is though to be a key step in the formation of these unstable vulnerable plaques (Moore & Tabas, 2011).

1.1.5 Plaque rupture and thrombosis

The advance plaque, often refered to as a "lesion" may further increase in size and subsequently rupture due to thining of the fibrous cap so exposing the underlying lipid-rich necrotic debris to the blood. This appears to trigger thrombus formation and precipitate acute vascular events (Mendis *et al.*, 2005). Plaque rupture is a serious clinical event because it exposes pro-thrombotic material from the core of the plaque (phospholipids, tissue factor and platelet-adhesive matrix molecules) to the blood (Figure 1.4) (Hansson, 2005). Plaque rupture preferentially occurs where the fibrous cap is thin and partially destroyed. At these sites, activated immune cells are abundant. They produce numerous inflammatory molecules and proteolytic enzymes that can weaken the fibrous cap and activate cells in the core, transforming the stable plaque into a vulnerable, unstable structure that can rupture, induce a thrombus, and elicit an acute coronary event i.e. heart attack or stroke (Hansson, 2005).

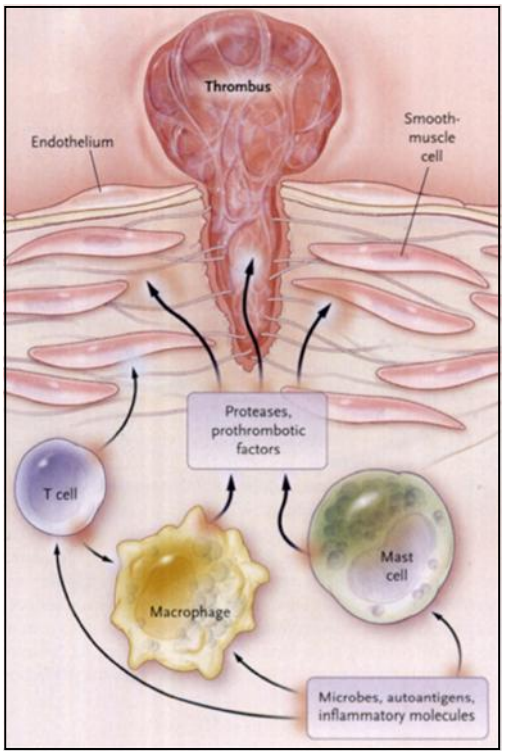

Figure 1.4 Atherosclerotic lesion thrombosis formation.
Microbes, auto-antigens, and various inflammatory molecules can activate T cells, macrophages, and mast cells, leading to the secretion of inflammatory cytokines (e.g., γ-interferon and tumour necrosis factor) that reduce the stability of plaque. The activation of macrophages and mast cells also causes the release of metalloproteinases and cysteine proteases, which directly attack collagen and other components of the tissue matrix. These cells may also produce prothrombotic and procoagulant factors that directly precipitate the formation of thrombus at the site of plaque rupture. Taken from (Hansson, 2005).

1.2 Low density lipoprotein

Low density lipoprotein (LDL) is the main carrier of cholesterol within the plasma, delivering cholesterol from the hepatocytes to the peripheral cells. In normolipidemic person, the serum LDL concentration is about 3 mg/ml total mass (total mass, protein plus lipid components with apoB portion making up 1/5 of mass) and typically this LDL carries about 60% of the total serum cholesterol (Esterbauer *et al.*, 1992). The amount of cholesterol and cholesterol esters associated with LDL are typically about two-thirds

of the total plasma cholesterol (total plasma cholesterol ranges from 1.3 to 2.6 mg/ml) (Mathews & Van Holde, 1996). In the artery wall, the LDL concentration is higher than that of other lipoproteins, although the range is still within that found in plasma (Steinbrecher & Lougheed, 1992).

1.2.1 LDL Composition

LDL is a particle with a spherical shape with diameter of 19-25 nm, relative molecular mass between 1.8 and 2.8 million and a density range of LDL is 1.090-1.063 g/ml. Each LDL particle has an average of 170 molecules of triglycerides, 600 molecules of cholesterol and 1600 molecules of cholesterol esters (mostly cholesterol linoleate) forming an inner core. The core is surrounded by phospholipid monolayer containing about 700 phospholipid molecules (mainly phosphatidylcholine) with their polar head groups oriented towards the aqueous phase. Of the fatty acids, half are polyunsaturated fatty acids (PUFAs) making LDL highly susceptible to free radical mediated oxidation (Parthasarathy *et al.*, 1990). The fatty acid contents vary

considerably among individuals. For instance, linoleic acid content varies from 1200 to 2400 nmol/mg LDL protein. This variation in the PUFA content affects the oxidation susceptibility of LDL in the laboratory and possibly clinically (Esterbauer *et al.*, 1992, Thomas *et al.*, 1994).

The LDL particle contains only one protein called apolipoprotein B100 (apoB100) which is made up of 4536 amino acids. Structurally apoB100 is made up of extensive β sheet with small amount of α-helices. The apoB100 protein is embedded in the lipid phase with extensive hydrophobic and hydrophilic sections (Obama *et al.*, 2007, Johs *et al.*, 2006). The interactions between apoB100 and the LDL receptor are critical for the normal, regulated receptor-mediated endocytosis of LDL by target cells (Brown & Goldstein, 1986).

Due to the high PUFAs content LDL contains a variety of antioxidants for protection. On average, each molecule of LDL has 6 α-tocopherol molecules and the remaining antioxidants are each reported to be present at less than one mole per mole of LDL and include γ-tocopherol, ubiquinol-10, retinoids and carotenoids (Esterbauer *et al.*, 1992). These lipid soluble antioxidants are present in both the core and phospholipid outer layer. Since the structure of LDL is reasonably fluid, the lipid soluble antioxidants can move freely between the core and the phospholipid coat (Schuster *et al.*, 1995). When LDL is exposed to oxidants, α-tocopherol is generally the first antioxidant to be consumed while β-carotene is the last (Esterbauer *et al.*, 1991). It is usually only after the antioxidants are consumed that significant lipid oxidation

occurs within the LDL particle. Under very low but extended exposure to oxidants α-tocopherol can be involved in the lipid oxidation (Bowry *et al.*, 1992).

1.2.2 LDL oxidation

Oxidative LDL modification, especially copper ion oxidation, involves the peroxidation of the PUFAs in the LDL particle (Esterbauer *et al.*, 1992). The lipid oxidation reactions in turn oxidise and damage the apoB100 protein moiety to give a particle that is not recognised as oxLDL by the cells scavenger receptors but is no longer recognised as LDL by the LDL receptor. The peroxidation starts when a reactive free radical ($R^{\bullet}$) detaches a hydrogen atom from PUFAs (LH) and yielding a carbon-centred lipid radical ($L^{\bullet}$). This in turn reacts with oxygen and forms lipid peroxyl radical ($LOO^{\bullet}$), which can then attack further PUFAs (LH) generating further lipid peroxyl radicals. The lipid peroxyl radicals also attack the apoB100 to generate protein hydroperoxides (LOOH) (Gieseg *et al.*, 2003). The resulting chain reactions would rapidly oxidise all the PUFAs in the particle except that the LDL antioxidant α-tocopherol (Vitamin E) scavenges the peroxyl radical preventing the chain reaction from occurring. In the plasma the resulting tocopherol radical is regenerated by ascorbate. In the absence of water soluble antioxidants, like ascorbate, lipid peroxidation occurs once all the α-tocopherol is consumed (Jessup *et al.*, 1990). The resulting lipid peroxides can break down via metal catalysed reactions to stable but often reactive end-products such as lipid aldehydes, hydrocarbon gases, epoxides and alcohols (Esterbauer *et al.*, 1992, Gieseg *et al.*, 2009b).

Lipid aldehydes, in particular, 4-hydroxy-2-nonenal (HNE) and malondialdehyde (MDA), reacted with lysine residues within the apoB100 protein of LDL. The aldehyde binding to the lysines destroys the LDL receptor binding site on the LDL and causes the LDL to be recognised/bound by macrophage scavenger receptors (section 1.2.4) (Hoff *et al.*, 1989). OxLDL is not observed in plasma. However, antibodies against oxLDL have been detected in the plasma of patients with heart disease (Salonen *et al.*, 1992, Shaw *et al.*, 2001). Antibodies against oxLDL are present in normal animal and human plasma, but in atherosclerosis, both oxLDL and oxLDL antibodies have been reported (Steinberg, 2009).

Several lines of evidence support the involvement of oxLDL in the development of atherosclerosis. Plasma LDL isolated from people with extensive atherosclerosis shows a mild degree of oxidation (Palinski *et al.*, 1995). Components of oxLDL have been shown to be present in human and animal models of atherosclerotic lesions. Analysis of plaques has detected cholesterol oxidation products, linoleic and arachidonic acid peroxides and hydroxides, and decomposition products of lipid peroxides (HNE and MDA) (Niki, 2009). In addition, antibodies that recognise a range of epitopes, including aldehydes and specific oxidised lipids present in oxLDL were found in the plasma from patients with coronary artery disease (Toshima *et al.*, 2000). The significance of these findings was shown by two separate studies. The first study showed that immunisation of mice or rabbits lacking LDL receptors with MDA-treated LDL led to high plasma antibody levels, and less atherosclerosis (Soto *et al.*, 2012). The second study showed that antibodies recognising oxidised mouse

LDL caused decreased atherosclerosis in LDL-receptor deficient mice (Shoenfeld *et al.*, 2004).

1.2.3 Types of oxLDL

There is a range of "oxidised" or high uptake LDL types all of which are taken up by the cells in a non-LDL receptor dependent mechanism. Types described in the literature include aggregated LDL (agLDL), minimally oxidised LDL (mLDL), moderately (mod-LDL) or mildly oxidised LDL (although some publications consider these as two different types), hypochlorite oxidised LDL (HOCl-oxLDL) and heavily oxidised LDL (oxLDL) usually made with copper ions with extended incubation periods more than 24 hours (Gieseg *et al.*, 2009a). The type of oxLDL made in the laboratory and the degree of oxidation is chosen according to the type of cells and the research. AgLDL contains little or no lipid peroxidation, less tocopherol or coenzyme Q10 (CoQ10). Technically, it is not oxidised and apparently not cytotoxic. AgLDL may initiate vascular disease due to low solubility, reduced diffusion potential and ability to act as a source of lipoprotein for oxLDL formation. Furthermore, it is rapidly taken up by macrophages (Khoo *et al.*, 1988, Asmis *et al.*, 2005). mLDL contains lipid hydroperoxides and greatly reduced α-tocopherol levels (30-50% compared with native LDL). It is not cytotoxic but has often been reported in the literature as being cytotoxic (Sparrow *et al.*, 1988, Massaeli *et al.*, 1999). Mildly oxidised LDL has been reported to be more toxic than moderately oxidised LDL. Mildly oxidised LDL is high in hydroperoxides, but low in oxysterols (e.g. 7-ketocholesterol, 7-KC) and MDA, contains no α-tocopherol and little protein damage

based on overall charge. The relatively high hydroperoxide levels of mildly oxidised LDL could be the cause of the observed increase in cell death and apoptosis. In contrast, mod-LDL is higher in oxysterols and less toxic (Carpenter *et al.*, 2003, Gerry *et al.*, 2007, Gerry & Leake, 2008). HOCl-oxLDL is characterised by heavy oxidation of the apoB100 residues of Cys, Met, Tyr, Trp, lipid oxidation and organic chloramine formation (Hazell *et al.*, 1994, Vicca *et al.*, 2003). During inflammation HOCl-oxLDL may be a significant product within the artery wall as chlorinated amino acid residues within atherosclerotic plaques have been detected (Hazen & Heinecke, 1997). The resulting HOCl is cytotoxic to cells including macrophages (Vicca *et al.*, 2000, Vicca *et al.*, 2003). Heavily oxLDL has the highest oxysterol levels and is the most cytotoxic. It is characterised by its colourless appearance and oxidation of all tocopherol and β–carotene, is often aggregated during preparation, and is high in oxysterols, protein carbonyls and isoprostanes. The resulting associated apoB100 appears heavily fragmented on sodium dodecyl sulfate polyacrylamide gel electrophoresis (SDS-PAGE) analysis (Esterbauer *et al.*, 1989, Lenz *et al.*, 1990, Reid *et al.*, 1993, Baird *et al.*, 2004, Gerry *et al.*, 2007). In heavily oxidised LDL, 50% of total cholesterol is oxidised, predominantly to 7-ketocholesterol. Few unoxidised sterolesters remain, all hydroperoxide-containing esters have further oxidised as well as and up to 90% of the steryl ester acyl groups (Brown *et al.*, 2000).

1.2.4 OxLDL uptake and scavenger receptors

Monocyte/macrophages in culture take up oxLDL much more rapidly than they take up native LDL. OxLDL does not bind to normal LDL receptors. Instead, oxLDL

binds with high affinity to macrophage-specific plasma membrane receptors called scavenger receptors. Scavenger receptors appear to be important for the binding of oxidised phospholipids for the recognision of apoptotic cells but also bind oxLDL (Shaw *et al.*, 2000). Macrophages possess several scavenger receptors for taking up oxLDL, including scavenger receptor A (SR-A), scavenger receptor B1 (SR-B1), CD36, CD68 and scavenger receptor for phosphatidylserine and oxidised lipoprotein (Linton & Fazio, 2001, Boullier *et al.*, 2001, Febbraio *et al.*, 2001). SR-A and CD36 mediate the uptake of oxLDL and promote the development of atherosclerosis (Linton & Fazio, 2001, Boullier *et al.*, 2001, Febbraio *et al.*, 2001). CD36 also functions as a fatty acid transport protein in adipose tissue and muscle (Febbraio *et al.*, 2001). Internalisation of oxLDL via CD36 generates oxLDL products (oxidised phospholipids and oxysterols), which is mediated by lipoxygenase (Febbraio *et al.*, 2001, Steinberg, 2002). These lipids provide ligands for the transcriptional regulator, peroxisome proliferator-activated receptor-γ (PPAR-γ) and activate LXR−RXR heterodimers, resulting in nuclear translocation and increased transcription of target genes (Li & Glass, 2002). The increased expression of CD36 on the cell surface leads to further internalisation of modified LDL and eventual foam cell formation (Febbraio *et al.*, 2001).

SR-B1 binds HDL with high affinity and mediates selective cholesterol delivery to liver and steroidogenic tissues by a mechanism distinct from the classic LDL receptor pathway (Acton *et al.*, 1996). Gene encoding studies showed that SR-B1 has an anti-atherogenic function (Braun *et al.*, 2002). In macrophages, SR-B1 facilitates cholesterol ester re-uptake by inhibiting net ATP-binding cassette 1 (ABCA1)-

mediated cholesterol efflux (Chen *et al.*, 2000). Thus, the overall actions of SR-B1 in the arterial wall seem to be protective (Li & Glass, 2002). As the cholesterol content of the macrophage increases, accumulation of cholesterol occurs to the point of foam cell generation, without down regulation of these receptors (Steinberg, 2009).

Macrophages possess at least two major pathways for the uptake of oxLDL. SR-A takes up both acetylated LDL (acLDL) and oxLDL. AcLDL was able to compete for around 40% of oxLDL uptake (Sparrow *et al.*, 1988). CD36 appears to only take up oxLDL and cannot be out competed with acLDL (Lougheed & Steinbrecher, 1996).

There are also non-receptor mediated mechanisms for the uptake of oxLDL by the cells. For example, aldehydes and oxysterols enter the cells' plasma membrane by partitioning from the lipid phase of oxLDL (Gotoh *et al.*, 1993, Brown *et al.*, 1997). OxLDL can also be taken up by non-specific receptor-mediated endocytosis, especially in the aggregated form (Khoo *et al.*, 1988, Brown *et al.*, 1997).

1.2.5 OxLDL metabolism

The oxLDL taken up by the receptor mediated endocytosis is delivered to lysosomes where the cholesterol esters are degraded into free fatty acids and free cholesterol by cholesteryl ester hydrolase (acid lipase) and proteases (cathepsins). Free cholesterol is readily esterified by the endoplasmic reticulum ER enzyme ACAT, leading to intra-cytoplasmic accumulation of cholesterol ester as membrane-free lipid droplets, so transforming the macrophage cells into foam cells (Li & Glass, 2002). Uptake of acLDL by macrophages leads to extensive cholesterol accumulation (Moore & Tabas,

2011). Free cholesterol is able to leave the lysosome to relocate in all cell membranes. Excess cholesterol in foam cells undergoes efflux onto HDL by ABCA1 and ABCG1 transporters and then is transported to the liver for excretion in the bile (Terasaka *et al.*, 2007). Loading foam cells with free cholesterol, oxLDL and 7-ketocholesterol, the major oxysterol present in oxLDL induced apoptosis (Freeman *et al.*, 2005). HDL exerted a protective effect against this apoptosis (Terasaka *et al.*, 2007). Excess cellular accumulation of oxLDL and oxysterols causes disfunction in ACAT and defect in ABCA1and ABCG1transporters lead to impaired efflux of free cholesterol from the cells onto HDL, trapped free cholesterol in the cells and induced cell death in advanced lesions (Moore & Tabas, 2011).

For reasons not fully understood, a portion of the cholesterol esters become resistant to acid esterases and remain trapped in the lysosomes and represent approximately 90% of the total ester pool in oxLDL-loaded macrophages. Cholesterol esters together with other undegradable components, such as oxidised apoB and oxidised sterylesters remain appearently trapped within the lysosomal in the form of particulate insoluble materials such as ceroid (Jessup & Kritharides, 2000).

1.2.6 OxLDL cytotoxicity

OxLDL triggers cell death in a wide number of different cell types such as ECs, SMCs, human monocyte-derived macrophage (HMDM) cells and human derived monocyte-like U937 and THP-1 cell lines (Henriksen *et al.*, 1979, Hessler *et al.*, 1979, Baird *et al.*, 2005, Gieseg *et al.*, 2010). There is a directly proportional relationship between oxLDL concentration and cell death. The cytotoxicity of oxLDL

in *vitro* experiments generally occurs between 100 and 400 μg/ml of apoB protein (0.25 to 2.0 mg/ml total mass of LDL) depending on the LDL preparation and type of cell (Gieseg *et al.*, 2009a).

The exact composition of oxLDL depends on the nature and amount of oxidant used, with the latter parameter related to oxidant concentration, duration and conditions of exposure. These conditions appear to affect the level of oxLDL cytotoxicity. For example, lipoxygenases catalyse peroxidation of fatty acids generating a less cytotoxic oxLDL than oxLDL made with hypochlorite which oxidises the apolipoprotein B100 protein (Jessup & Kritharides, 2000). Some of the oxidation products that are present in oxLDL after exposure to copper are oxysterols (e.g. 7-ketocholesterol), hydroperoxides (e.g. linoleyl hydroperoxide), hydroxides (e.g. linoleyl hydroxide), ketones (e.g. oxo-octadecadienote), F2-isoprostanes (e.g. 8-epi-prostaglandin $F_2\alpha$), core aldehydes (e.g. 9-oxononanoate), fragmentation (e.g. 3-chlorotyrosine), cross-linking (e.g. dityrosine), amino acid oxidation (e.g. hydroxyleucine) and amino acid dervativatisation products (Jessup & Kritharides, 2000). Many of these compounds are cytotoxic when given directly to cells. OxLDL is therefore thought to cause macrophage cell death due to the cytotoxic chemicals, within the particle (Darley-Usmar *et al.*, 1991, Clare *et al.*, 1995). OxLDL induces intracellular oxidant production by decreasing antioxidant enzymes or increasing production of reactive oxygen species (ROS) such as H_2O_2 and HOCl (Dimmeler *et al.*, 1997). The binding of oxLDL to CD36 causes H_2O_2 release (Maxeiner *et al.*, 1998). Also the binding of oxLDL to CD36 activates caspase-3 to induce apoptosis in human macrophages (Wintergerst *et al.*, 2000). In addition, oxLDL and oxysterols

cause loss of the intracellular antioxidant GSH (Baird *et al.*, 2004, Rutherford & Gieseg, 2011).

The nature of the cell death does appear to depend on the type of death mechanism stimulated by oxLDL. Cell death induced by oxLDL can be either necrotic or apoptotic or both depending on cell type and incubation conditions (Gieseg *et al.*, 2009a). Direct observations of plaque have shown foam cells dying by an apoptosis-like mechanism as indicated by TUNEL staining (DNA fragmentation) of the cells (Hegyi *et al.*, 1996). Monocytes and macrophages derived from human blood showed caspase-dependent and -independent cell death (Nhan *et al.*, 2003, Asmis & Begley, 2003). In the absence of human serum, oxLDL induces apoptosis via the caspase-3 activation mechanism in HMDM cells (Asmis & Begley, 2003). In this laboratory, in the presence of 10% human serum, oxLDL induces cell death via necrosis with a rapid loss of GSH and without caspase-3 activation (Gieseg *et al.*, 2009a, Baird *et al.*, 2004).

With human derived monocyte-like THP-1 cells, increasing oxLDL concentration results in increasing activity of caspase-3 (Baird *et al.*, 2004). THP-1 cells undergo classic apoptosis with the appearance of annexin V staining morphology due to the flipping of phosphatidylserine to the outer surface of the membrane, caspase-3 activation and a small reduction in cellular thiol after exposure to oxLDL (Baird *et al.*, 2004, Vicca *et al.*, 2000). In U937 cells, incubation with oxLDL causes phosphatidylserine exposure (a marker of apoptosis), but with the absence of caspase activity. The oxLDL also causes a dramatic loss of intracellular thiol, which may

cause the inhibition of caspase activity. The failure of caspase-3 appears to lead to necrosis with cell swelling and lysis with no phosphatidylserine exposure on the cell membrane (Baird *et al.*, 2004). The difference in responses to oxLDL could be related to the varying mechanisms of uptake of oxLDL. U937 cells uptake by CD36 scavenger receptor four-fold higher than THP-1 cells (Nguyen-Khoa *et al.*, 1999), which causes oxidative stress. In contrast, THP-1cells uptake by scavenger receptors were partially regulated by the transcriptional regulator PPAR- γ, in response to oxLDL (Inoue *et al.*, 2001).

OxLDL uptake via scavenger receptors is important for cell death because it alters the cellular response to oxLDL. Antibodies to CD36 do not inhibit oxLDL uptake but do significantly reduce the level of ROS produced, caspase activation and cell death in human aortic smooth muscle cells (HASMCs) (Sukhanov *et al.*, 2006) and in HMDM cells (Wintergerst *et al.*, 2000). OxLDL result in the generation of more ROS in U937 cells than THP-1 cells possibly because THP-1 cells have lower level of CD36 expression than U937 cells (Nguyen-Khoa *et al.*, 1999). In THP-1 cells where oxLDL is though to be mainly taken up via the SR-A receptor which seems to alter the type of cell death (Liao *et al.*, 2000). Interestingly, there is no appearent difference in the degree of oxLDL toxicity between U937 and THP-1 cells (Baird *et al.*, 2004).

Aggregation of oxLDL causes a decrease in macrophage injury and necrotic core formation. Aggregation of oxLDL also causes increase in oxLDL uptake, so increaseing cholesterol ester accumulation and foam cell formation. Aggregated oxidised low density lipoprotein (aggoxLDL), is taken up through the SR-A receptor

but not by the CD36 receptor. AggoxLDL enhances oxLDL clearences by macrophages without damage to the cells (Asmis *et al.*, 2005) which may explain why aggoxLDL does not appear to increase free cholesterol levels.

1.3 Antioxidants

Antioxidants are substances which at at low concentrations are able to react with and neutralise free radicals faster than the radical reaction with key biomolecules such as proteins, lipids or DNA. Antioxidants can be enzymatic and non-enzymatic compounds. The main antioxidant enzymes are superoxide dismutase's (SOD), catalases and glutathione peroxidases. The most commonly studied non-enzymatic antioxidants are glutathione, ascorbate, α-tocopherol and β-carotene (Halliwell & Gutteridge, 2007).

1.3.1 Oxidative stress

Oxidative stress is defined as an increase in the production of ROS due to an imbalance between oxidants and antioxidants leading to damage of lipids, proteins, nucleic acids, membrane and genes (Sies, 1991). Oxidative stress can result either from low levels of antioxidants and/or from an increased production of reactive species (Halliwell & Whiteman, 2004). Free radicals and ROS interact with other molecules within cells inducing oxidative stress and oxidative damage. Oxidative damage has been implicated in the cause of many diseases, such as cardiovascular disease, cancer and Alzheimer's disease (Sies, 1991). In this research the antioxidant activities of two specific antioxidants, GSH and 7,8-dihydroneopterin (7,8-NP) will be examined in oxLDL treated cells.

1.3.2 The antioxidant effect of glutathione

Glutathione (L-γ-glutamyl-L-cysteinylglycine, GSH) is synthesized from its constituent amino acids by the sequential action of cytosolic enzymes, γ-glutamylcysteine synthetase (γ-GCS) and GSH synthetase. GSH is important in maintaining various proteins in a reduced state. GSH is the key thiol controlling the redox potential and state of reduction within the cell. GSH plays a critical role in cellular defenses against electrophiles, oxidative stress and nitrosating species (Griffith, 1999, Meister, 1988). The intracellular GSH concentration, typically 1-8 mM, reflects a dynamic balance between the rate of GSH synthesis and the combined rate of GSH consumption within the cell and loss through efflux.

Approximately 70% of the cells total antioxidant capacity is due to the presence of free thiol, whose reduction is partially dependent on the GSH concentration (Balcerczyk & Bartosz, 2003). Administration of L-cysteine precursors and other strategies allow GSH levels to be maintained under conditions that would otherwise result in GSH depletion and cytotoxicity. Conversely, inhibitors of γ-GCS have been used to deplete GSH as a strategy for increasing the sensitivity of tumours and parasites to certain therapeutic interventions (Griffith, 1999). Excessive accumulation of lipids derived from oxLDL, induces oxidative stress in foam cells and causes a compensatory increase in the synthesis of the endogenous antioxidant, GSH (Bea *et al.*, 2003, Shen & Sevanian, 2001, Darley-Usmar *et al.*, 1991). The oxidised GSH (GSSG) is converted back to GSH by the action of GSH-reductase using NADPH, which means the cell can withstand a certain level of oxidative stress (Gieseg *et al.*,

2009b). A number of the key enzymes in metabolism such as glyceraldehyde-3-phosphate dehydrogenase (GAPDH) enzyme, as well as regulatory enzymes like caspases, require key cysteine residues to be in a reduced free thiol state for activity (Baty *et al.*, 2002, Hampton *et al.*, 2002b). The interaction between ascorbate and GSH is an essential part of the cellular defence mechanism. Ascorbate reduces the level of GSH loss and subsequent DNA base and protein damage in human arterial smooth muscle cells (Jenner *et al.*, 2002).

In macrophages, depletion of intracellular GSH disables caspases and thus apoptosis is inhibited (Boggs *et al.*, 1998). A high GSH status in monocytes and macrophages is important in both controlling the foam cell formation and detoxification of oxLDL (Gotoh *et al.*, 1993). In HMDM cells, oxLDL depleted intracellular GSH and inhibited glutathione reductase, resulting in a marked diminution of the GSH/GSSG ratio (Gotoh *et al.*, 1993). Since GSH/GSSG ratio is one of the principal determinants of the cellular redox environment, any alteration in the redox environment can lead to cellular dysfunction and cell death (Schafer & Buettner, 2001). In the absence of oxLDL, an 80% depletion of intracellular GSH levels did not affect cell viability, but GSH depletion dramatically increased oxLDL-induced cell death. Conversely, supplementation of intracellular GSH stores with glutathione diethyl ester substantially diminished oxLDL toxicity (Wang *et al.*, 2006). In *vitro*, exposure of macrophages and THP-1 cells to oxLDL or HNE (a reactive aldehyde formed during LDL oxidation) causes oxidative stress and depletion of GSH, followed by re-synthesis and elevated levels of GSH after 24 hours and in turn, increases in availbale antioxidant (Darley-Usmar *et al.*, 1991). Also, increases in GSH and antioxidant

vitamins such as vitamins C and E play a central role in the antioxidant defences of human umbilical artery smooth muscle cells (HUASMCs) and may help to prevent oxLDL-mediated alterations in cell signalling, gene transcription and vascular reactivity occurring during atherogenesis (Siow *et al.*, 1998). Similarly, increasing GSH levels by treatment with GSH-ethyl ester decreased mouse-derived IC21 macrophage death resulting from oxLDL-induced apoptosis (Rosenson-Schloss *et al.*, 2005). The intracellular GSH status plays an important role in the differentiation and phagocytic activity of macrophages (Kim *et al.*, 2004).

1.3.3 Synthesis of 7,8-dihydroneopterin

Macrophages do not just release oxidants but they also release antioxidants. As mentioned previously, macrophages are a major source of the oxidants that can oxidise LDL to oxLDL including $O_2^{\bullet -}$, HOCl and reductants that increase the level of Fenton active metal ions on LDL (Firth *et al.*, 2008a). Macrophages appear to respond to inflammatory mediators by increasing their antioxidant capacity. During inflammation, γ-interferon released by Th-1 cells has been shown to stimulate macrophages to synthesise a potent antioxidant, 7,8-dihydroneopterin, which is generated through the enzymatic breakdown of guanosine triphosphate (GTP) by GTP-cyclohydrolase (Figure 1.5) (Gieseg *et al.*, 2008).

Interferon-γ generally prepares immune cells for inflammation by stimulating the macrophages in to various cellular changes such as increasing the NOX superoxide generating capacity (Cassatella *et al.*, 1985, Kikuchi *et al.*, 1994).

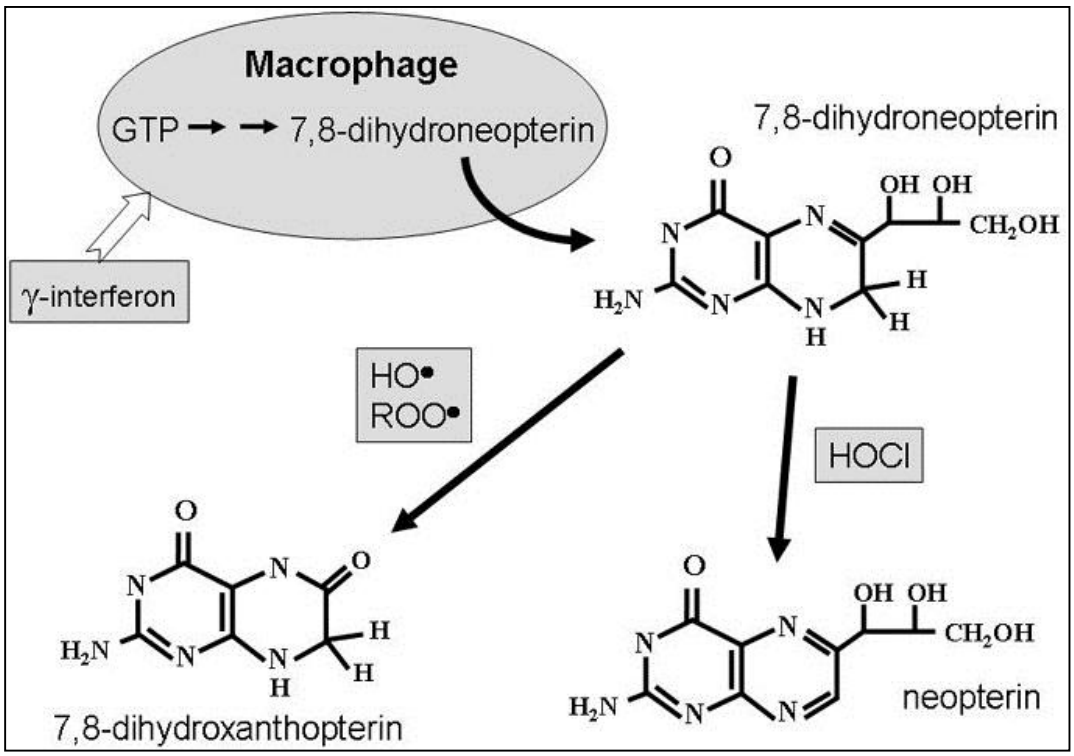

Figure 1.5 Generation and oxidation of 7,8-dihydroneopterin.
Interferon-γ stimulation of macrophages causes the enzymatic breakdown of intracellular GTP to 7,8-dihydroneopterin which can either be oxidised to the highly fluorescent neopterin by HOCl or to 7,8-dihydroxanthopterin by peroxyl and hydroxyl radicals. Adapted from (Gieseg *et al.*, 2009b).

Interferon-γ also up regulates synthesis of indoleamine2,3-dioxygenase (IDO) which catalyses the breakdown of tryptophan to 3-hydroxyanthranilic acid (3HAA) which also has antioxidant activity in *vitro* (Christen *et al.*, 1994, Gieseg *et al.*, 1995). Together these two antioxidants appear to play a role in protecting macrophages from oxidative stress but this research will focus solely on 7,8-dihydroneopterin (Gieseg *et al.*, 2008).

In *vivo*, 7,8-dihydroneopterin is oxidised to the highly fluorescent compound neopterin, which has been used clinically as a marker of immune cell activation for a number of years (Gieseg *et al.*, 2009a, Wachter *et al.*, 1989). During vascular disease high levels of neopterin are detected in the plasma and at micro-molar concentrations in atherosclerotic plaques (Firth *et al.*, 2008a, Ray *et al.*, 2007, Adachi *et al.*, 2007).

1.3.4 The antioxidant effect of 7,8-dihydroneopterin

It is possible that micro-molar concentrations of 7,8-dihydroneopterin are capable of exerting a biological effect on oxidative processes (Firth *et al.*, 2008b). This and other laboratories have reported that 7,8-dihydroneopterin was relatively a good antioxidant and inhibitor of oxidant-induced cell death when added at low micro-molar concentrations to cell culture media (Duggan *et al.*, 2002, Gieseg *et al.*, 1995). 7,8-Dihydronepterin has a protective effect against oxidant damage on cells, cellular membranes, free proteins, cellular protein and protein thiol (Gieseg *et al.*, 2000, Gieseg *et al.*, 2001b, Duggan *et al.*, 2002, Gieseg *et al.*, 2008). The protective effect of 7,8-dihydronepterin is due to the potent radical-scavenging ability of 7,8-

dihydronepterin with peroxyl radical ($ROO^{\bullet}$), $O_2^{\bullet-}$ and HOCl (Duggan *et al.*, 2002, Oettl *et al.*, 1997).

In *vitro*, it was shown that 7,8-dihydroneopterin neutralised lipid peroxyl radicals, inhibited copper, 2,2'-azobis (2-amidinopropane) hydrochloride (AAPH) and cell-mediated LDL oxidation (Gieseg *et al.*, 2003, Gieseg *et al.*, 1995).

It has been hypothesised that in *vivo*, this may slow the rate of LDL oxidation, therefore lowering the concentration of oxLDL within plaques (Gieseg *et al.*, 1995, Gieseg *et al.*, 2003, Gieseg & Cato, 2003, Firth *et al.*, 2007b). In U937 cells but not in THP-1 cells, 7,8-dihydroneopterin was shown to inhibit the cytotoxicity of oxLDL, possibly by preventing the loss of the intracellular antioxidant GSH by scavenging ROS generated in the presence of oxLDL (Baird *et al.*, 2005). 7,8-Dihydroneopterin has been shown to inhibit oxLDL-induced loss of GSH and cell death in HMDM cells in this laboratory (Gieseg *et al.*, 2010, Amit, 2008). 7,8-dihydroneopterin was unable to reduce the oxidised protein thiol and it is unlikely that 7,8-dihydroneopterin can regenerate or increase the intracellular GSH levels (Duggan *et al.*, 2002).

Micro-molar concentrations of 7,8-dihydroneopterin protect U937 but not THP-1 (Baird *et al.*, 2005, Duggan *et al.*, 2002) or HMDM cells (Firth *et al.*, 2007b) from AAPH-derived peroxyl radicals (Gieseg *et al.*, 2000). The reason for this was initially thought to be due to the poor uptake of 7,8-dihydroneopterin in HMDM cells but these cells have been shown to readily take up the 7,8-dihydroneopterin (Gieseg *et al.*, 2010). The reason for these differences in protection is still being investigated and may be due to the speed at which oxidative stress occurs in these cells.

7,8-Dihydroneopterin has been shown to protect U937 cells from a number of other oxidants including H_2O_2, HOCl and free iron ions, which reduce cell viability loss as well as protein and lipid hydroperoxide formation (Gieseg *et al.*, 2001b, Duggan *et al.*, 2001). TNF-α-induced apoptosis in U937 cells is also inhibited by 7,8-dihydroneopterin (Baier-Bitterlich *et al.*, 1995).

1.3.5 The effect of other antioxidants on oxLDL induced cell death

It has been shown in animal models that the extent and progression of atherosclerotic plaques is decreased by the administration of antioxidants. Cardiovascular disease is also associated with low plasma concentrations of ascorbate, tocopherol and β–carotene (Gey *et al.*, 1991). The modification of LDL to oxLDL in atherosclerotic plaques by macrophages can be inhibited by antioxidants such as α-tocopherol (vitamin E) (Morel *et al.*, 1983, Steinbrecher *et al.*, 1984). α-Tocopherol inhibited oxLDL-induced apoptosis in mouse mesangial cells (Tashiro *et al.*, 1999) and in SMCs (Guyton *et al.*, 1995). Treatment of HASMCs with water-soluble γ-tocopherol derivative (6-hydroxy-2,5,7,8-tetramethylchroman-2-carboxylic acid, Trolox), suppressed oxLDL-specific increase in ROS and prevented down-regulation of GAPDH (Sukhanov *et al.*, 2006). In human coronary artery endothelial cells (HCAECs), γ-tocopherol significantly decreased oxLDL-induced apoptosis by inhibiting the activation of nuclear factor kappa-light-chain-enhancer of activated B cells (NF-kB) (Li *et al.*, 1999). Interestingly, α-tocopherol supplementation of HMDM cells did not prevent foam cell formation or alter the susceptibility of foam

cells to lysis by oxLDL (Asmis & Jelk, 2000b) suggesting that plasma membrane oxidation is not a significant factor in oxLDL toxicity. Additionally, other antioxidants such as GSH and vitamin C can also inhibit LDL oxidation (Siow *et al.*, 1998, Lizard *et al.*, 2000). Copper-induced LDL oxidation is inhibited by vitamin C (L-ascorbic acid, AA) and dehydro-L-ascorbic acid (DHAA), the oxidative product of vitamin C (Retsky *et al.*, 1999). Results with ascorbic acid inhibition of oxLDL have been rather inconsistent. Ascorbate gave almost complete inhibition of apoptosis in human ECs (Dimmeler *et al.*, 1997). Ascorbic acid also protected human vascular smooth muscle cells (HVSMCs) against apoptosis induced by "moderately oxidised LDL" which contained high levels of lipid hydroperoxides (Siow *et al.*, 1999). However, later the same laboratory reported that ascorbic acid did not protect the murine macrophage cell line J774 against moderately oxidised LDL, but produced a modest increase in apoptosis (Harris *et al.*, 2006). Detoxification of oxLDL by DHAA but not ascorbic acid and isoascorbic acid completely inhibited apoptosis induced by oxLDL. In contrast to oxLDL treated with ascorbic or isoascorbic acid, thiobarbituric acid reactive substances (TBARS) levels and lipid peroxide levels of oxLDL treated with DHAA were not substantially reduced. This suggests that reduction of oxLDL is an unlikely mechanism for the inhibition of oxLDL-induced apoptosis by DHAA. There is a possibility that the inhibitory effect of DHAA is due to it reacting with reactive groups within apoB100 (Asmis & Wintergerst, 1998).

Results with butylated hydroxytoluene (BHT) were also varied. BHT has no protective effect against oxLDL induced death of rabbit aortic smooth muscle cells (RASMCs) (Liu *et al.*, 1998), but gave partial protection in SMCs (Guyton *et al.*,

1995) and gave complete protection to human umbilical vein endothelial cells (HUVECs) (Harada-Shiba *et al.*, 1998). BHT also blocked oxLDL-induced apoptosis of mouse peritoneal macrophages (Niu *et al.*, 1996).

Antioxidant thiols could also prevent oxLDL-induced apoptosis. N-Acetylcysteine (NAC) as well as GSH were successful in protecting mouse vascular smooth muscle cells (MVSMCs) (Hsieh *et al.*, 2001) and mesanglia cells with oxLDL (Tashiro *et al.*, 1999). Also, NAC and GSH have been reported to inhibit oxLDL- and 7-ketocholesterol-induced apoptosis by increasing the intracellular thiol pool in macrophages and U937 cells (Kinscherf *et al.*, 1998, Lizard *et al.*, 2000).

Increases in putative cystine protease (CPP32-like) activity triggered by oxLDL were drastically reduced by NAC, vitamin C and α-tocopherol. The decreased CPP32-like protease activity correlated with a reduction in proteolytic cleavage of the CPP32 into the active p17 subunit and therefore, probably inhibits apoptosis through inhibition of caspase-3 activation (Dimmeler *et al.*, 1997).

In *vitro*, LDL oxidation has been shown to be suppressed by several garlic compounds (Lau, 2006). Pomegranate juice inhibits oxLDL uptake and cholesterol biosynthesis in macrophages, which leads to a reduction in cellular cholesterol accumulation and macrophage foam cell formation (Fuhrman *et al.*, 2005).

Serum albumin, which is the most abundant circulating protein in the plasma constitutes the major plasma protein target of oxidant stress (Roche *et al.*, 2008). In *vitro*, albumin acts as a multifaceted antioxidant. Albumin binds fatty acids and

protects them from oxidation; binds copper, cysteine, GSH, bilirubin and pyridoxal-5'-phosphate and in doing so protects them from oxidation (Kouoh *et al.*, 1999). The presence of serum has been shown to protect macrophages cells against the cytotoxic effects of oxLDL (Leake & Rankin, 1990, Henriksen *et al.*, 1979).

1.4 Metabolic functions of the cell

One of the most basic functions of a cell is energy release. Cell viability assays like the thiazolyl blue tetrazolium bromide (MTT) reduction assay essential measure cell viability by the activity of the metabolism. In the case of the MTT assay this is a measure of the cells ability to maintain a reductive level of nicotinamide adenine dinucleotide phosphate (NADPH) and nicotinamide adenine dinucleotide (NADH). The loss of metabolism is therefore both a cause and consequence of cell death. This research will be examining cell metabolism failure as a cause of macrophage cell death following exposure to oxLDL. To reliably measure cell metabolism we have focussed on key enzymes and products of glycolysis in the cells.

1.4.1 Lactate

Lactate is synthesised from the pyruvic acid derived from glycolysis. Under hypoxic conditions the animal cells will regenerate nicotinamide adenine dinucleotide (NAD^+) from NADH by the reduction of pyruvate to lactate, which is catalysed by lactate dehydrogenase (LDH) enzyme. Some tissues and cell types, which have no mitochondria and thus cannot oxidise pyruvate to carbon dioxide (CO_2), produce lactate from glucose even under aerobic conditions. The resulting lactate is mainly utilised in the liver and the kidney. During starvation and strenuous muscular activity,

lactate can also serve as one of the gluconeogenic precursors. The rate of lactate synthesis is dependent on the activity of the glycolytic pathway relative to the oxidative capacity of the pyruvate dehydrogenase enzymatic complex. An acceleration of lactate synthesis may be observed in conditions of increased glucose uptake from circulation, of increased glycogenolysis and glycolysis due to enhanced epinephrine secretion, of inhibition of pyruvate dehydrogenase or of glycogen synthesis in sepsis and, finally, during tissue hypoxia (Nelson & Cox, 2005). Lactate measurement of cells such as macrophages therefore represents a very basic measure of overall glycolytic flux within a cell.

Lactate, which is present in biological fluids as its dissociated canionic form, is widely distributed among the pathways involved in the intermediary metabolism of living systems. While, from the physiologists' point of view, it is one of the most crucial intermediates of carbohydrate metabolism, for most physicians, it is merely considered a marker of bad prognosis significantly related to a high mortality rate in acutely ill patients (Bakker *et al.*, 1991, Marecaux *et al.*, 1996). The concentration of blood lactate is usually 1–2 mmol/L at rest, but can rise to over 20 mmol/L during intense exertion. The increased lactate that is produced can be removed by oxidation to pyruvate for use in the Krebs cycle in the mitochondrion matrix, or by conversion to glucose via gluconeogenesis in the liver before being released back into the circulation, otherwise known as the Cori cycle (Nelson & Cox, 2005). It is known that the blood lactate concentration is increased in patients with obesity, hypertension, and type 2 diabetes mellitus (non-insulin-dependent) (Digirolamo *et al.*, 1992). The lactate level is also elevated locally in tissues suffering injury, infection,

inflammation or ischemia. This is probably due to increased tumour necrosis factor secretion and transcription during lactic acidosis (Jensen *et al.*, 1990). Although tissue hypoxia plays a role in the elevation of lactate concentration, the high activity of anaerobic glycolysis in activated macrophages and adipose tissue can also lead to high lactate production (Digirolamo *et al.*, 1992, Beckert *et al.*, 2006). Lactate has been shown to be not only an important intermediary in metabolic processes, but also an active player in inflammation (Iscra *et al.*, 2002, Hunt *et al.*, 1978, Mustafa & Leverve, 2002). Lactate enhances lipopolysaccharide (LPS)-stimulated cytokine expression by macrophages, indicating that lactate promotes the innate immune activation (Nareika *et al.*, 2005). It is known that bacterial infection and LPS lead to increased lactate production (Jensen *et al.*, 1990, Tsai *et al.*, 2005). Elevated plasma lactate is also a marker for cellular stress (Miller *et al.*, 2007). Lactate increased ROS production and upregulated 673 genes in L6 myogenic cells; many known to be responsive to ROS (Hashimoto *et al.*, 2007). Lactate and ROS boosted LPS signalling-mediated inflammatory gene expression. Lactate and LPS promotes TLR4-mediated inflammation and contributes to a number of diseases, including type 2 diabetes and cardiovascular disease (Samuvel *et al.*, 2009). Extracellular lactate in wounds stimulates macrophages to secrete vascular endothelial growth factor and TGF-β, both known to be immunosuppressive factors (Trabold *et al.*, 2003). Pre-incubation of myeloid U937 and HMDM cells with lactate increases the expression of inflammatory cytokines, IL-6 and IL-8 (Samuvel *et al.*, 2009). It was also shown that low pH environment and high concentration of lactate in peritoneal dialysis fluids inhibits macrophage/monocyte IL-1 β and TNF-α (Douvdevani *et al.*, 1993). Lactate

can have opposing effects on the activation of different types of immune cells. Tumour environment have low pH (Gatenby & Gillies, 2004) due to accumulation of lactate as a result of accelerated glycolysis. Lactate upregulates transcription and secretion of IL-23, a tumour-promoting cytokine, in human monocytes (Shime *et al.*, 2008). Tumour-derived lactate strongly inhibits both the differentiation of monocytes to DCs (Dietl *et al.*, 2010, Gottfried *et al.*, 2006) and the activation of T cells (Fischer *et al.*, 2007). TNF-α secretion of monocytes depends on both glycolysis and export of its end product lactate. Monocytes take up extracellular lactate, which results in a decreased glycolytic flux and an inhibition of TNF-α release. Tumour-derived lactate and concomitant acidification could modulate and disturb monocyte cytokine production by blocking lactate export and glycolytic flux. Impairment of glycolysis may contribute to the immunosuppressive effects of lactate in wounds and tumours (Dietl *et al.*, 2010).

1.4.2 Lactate dehydrogenase enzyme

Lactate dehydrogenase (LDH) catalyses the reaction that transforms pyruvic acid into lactate (under anaerobic conditions) in many cells, and vice versa, transforming lactate into pyruvic acid under aerobic conditions. The essential coenzyme for this reaction is NAD^+ which is converted to NADH. LDH is found in many human tissues, and is found in the greatest concentration in kidneys, myocardial, skeletal muscles and liver. Within cells it is located in the cytoplasm. Its concentration in serum and other tissue fluids is lower than in body tissues. There are at least five different LDH isoenzymes (LDH_1-LDH_5) (Bansal & Kaw, 1981, Jovanovic *et al.*,

2010, Barrett *et al.*, 1988) separable by electrophoresis. LDH_1 founded in the heart and red blood cells, LDH_2 in the reticuloendothelial system LDH_3 in the lungs, LDH_4 in the kidneys, placenta, and pancreas, LDH_5 in the liver and striated muscle (Nelson & Cox, 2005). LDH_1 is called α-hydroxybutyrate dehydrogenase (HBDH) (Barrett *et al.*, 1988). The extracellular activity of this intracellular enzyme increases under the conditions of oxidative stress, due to the loss of integrity of the cell membrane in the course of lipid peroxidation by the influence of free radicals. This leads to an increase in lactate concentration (Jovanovic *et al.*, 2010). Accumulation of lactate in myocardial cells has been proposed as a primary trigger of ischemic damage in the heart (Geisbuhler & Rovetto, 1990). Damage to heart tissues results in the release of LDH into the blood and the differences in the isoenzyme content of tissues can be used to assess the timing and extent of heart damage.

The release of LDH is also used as a marker of cell lysis and therefore loss of cell viability (Legrand, 1992). Measurement of lactate production in cells where cell death is occurring need to take into accounts this possible loss of LDH activity from the cells. Unlike the glycolytic enzyme GAPDH to be discussed below, LDH has not been reported to be sensitive to inactivation by general intracellular oxidative stress mediated by $O_2^{\bullet -}$, H_2O_2 or $ROO^{\bullet}$ though it is likely that HOCl will inactivate the enzyme.

1.4.3 Glyceraldehydes-3-phosphate dehydrogenase enzyme

Glyceraldehydes-3-phosphate dehydrogenase (GAPDH) is an enzyme that catalyses the sixth step of glycolysis. In the cytosol, GAPDH catalyes the oxidation of

glyceraldehyde-3-phosphate (GAP) to 1, 3-diphospho-glycerate (1, 3-PGA) with the conversion of NAD^+ to NADH. NADH must be re-oxidised to keep the glycolytic pathway supplied with NAD^+. Usually this oxidation happens within the mitochondria to produce adenosine triphosphate (ATP) (Nelson & Cox, 2005). GAPDH, therefore, maintains glycolysis and provides substrates for the Krebs cycle and electron transport chain (ETC) during the metabolism of sugars (Nelson & Cox, 2005, Yamaguchi *et al.*, 2003).

The molecular mass of the GAPDH enzyme is 36 kDa (Torchinsky, 1981) and is made up of two domains; one of the domains binds NAD^+ and the second domain binds GAP (Yamaguchi *et al.*, 2003). The loss of GAPDH activity in the cell can be partly attributed to the loss of NAD^+, a cofactor required for the activity of GAPDH (Schraufstatter *et al.*, 1990). The types of GAPDH can be differentiated by their cysteine residue active site and GAPDH reversibility and irreversibility.

The GAPDH molecule has four cysteine residues (Cys^{149}, Cys^{153}, Cys^{244} and Cys^{281}) (Nakajima *et al.*, 2007) that contain sulfhydryl (-SH) groups. Cys^{149} and Cys^{153} are essential for GAPDH catalytic activity and sensitive to thiol modification and oxidation (Schuppe-Koistinen *et al.*, 1994). In rat GAPDH the -SH group of Cys^{150} is essential for its catalytic activity (Hara *et al.*, 2006). The cysteine thiol group is sensitive to oxidants as detected by fluorescence labelling (Baty *et al.*, 2002) and can be oxidised to sulfenic (-SOH), sulfinic ($-SO_2H$) and sulfonic ($-SO_3H$) acids, S-nitrosothiols (-SNO) and disulfides (R-S-S-R) (Cuddihy *et al.*, 2009b, Sukhanov *et al.*, 2006, Pullar *et al.*, 2000, Albina *et al.*, 1999).

Reversible GAPDH enzyme inhibition is mediated by S-nitrosylation of its active site Cys^{149} (Mohr *et al.*, 1996). S-Nitrosylation modification protects thiol-containing enzymes such as GAPDH from oxidative inactivation in settings of cytokine overproduction and regulates glycolysis, seen in cellular systems activated with inflammatory cytokines (Horton *et al.*, 1994). In contrast, irreversible enzyme inhibition in some cellular systems (Molina Y Vedia *et al.*, 1992) is likely to be explained by covalent attachment of NADH. This modification is more likely to be a pathophysiological event associated with inhibition of gluconeogenesis.

In nitric oxide-producing rat peritoneal macrophages, NO inhibits GAPDH activity and decreases ATP content, synthesis and turnover by uncoupling of glycolytic flux from substrate level phosphorylation by the acyl phosphatase activity of NO-modified GAPDH (Albina *et al.*, 1999). In HUVECs, GAPDH can be inhibited by S-thiolation after H_2O_2 treatment, which is reversed upon removal of the oxidative stimulus (Schuppe-Koistinen *et al.*, 1994). The post-translational modification of GAPDH by reversible thiol redox reactions with GSH may represent a physiologically relevant mechanism for the control of the enzyme in HUVECs (Schuppe-Koistinen *et al.*, 1994). NO has been shown to react with the four thiols of each of the GAPDH tetramer. This reaction of NO causes a decrease in GAPDH activity as the modified thiol group in the active site of GAPDH is converted to sulfenic acid. This inhibition cannot be reversed by dithiothreitol (DTT). GAPDH activity is inhibited also by NO donors such as sodium nitroprusside (SNP), and S-nitroso-N-acetyl-DL-penicillamine (SNAP). SNAP but not SNP modifies the active site thiol via process called S-nitrosylation which can be reversed by treating with DTT after the SNAP treatment.

The DTT prevents the thiol from oxidising to sulfenic acid (Ishii *et al.*, 1999). NADH and DTT are required for the S-nitrosylation of GAPDH caused by the NO-generating compound sodium nitroprusside. S-Nitrosylation of GAPDH may be a key covalent modification of multiple regulatory consequences in chronic liver inflammation (Molina Y Vedia *et al.*, 1992). In macrophage cells, NO gas has been shown to inhibit of lactate production due to NO-modified GAPDH and also inactivate the Krebs cycle enzyme aconitase (Messmer *et al.*, 1996). In the colon, epithelial cells of patients with inflammatory bowel disease, NO and ROS-mediated oxidation of GAPDH thiol has been reported resulting in GAPDH inactivation (Mckenzie *et al.*, 1996).

OxLDL has been shown to cause increased ROS formation, including rapid elevation of H_2O_2. OxLDL has been shown to induce the down-regulation of GAPDH via a H_2O_2-dependent mechanism resulting in inhibition of glycolysis and marked depletion of cellular ATP levels in HASMCs (Sukhanov *et al.*, 2006) and in U937 cells (Colussi *et al.*, 2000). OxLDL down-regulated-GAPDH appears to play an important role in the mechanisms of atherogenesis (Sukhanov *et al.*, 2006). In U937 cells, GAPDH is also inhibited by HNE and 4-hydroxy-2-hexenal (HHE), which are produced during the oxidative modification of LDL (Tsuchiya *et al.*, 2005).

1.5 Research programme

1.5.1 Aim

The major aim of this PhD research is to determine the effect of oxidised low-density lipoproteins (oxLDL) on macrophage cell metabolic functions using U937 cells and human monocyte-derived macrophage (HMDM) cells.

1.5.2 Hypothesis experimental approach

The central hypothesis to this research was that oxLDL induced cell death in macrophages was due to the oxidative loss of glycolysis activity as a result of the oxidative inactivation of glyceraldehyde-3-phosphate dehydrogenase (GAPDH).

In chapter 3, initial characterisation of oxLDL and its effect on both U937 and human monocyte derived macrophage (HMDM) on both cell morphology and viability was characterised and standardised for further experimentation on GAPDH and the relationship to cell death. The protective effect of the antioxidant 7,8-dihydroneopterin was also characterised to establish appropriate concentrations and incubation times for further analysis. Much of this analysis was aimed at extending and confirming the studies of previous researchers within the laboratory.

Chapter 4 will examine the effect of oxLDL on U937 cell metabolism by measuring lactate production and the activity of lactate dehydrogenase (LDH) and GAPDH. The loss of these enzyme activities will be related in time and oxLDL concentration to the changes in cell glutathione (GSH) level and adenosine triphosphate (ATP) formation. The oxidative inhibition of GAPDH will be confirmed by sodium dodecyl sulfate

polyacrylamide gel electrophoresis (SDS-PAGE) analysis of changes in thiol oxidation states of GAPDH. The effectiveness of intracellular reactive oxygen species (ROS) scavenging by 7,8-dihydroneopterin (7,8-NP) will be further quantified by measuring the protection of cell metabolism from oxLDL inhibition. Changes in metabolic function will be further characterised by measuring changes in the rate of oxygen consumption (VO_2) following the addition of oxLDL and the protection of metabolism by 7,8-dihydroneopterin.

Chapter 5 will examine the same glycolytic metabolic markers as the study with the U937 cells using the clinically more relevant HMDM cells. This will provide some validation to the effects observed in U937 cells. However, VO_2 will not be studied due to the difficultly of culturing the strongly adherent HMDM cells in the oxygen sensing ringers of the chamber of the respirometers. The effect of 7,8-dihydroneopterin in protecting HMDM cell metabolism will be quantified and compared to that observed in U937 cells. The uptake of oxLDL by HMDM cells and the effect of 7,8-dihydroneopterin on this uptake is examined to observe whether oxLDL uptake is critical to the loss in cell viability.

This study will provide strong evidence that oxLDL triggers a rapid cell death mechanism resulting in necrosis, by causing oxidative inactivation of glycolysis and specifically, GAPDH activity. The resulting loss of ATP generation is proposed to lead to a systematic failure of cellular function leading to cell necrosis. The study also shows clearly how the protection of the cellular GSH levels by 7,8-dihydroneopterin prevents the loss of GAPDH activity. This work provides an alternative mechanism

to that proposed by others where specific oxysterols causes activation of apoptopic mechanism causing cell death within the atherosclerotic plaque.

2 Materials and methods

2.1 Materials

2.1.1 Reagents and media

All reagents and media used were of analytical grade or better (Table 2.1 and Table 2.2). All solutions were prepared using ion-exchanged ultra filtered water, obtained using a nanopure ultrapure water system from Barnstead/Thermolyne (IA/USA).

Table 2.1 Names of chemicals and suppliers.

Chemical Name/Abbreviations/Formula/MW in g/mol	Company/ Supplier
β-Mercaptoethanol (C_2H_6OS) (MW 78.13)	Sigma Chemical Co., St. Louis, USA/ NZ Sigma
1,1'-Dioctadecyl-3,3,3',3'-tetramethylindo carbocyanine perchlorate (DiI) (MW 5341)	Sigma-Aldrich Chemical Co., Wisconsin, USA/ NZ Sigma-Aldrich
1,1,3,3-Tetramethoxypropane (TMP) $(CH_3O)_2CHCH_2CH(OCH_3)_2$ (MW 164.2)	Sigma Chemical Co., Missouri, USA/ NZ Sigma
2-Thiobarbituric acid (TBA) ($C_4H_4N_2O_2S$) (MW 144.15)	Merck, Darmstadt, Germany/ NZ Merck
3-[(3Cholamidopropyl) dimethylammonio]-1-propanesulfonate (CHAPS) ($C_{32}H_{58}N_2O_7S$) (MW 614.9)	Sigma-Aldrich Chemical Co., Missouri, USA/ NZ Sigma-Aldrich
4-Morpholine-propanesulfonic acid (MOPS) ($C_7H_{15}NO_4S$) (MW 209.3)	Sigma Chemical Co., Missouri, USA/ NZ Sigma
5-(Iodoacetamido) flurescein (5-IAF) ($C_{22}H_{14}INO_6$) (MW 515.26)	Molecular Probes, Eugene, Oregon, USA/ NZ Global
7,8-Dihydroneopterin (7,8-NP) (MW 255.2)	Schircks Laboratory, Switzerland/ NZ Schircks laboratory

Chemical Name/Abbreviations/Formula/MW in g/mol	Company/ Supplier
Acetic acid (CH_3COOH) (MW 60.05)	Merck Ltd, Poole, England/ NZ Merck
Acetone (CH_3COCH_3) (MW 58.08)	Merck Ltd, Poole, England/ NZ Merck
Acetonitrile (Acn) (CH_3CN) (MW 41.05)	Merck, Darmstadt, Germany/ NZ Merck
Adenosine diphosphate (ADP) (MW 427.2)	Sigma-Aldrich Chemical Co., Missouri, USA/ NZ Sigma-Aldrich
Adenosine monophosphate (AMP) (MW 347.2)	Sigma-Aldrich Chemical Co., Missouri, USA/ NZ Sigma-Aldrich
Adenosine triphosphate (ATP) (MW 551.14)	Sigma-Aldrich Chemical Co., Missouri, USA/ NZ Sigma-Aldrich
Argon gas	BOC Gasses; Auckland, NZ
Bicinchoninic acid (BCA) protein kit	Pierce, Illinois, USA/ NZ Global
Butylated hydroxytoluene (BHT) ($C_{15}H_{24}O$) (MW 220.4)	Sigma Chemical Co., Missouri, USA/ NZ Sigma
Bovine serum albumin (BSA)	Sigma Chemical Co., Missouri, USA/ NZ Sigma
Bromophenol blue (MW 670.02)	Sigma Chemical Co., Missouri, USA/ NZ Sigma
Chelex 100 resin	Bio-Rad Laboratories, California, USA/ NZ Global
Cholesterol reagent	Roche Diagnostics GmbH, Mannheim, Germany/ NZ Global
Copper chloride (Cu_2Cl) (MW 170.48)	AnalaR®, B.D.H. Laboratory Chemicals Division Poole, England/ NZ Biolab
Coumassie blue	Bio-Rad Laboratories, California, USA/ NZ Global
Dialysis tubing	Biolab Scientific, Auckland, NZ
Dimethyl sulphoxide (DMSO) $(CH_3)_2SO$ (MW 78.18)	AnalaR®, B.D.H. Laboratory Chemicals Division Poole, England/ NZ Biolab

Chemical Name/Abbreviations/Formula/MW in g/mol	Company/ Supplier
Ethanol (C_2H_5OH) (MW 46.07)	Merck, Darmstadt, Germany/ NZ Merck
Ethylene diamine tetraacetic acid (EDTA) ($C_{10}H_{16}N_2O_8$) (MW 292.24)	AnalaR®, B.D.H. Laboratory Chemicals Division Poole, England/ NZ Biolab
Ethlylene glycol-bis(2-aminoethylether) N,N,N',N'-tetracetic acid (EGTA) (-$CH_2OCH_2CH_2N(CH_2CO_2H)_2)_2$ (MW 380.4)	Sigma Chemical Co., Missouri, USA/ NZ Sigma
Glyceraldehyde-3-phosphate (GAP) (MW 170.6)	Sigma Chemical Co., Missouri, USA/ NZ Sigma
Glyceraldehyde-3-phosphatedehydrogenase (GAPDH), marker from rabbit muscle (36 kDa)	Sigma Chemical Co., Missouri, USA/ NZ Sigma
Glycerol ($C_3H_8O_3$) (MW 92.10)	Sigma Chemical Co., Missouri, USA/ NZ Sigma
Glycine ($C_2H_5NO_2$) (MW 75.07)	Bio-Rad Laboratories, California, USA/ NZ Global
Glutathione (reduced form) (GSH) (MW 307.3)	Sigma Chemical Co., Missouri, USA/ NZ Sigma
Hexane 85% ($CH_3(CH_2)_4CH_3$) (MW 86.18)	Merck, Darmstadt, Germany/ NZ Merck
Hydroxy ethyl prazine ethane sulphonic acid (HEPES) ($C_8H_{18}N_2O_4S$) (MW 238.3)	Sigma Chemical Co., Missouri, USA/ NZ Sigma
Hydrochloric acid (HCl) (MW 36.46)	Merck, Darmstadt, Germany/ NZ Merck
Isopropanol ($CH_3CHOHCH_3$) (MW 60.1)	J.T. Baker, New Jersey, USA/ NZ Merck
Lactic acid kit	Roche, Darmstadt, Germany/ NZ Global
Malondialdehyde (MDA) ($CH_3H_4O_2$) (MW 72.06)	Sigma Chemical Co., Missouri, USA/ NZ Sigma
Methanol (CH_3OH) (MW 32.04)	Merck, Darmstadt, Germany/ NZ Merck
Molecular Weight Proteins Marker	Fermentas International Inc, Ontario, Canada/ NZ Global

Chemical **Name/Abbreviations/Formula/MW in g/mol**	**Company/ Supplier**
Monobromobimane (MBB) ($C_{10}H_{11}BrN_2O_2$) (MW 271.1)	Sigma-Aldrich, Steinheim, Switzerland/ NZ Sigma-Aldrich
Nicotinamide adenine dinucleotide (NAD^+) (MW 663.43)	Sigma Chemical Co., Missouri, USA/ NZ Sigma
Nicotinamide adenine dinucleotide (Reduced form) (NADH) (MW 709.4)	Sigma Chemical Co., Missouri, USA/ NZ Sigma
Nicotinamide adenine dinucleotide phosphate ($NADP^+$) (MW 743.4)	Sigma Chemical Co., Missouri, USA/ NZ Sigma
Nitrogen gas	BOC Gasses, Auckland, NZ
NuPAGE 4-12 % Bis-Tris Gel, 1.0 mm x 10 well	Invitrogen, California, USA/ NZ Invitrogen
Perchloric acid (PCA) ($HClO_4$) (MW 100.46)	AnalaR®, B.D.H. Laboratory Chemicals Division Poole, England/ NZ Biolab
Phosphoric acid 85% (H_3PO_4) (MW 97.994) (1L=1.71kg)	Merck, Darmstadt, Germany/ NZ Merck
Potassium bromide (KBr) (119.01)	Merck, Darmstadt, Germany/ NZ Merck
Potassium carbonate (K_2CO_3) (MW 138.21)	Merck, Darmstadt, Germany/ NZ Merck
Protease inhibitors	Roche, Mannheim, Germany/ NZ Global
Pyruvate ($C_3H_4O_3$) (MW 88.06)	Sigma Chemical Co., Missouri, USA/ NZ Sigma
Sodium arsenate ($Na_2H_2AsO_4.7H_2O$) (MW 312.01)	AnalaR®, B.D.H. Laboratory Chemicals Division Poole, England/ NZ Biolab
Sodium chloride (NaCl) (MW 58.44)	Merck, Darmstadt, Germany/ NZ Merck
Sodium dihydrogen orthophosphate ($NaH_2PO_4H_2O$) (MW 137.99)	Merck, Darmstadt, Germany/ NZ Merck
Sodium dodecyl sulfate (lauryl sulfate) (SDS) (MW 288.38)	Sigma-Aldrich Chemical Co., Missouri, USA/ NZ Sigma-Aldrich

Chemical Name/Abbreviations/Formula/MW in g/mol	Company/ Supplier
Sodium hydrogen carbonate ($NaHCO_3$) (MW 84.01)	Sigma Chemical Co., Missouri, USA/ NZ Sigma
Sodium hydroxide (NaOH) (MW 39.9971)	Merck, Darmstadt, Germany/ NZ Merck
Tetrabutylammonium bisulfate ($C_{16}H_{37}NO_4S$) (MW 339.54)	Merck, Darmstadt, Germany/ NZ Merck
Thiazolyl blue tetrazolium bromide (MTT) ($C_{18}H_{16}N_5SBr$) (MW 414.33)	Sigma-Aldrich Chemical Co., Missouri, USA/ NZ Sigma-Aldrich
Trichloroacetic acid (TCA) (CCl_3COOH) (MW 163.39)	Merck, Darmstadt, Germany/ NZ Merck
Tris(hydroxymethyl)aminomethane (Tris) ($C_4H_{11}NO_3$) (MW 121.1)	Roche Diagnostics GmbH, Mannheim, Germany/ NZ Global
Triton X-100	AnalaR®, B.D.H. Laboratory Chemicals Division Poole, England/ NZ Biolab
Trypan blue solution (0.4 %)	Sigma-Aldrich Chemical Co., Missouri, USA/ NZ Sigma-Aldrich

Table 2.2 Chemicals and suppliers of cell culture media.

Chemical	Company/ Supplier
Granulocyte macrophage colony stimulating factor (GM-CSF)	Bayer Health Care Pharmaceuticals, LLC. Seattle, WA/ Shipping to NZ
Heat-inactivated foetal calf serum	Invitrogen, California, USA/ NZ Invitrogen
Penicillin/streptomycin (containing 5000 units of penicillin and 5000 μg of streptomycin/ml)	Invitrogen, California, USA/ NZ Invitrogen
Roswell Park Memorial Institute-1640 (RPMI-1640) media, with phenol red	Sigma-Aldrich Chemical Co., Missouri, USA/ NZ Sigma-Aldrich
Roswell Park Memorial Institute-1640 (RPMI-1640) media, without phenol red	Sigma-Aldrich Chemical Co., Missouri, USA/ NZ Sigma-Aldrich

2.1.2 General buffers, media and solutions

2.1.2.1 Phosphate buffered saline

Phosphate buffered saline (PBS) was prepared by adding 150 mM sodium chloride (NaCl, MW 58.44) to 10 mM sodium dihydrogen orthophosphate ($NaH_2PO_4H_2O$, MW 137.99), pH 7.4. It was stirred with 1 g of washed Chelex 100 resin for at least 4 hours to remove metal ions. Subsequently, it was vacuum-filtered through a 0.45 µm Phenex filter membrane (Phenomenex). PBS used for cell culture work was autoclaved for 15 minutes, at 121°C and 15 psi.

2.1.2.2 Roswell park memorial institute media-1640

The Roswell park memorial institute-1640 (RPMI-1640) media was prepared as per the manufacturer's instructions. Powdered RPMI-1640 (with or without phenol red) was dissolved in nanopure water, then sodium hydrogen carbonate ($NaHCO_3$) was added and the solution adjusted to pH 7.4 with 1 M sodium hydroxide (NaOH). The media was put into sterile bottles in a Class II biological safety cabinet (Clyde-Apex BH 200) and was sterilised using a peristaltic pump (CP-600, Life Technologies, Maryland, USA) and a 0.2 µm Millex®-GP_{50} filter (Sartorius AG, Goettingen, Germany). The media was stored at 4°C.

2.1.2.3 7, 8-Dihydroneopterin solution

7,8-Dihydroneopterin (7,8-NP, MW 255.2) was prepared fresh prior to each experiment. The stock concentration was 2 mM, which was dissolved in a degassed ice cold RPMI-1640 medium followed by 5 minute sonication. The 7,8-dihydroneopterin stock solution

was sterilised by filtering through a 0.22 μm membrane filter with 25 mm diameter (Sartorius AG, Goettingen, Germany) in a Class II biological safety cabinet (Clyde-Apex BH 200).

2.1.2.4 Determination of protein concentration

Protein concentration was determined using the bicinchoninic acid (BCA) protein determination kit from Pierce (supplied by Global Scientific). The working reagent was freshly prepared by mixing Reagent A (sodium carbonate (Na_2CO_3), $NaHCO_3$, BCA and sodium tartrate ($Na_2C_4H_4O_6$) in 0.1 M NaOH) and Reagent B (4% copper sulfate pentahydrate, $CuSO_4.5H_2O$) in a 50:1 ratio. The assay was carried out by mixing 50 μl of cell suspension with 1 ml of working reagent and incubated at 60°C for 30 minutes while being gently shaken in a heated shaking block. The reaction was subsequently stopped by placing samples on ice before reading the absorbance at 562 nm against the water blank. Protein concentration was determined from a standard curve prepared by the incubation of known concentrations of BCA (0-250 μg/ml) in 1 ml of working reagent.

2.2 Methods

Experiments were carried out on the U937 monocyte-like cell line and human monocyte-derived macrophage (HMDM) cells. The cells were incubated with and without oxidised low density lipoprotein (oxLDL) to determine its effect on cells' metabolic function along with 7,8-dihydroneopterin (7,8-NP) production.

2.2.1 Cell culture

Cells were manipulated for experiments under aseptic conditions in a Class II biological safety cabinet (Clyde-Apex BH 200). Sterile plasticware was supplied by Becton Dickinson & Co., Falcon, Nunc, Terumo, Unomedical, and Greiner Bio-one. Media and solutions were sterilised either by autoclaving or by filtration through a sterile membrane filter, or both. All equipment for cell culture experiments was sprayed with 70% (v/v) ethanol before being transferred into the Class II biological safety cabinet.

Experiments were conducted on both the U937 and HMDM cells. The cells were incubated at 37°C in a humidified incubator, with an atmosphere calibrated to 5% carbon dioxide: 95% air (Nuaire™ IR Autoflow).

2.2.1.1 Cell culture media

RPMI-1640 medium (with phenol red) (see section 2.1.2.2) containing 100 U/ml penicillin-G and 100 µg/ml streptomycin (pen/strep) was supplemented with either 5% (v/v) heat-inactivated foetal calf serum (HI-FCS) or 10% (v/v) heat-inactivated human serum (HIHS) for culturing U937 cells or HMDM cells, respectively. The cell culture medium was warmed to 37°C before use in maintaining the cells. In this thesis, the above described cell culture media for U937 cells is referred to as U937 culture medium and for HMDM cells as HMDM culture medium.

2.2.1.2 Preparation of heat-inactivated human serum

Unlinked (anonymised) blood from consenting haemochromatosis patients was collected in 600 ml dry bags by the NZ Blood Bank (Riccarton Road, Christchurch). The blood bag

was incubated in a vertical position at room temperature for 2 hours and then at 4°C overnight. This treatment allowed the blood to coagulate and the serum to separate from the blood clot. In a Class II biological safety cabinet (Clyde-Apex BH 200) the serum was subsequently collected into 50 ml centrifuge tubes and centrifuged at 4,100 g for 15 minutes to pellet any remaining blood cells. The resulting serum was transferred into new 50 ml centrifuge tubes, heat inactivated in a water bath at 56°C for 30 minutes and then stored at –80ºC (Freshney, 2000).

2.2.1.3 Culture of U937 human monocyte-like cell line

The human monocyte-like cell line U937 cells were a gift from the Haematology Research laboratory at the Christchurch School of Medicine, University of Otago. Originally, the U937 cell line was obtained from a human haematopoietic cell line derived from histiocytic lymphoma. It was derived from a 37 year old man with a generalized lymphoma (Sundstrom & Nilsson, 1976).

Two vials of U937 cells at 20 $\times 10^6$ cells/ml, at 1 ml per vial, were removed from liquid nitrogen storage and defrosted in a 37°C water bath until only a small piece of frozen liquid remained in the vials. In a Class II biological safety cabinet (Clyde-Apex BH 200) the liquid in both vials was then poured into 30 ml of U937 culture medium in a 50 ml centrifuge tube, followed by centrifugation at 500 g for 5 minutes to remove the dimethyl sulfoxide (DMSO) freezing medium.

The resulting cell pellet was re-suspended in 10 ml of U937 culture medium in a 25 cm^2 tissue culture flask. Cell concentration was maintained at 0.5-1 $\times 10^6$ cells/ml by changing

media and transferring cells to 75 cm^2 tissue culture flasks every 3 days after counting cells under a microscope using a haemocytometer and trypan blue dye to distinguish between intact and damaged cells. The cells were counted by adding 100 µl of cells suspension to 100 µl trypan blue and mounting onto a haemocytometer.

2.2.1.4 Preparation and culture of human monocyte-derived macrophage cells

Human monocyte-derived macrophage (HMDM) cells were prepared from whole blood donated by clinically healthy haemochromatosis patients at the New Zealand Blood Services (Christchurch) under ethics approval CTY/98/07/069 granted by the New Zealand Upper South B Ethics Committee. The monocytes were purified by centrifugation of leukocytes to within a rich buffy coat layer using Lymphoprep™ and differentiated into adherent macrophages in adherent 12-well plates (Firth *et al.*, 2007a). This method was developed in the laboratory over a number of years from that originally used by Professor Wendy Jessup (University of New South Wales, Sydney).

All the media and solutions were warmed up to room temperature prior to use, except for the HMDM culture medium, which was warmed up to 37°C in a water bath.

Unlinked blood was collected by the NZ Blood Bank (Riccarton Road, Christchurch) from consenting haemochromatosis patients into 600 ml autologous bags containing the anticoagulant citrate-phosphate-dextrose-adenine-1 (CPDA-1).

At the Free Radical Biochemistry Laboratory, the blood bag was gently inverted five times to ensure even distribution of blood cells. Then the bag was placed in a Class II

biological safety cabinet (Clyde-Apex BH 200) and blood poured gently into 50 ml centrifuge tubes. The blood was then centrifuged (Multifuge 1 S-R, Heraeus) for 20 minutes at 3000 g, with slow deceleration.

The resulting buffy coat layer was collected using a mixing cannula attached to a 10 ml syringe after removing a plasma layer above this buffy coat layer. The buffy coat layer was then transferred into new centrifuge tubes at 15 ml per tube, and mixed well with PBS at 20 ml per tube. The mixture was then under laid with 15 ml of Lymphoprep, and centrifuged at 1000 g for 20 minutes with slow acceleration and deceleration.

After centrifugation, a white layer of monocytes/lymphocytes appearing about half-way down each the centrifuge tube was transferred to new centrifuge tubes, with 15 ml per tube. Each tube was topped up to 45 ml with sterile PBS and centrifuged at 500 g for 15 minutes. The resulting cell pellet was washed three times in 45 ml of PBS at 500 g for 10 minutes.

The cell pellet was subsequently re-suspended in 30 ml serum-free HMDM culture medium (RPMI-1640 medium containing pen/strep). Cells were then counted by adding 20 µl of cell suspension to 180 µl trypan blue and transferring 20 µl of the mixture to a haemocytometer for counting. The cell concentration was adjusted to 5 $x10^6$ cells/ml in serum-free HMDM culture medium and 6-8 ml of this suspension placed into each well of a 6-well suspension culture plates (Greiner Bio-one). The plates were then incubated at 37ºC/5% CO_2 for 40 hours to allow T cell death and platelet adhesion to the plates, while monocytes remained viable in suspension.

After 40 hours incubation, the cell suspension was transferred from each well into 50 ml centrifuge tubes and the viable monocytes were pelleted by centrifugation at 500 g for 15 minutes at room temperature. The cells were then re-suspended in 30 ml serum-free HMDM culture medium. The cells were counted as described above and the concentration was adjusted to 5.0 x10^6 cells/ml in RPMI-1640 with pen/strep and supplemented with 10% (final concentration in total media volume) HIHS. To each well 1 µl of 25 µg/ml granulocyte macrophage colony stimulating factor (GM-CSF) was added (Leukine® GM-CSF prepared in filtered (0.22 µm filter) sterilised nanopure water) per 1 ml of cell suspension. The cells were then plated at 5.0 ×10^6 cells/well in 12-well adherent plates (Nunclon- Surface Nunc) and then incubated at 37°C.

The HMDM culture medium was replaced every 3-4 days. Experiments were not conducted until more than 70% of monocytes had matured to macrophages, which usually took up to 14 days after plating.

2.2.2 Preparation of low density lipoprotein

Low density lipoprotein (LDL) was isolated from human plasma using a Beckman Near Vertical Rotor (NVTi-65) and involved the preparation of a single step gradient. LDL prepared via this simple method generated highly toxic oxLDL after oxidation with $CuCl_2$. Previously, LDL was prepared using a Beckman Swing out Bucket Rotor (SW41-Ti) which required a much more complex preparation procedure. Both methods are described in detail in sections 2.2.2.3 and 2.2.2.7.

2.2.2.1 Blood collection for isolation of plasma

A written consent was first obtained from the healthy blood donors who were required to fast overnight. Blood was collected from donors by venipuncture using a 21G x ¾ inch or 19G needle attached to a 30 ml syringe. The blood was transferred into 50 ml centrifuge tubes containing 0.5 ml of 10% (w/v) ethylene diamine tetraacetic acid (EDTA, MW 292.24) (pH 7.4). The blood containing tubes were centrifuged (Multifuge 1 S-R, Heraeus) for 20 minutes at 4°C in a swing-out rotor at 4,100 g with a soft start.

The resulting yellow plasma at the top of the tube was transferred to 50 ml round bottom centrifuge tubes and spun for 30 minutes at 11,000 g in a fixed angle rotor to remove any remaining traces of cells. Plasma from all donors (between 5 and 7 donors) was pooled and the total volume was recorded. The pooling of plasma minimised inter-individual variation. The plasma was stored in 20 ml or 32 ml aliquots at –80°C for a maximum of 6 months (Gieseg & Esterbauer, 1994).

2.2.2.2 Preparation of dialysis tubing

The dry dialysis membrane tubing (Medical International Ltd, London, England) with a 14.4 mm flat width and molecular weight cut-off of 14,000 Daltons was pre-treated before use. The dialysis tubing was first cut into 22 cm lengths.

The tubes were boiled in a glass beaker containing a solution of 5% w/v $NaHCO_3$ (MW 84.01) and 1 mM EDTA (MW 292.24). After 20 minutes boiling, the tubes were washed with reverse osmosis-water (RO-H_2O) and boiled again in a glass beaker containing RO-H_2O. After 20 minutes the tubes were washed thoroughly with RO-H_2O and stored in a

solution of RO-H_2O: ethanol (50:50 v/v) at 4°C. The tubes were washed thoroughly with RO-H_2O before being used for dialysis.

2.2.2.3 Preparation of LDL using Beckman Near Vertical (NVTi-65) rotor method

This method of LDL isolation utilises a Beckman Near Vertical (NVTi-65) rotor and employs the method of (Chung *et al.*, 1986), with modifications described by (Gieseg & Esterbauer, 1994). The protocol requires a single gradient that redistributes during ultracentrifugation to form a density gradient, which separates lipoproteins.

A 32 ml tube of frozen human plasma was defrosted under cold running water and centrifuged at 4700 rpm for 10 minutes at 4ºC to pellet precipitated fibrinogen. The supernatant was decanted into a beaker and placed immediately on ice. Potassium bromide (KBr) was gradually dissolved in plasma, to a final concentration of 382 mg KBr/ml plasma, altering the plasma density to 1.24 g/ml. Plasma was stirred gently to prevent foam formation, which is an indication of LDL denaturation. Plasma was maintained on ice and under argon gas until ultracentrifugation.

Eight millilitres of 1 mg/ml EDTA (pH 7.4) was added to each of eight OptiSeal™ polyallomer centrifuge tubes (Beckman Coulter, USA) before under-layering with 4 ml or less of KBr-plasma, using a needle attached to a 5 ml syringe. Ultracentrifuge tubes were transferred to the NVTi-65 rotor and centrifuged at 60,000 rpm for 2 hours at 10ºC with slow acceleration/deceleration using an Optima™ L-90K Preparative Ultracentrifuge (Beckman Coulter, Inc., Fullerton, California). Following centrifugation,

a yellow/orange coloured band of LDL in the density range of 1.019 – 1.063 g/ml was collected using a 20 ml syringe attached to a 90º bend needle (Figure 2.1).

2.2.2.4 Measurement of LDL concentration

LDL concentration was determined by enzymatic cholesterol assay using a CHOL kit (Roche Diagnostic). Ten microlitres of LDL was incubated with 1 ml of cholesterol reagent at room temperature for 10 minutes. The absorbance was read at 500 nm against a blank containing only cholesterol reagent.

LDL concentration as total mass was then calculated from the absorbance, based on the estimate that cholesterol accounts for 31.69% of the entire LDL particle, by weight, and that LDL has a molecular weight of 2.5 $x10^3$ kDa and the cholesterol molecular weight was 386.64 (g/mol) (Gieseg & Esterbauer, 1994). The extinction coefficient for the assay was 14.9 at 500 nm.

LDL total mass (mg/ml) = Absorbance x 14.9 x (1/1000) x 386.64 x (100/31.69)

2.2.2.5 LDL washing and concentration

The LDL was adjusted to a final concentration of 10 mg/ml (total mass) before any subsequent manipulations or use in experiments. LDL was concentrated using Amicon® Ultra-15 ultrafiltration tubes (Millipore, USA). LDL was transferred to two filter tubes. Each was made up to 15 ml with chelex-treated PBS and centrifuged at 3000 g for 30 minutes at 10ºC. This step was then repeated twice. The duration of the third centrifugation was adjusted according to the desired final volume/concentration of LDL, as determined by cholesterol assay (see section 2.2.2.4).

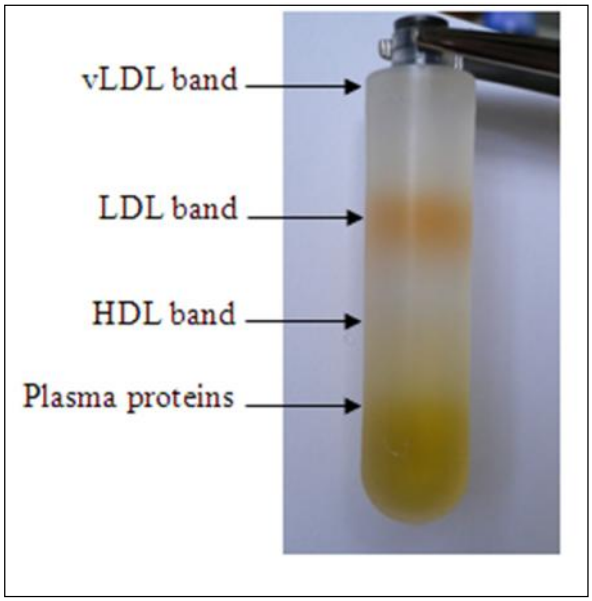

Figure 2.1 Location of different density lipoproteins bands after ultracentrifugation using NVTi-65 rotor.
The top yellow layer is very low density lipoprotein (vLDL). The second yellow/orange layer is low density lipoprotein (LDL). The third yellow layer is high density lipoprotein (HDL). The bottom yellow layer is plasma proteins.

If no further manipulations were to be made to the LDL, it was filter-sterilised through a 0.22 μm membrane filter with 25 mm diameter (Sartorius AG, Goettingen, Germany) and stored at 4ºC in the dark, under argon gas.

2.2.2.6 LDL oxidation

LDL at 10 mg/ml (total mass) was transferred to 12-14 kDa dialysis tubing (Medicell International, UK) secured at one end with a double knot and a weighted closure at the other. Fifty millimolar copper chloride ($CuCl_2$) solution was combined with the LDL inside the dialysis tubing to give a final concentration of 0.5 mM $CuCl_2$. The LDL-containing dialysis tubing was placed in a large bottle containing 1 L PBS/50 mg LDL, plus $CuCl_2$ at a final concentration of 0.5 mM $CuCl_2$. LDL was dialysed against 0.5 mM $CuCl_2$ in PBS for 24 hours at 37ºC in a heated shaker.

The dialysis bag containing oxLDL was then transferred to a fresh bottle containing 1L of PBS and stirred with 1 g of washed chelex-100 at 4ºC for 2 hours. This was repeated twice, with the final incubation taking place overnight. OxLDL was filter-sterilised using a 0.22 μm membrane filter with 25 mm diameter (Sartorius AG, Goettingen, Germany) and stored at 4ºC (Gerry *et al.*, 2007).

2.2.2.7 Preparation of LDL using Beckman Swing out Bucket (SW41-Ti) rotor method

During few of the U937 cell studies, LDL was prepared using a (SW41-Ti) rotor method. Previous studies have shown there is no difference in the LDL prepared by Beckman

Near Vertical NVTi-65 rotor and Beckman Swing out Bucket (SW41-Ti) rotor (Gieseg & Esterbauer, 1994).

Density gradient solutions for ultracentrifugation were prepared by dissolving the required amount of NaCl (MW 58.44) in nanopure water. Firstly, a 10 mg/ml EDTA solution was prepared by dissolving EDTA (MW 292.24) in nanopure water and adjusting the pH to 7.4 with 10 M NaOH. Solution A of density 1.08 g/ml was made up by adding 8 g NaCl to 10 ml of 10 mg/ml EDTA solution and made up to 100 ml with nanopure water. Solution B of density 1.05 g/ml was made up by adding 5 g NaCl to 10 ml of 10 mg/ml EDTA solution and made up to 100 ml with nanopure water. Finally, solution C of density 1.0 g/ml was made up by adding 10 ml of 10 mg/ml EDTA solution to 90 ml of nanopure water.

A 20 ml tube of plasma was thawed under cold running water (at approximately 6°C) and centrifuged at 4,700 rpm for 10 minutes at 4°C to remove any precipitated fibrinogen. The supernatant was decanted into a beaker placed on ice. Potassium bromide (KBr) (MW 119.01, 410 mg/ml) was gradually added to the plasma with continuous stirring using a magnetic flea to produce a plasma density of 1.41 g/ml. The plasma was pipetted evenly between six Beckman ultracentrifuge tubes. Three millilitres of solution A was gently layered onto the plasma using a syringe attached to a 180°-bend needle followed by 3 ml of solution B and finally solution C.

The centrifuge tubes were then transferred to a Beckman SW41-Ti rotor and centrifuged at 40,000 rpm for 22 hours at 10°C using an Optima^{TM} L-90K Preparative Ultracentrifuge (Beckman Coulter, Inc., Fullerton, California). The top very low density lipoprotein

(vLDL) layer was first discarded. A yellow/orange band of LDL in the density range of 1.019 g/ml to 1.063 g/ml was collected using a 20 ml syringe attached to a 90°-bend needle (Figure 2.2). The high density lipoprotein (HDL) band which was the second yellow band from the bottom of the tube was discarded.

The LDL was transferred to a treated dialysis tube, layered with argon gas and dialysed for 24 hours at 4°C against four changes of degassed PBS containing Chelex 100 resin in order to remove all traces of EDTA.

Freshly dialysed LDL was stored under argon and filter-sterilised through a 0.22 μm membrane filter with 25 mm diameter (Sartorius AG, Goettingen, Germany) and stored at 4°C until the oxidation was carried out.

For LDL oxidation $CuCl_2$ (MW 170.48) from a sterile 50 mM stock was added to filter-sterilised 3 mg/ml LDL in a 25 ml cell culture flask at a final concentration of 300 to 400 μM. The mixture was incubated overnight at 37°C. Complete oxidation of LDL occurred after 24 hours when the LDL became colourless.

The copper ions were removed by mixing the oxLDL with 1 g Chelex 100 resin and placing the tube on a rotating turntable which inverts the tube 8 times per minute. This was done at 4°C for 2 hours. The Chelex 100 resin was allowed to settle down by centrifugation at 500 g for 2 minutes before collecting the oxLDL from above it.

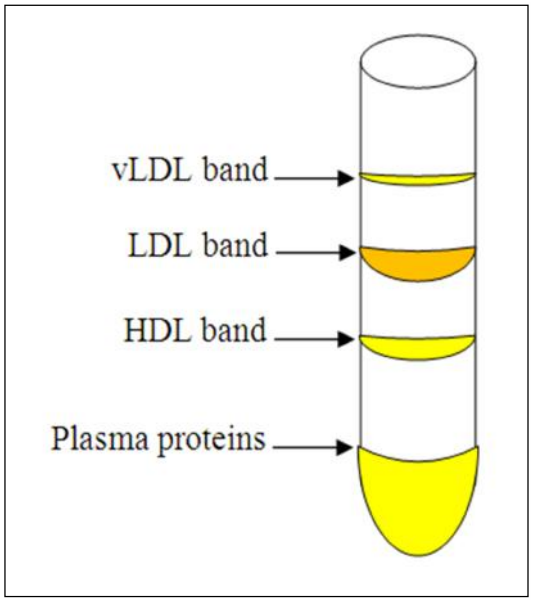

Figure 2.2 Location of different density lipoproteins bands after ultracentrifugation using SW41-Ti rotor.

The top yellow layer is very low density lipoprotein (vLDL). The next yellow/orange layer is low density lipoprotein (LDL). The following yellow layer is high density lipoprotein (HDL). The bottom yellow layer is plasma proteins.

OxLDL was concentrated using an Amicon® Ultra-15 filter tubes (Millipore, USA) to the concentration (usually between 10 to 12 mg/ml) necessary to allow a small volume of oxLDL to be added to the medium during subsequent use in experiments. OxLDL was filter-sterilised through a 0.22 μm membrane filter with 25 mm diameter (Sartorius AG, Goettingen, Germany) and stored at 4°C.

2.2.3 Lipoprotein gel electrophoresis of LDL and oxLDL

Relative electrophoretic mobility (REM) on native gels was determined using a SEBIA HYDRAGEL LIPO K20 kit and apparatus according to the manufacturer's instructions.

Two 10 μl applications of native LDL (nLDL) or oxLDL (from 10 mg/ml stock) were applied per lane, allowing 7 minutes for absorption between each application. The gel was electrophoresed for 90 minutes at 50 volts. The gel was dried at 90°C for 45 minutes before staining for 15 minutes in Sudan black stain. The gel was then destained, washed in distilled water and dried as before.

2.2.4 OxLDL labelling and uptake measurement using DiI

1,1'-Dioctadecyl-3,3,3',3'-tetramethylindocarbocyanine perchlorate (DiI, MW 5341) is a highly lipophilic molecule and it is extensively used in studies of receptor–mediated metabolism of LDL. The lipoproteins were labelled with the fluorescent probe DiI as described by (Stephan & Yurachek, 1993) and (Devaraj *et al.*, 2001). Sterilised oxLDL of known lipoprotein concentration (1-2 mg protein/ml) was incubated with 25 μl of 3 mg/ml DiI in DMSO for each milligram of lipoprotein in a 25 cm^2 tissue culture flask. The flask was covered with aluminium foil to prevent exposure to light. The mixture was

then incubated overnight for between 15 to 18 hours at 37°C. DiI-oxLDL was kept at 4°C in the dark and used immediately due to the instability of DiI.

Measurement of DiI-oxLDL uptake was conducted according to the method of (Stephan & Yurachek, 1993). HMDM cells at 5.0 x10^6 cells/ml were incubated at 37°C to measure cell-associated DiI-oxLDL. At the end of the incubation period, the medium was removed and cells were washed three times with warm PBS. Then 1ml isopropanol was added to each well and plates were gently shaken on an orbital shaker (Bioline, Edwards Instrument Company, Australia) for 15 min. The cells were harvested and the cell lysates were transferred into 1.7 ml microtubes and centrifuged at 3000 rpm for 15 min.

The supernatant was taken out for determination of fluorescence intensity using a fluorescence spectrophotometer (Cary Eclipse). The excitation and emission wavelengths were set at 520 and 580 nm, respectively. The cell pellets were dissolved in 2 M NaOH for protein determination. Results were expressed as mean fluorescence intensity (MFI) of cell associated (37°C) DiI-oxLDL per mg of cell protein.

2.2.5 Measurement of cell viability using MTT reduction assay

The thiazolyl blue tetrazolium bromide (MTT, MW 414.33) assay provides an indirect measure of cell viability. Metabolically active cells can endocytose and metabolise the yellow MTT compound, via the action of cellular nicotinamide adenine dinucleotide phosphate dehydrogenases (NAD(P)H-dehydrogenases), into a purple insoluble MTT-formazan product that, when dissolved in detergent, that can be quantified

spectrophotometrically at 570 nm (Mosmann, 1983a). The colour intensity provides an indication of the concentration of cells and their metabolic activity.

MTT was dissolved in RPMI-1640 medium (without phenol red), at a concentration of 5 mg/ml. The mixture was then sterilised through a 0.22 μm membrane filter (Sartorius AG, Germany) and stored at –20°C in the dark. Ten percent (w/v) sodium dodecyl sulfate (SDS, MW 288.38) in 0.01 M hydrochloric acid (HCl) was stored at room temperature.

After experimental treatments, U937 cells at 0.5 x10^6 cells/ml were transferred to a 1.7 ml microtube for washing with PBS (see section 2.1.2.1) then re-suspended in suspension culture plates (Greiner Bio-one). With HMDM cells, (at 5.0 x10^6 cells/ml) they were washed with PBS (see section 2.1.2.1) in the adherent plates (Nunclon- Surface, Nunc).

Cells in each well were incubated at 37°C with 1 ml of RPMI-1640 without phenol red containing 0.5 mg/ml MTT for 2 hours (U937 cells) or 10 minutes (HMDM cells). The insoluble purple crystals that developed in each well were then dissolved by mixing with 1 ml of 10% (w/v) SDS. The absorbance was read at 570 nm, against a blank lacking cells but containing all other reagents.

2.2.6 Measurement of lactate production

Lactate within cell culture media was measured using a lactate kit (Roche Pharmaceuticals and supplied through Global Science NZ Ltd) as per the manufacturer's instructions. The kit measured lactate via its enzymatic oxidation to pyruvate by lactate dehydrogenase (LDH) which is coupled to the reduction of NAD^+ to NADH, and is measured by its absorption at 340 nm. The reaction equilibrium becomes shifted towards

pyruvate by the presence of glutamate-pyruvate transaminase which converts the pyruvate to 2-oxoglutarate. The lactate concentration was calculated using the molar extinction coefficient of NADH (6220 $M^{-1}cm^{-1}$).

For experiments measuring lactate production U937 cells at 0.5 $x10^6$ cells/ml or HMDM cells at 5.0 $x10^6$ cells/ml were incubated in RPMI-1640 (no phenol red). For HMDM cells pen/strep and 10% HIHS were added. Samples of media were centrifugated at 21,000 g to remove any particulates before placing on ice before analysis. The analysis was carried out using the kit's reagents in a semi-micro cuvette which containing 500 µl glycylglycine buffer, 100 µl NAD^+, 10 µl glutamate-pyruvate transaminase suspension, 50 µl sample and 450 µl water (H_2O), for blank 500 µl H_2O, in this order, followed by mixing. The absorbance was recorded after 5 minutes at 340 nm. The absorbance was then recorded at 340 nm, 30 minutes after the reaction was started by adding 10 µl lactate dehydrogenase solution.

The lactate concentration was calculated from the difference between the absorbance using as the molar extinction coefficient of NADH (6220 $M^{-1}cm^{-1}$) and the lactate molecular weight (90.1 g/mol).

2.2.7 Measurement of LDH activity

Lactate dehydrogenase (LDH) is an enzyme found in all cell types. It is rapidly released into the cell culture medium upon damage to the plasma membrane. LDH catalyses the reduction of pyruvate to lactate and is coupled to the oxidation of NADH to NAD^+. NADH has an absorbance peak at 340 nm, so LDH activity can be measured by

monitoring the loss of absorbance using excess pyruvate and NADH. Extracts are taken from both the cell culture media and the lysed cells, which gives a calculation of released LDH and cellular LDH (Decker & Lohmann-Matthes, 1988).

U937 cells and HMDM cells were incubated in RPMI-1640 (no phenol red) at 0.5 $x10^6$ cells/ml and 5.0 $x10^6$ cells/ml, respectively. For the HMDM cells pen/strep and 10% HIHS were added. LDH activity was measured in the cell culture medium which was removed and stored on ice before analysis. The intracellular LDH activity was also measured following the resuspension of cell pellets with 480 µl PBS and 20 µl Triton X-100 (5% solution in PBS) before incubation for 30 minutes at 37°C. A small amount of resuspended pellets, 10 µl, was used for protein assay (see section 2.1.2.4). The LDH assay was carried out in a semi-micro cuvette which contained 870 µl of PBS, 90 µl cell extract (supernatant or pellets), 60 µl of 3 mg/ml NADH (made up fresh, wrapped with foil and kept on ice during use) and 30 µl of 0.8 mg/ml pyruvate, added in this order and followed by mixing.

The absorbance at 340 nm was recorded at 0.1-minute intervals over 5 minutes at 340 nm. The molar extinction coefficient of NADH (6220 $M^{-1}cm^{-1}$) was used to calculate the rate of NADH release in µmol per minute.

2.2.8 Measurement of GAPDH activity

Glyceraldehyde-3-phosphate dehydrogenase (GAPDH) is a glycolytic enzyme that catalyses the oxidative phosphorylation of glyceraldehyde-3-phosphate (GAP) to 1,3-diphospho-glycerate (1,3-PGA). In the process, the NAD^+ cofactor is reduced to NADH,

which has a strong absorbance at 340 nm. The activity of GAPDH can hence be monitored spectrophotometrically by measuring the rate of NADH formation using an assay modified from (Steck & Kant, 1974).

The solutions, 30 mM $NaH_2PO_4H_2O$, pH adjusted to 8 with 10 M NaOH in nanopure water, 0.2 M sodium arsenate ($Na_2H_2AsO_4.7H_2O$, MW 312.01) in nanopure water, and 0.2% (v/v) Triton X-100 in 30 mM $NaH_2PO_4H_2O$ (pH 8.0) were stored at room temperature. A 294 mM GAP (MW 170.6) solution in nanopure water was stored at -80°C, which was diluted to 15 mM working concentration in nanopure water. The 20 mM NAD^+ (MW 663.43) was made up fresh on the day of analysis in cold nanopure water. Both substrates were stored on ice during use.

U937 cells at 0.5 $x10^6$ cells/ml were transferred to 1.7 ml microtubes and the cells were pelleted by centrifugation. After washing the cell pellet in PBS (see section 2.1.2.1), the cell mixture was placed on ice. For HMDM cells, (at 5.0 $x10^6$ cells/ml) the cells were scraped off using cell scrapers (Greiner bio-one, Germany) into 1 ml of cold PBS (see section 2.1.2.1). The resulting cell mixture was transferred to 1.7 ml microtubes and stored on ice.

In a semi-micro cuvette 100 µl of cell mixture and 100 µl of 0.2% (v/v) Triton X-100 were mixed, which was then incubated for 1 minute in the spectrophotometer at 37°C. To this was added 600 µl of 30 mM $NaH_2PO_4H_2O$ (pH 8.0) that had already been equilibrated to 37°C, 50 µl of 0.2 M sodium arsenate, 50 µl of 20 mM NAD^+, and 100 µl of 15 mM GAP in this order and followed by mixing.

The absorbance at 340 nm was recorded at 0.1-minute intervals over 3 minutes at 340 nm. The molar extinction coefficient of NADH (6220 M^{-1} cm^{-1}) was used to calculate the rate of NADH release in μmol per minute.

2.2.9 Measurement of the sensitivity of free thiol in GAPDH enzyme

The sensitivity of the thiol groups in GAPDH to oxidation was measured by fluorescent labelling of reduced thiol in combination with sodium dodecyl sulfate polyacrylamide gel electrophoresis (SDS-PAGE) to detect changes in the redox state of cultured cells and to show the loss of reactive thiol in the GAPDH enzyme. Reduced thiol were labelled with the fluorescent compound 5-iodoacetamidofluorescein (5-IAF). Gel electrophoresis was conducted using a simpler modification of a technique developed by Dr. Mark Hampton (Cuddihy *et al.*, 2009a).

2.2.9.1 Solutions for thiol analysis

The extraction buffer consisted of (40 mM hydroxy ethyl prazine ethane sulfonic acid (HEPES, MW 238.31), 50 mM NaCl (MW 58.44), 1 mM EDTA (MW 292.24), 1 mM ethlylene glycol-bis(2-aminoethylether)-N,N,N',N'-tetracetic acid (EGTA, MW 380.4), protease inhibitors solution and 1% 3-[(3-cholamidopropyl)dimethylammonio]-1-propanesulfonate (CHAPS, MW 614.9) w/v (prepared fresh) in nanopure water, with the pH adjusted to 7.4 using 10 M NaOH and was stored on ice until use.

Complete mini protease inhibitor stock (25×) was added to the extraction buffer, with 40 μl added per 1 ml of buffer. The 25× stock protease inhibitor solution was prepared as per the manufacturer's instructions. One complete mini protease inhibitor cocktail tablet

(Roche, Germany) was dissolved in 1.5 ml of nanopure water to give a 25× stock solution. Tablets were stored in 4ºC fridge and stocks in a -20ºC freezer.

The cracker buffer was prepared by dissolving SDS (MW 288.38), glycerol (MW 92.10), and bromophenol blue (MW 670.02) in 0.5 M Tris-HCl in nanopure water (pH adjusted to 6.8 using 11.4 M HCl) and s making up to a final volume of 50 ml. Prior to use 1 ml of the above solution was mixed with 20 µl of β-mercaptoethanol and 2 µl of 100 mg/ml EDTA. The complete cracker buffer consisted of 0.125 M Tris-HCl (pH 6.8), 1% (w/v) SDS, 20% (w/v) glycerol, 0.1% (w/v) bromophenol blue, 2% (v/v) β-mercaptoethanol, and 0.5 mM EDTA.

4-Morpholine-propanesulfonic acid (MOPS) buffer consisted of 50 mM MOPS (MW 209.3), 50 mM Tris(hydroxymethyl)aminomethane (Tris, MW 121.1), 0.1% (w/v) SDS (MW 288.38), and 1 mM EDTA (MW 292.24) in nanopure water, with the pH adjusted to 7.7 by adding concentrated HCl.

2.2.9.2 IAF labelling of reduced thiol

U937 cells at 5.0 x10^6 cells/ml were washed with PBS (see section 2.1.2.1) after the culture medium was removed by centrifugation. The pellets were suspended in 100 µl of extraction buffer (see section 2.2.9.1), and incubated at room temperature for 15 min. Ten microlitres of 10% CHAPS was added to the final concentration of 1% w/v for cells, before the extract was mixed and incubated for another 15 min. One millilitre of -20°C acetone was added, mixed and placed on ice, before being centrifuged at 15,000 rpm for

5 min, at 4°C to precipitate proteins and insoluble material. The supernatant was gently removed by aspiration.

Cell pellets were suspended in 100 µl of extraction buffer and then centrifuged at 15,000 rpm for 5 min at 4°C to separate the insoluble material and remove cell debris. Eighty microlitres of supernatant was transferred to clean 1.7 ml microtubes. Sixteen microlitres of 1 mM IAF (prepared in DMSO) was added to the extract to a final concentration of 200 µM. The extract was incubated in the dark at room temperature for 10 min. One millilitre of -20°C acetone was added before the mixture was centrifuged at 15,000 rpm for 5 min, at 4°C to remove excess IAF. The supernatant was gently removed by aspiration.

The resulting pellets were dissolved in 20 µl of 100 mM Tris (to stop the reaction). Then 5 µl was taken for protein assay (see section 2.1.2.4). After protein analysis, the protein concentration in the remaining 15 µl of each sample was adjusted with excess Tris to give the same protein concentration in all samples. Then the same amount of each sample was then transferred to new 1.7 ml microtubes.

The cracker buffer (see section 2.2.9.1) was added (to dissolve the precipitated protein) with an amount equivalent to the cells lysate to give a final protein concentration of 1.25 µg/µl (at this time the samples may be stored at -20°C until used). The samples were then heated in a heating block at 95ºC for 3 minutes and centrifuged for 5 minutes at 15,000 rpm at 4°C (to remove any cell debris) before SDS-PAGE analysis (see section 2.2.9.3).

2.2.9.3 SDS-PAGE analysis

A 4-12% gradient polyacrylamide gel (Bis-Tris Gel, Invitrogen, Carslband, CA, USA), was placed in the XCell SureLock™ Mini-Cell system (Invitrogen, US) and the MOPS running buffer (see section 2.2.9.1) was added to the buffer reservoir. Five microlitres of Fermentas pre-stained molecular weight marker mix (Fermentas International Inc, Canada), 5.0 µl of GAPDH marker for identification of thiol sensitivity and 20 µl of samples (containing 25 µg proteins) were loaded into the wells of the gel, before electrophoresis in the dark at 200 V for approximately 1 hour until the buffer loading dye reached the bottom of the gel.

The gel was kept wet in a running buffer in a dark box until it was scanned using a Bio-Rad Molecular Imager FX (Bio-Rad Laboratories, Hercules, CA, USA) with an excitation wavelength of 488 nm and an emission/detection wavelength of 530 nm. Then the gel was stained with coomassie blue to show the position of the authentic GAPDH marker (supplied by Sigma), which has a molecular size of 36 kDa.

2.2.10 Measurement the rate of oxygen consumption

The rate of oxygen consumption (VO_2) was determined by measuring the change in the partial pressure of oxygen (PO_2) (Forgan & Forster, 2009). U937 cells at 2.0 $x10^6$ cells/ml were placed into 1 ml of appropriately stirred air-saturated ringer solution of the chamber in a temperature controlled 37°C Strathkelvin Instruments model RC 300 respirometers (Strathkelvin, Glasgow, Scotland). These were fitted with model IL1302 O_2 electrodes and model 781 metres. The signal was fed via a Powerlab 4/25 into a notebook computer running Chart 5 software (both AD Instruments, Castle Hill, Waverley, NSW,

Australia) recording at 1 Hz. The air supply was disconnected and the cells were allowed to deplete the oxygen contained within the respirometers. The experiment was terminated when the PO_2 fell from air saturation (PO_2 155 mmHg) to zero. The VO_2 was determined from the equation 2.1.

$$VO2 = \frac{\Delta PO2}{t \times M} \times \alpha O_2 \times V \qquad 2.1$$

Where VO_2 is the rate of oxygen consumption ($\mu l\ O_2.\ 10^6 cells^{-1}\ .hr^{-1}$), ΔPO_2 is the change in the PO_2 during the treatment period ($mmHg.time^{-1}$ (sec)), αO_2 is the oxygen solubility of the ringer based on the osmolarity ($0.0021\ mmol\ O_2.L^{-1}.mmHg^{-1}$), V is the volume in the respirometers (ml), t is the time (hour) between the PO_2 measurements and M is the number of the cells in the respirometers. The instantaneous VO_2 was calculated in two different ways, both using linear regression. For the first method, the VO_2 is calculated during every 10 minutes period over the time course of the experiment (7 hours) and for the second method, the VO_2 is calculated at 0, 3, 5, 7 hours where the cells were placed in the cell chambers at each time point, after being held at 37°C in a humidified incubator, with an atmosphere calibrated to 5% CO_2: 95% air (Nuaire™ IR Autoflow), in the absence of HI-FCS and pen/strep.

2.2.11 HPLC instrumentation

The High Performance Liquid Chromatography (HPLC) system used in this research was supplied by Shimadzu Corporation, Japan and consisted of a 2LC-20ADvp pumps with prepump solvent mixing, inline vacuum degasser (DGU-20A5), an autosampler (SIL-20AD vp), a column oven (CTO-20A(C)vp), a fluorescence detector (RF-20AXL), a UV-Vis diodearray (SPD-20A(V)vp), and a communication bus module (CBM-20A) connected to a PC. Peak areas were quantified using the Shimadzu LC solution software package.

All aqueous mobile phases used were filtered through a 0.45 μm Phenex filter membrane (Phenomenex) and sonicated (Alphatech Systems Ltd & Co., Auckland) for 10 minutes. Analytes in samples were standardised against particular standards of known concentrations.

2.2.12 TBARS-HPLC lipid analysis

The thiobarbituric acid reactive substances (TBARS) assay provides a means of quantifying general lipid peroxidation. It relies on the ability of 2-thiobarbituric acid (TBA) to readily react with the malondialdehyde (MDA) lipid hydroperoxide break-down product, forming the pink TBA-MDA adduct which is fluorometrically detectable via the HPLC system. The method used here is slightly modified from the 1993 Drapper method which uses butylated hydroxytoluene (BHT) in the incubation media to prevent further lipid oxidation and fluorescent detection of the TBA-MDA (Draper *et al.*, 1993).

Lipoproteins samples (200 µl; 50 µl of sample from 10 mg/ml stock and 150 µl of PBS) were mixed with 100 µl of 150 mM phosphoric acid (H_3PO_4, MW 97.994) and any further oxidation was inhibited by the addition of 20 µl of 20 mg/ml BHT (MW 220.4). After addition of 100 µl of fresh 42 mM TBA (MW 144.15) reagent the tubes were mixed by inversion and placed in a heating block at 95°C for 30 minutes with very gentle shaking. Samples were then cooled on ice and centrifuged at 4°C for 10 minutes at 15000 rpm.

The resulting supernatant (100 µl) was transferred to auto sampler vial and 20 µl was injected onto the HPLC. The HPLC was equipped with a phenosphere reverse phase C-18, 4.6 x150 mm, 5 µm column (Phenomenex; Auckland, NZ), heated to 30°C. TBARS were fluorometrically detected using excitation and emission wavelengths of 525 nm and 550 nm, respectively. The mobile phase consisted of 50 mM $NaH_2PO_4H_2O$ with pH adjusted to 6.8 with 10 M NaOH and filtered through 0.45 µm filter. This was mixed with HPLC grade methanol in a ratio of 65:35 before degassing by sonication. The mobile phase was pumped through the system at a flow rate of 1 ml/min.

TBARS concentrations in all samples were quantified by comparison with the peak areas of 1 µM MDA (MW 72.06) standards. A fresh MDA standard was prepared before each assay by hydrolysis of 6.07 M of 1,1,3,3-tetramethoxypropane (TMP, MW 164.2) in 2:3 (v/v) ethanol:water, with subsequent dilution in water to the appropriate concentration. H_3PO_4 and BHT were then added, as per the experimental samples.

2.2.13 Free 7-ketocholesterol analysis

Free 7-ketocholesterol (7-KC) was analysed by HPLC analysis (Kritharides *et al.*, 1993). Lipid extraction of 100 µl of lipoprotein (20 µl of samples from 10 mg/ml stock and 80 µl water) was carried out by the addition of 10 µl of 20 mg/ml BHT, 20 µl of 100 mg/ml EDTA, 500 µl ethanol and 2 ml of hexane, before vortexing for 60 seconds. Samples were then centrifuged at 200 g for 10 minutes at 4ºC to obtain complete phase separation. Then 1400 µl of the top hexane layer was removed, transferred to a tapered glass test tube and dried completely under nitrogen gas. The dried residue was re-solubilised in 100 µl of solvent mix (ACN/isopropanol, 4:5).

Then 80 µl of the resulting supernatant was transferred to a glass auto sampler vial insert and 20 µl was injected onto a phenosphere reverse phase C-18, 250 ×4.6 mm, 5 µm column (Phenomenex, Auckland, NZ), heated to 35°C. Mobile phase was acetonitrile:isopropanol:H_2O in a ratio of 44:54:2. Detection of free 7-ketocholesterol was via monitoring 234 nm absorbance. Quantification of the oxysterol was by comparison of peaks from known concentrations of the standard.

2.2.14 Intracellular GSH analysis

Monobromobimane (MBB) is a cell-permeable fluorescent dye that binds thiol groups, specifically those of glutathione (GSH). The GSH-MBB adducts can then be detected by the HPLC after protein precipitation (Cotgreave & Moldeus, 1986). The procedures were carried out under minimum exposure to light as MBB is light sensitive. MBB (MW 271.1) was dissolved in acetonitrile to give a 40 mM stock, which was stored in darkness at 4°C for up to two weeks. Reduced GSH (MW 307.3 g/mol), at 5 and 10 µM

concentrations, was prepared in cold PBS immediately before HPLC analysis to serve as a standard. For analysis, U937 cells at 0.5 x10^6 cells/ml were washed with PBS (see section 2.1.2.1). Then 400 µl of PBS, 9 µl of 0.1 M NaOH (to bring up the pH to 8), and 10 µl of 40 mM MBB were added to each sample of U937 cells. After 20 minutes of incubation in the dark at room temperature, 20 µl of 100% (w/v) trichloroacetic acid (TCA, MW 163.39) was added to lyse the cells and precipitate cellular proteins. The cell lysate was collected and centrifuged in 1.7 ml microtubes at 15,000 rpm for 5 minutes at 4°C. Ten microlitres of the resulting supernatant was injected onto the phenosphere reverse phase C-18, 150 ×4.6 mm, 5 µm column (Phenomenex, Auckland, NZ), heated to 35°C. GSH-MBB adducts were detected by the fluorescence detector with excitation and emission wavelengths set at 394 nm and 480 nm, respectively. Mobile phase A (consisting of 0.25% acetic acid in nanopure water) and mobile phase B (consisting of 100% acetonitrile) were pumped through the column at a flow rate of 1.5 ml/minute with gradient program as described in Table 2.3.

Table 2.3 HPLC gradient for GSH measurement.

Time (minutes)	Mobile phase A (0.25% acetic acid)	Mobile phase B (100% acetonitrile)
0	90%	10%
10	90%	10%
11	0%	100%
15	0%	100%
16	90%	10%
20	90%	10%

2.2.15 Measurement of intracellular purine nucleotides ATP, ADP, AMP, NAD^+ and $NADP^+$

The effect of oxLDL on purine nucleotides which are adenosine triphosphate (ATP), adenosine diphosphate (ADP), adenosine monophosphate (AMP), nicotinamide adenine dinucleotide (NAD^+) and nicotinamide adenine dinucleotide phosphate ($NADP^+$) in U937 cells and HMDM cells was examined by measuring intracellular purine nucleotides levels upon oxLDL exposure via HPLC analysis.

Purine nucleotides (ATP, ADP, AMP, NAD^+ and $NADP^+$) were quantified by reverse phase ion pair-HPLC with UV detection at 254 nm (Tuckey *et al.*, 2010, Pelzmann *et al.*, 2003, Furst & Hallstrom, 1992). A purine nucleotides stock of 1 mM concentration was prepared in 50 mM $NaH_2PO_4H_2O$, pH 7.2 and stored at -20°C. The stock was diluted to 25 µM in cold nanopure water immediately before use to serve as a standard for quantifying the elution time and peak size of purine nucleotides.

For a sufficient signal to be detected by the HPLC system, U937 cells were used at 5.0 $x10^6$ cells/ml. Cells were transferred to 1.7 ml microtubes and centrifuged at 1500 rpm for 5 min at 4ºC before washing with PBS. Then 100 µl of cold 0.07 M perchloric acid (PCA, MW 100.46) in nanopure water was added. In the case of HMDM cells, for a sufficient signal to be detected by the HPLC, a combination of three wells containing 5.0 $\times 10^6$ HMDM cells was required. HMDMs were collected by scraping, using a total of 125 µl cold 0.07 M PCA in nanopure water after washing with cold PBS.

The cell lysate was then sonicated for 1 minute, left on ice for 30 minutes and centrifuged at 15,000 g for 5 minutes at 4°C to remove proteins. The supernatant was neutralised with

10 or 12.5 µl of 2 M potassium carbonate (K_2CO_3, MW 138.21) in nanopure water (the ratio between 0.07 M PCA and 2 M K_2CO_3 was 10:1) for U937 cells or HMDM cells, respectively, and then centrifuged as above.

The supernatant (40 µl) was injected onto a reverse phase 5 µm ODS (C18), 250 x 4.6 mm, 5 µm column (Phenomenex). This column was developed with gradient of mobile phases A and B. Mobile phase A consisted of 6.9 g/L of $NaH_2PO_4H_2O$ and 2 g/L of tetrabutylammonium bisulfate ($C_{16}H_{37}NO_4S$, MW 339.54) in nanopure water, pH adjusted to 5.5 using 10 M NaOH. Mobile phase B consisted of mobile phase A and acetonitrile at a ratio of 75:25. Both were pumped at a flow rate of 1 ml/minute with gradient program as described in Table 2.4.

Table 2.4 HPLC gradient for purine nucleotides measurement.

Time (minutes)	Mobile phase A	Mobile phase B
0	100%	0%
5	100%	0%
25	30%	70%
28	30%	70%
30	100%	0%
50	100%	0%

2.3 Statistical analysis

Data was graphed and statistically analysed using the Prism software (version 4.0; GraphPad Software, USA). The significance was confirmed by a one-way analysis of variance (ANOVA), followed by Tukey's multiple comparison test to provide a more quantitative indication of significance between treatments and/or time points. Where appropriate, linear regression and correlation analyses were also applied with r2 values calculated assuming a Gaussian distribution. Significance levels are indicated in the following manner: * $p \leq 0.05$; ** $p \leq 0.01$; *** $p \leq 0.001$.

Results displayed in this thesis are taken from one experiment, which is representative of at least three separate experiments. The means and standard errors of the mean (SEM) shown within each experiment were calculated from triplicate samples.

3 Characterisation of oxLDL, the effect of oxLDL and the effect of 7,8-dihydroneopterin on cell viability and morphology

3.1 Introduction

The formation of oxidised low density lipoprotein (oxLDL) within the atherosclerotic plaque is a significant event in the progression and development of atherosclerosis (Niu *et al.*, 1999, Salvayre *et al.*, 2002). In contrast to low density lipoprotein (LDL), oxLDL is taken up by macrophages in a rapid and uncontrolled manner leading to the formation of cholesterol filled macrophages (foam cells). OxLDL at high concentrations is cytotoxic in tissue culture and most likely within atherosclerotic plaques. OxLDL causes death of a variety of cell types including macrophages by both necrosis and apoptosis. Therefore, the change from fatty streak to complex plaque may be driven in part by the oxLDL-induced death of macrophages within the plaque (Hardwick *et al.*, 1996, Hegyi *et al.*, 1996).

This laboratory had shown that oxLDL was cytotoxic to two different human monocyte-like cell lines, THP-1 and U937 cells (Baird et al., 2004) and human blood monocyte-derived macrophage (HMDM) cells (Gieseg *et al.*, 2010). However, only in the U937 and HMDM cells oxLDL induced death shows high levels of oxidative stress which can be inhibited by the addition of the antioxidant 7,8-dihydroneopterin. Previous studies have highlighted a significant variation in the potency and type of cell death caused by different preparation of oxLDL, especially between different laboratories (Darley-Usmar *et al.*, 1991, Draper *et al.*, 1993, Kritharides *et al.*, 1993) and surprisingly we have seen

small changes in potency within our laboratory between individuals oxLDL preparation over the years (Baird, 2003, Amit, 2008).

Primary goal of the research reported in this chapter was to characterise the potency of the oxLDL prepared against U937 and HMDM cells prepared from human blood. Previous studies have shown that oxLDL at cytotoxic concentrations causes both U937 cells and HMDM cells to undergo necrosis after the loss of cellular glutathione (GSH). U937 cells normally appear more sensitive to the oxLDL than the HMDM cells. A number of published studies have shown HMDM cells to undergo caspase independent "apoptosis" but these studies have been conducted in the absence of serum or with only a trace amount of serum suggesting the cells were already in a highly stressed, apoptosis primed state which is then activated by the oxLDL (Baird *et al.*, 2004, Asmis & Begley, 2003). The HMDM cells studies were therefore conducted in the same heat-inactivated human serum (HIHS) containing media that they were cultured in.

This first results chapter begins by reporting measurements key biochemical characteristics of native low density lipoprotein (nLDL) and heavily oxidised low density lipoprotein (oxLDL). Previous studies in this laboratory have prepared the oxLDL by incubating the LDL in a concentrated solution of copper ions. To gain a more reproducible oxidation this study used the method of Dr. David Leake (Gerry *et al.*, 2007) which oxidises the LDL in a dialysis bag placed in a large volume of copper ions so maintaining the overall copper ion concentration even though the LDL binds significant amounts of these ions. The prepared oxLDL is analysed for an increase in relative electrophoretic mobility (REM), unesterified 7-ketocholesterol (7-KC) formation,

and lipid oxidation, measured as thiobarbituric acid reactive substances (TBARS). The second part of the chapter characterises the cytotoxicity of the oxLDL prepared in this laboratory in U937 and HMDM cell viability and morphology.

Previous studies in the laboratory have usually measured cell death after a standard 24 hours incubation (Baird, 2003, Amit, 2008). In order to obtain a more detailed understanding of the nature of both oxLDL-induced cytotoxicity and any; present form makes an unjustified assumption corresponding protective effect of 7,8-dihydroneopterin on U937 and HMDM cells, this chapter presents the oxLDL induced changes in U937 and HMDM cell morphology over time and with different levels of 7,8-dihydroneopterin protection. These morphological changes will be compared to the loss of cell viability measured by the thiazolyl blue tetrazolium bromide (MTT) reduction assay and will establish the concentration of oxLDL that will be used for further study in chapters 4 and 5. Finally, time course studies of the mechanism of 7,8-dihydroneopterin protection on U937 and HMDM cells against oxLDL-induced cytotoxicity were conducted.

3.2 Results

3.2.1 Characterisation of native LDL and heavily oxidised LDL

Heavily oxidised low density lipoprotein (oxLDL) was prepared by added 50 mM copper chloride ($CuCl_2$) solution to 10 mg/ml native low density lipoprotein (nLDL) (total mass) in 12-14 kDa dialysis tubing and in to the baaathing fluid to give a final concentration of 0.5 mM $CuCl_2$ for 24 hours at 37ºC (Gerry *et al.*, 2007). This procedure keeps the copper ion level at a stable concentration which was not affected by the level of copper binding

by the relatively low amount of LDL. This oxLDL was used for the majority of the experiments.

The properties of nLDL and oxLDL are most commonly assessed by measurement of relative electrophoretic mobility (REM), unesterified 7-ketocholesterol (7-KC) content and thiobarbituric acid reactive substances (TBARS) levels (Darley-Usmar *et al.*, 1991, Draper *et al.*, 1993, Kritharides *et al.*, 1993, Ehrenwald & Fox, 1996). In gel mobility analysis, LDL oxidation leads to the loss of positive charge on LDL and hence the shift in REM. OxLDL mobility was 3-fold greater than that of nLDL showing a significant level of LDL oxidation had been achieved. Native LDL contained very low levels of 7-ketocholesterol, which was significantly increased after oxidation by approximately 53–fold in the oxLDL. Native LDL also contained very low levels of TBARS, which was significantly increased after oxidation, by approximately 130–fold in the oxLDL (Table 3.1 and Figure 3.1). These data are consistent with previous characterisations of heavily oxidised LDL in our laboratory (Gieseg *et al.*, 2009a).

Table 3.1 Characterisation of native LDL (nLDL) and heavily oxidised LDL (oxLDL).

	nLDL	**oxLDL**
REM	8 mm	24 mm
Free 7-KC	6.5 µM ± 0.5	347.2 µM ± 18.6
TBARS	0.0025 mol/mol LDL±0.004	0.324 mol/mol LDL± 0.015

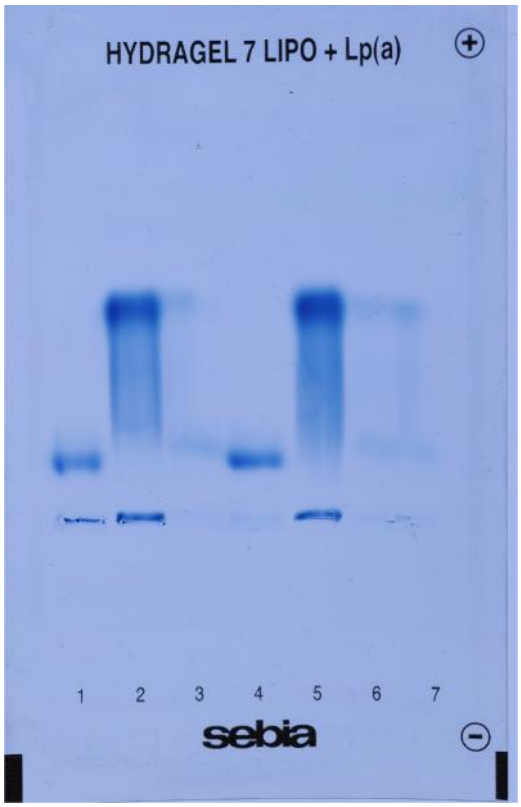

Figure 3.1 Lipoprotein gel of native LDL (nLDL) and heavily oxidised LDL (oxLDL).
Electrophoresis was performed on 1% agarose gel and Sudan black stain was used. Lanes 1 and 4 represent the REM position of nLDL; lanes 2 and 5 represent the REM position of oxLDL.

3.2.2 Effect of oxLDL on U937 and HMDM cells' morphologies

The effect of oxLDL on the U937 and HMDM cells was monitored by observing changes in morphology under a Leica light microscope at 40x magnification (Figure 3.2 and Figure 3.3).

U937 cells were incubated in serum free RPMI-1640 media with or without 0.5 mg/ml oxLDL over 24 hours. The control cells showed a round shape and classic U937 cell morphology which did not change over the course of the incubation in the serum free media (Figure 3.2). With the addition of oxLDL, the U937 cells started to have a swollen appearance after 3 hours which became more noticeable with time (Figure 3.2). By 12 hours many cells had distorted cellular membranes with some blebbing structures. At 24 hours, a large amount of damage to the cells was apparent which included the loss of cellular contents, disruption of cellular membranes and the presence of cellular debris from lysed cell (Figure 3.2). These cellular morphologies appear to be consistent with the necrotic cell death process.

HMDM control cells incubated in RPMI-1640 media containing 10% HIHS showed a poached egg-like appearance, which is the classic morphology of macrophage cells (Figure 3.3). HMDM cells treated with 2.0 mg/ml oxLDL did not show significant morphological changes after 3 hours of incubation but by 6 hours of incubation, the cells appeared swollen and enlarged compared to the control cells (Figure 3.3). After 9, 12 and 24 hours of incubation with oxLDL, the cellular membranes looked distorted and disrupted, and cell debris was observed. A number of cells were also found detached and

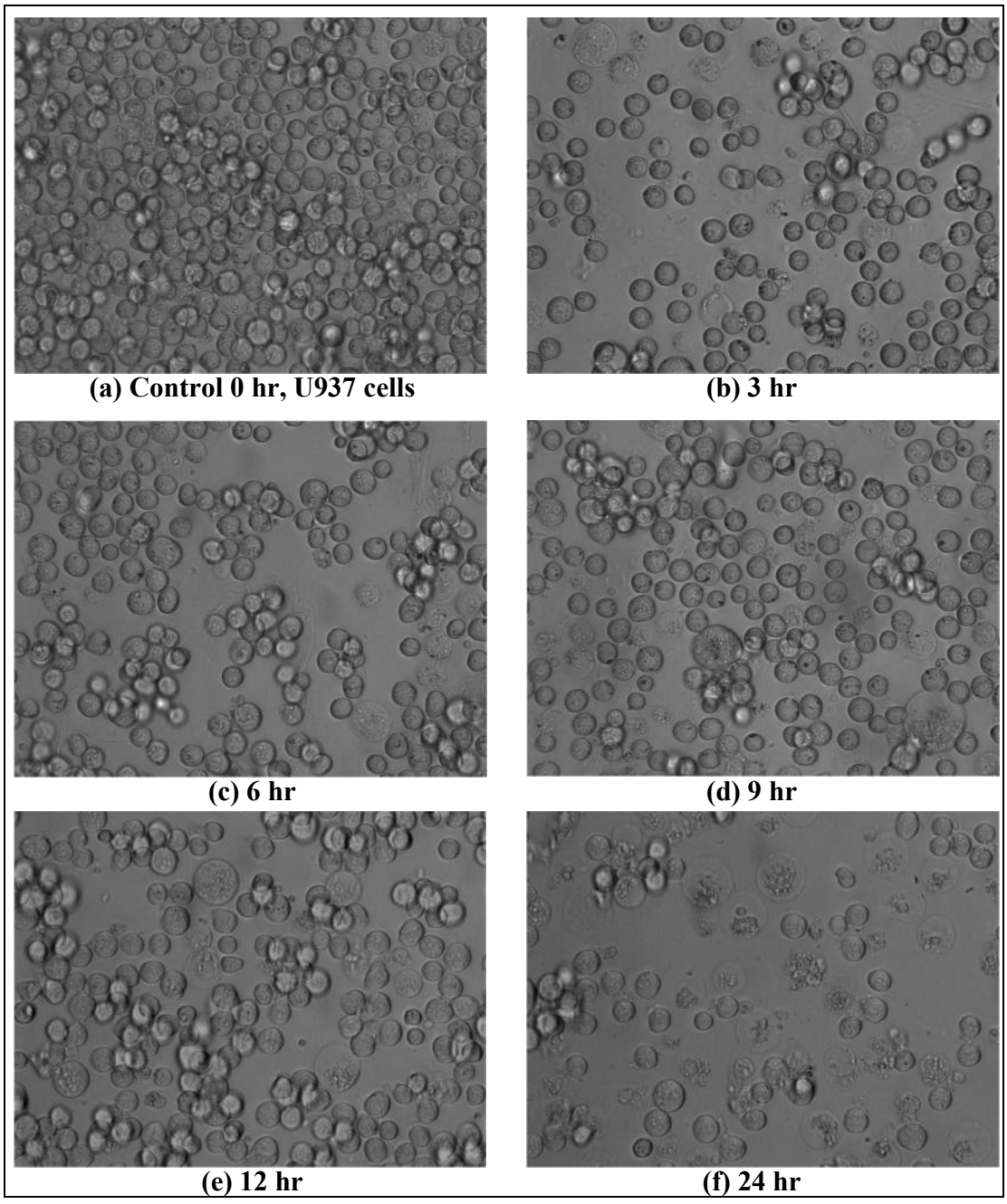

Figure 3.2 Changes in U937 cell morphology during incubation with oxLDL.
U937 cells at 0.5 x10^6 cells/ml were incubated with or without 0.5 mg/ml oxLDL over a 24 hour period. (a) Control U937 cells (b) U937 cells with oxLDL after 3 hr; (c) 6 hr; (d) 9 hr; (e) 12 hr; (f) 24 hr.

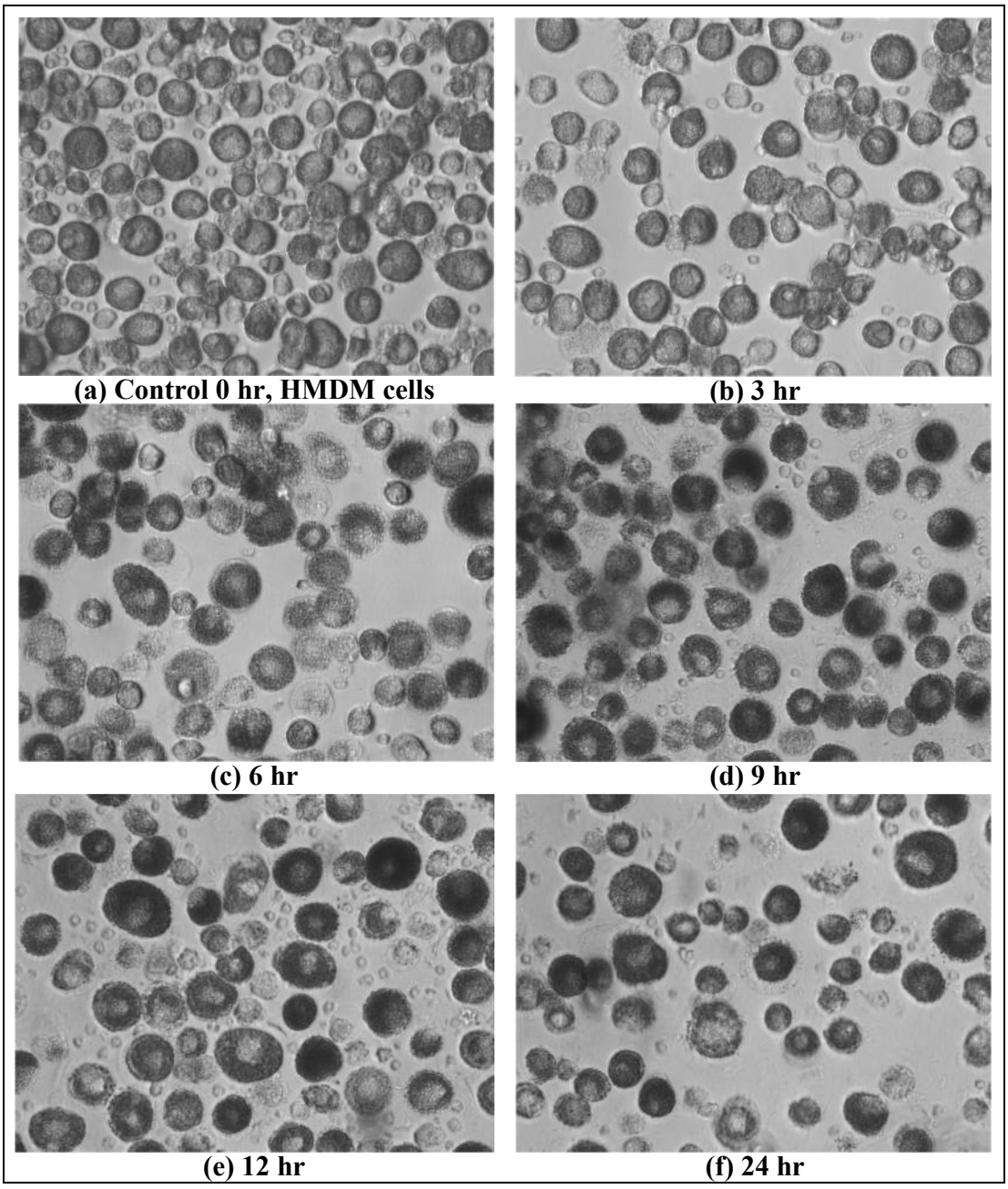

Figure 3.3 Changes in HMDM cell morphology during incubation with oxLDL. HMDM cells seed at 5.0 x10^6 cells/ml were incubated with and without 2.0 mg/ml oxLDL over a 24 hour period. (a) Control HMDM cells without oxLDL added (b) HMDM cells with oxLDL after 3 hr; (c) 6 hr; (d) 9 hr; (e) 12 hr; (f) 24 hr.

floating in the medium. Like the U937 cells, the morphological changes induced by the oxLDL appear to be characteristic of necrotic cell death (Figure 3.3). The results clearly showed that the cytotoxic effect of oxLDL on U937 cell morphology appeared from the initial 3 hours of incubation. In contrast, the oxLDL only appear to affect HMDM cell morphology after 6 hours of incubation.

3.2.3 Effect of oxLDL concentration on U937 cell viability

U937 cells were incubated in serum free RPMI-1640 media for 24 and 48 hours with a range of oxLDL concentrations. This study also aimed to determine a suitable concentration of oxLDL that can cause approximately 50% loss in U937 cell viability. Loss of cell viability was determined by MTT reduction assay and the results are displayed as a percentage of the viability of control cells (no treatment).

OxLDL caused a concentration dependent loss in U937 cell viability after 48 hours incubation with high oxLDL concentrations (Figure 3.4). A drastic 94% loss in cell viability was observed with 0.5 mg/ml oxLDL and near total loss of cell viability occurred with 1.5 and 3.0 mg/ml oxLDL, suggesting that these concentrations were very cytotoxic (Figure 3.4). The study also showed that by 48 hours of incubation the cell death process was complete with the majority of cells losing viability.

The cell death was therefore re-examined using lower oxLDL concentrations. The oxLDL caused a concentration dependent loss in U937 cell viability after 24 and 48 hours (Figure 3.5). Incubation of U937 cells for 24 hours with 0.2 mg/ml oxLDL caused a loss of viability of 61%, 0.5 mg/ml oxLDL caused a 66% loss in cell viability and only 24%

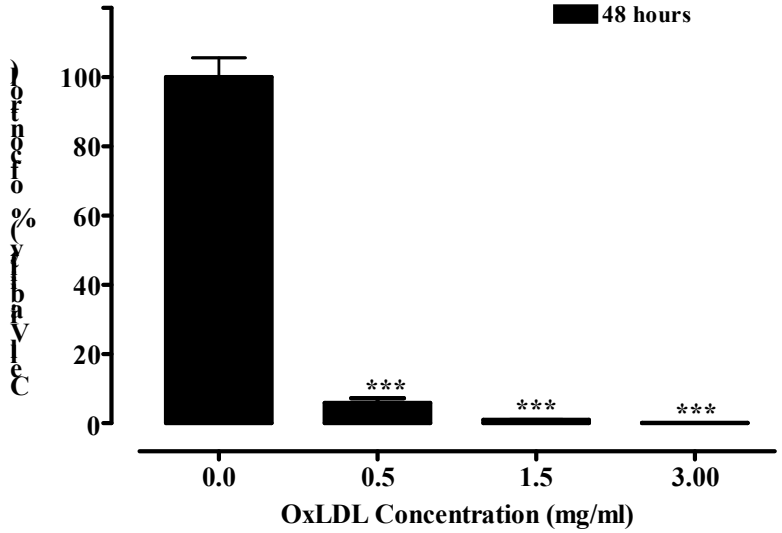

Figure 3.4 Effect of high concentrations of oxLDL on U937 cell viability after 48 hours.
U937 cells at 0.5 x10^6 cells/ml were incubated with increasing oxLDL concentrations for 48 hours before viability analysis by measuring MTT reduction. Significance is indicated as *** $P < 0.001$ vs 0.0 mg/ml oxLDL control. Results shown are the mean ± SEM of triplicate samples.

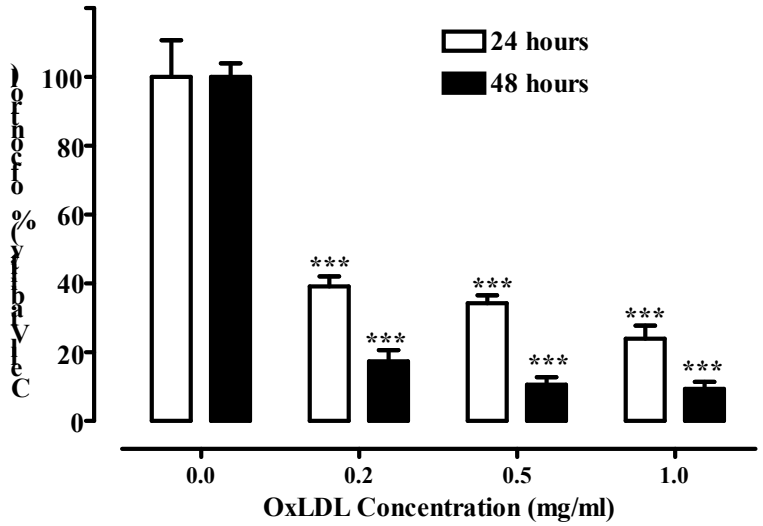

Figure 3.5 Effect of low concentrations of oxLDL on U937 cell viability.
U937 cells at 0.5 x10^6 cells/ml were incubated with increasing oxLDL concentrations for 24 and 48 hours before viability analysis by measuring MTT reduction. Significance is indicated as *** $P < 0.001$ vs respective 0.0 mg/ml oxLDL control. Results shown are the mean ± SEM of triplicate samples.

were still viable after incubation with 1.0 mg/ml oxLDL (Figure 3.5). However, 48 hours appeared to be a relatively long time to expose the cells to a toxic agent and showed similar result as above. From this data it was decided to only incubate U937 cells for 24 hours with 0.5 mg/ml oxLDL.

3.2.4 Rate of U937 cell viability loss induced by oxLDL

A time course study of oxLDL-mediated cellular damage was conducted by incubating U937 cells in serum free RPMI-1640 media with 0.5 mg/ml oxLDL for 24 hours (Figure 3.6). The cell viability dropped drastically over the first 3 hours by 44% compared to the control. The U937 cell viability continued to decline reaching a level 59% lower than the control after 6 hours. After 10 hours of incubation only 20% of cells were still viable and no further change was measured after 24 hours. Therefore, oxLDL exerts its toxic effect on U937 cells within the initial 3 hours. This result is consistent with the finding in section 3.2.2 where U937 cells morphology changed after 3 hours of incubation with oxLDL (Figure 3.2).

3.2.5 Effect of serum on U937 cell viability loss induced by oxLDL

Heat-inactivated foetal calf serum (HI-FCS) is a commonly used supplement in cell culture as it provides growth factors and cytokines necessary for cell growth and stability of phenotype. However the albumin in the serum is a well documented radical scavenger so may mask the cytotoxicity of the oxLDL in *vitro*. It is possible that atherosclerotic plaques may have lower levels of albumin than plasma due to filtration.

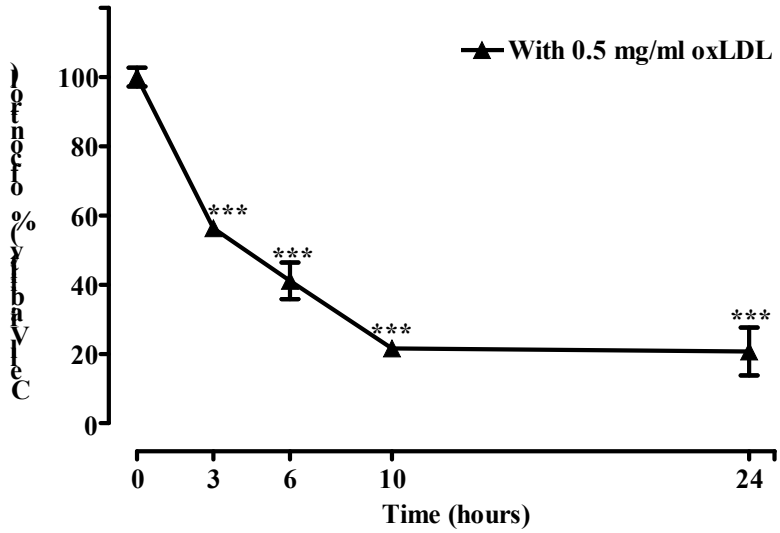

Figure 3.6 Time course showing the effect of oxLDL on U937 cell viability.
U937 cells at 0.5 x10^6 cells/ml were incubated with 0.5 mg/ml oxLDL over a 24 hour period. The cell viability was measured by MTT reduction at various time points. Significance is indicated as *** $P < 0.001$ vs 0 h control. Results shown are the mean ± SEM of triplicate samples.

The effect of HI-FCS on U937-treated oxLDL cell viability loss was studied by incubating U937 cells in RPMI-1640 media containing 10% HI-FCS and 0.5 mg/ml oxLDL for up to 24 hours. The cell viability was determined at the indicated times by MTT reduction assay (Figure 3.7). Results showed that 0.5 mg/ml oxLDL did not cause U937 cell viability loss when 10% HI-FCS was added to the RPMI-1640 media. There was a slight increase in the cell viability but this was not significant. This result clearly shows, HI-FCS has a protective effect on U937 cells when exposed to oxLDL. This will discussed further in the discussion section 3.3.

3.2.6 Effect of oxLDL concentration on HMDM cell viability

HMDM cells were incubated in RPMI-1640 media containing 10% HIHS for 24 hours with oxLDL at a range of concentrations. This study determined a suitable concentration of oxLDL that can cause approximately 50% loss in HMDM cell viability. Serum was included in the incubations as the HMDM cells become unstable in serum free RPMI-1640 media over extended incubation periods. OxLDL caused a concentration dependent loss in HMDM cell viability after 24 hours as measured by MTT reduction assay (Figure 3.8a).The HMDM cells appeared to be more resistant to the cytotoxic effect for the oxLDL than the U937 cells requiring more oxLDL to cause significant viability loss. As 2.0 mg/ml oxLDL caused approximately 50% viability loss, this was the oxLDL concentration chosen in the subsequent experiments involving HMDM cells.

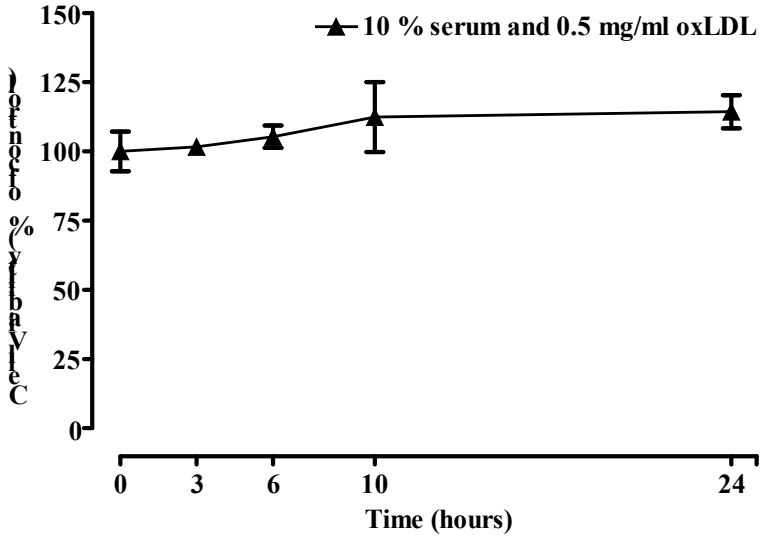

Figure 3.7 Time course showing the effect of oxLDL on U937 cell viability in the presence of HI-FCS.
U937 cells at 0.5 x10^6 cells/ml were incubated with 0.5 mg/ml oxLDL and 10 % HI-FCS over a 24 hour period. The cell viability was measured by MTT reduction at various time points. Results compared to 0 h control and are the mean ± SEM of triplicate samples.

(a)

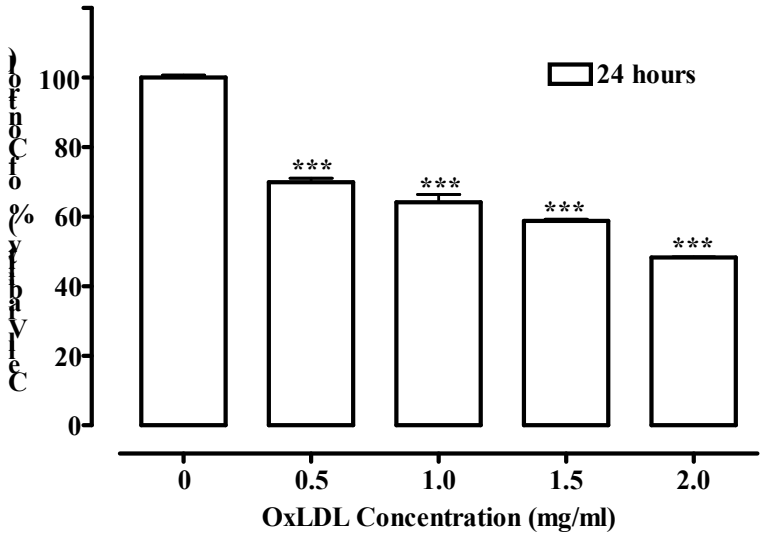

(b)

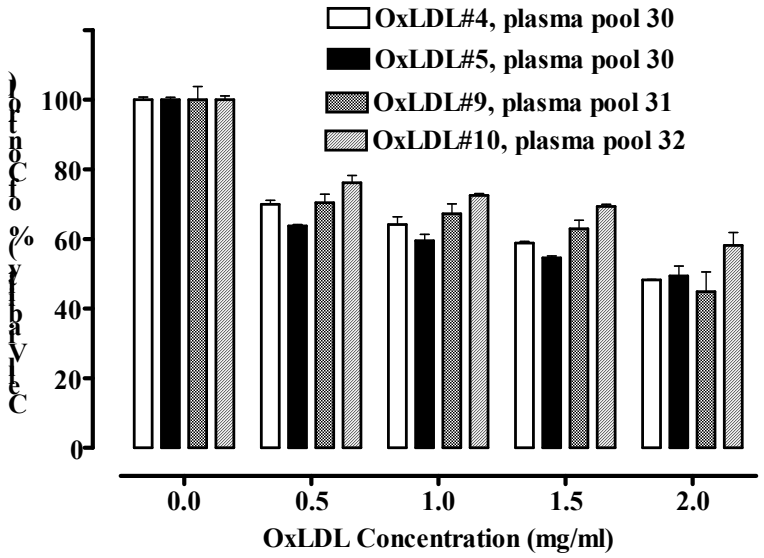

Figure 3.8 Effect of different oxLDL concentration on HMDM cells viability.
HMDM cells at 5.0 x10^6 cells/ml were incubated with different oxLDL concentrations (0, 0.5, 1.0, 1.5 and 2.0 mg/ml) for 24 hours before viability analysis by measuring MTT reduction. (a) Shows effect of oxLDL#4 of plasma pool 30; (b) Shows comparison between the effects of oxLDL from different plasma pools. Significance is indicated as *** $P < 0.001$ vs 0.0 mg/ml oxLDL control. Results shown are the mean ± SEM of triplicate samples.

Previous study in this laboratory used 1.0 mg/ml oxLDL to cause approximately 50% loss in the cell viability (Amit, 2008). The reason for this change is not fully understood and will be discussed further in the discussion section 3.3.

It was observed over the course of the research that there was no significant difference oxLDL cytotoxicity to HMDM cells between different oxLDL preparations prepared from different plasma pools (Figure 3.8b).

3.2.7 Time course study the effect of oxLDL on HMDM cell viability

A time course study of oxLDL-mediated damage was conducted by incubating HMDM cells in RPMI-1640 media containing 10% HIHS with 2.0 mg/ml oxLDL for 24 hours (Figure 3.9). The cell viability did not show any significant change compared with the control until 6 hours of incubation. Between 6 and 9 hours, the cell viability dropped drastically, by 41% compared to the control. After 12 hours of incubation the cell viability continued to decline to 47% of the control value. After 24 hours of incubation, only 38% of cells were still viable (Figure 3.9). This shows that the toxic effect of oxLDL on cell viability only becomes apparent in HMDM cells after 6 hours of incubation. This corresponds with the timing of the major morphological changes that were observed in HMDM cells as discussed in section 3.2.2 and showed in Figure 3.3.

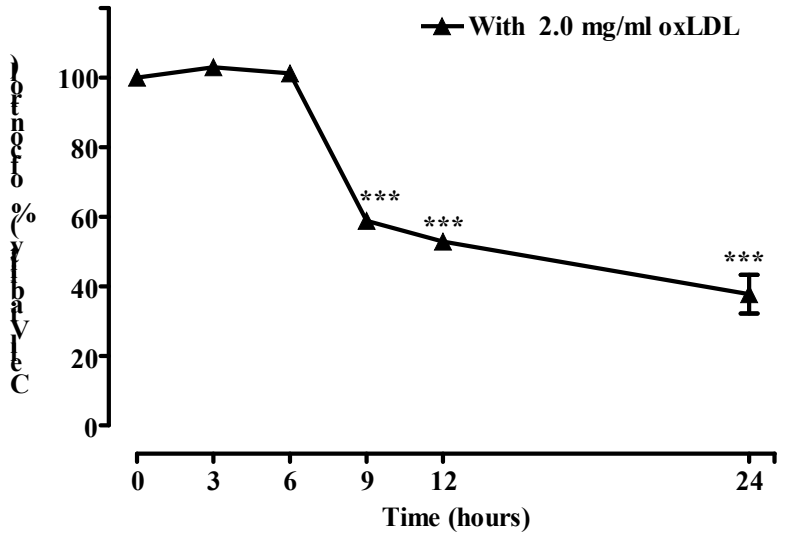

Figure 3.9 Time course showing the effect of oxLDL on HMDM cells viability.
HMDM cells at 5.0 x10^6 cells/ml in RPMI-164 with 10% HIHS were incubated with 2.0 mg/ml oxLDL over a 24 hour period. The cell viability was measured by MTT reduction at various time points. Significance is indicated as *** $P < 0.001$ vs 0 h control. Results shown are the mean ± SEM of triplicate samples.

3.2.8 Effect of 7,8-dihydroneopterin concentration on oxLDL-treated U937 cells

The antioxidant effect of 7,8-dihydroneopterin on cell viability loss was characterised by pre-incubated U937 cells for 10 minutes with various concentrations of 7,8-dihydroneopterin (0, 20, 50, 100 and 200 μM) in serum free RPMI-1640 media with and without 0.5 mg/ml oxLDL for 24 hours (Figure 3.10). Previous studies have shown the pre-incubation period is required for consistent results (Gieseg *et al.*, 1995). The presence of up to 200 μM 7,8-dihydroneopterin alone did not affect U937 cell viability, while the presence of 0.5 mg/ml oxLDL alone caused 70% loss of cell viability comparing to the cell control (Figure 3.10).

The presence of 7,8-dihydroneopterin caused a significant concentration dependent protection against oxLDL-induced loss of cell viability but only at 7,8-dihydroneopterin concentrations of 50 μM and above. At 100 μM 7,8-dihydroneopterin, the cell viability was increased by approximately 68% compared to the oxLDL treated U937. An oxLDL cytotoxicity was completely inhibited with 200 μM 7,8-dihydroneopterin therefore, 200 μM 7,8-dihydroneopterin was used in subsequent experiments for testing the protective effect of 7,8-dihydroneopterin against oxLDL-induced damage in U937 cells.

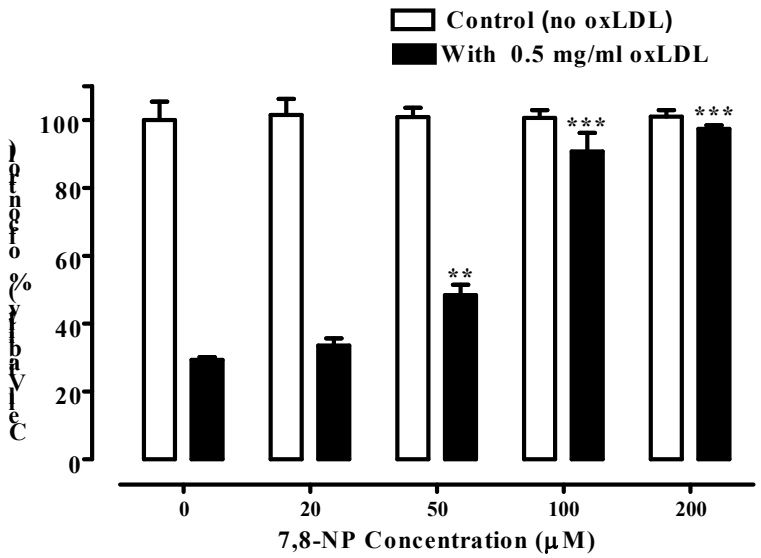

Figure 3.10 Effect of 7,8-NP concentration on cell viability of oxLDL-treated U937 cells.

U937 cells at 0.5 x10^6 cells/ml were incubated with different concentrations of 7,8-NP (0, 20, 50, 100 and 200 μM) before incubation with or without 0.5 mg/ml oxLDL for 24 hours before viability analysis by measuring MTT reduction. Significance is indicated as ** $P < 0.01$, *** $P < 0.001$ vs oxLDL only control. Results shown are the mean ± SEM of triplicate samples.

3.2.9 Effect of 7,8-dihydroneopterin concentration on oxLDL-treated HMDM cells

The antioxidant effect of 7,8-dihydroneopterin on cell viability loss was characterised by pre-incubated HMDM cells for 10 minutes with various concentrations of 7,8-dihydroneopterin (0, 50, 100, 150 and 200 μM) in RPMI-1640 media containing 10% HIHS with and without 2.0 mg/ml oxLDL for 24 hours (Figure 3.11). The presence of 7,8-dihydroneopterin alone, up to a concentration of 200 μM did not affect HMDM cell viability, while the presence of 2.0 mg/ml oxLDL alone caused 52% loss of cell viability comparing to the only cells control (Figure 3.11).

The presence of 7,8-dihydroneopterin caused a significant concentration-dependent protection against oxLDL-induced loss of HMDM cell viability but only at 7,8-dihydroneopterin concentrations of 100 μM and higher. At 100 and 150 μM 7,8-dihydroneopterin the cell viability increased by approximately 40% and 47% compared to the oxLDL only control, respectively, while 50 μM had no protective effect. Complete protection against oxLDL was observed with 200 μM 7,8-dihydroneopterin. Therefore, 200 μM 7,8-dihydroneopterin was used in subsequent experiments for testing the protective effect of 7,8-dihydroneopterin against oxLDL-induced damage in HMDM cells.

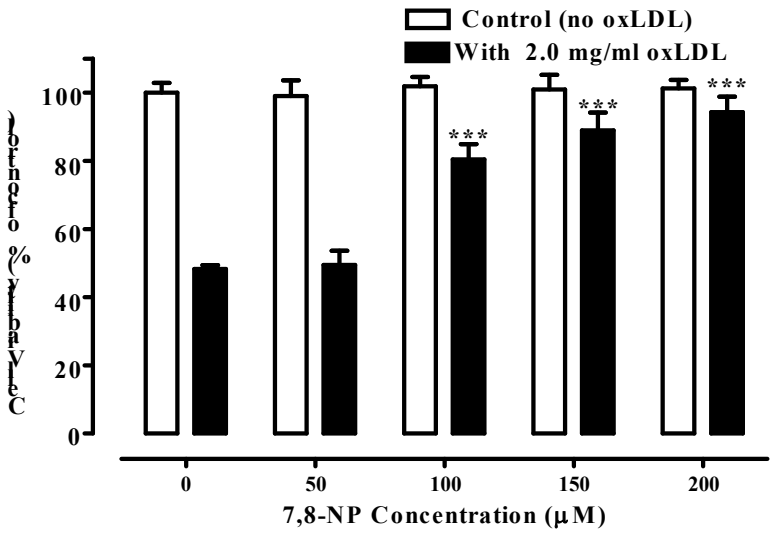

Figure 3.11 Effect of 7,8-NP concentration on cell viability of oxLDL-treated HMDM cells.

HMDM cells at 0.5 x10^6 cells/ml were incubated with different concentrations of 7,8-NP (0, 50, 100, 150 and 200 μM) before incubation with or without 2.0 mg/ml oxLDL for 24 hours before viability analysis by measuring MTT reduction. Significance is indicated as *** $P < 0.001$ vs oxLDL only control. Results shown are the mean ± SEM of triplicate samples.

3.2.10 Effect of 7,8-dihydroneopterin on oxLDL treated-U937 and HMDM cells morphologies

The effect of 7,8-dihydroneopterin on the U937 and HMDM cells was monitored by observing U937 and HMDM cell–morphology under a Leica light microscope at 40x magnification. The change in U937 cell morphology was studied by pre-incubated U937 cells for 10 minutes with various concentrations of 7,8-dihydroneopterin (0, 20, 50, 100 and 200 μM) with and without 0.5 mg/ml oxLDL in serum free RPMI-1640 media for 24 hours (Figure 3.12) and via time course study of cells incubated with 0.5 mg/ml oxLDL (0, 3, 6, 9, 12 and 24 hours) with and without 200 μM 7,8-dihydroneopterin in serum free RPMI-1640 media for 24 hours (Figure 3.13).

In Figure 3.12 the presence of 7,8-dihydroneopterin alone, up to a concentration of 200 μM (b ,c, d and e) did not result in any change in U937 cell morphology compared to control cells (a), which showed a typical, round shape. In the presence of 0.5 mg/ml oxLDL alone, the U937 cells showed morphological changes consistent with necrosis as previously described. In the presence of 20 and 50 μM 7,8-dihydroneopterin with 0.5 mg/ml oxLDL (f and g) the U937 cells also showed levels of cellular damage compared to their respective controls (a and b). There was no change in U937 cell morphology compared to the respective controls (c, d and e) in the presence of 100 and 200 μM 7,8-dihydroneopterin with 0.5 mg/ml oxLDL (h, i and j). 7,8-Dihydroneopterin, at a concentration between 100 and 200 μM, protects U937 cells from the cytotoxic effect of oxLDL characterised by changes in cell morphology.

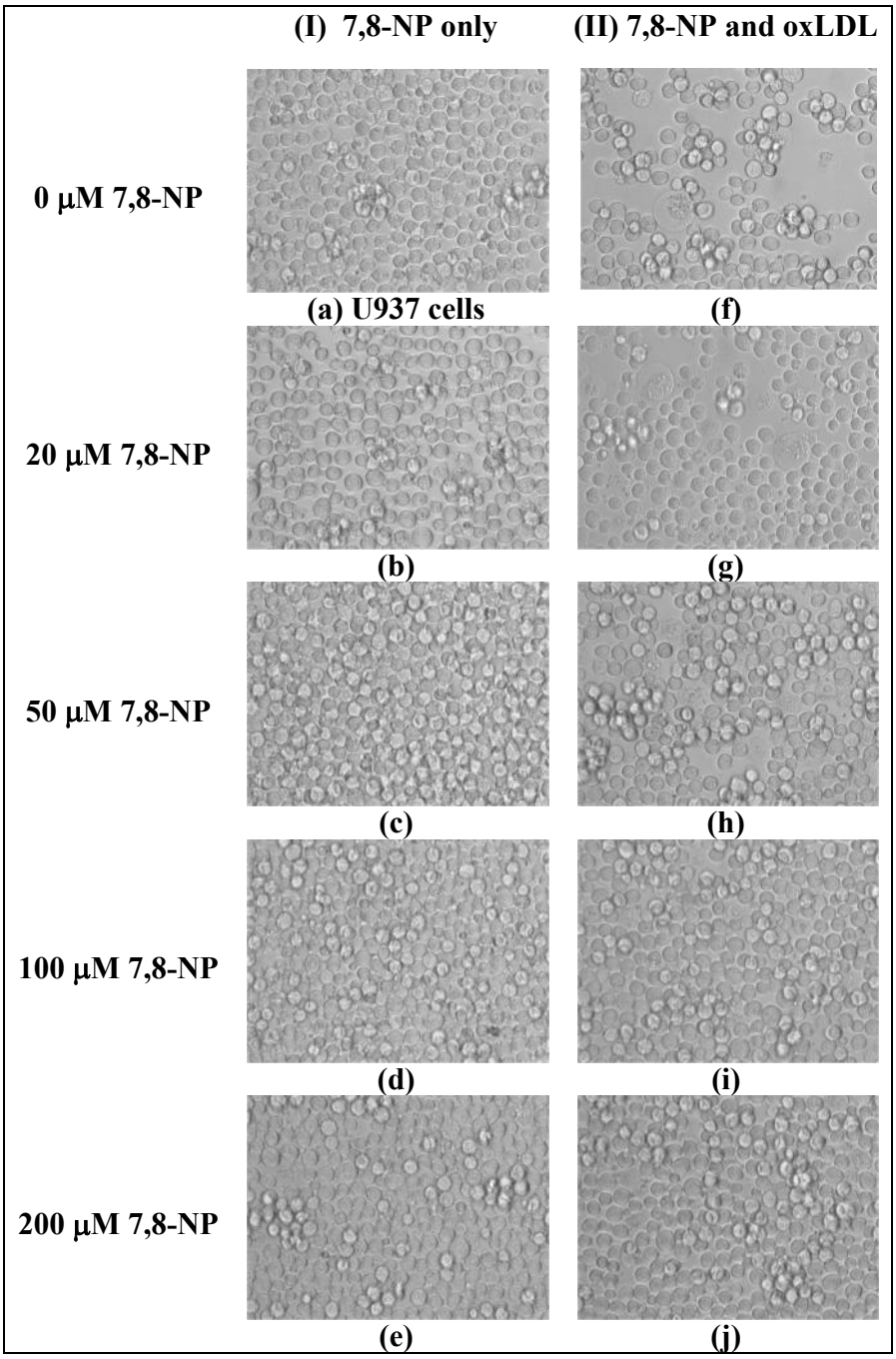

Figure 3.12 Changes in U937 cell morphology during incubation with different concentrations of 7,8-dihydroneopterin.

U937 cells at 0.5 x10^6 cells/ml were incubated with 200 μM 7,8-NP and without 0.5 mg/ml oxLDL (I) or with 0.5 mg/ml oxLDL (II) for 24 hours. (a), (f) 0 μM 7,8-NP; (b), (g) 20 μM 7,8-NP; (c), (h) 50 μM 7,8-NP; (d), (i) 100 μM 7,8-NP; (e), (j) 200 μM 7,8-NP.

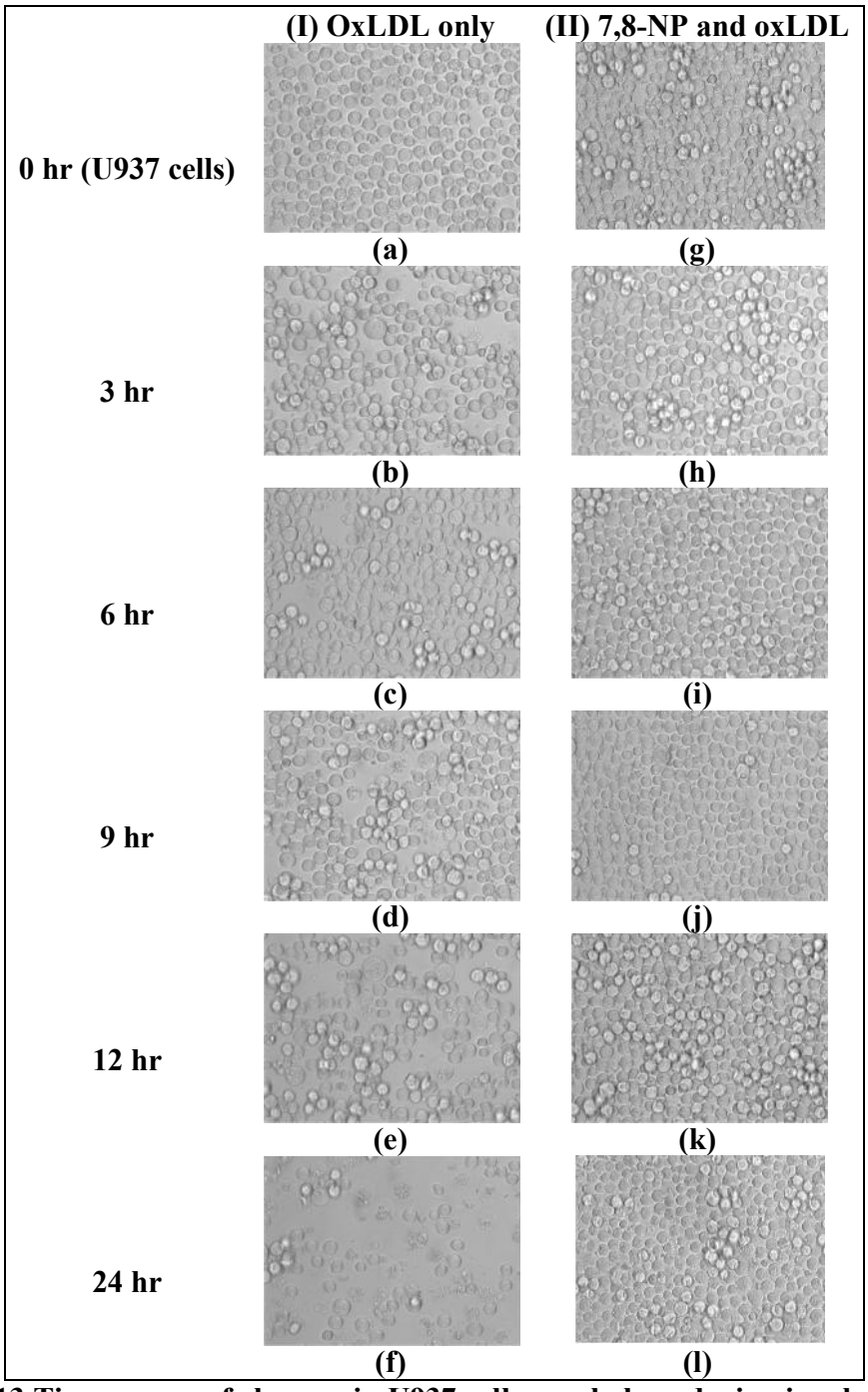

Figure 3.13 Time course of changes in U937 cell morphology during incubation with 7,8-NP.

U937 cells at 0.5 x10^6 cells/ml were incubated with 0.5 mg/ml oxLDL and without 200 μM 7,8-NP (I) or with 200 μM 7,8-NP (II) over a 24 hour period. (a), (g) 0 hr; (b), (h) 3 hr; (c), (i) 6 hr; (d), (j) 9 hr; (e), (k) 12 hr; (f), (l) 24 hr.

The time course study of U937 cell morphology showed cell damage in cells incubated for 3 to 24 hours with 0.5 mg/ml oxLDL alone (b, c, d, e and f) compared to control cells (a). There was no difference in cell morphology between control cells (g) and cells incubated with 200 μM 7,8-dihydroneopterin with 0.5 mg/ml oxLDL for any time point (h, i, j, k and l) (Figure 3.13). Therefore, 200 μM 7,8-dihydroneopterin protected the U937 cells from the changes in cell morphology caused by the oxLDL during the initial 3 hours of incubation.

With HMDM cells, the change in morphology was studied by pre-incubated HMDM cells for 10 minutes with various concentrations of 7,8-dihydroneopterin (0, 50, 100, 150 and 200 μM) in RPMI-1640 containing 10% HIHS with and without 2.0 mg/ml oxLDL for 24 hours (Figure 3.14). The timing of the changes in morphology were studied in a time course experiment where the HMDM cells were incubated with 2.0 mg/ml oxLDL for up to 24 hours with and without 200 μM 7,8-dihydroneopterin in RPMI-1640 containing 10% HIHS (Figure 3.15).

The presence of 7,8-dihydroneopterin alone (b, c, d and e), up to a concentration of 200 μM did not cause any change in HMDM cell morphology compared to control cells (a). The control cells were the typical, round shaped poached egg like morphology of HMDM cells. However, in the presence of 2.0 mg/ml oxLDL alone (f), the HMDM cells showed morphological changes characteristic of severe cellular damage characterised by swollen cells, appearance of large vacuoles, distorted cellular membranes and cell debris. Also, some cells were detached and floating in the medium.

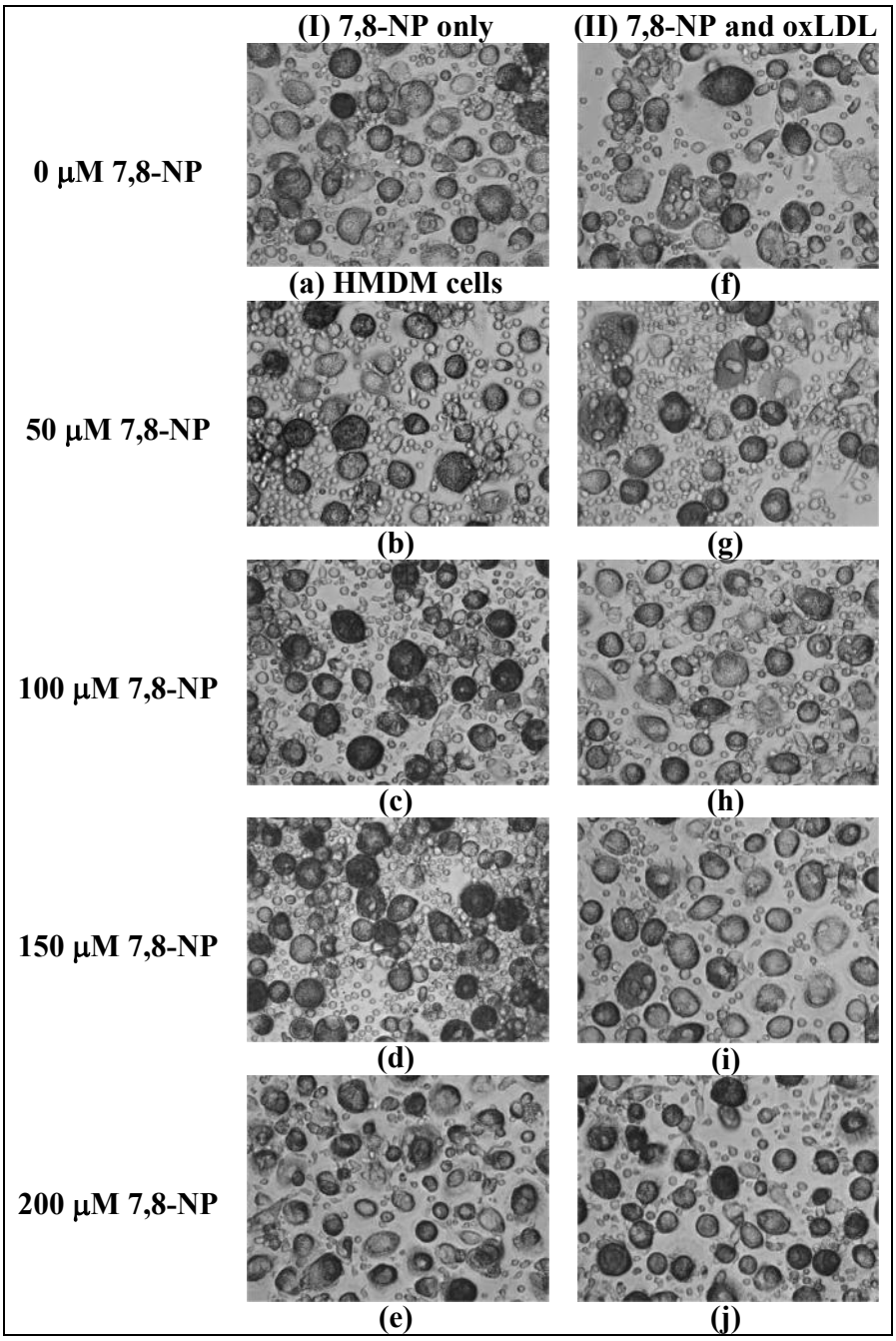

Figure 3.14 Changes in HMDM cell morphology during incubation with different concentrations of 7,8-NP.

HMDM cells at 5.0 x10^6 cells/ml were incubated with 200 μM 7,8-NP and without 2.0 mg/ml oxLDL (I) or with 2.0 mg/ml oxLDL (II) for 24 hours. (a), (f) 0 μM 7,8-NP; (b), (g) 50 μM 7,8-NP; (c), (h) 100 μM 7,8-NP ; (d), (i) 150 μM 7,8-NP; (e), (j) 200 μM 7,8-NP.

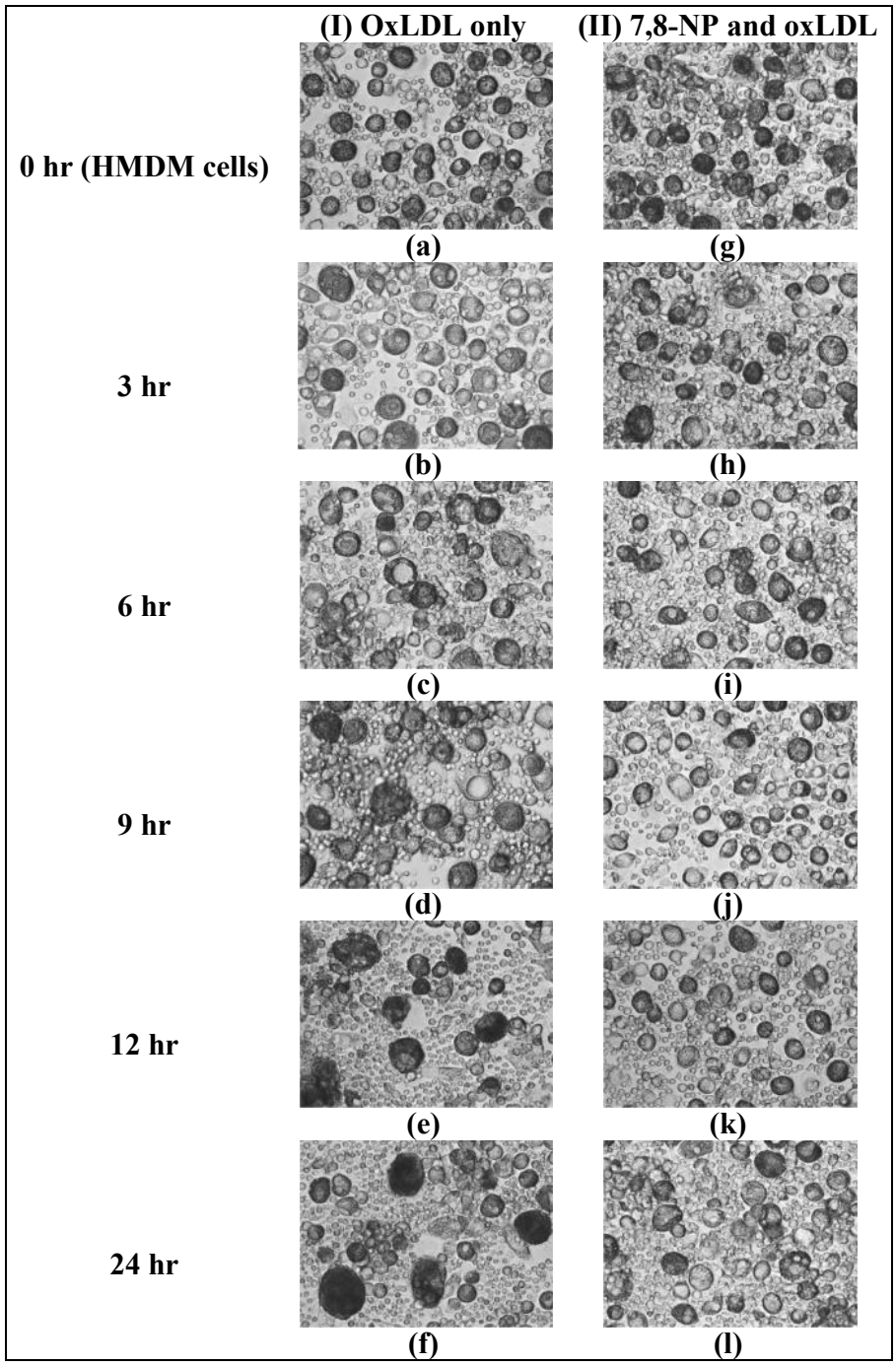

Figure 3.15 Time course of changes in HMDM cell morphology during incubation with 7,8-NP.

HMDM cells at 5.0 x10^6 cells/ml were incubated with 2.0 mg/ml oxLDL and without 200 μM 7,8NP (I) or with 200 μM 7,8NP (II) over a 24 hour period. (a), (g) 0 hr; (b), (h) 3 hr; (c), (i) 6 hr; (d), (j) 9 hr; (e), (k) 12 hr; (f), (l) 24 hr.

With 50 μM 7,8-dihydroneopterin (g) there was no observable reduction in the observed cellular damage compered to their respective control (b), but at a concentration of 100 μM (h) or greater (i and j) the cells morphology was the same as the control cell not treated with oxLDL (c, d and e) (Figure 3.14).

The time course study of the morphology of HMDM cells treated with 2.0 mg/ml oxLDL only showed cells with normal morphology after 3 hours (b) but damaged cells at 6 hours on wards (c) compered to control cells (a). There was no difference in cell morphology between control cells (g) and cells incubated with 200 μM 7,8-dihydroneopterin in the presence of 2.0 mg/ml oxLDL for any time point (h, i, j, k and l) (Figure 3.15). The data shows 100 μM 7,8-dihydroneopterin protects the HMDM cells from the effect of oxLDL on cell morphology after 6 hours.

3.3 Discussion

3.3.1 Characterisation of native LDL and oxidised LDL

There are significant differences in the characteristics of oxLDL prepared by different laboratories. A few factors can contribute to these differences and they include the concentration of LDL when oxidised, the types of oxidants used and their concentrations, the length of the oxidation, temperature of oxidation and transition metal or metal chelator concentration (Lougheed & Steinbrecher, 1996, Ziouzenkova *et al.*, 1998).

The REM of oxLDL used in this study was 3-fold greater than that of nLDL. The REM values of nLDL and oxLDL prepared in this study were similar to those reported in the literature (Darley-Usmar *et al.*, 1991, Asmis & Jelk, 2000a, Baird, 2003, Amit, 2008).

OxLDL used in the present study contained very high levels of 7-ketocholesterol, approximately 53–fold more than that of the nLDL. Analysis of highly oxidised LDL revealed that, in terms of oxysterol content, it contained almost exclusively unesterified 7-ketocholesterol (Harris *et al.*, 2006). In some studies, 7-ketocholesterol, when delivered directly to cell cultures, has been shown to be a potent inducer of apoptosis in various cell types (Berthier *et al.*, 2004, Leonarduzzi *et al.*, 2006, Lizard *et al.*, 1998). OxLDL prepared in this study also had a very high TBARS level, i.e. 130-fold greater than the nLDL. In contrast, oxLDL prepared by this laboratory using alternative methods contained between 9-fold (Baird, 2003) and 52-fold (Amit, 2008) greater TBARS than the corresponding nLDL. The present study used 500 μM $CuCl_2$ to oxidise 10 mg/ml LDL whereas Amit, (2008) used 300-350 μM $CuCl_2$ to oxidise 3 mg/ml LDL and Baird, (2003) used 50 μM $CuCl_2$ to oxidise 0.5 mg/ml oxLDL. The most likely explanation for the disparity in the TBARS values is that nLDL is very heterogeneous also, differences in conditions used would have large bearing. It contains different ratios of components such as polyunsaturated fatty acids (PUFAs) and antioxidants from each group of donors, which will then affect the properties of the resulting oxLDL (Esterbauer *et al.*, 1990). The high value of TBARS gives an indication that the resulting oxLDL is highly toxic. All three characteristics mentioned above (REM, 7-KC, TBARS) suggest that the oxLDL prepared in this study was heavily oxidised.

3.3.2 Cytotoxicity of oxLDL

3.3.2.1 Cell Viability

Following the characterisation of the heavily oxidised LDL, the MTT reduction assay was used to assess the degree of toxicity of the oxLDL to U937 cells and HMDM cells. The MTT assay measures the cells' ability to reduce MTT to formazan by NADPH oxidase enzymes (Mosmann, 1983b). This makes the assay very sensitive to changes in the cells' metabolic state. Other studies have used the trypan blue assay to measure the failure of the cell membrane and therefore, tends to be less sensitive to changes in cell metabolic activity (Duggan *et al.*, 2001). However, the MTT assay has previously been shown to correlate strongly with cell viability results obtained by trypan blue exclusion assay and phosphatidylserine exposure/propidium iodide staining in human monocyte-like U937 and THP-1 cells (Baird *et al.*, 2004). The loss of cell viability measured using the MTT assay was dependent on the oxLDL concentration and the duration of incubation. In this study, oxLDL concentrations between 0.2 mg/ml and 0.5 mg/ml oxLDL were toxic to U937 cells in terms of cell viability loss with 0.5 mg/ml oxLDL causing approximately 50% loss in cell viability after 24 hours incubation. With HMDM cells, oxLDL concentrations greater than 0.5 mg/ml and up to 2.0 mg/ml were toxic in terms of cell viability loss with 2.0 mg/ml oxLDL causing approximately 50% loss in cell viability after 24 hours incubation. The concentrations of oxLDL used in the present experiments are within the range of LDL concentrations in *vivo*, as serum concentrations of LDL in normolipidemic persons are maintained at approximately 3.0 mg/ml total mass (Esterbauer *et al.*, 1992). Previous results indicate that the equivalent median lethal dose

was between 1.5 and 2.0 mg/ml oxLDL in U937 cells (Baird, 2003) and between 1.0 and 2.0 mg/ml oxLDL in HMDM cells (Amit, 2008) depending upon the individual oxLDL preparation. A likely explanation for this difference in cytotoxicity is that different methods of copper ion-mediated LDL oxidation were used. The recently adapted method for LDL oxidation employed in this study eliminates the possibility of decreased yield during processing, and instead involves contained dialysis against copper ions at 37ºC (Gerry *et al.*, 2007).

The exact mechanism of oxLDL cytotoxicity is difficult to ascertain since oxLDL is not a single set of molecules but a large collection of different oxidation products. The structural and physical properties of the oxLDL vary according to method and degree of oxidation. The nature of oxLDL prepared by different laboratories is different due to variations in the conditions of oxidation and the source of the LDL (Gieseg *et al.*, 2009a). Slight variations in the conditions of oxidation might also result in a different degree of toxicity of oxLDL. Surprisingly, few authors characterise the oxLDL used in their studies except for stating that it is oxidised. This appears to have given rise to discrepancies in the reported biological effects or mechanisms implicated in oxLDL-induced death. The effect of oxLDL on various types of cells has been discussed in great detail in chapter 1 (section 1.2.6). The differences in oxLDL-induced cell death between U937 and HMDM cells may be due to the differences in cell type, cell size, varying mechanisms of uptake of oxLDL, cell metabolism, incubation conditions and the presence or absence of serum would also surly play a part. In previous studies, oxLDL showed a high degree of toxicity to U937 cells and HMDM cells (Firth *et al.*, 2008a, Gieseg *et al.*, 2001a, Gebicki *et al.*, 2000, Vicca *et al.*, 2003, Baird *et al.*, 2005). In U937 cells the time course studies

indicated that the loss of cell viability caused by oxLDL in the absence of serum occurred rapidly within 3 hours. With HMDM cells, the time course studies indicated a loss of cell viability in the following 6 hours of incubation with oxLDL in the presence of 10% HIHS. The presence of the serum in HMDM cells may affect the toxicity of the oxLDL in the first 3 hours and delay the drop in cell viability after 6 hours of incubation. In contrast, incubation of U937 cells with 10% HI-FCS in the presence of oxLDL did not result in a loss of cell viability. Therefore, HI-FCS in the cell culture media of U937 cells has a protective effect when cells are exposed to oxLDL. It is unknown whether this effect of serum protecting the U937 cell line is the results of serum antioxidants or a general cell stabilisation effect through various cytokines and/or nutrients. After ascorbate and urate, albumin by its concentration is the next most significant scavenger of ROS in the plasma (Kouoh *et al.*, 1999, Roche *et al.*, 2008). Albumin readily forms carbonyls and has a free thiol, Cys^{34}, which may play a further antioxidant role through thiol oxidation. Oxidised albumin is effectively cleared from the systemic circulation by the liver (Anraku *et al.*, 2004). However, in inflammation, the antioxidant properties of albumin have been considered biologically insignificant to protect cells but significant amounts of oxidised albumin has been found in the plasma in certain pathological conditions such as atherosclerosis, anemia, kidney and liver diseases (Anraku *et al.*, 2004, Quinlan *et al.*, 2005). Other studies in this laboratory have failed to demonstrate albumin damage during oxLDL incubation either. Other studies within this laboratory have clearly shown that the oxLDL induced stress is intracellular as dihydroethidium (DHE) staining and GSH loss are intracellular (Gieseg *et al.*, 2010). The significant amount of albumin could not enter the cell to provide the needed antioxidant protection

suggesting that the serum albumin protection is not via an antioxidant effect. The ascorbate within the serum would be taken up by the cell but with a serum concentration of only 10% it is unlikely that enough would be absorbed to have an effect. The combination of ascorbate and urate may be sufficient however. More revealing is that the same concentration of albumin is not protecting the HMDM cells suggesting that the serum protection effect is more cell stabilisation.

3.3.2.2 Morphology

Many published studies extensively use a single cell viability assay with little or no comment on what was actually happening to the cells physically. In this research we linked the MTT assay with an examination of U937 and HMDM cell morphology during incubation with a toxic concentration of oxLDL. This study clearly showed that oxLDL caused U937 cells and HMDM cells to show the classic morphology of necrotic cell death. Cell swelling and lysis was observed in both U973 and HMDM cells treated with oxLDL. Previous studies by this laboratory have shown that oxLDL caused necrotic death in HMDM cells in the presence of serum with a rapid loss of intracellular GSH without caspase-3 activation (Gieseg *et al.*, 2009b). Other studies found that the presence of toxic concentrations of oxLDL caused HMDM cells to undergo death processes of both apoptotic mechanism (in the absences of serum) due to cell membrane phosphatidylserine exposure and intracellular caspase-3 activation (Nhan *et al.*, 2003, Asmis & Begley, 2003). In U937 cells, oxLDL caused necrotic death with a rapid loss of intracellular glutathione, resulting in caspase-3 inactivation due to oxidation of the essential free thiol groups in the active site, with no phosphatidylserine exposure on the

plasma membrane (Baird *et al.*, 2004). In contrast, in THP-1 cells, oxLDL caused apoptotic death with a small reduction in cellular thiol, caspase-3 activation and plasma membrane phosphatidylserine exposure (Baird *et al.*, 2004). The difference in cellular response to oxLDL could be related to the varying mechanisms of uptake of oxLDL. There is growing evidence that CD36 has an important physiological function in the uptake of oxLDL by macrophages (Acton *et al.*, 1994) and by U937 cells (Nguyen-Khoa *et al.*, 1999). Macrophage scavenger receptors have been implicated as key players in the pathogenesis of atherosclerosis (Febbraio et al., 2000). OxLDL scavenger receptor A (SR-A) and CD36 are involved in foam cell formation and oxLDL mediated cell death (Plüddemanna *et al.*, 2007). During oxidative stress, an initial burst of oxLDL uptake may be the result of U937 cells expressing four-fold higher levels of CD36 scavenger receptor than seen in THP-1 cells (Nguyen-Khoa *et al.*, 1999). THP-1 cells have been shown to express the transcriptional regulator peroxisome proliferator-activated receptor-γ (PPAR-γ) in response to oxLDL. However, it has been found that this is not the case with U937 cells (Inoue *et al.*, 2001).

3.3.3 7,8-Dihydroneopterin protection to cell viability

7,8-Dihydroneopterin is a redox active compound capable of acting as either a pro-oxidant or antioxidant depending on the chemical environment. This laboratory has previously shown that at low micromolar concentrations, 7,8-dihydroneopterin is a very potent antioxidant (Gieseg *et al.*, 2009b, Gieseg *et al.*, 2008). It protects erythrocytes from lysis induced by peroxyl radicals ($ROO^{\bullet}$), hydrogen peroxide (H_2O_2) and hypochlorite (HOCl) (Gebicki *et al.*, 2000, Duggan *et al.*, 2001). In separate studies, 7,8-

dihydroneopterin has been demonstrated to protect free proteins, cellular proteins and protein thiol from oxidant damage (Duggan *et al.*, 2001, Duggan *et al.*, 2002). 7,8-dihydroneopterin has also been shown to dramatically increase, in a dose dependent manner, the lag time of LDL oxidation mediated by copper and $ROO^{\bullet}$ (Gieseg *et al.*, 1995). The present study found that 100-200 μM 7,8-dihydroneopterin provided significant protection for U937 and HMDM cells against toxic concentrations of heavily oxLDL that caused approximately 50% loss in cell viability in the absence of 7,8-dihydroneopterin. An examination of cell morphology during incubation with a toxic concentration of oxLDL with or without 7,8-dihydroneopterin showed that oxLDL-induced changes in cell morphology did not occur in the presence of 100 μM 7,8-dihydroneopterin.

These results are consistent with the findings from previous studies by this laboratory which showed that 7,8-dihydroneopterin provides protection for U937 cells (Baird *et al.*, 2005) and for HMDM cells (Amit, 2008, Gieseg *et al.*, 2010) against the toxic effect of oxLDL. The protective effect of 7,8-dihydroneopterin appears to depend on the nature of the cell and of the oxidant. For example, the addition of 7,8-dihydroneopterin to THP-1 cells failed to inhibit oxLDL-dependent loss of cell viability or restore the THP-1 cellular thiol content. Surprisingly, 7,8-dihydroneopterin was very effective at protecting U937 cells from oxLDL-induced cell viability and intracellular GSH loss (Baird *et al.*, 2005). The peroxyl radical scavengers, Trolox and α-tocopherol, have been shown to inhibit oxLDL- and 7β-hydroperoxycholesterol-induced apoptosis in blood derived macrophages and U937 cells, respectively (Asmis & Begley, 2003, Coffey *et al.*, 1995). It is possible that a similar mechanism is established in the U937 cells since 7,8-dihydroneopterin is a

potent peroxyl radical scavenger (Kappler *et al.*, 2007, Gieseg *et al.*, 1995). This suggests that 7,8-dihydroneopterin may protect cells from intracellular oxidative stress by scavenging oxidants generated within the cells due to the binding of oxLDL. This possible mechanism is further explored in the following chapters.

4 Effect of oxLDL and 7,8-dihydroneopterin on the metabolic function of U937 cells

4.1 Introduction

In chapter 3 the cytotoxic activity of laboratory prepared copper oxidised low density lipoprotein (oxLDL) was examined in both human derived monocyte-like (U937) cell line and human monocyte-derived macrophage (HMDM) cells by measuring the loss of cell viability. The main method for measuring the cell viability loss was the thiazolyl blue tetrazolium bromide (MTT) reduction assay which measures the ability of cells to generate reducing potential as nicotinamide adenine dinucleotide phosphate/nicotinamide adenine dinucleotide (NADPH/NADH). We therefore hypothesised that much of the cytotoxic process induced by oxLDL is through the loss of cellular metabolic function and 7,8-dihydroneopterin (7,8-NP) acts to prevent this loss of cellular function. Cellular activity is a complex network of enzymatic functions. To measure this activity, a number of key indicators are available to measure a cells metabolic activity which are lactate production, the activity of lactate dehydrogenase (LDH) and the glyceraldehyde-3-phosphate dehydrogenase (GAPDH) and adenosine triphosphate (ATP) formation.

Lactate is the end product of anaerobic glycolysis, which is one of the major metabolic pathways in macrophage cells. Lactate, which plays a role in cell metabolic functions, is produced by anaerobic respiration (fermentation) during normal metabolism. The enzymatic reduction of pyruvate to lactate by the LDH enzyme is coupled to the oxidation of NADH to NAD^+. Regeneration of NAD^+ is important for the continuity of glycolysis, when oxygen levels are restricted such that NAD^+ is being released from the

mitochondria. During inflammation macrophages produce a high lactate concentration (Loike *et al.*, 1993). Cancer cells such as U937 cells (a human histocytic lymphoma cell line) (Sundstrom & Nilsson, 1976), produce excessive lactate because of their dysfunctional mitochondria, which prevents their use of the citric acid or Krebs cycle. Consequently, pyruvic acid, the end product of glycolysis, which normally would enter the mitochondria for its total combustion into energy, is instead converted to lactate (John, 2001). Lactate has been shown to be not only an important intermediary in metabolic processes, but also an active player in inflammation (Leverve & Mustafa, 2002). Lactate enhanced lipopolysaccharide (LPS) stimulated inflammatory gene expression by U937 cells and monocyte derived macrophages indicating that lactate promotes the innate immune activation (Samuvel *et al.*, 2009, Nareika *et al.*, 2005).

Therefore, the LDH enzyme is one of the key enzymes in glycolysis (Nelson & Cox, 2005). LDH is an enzyme found in all cell types. LDH is rapidly released into the cell culture medium upon damage to the plasma membrane but appears to be relatively resistant to oxidative damage. This makes measurement of intracellular and extracellular LDH activity a useful marker of cell integrity and when coupled with lactate generation, overall glycolysis activity.

In contrast, the GAPDH is a key glycolytic enzyme in the cytosol which is known to be sensitive to oxidative stress (Sukhanov *et al.*, 2006). GAPDH enzyme has active site cysteine residue (Cys^{149}) that is relatively easily oxidised to a sulfenic acid, disulfides or other high oxidation product(s) (Torchinsky, 1981). The cysteine thiol group has been shown to be sensitive to oxidants by fluorescence labelling (Baty *et al.*, 2002). Loss of

the free thiol group within the enzymes catalytic site causes the loss of enzyme activity (Sukhanov *et al.*, 2006). Treatment of NOC18-HeLa cells, a human carcinoma cell line with NOR3 a nitric oxide donor induces oxidative stress that causes dimerisation, oligomerisation and aggregation of GAPDH through formation of intermolecular disulfide bonds and lead to cell death (Nakajima *et al.*, 2007). Combined with lactate measurement GAPDH activity measurement provides a sensitive measure of cellular glycolytic potential. Other studies have found that nitric oxide (NO) also denatures GAPDH (Mcdonald & Moss, 1993, Minetti *et al.*, 1996).

The role of catabolic metabolism is the production of adenosine triphosphate (ATP). Adenine and pyrimidine nucleotides are involved in the energetic charge and redox state of cells and participate as cofactors in enzymic reactions. It is, therefore, of interest to determine levels of both the high-energy phosphates, which are directly related to the cell energy level, and of the purine metabolites, which serve as substrates for the generation of oxygen-free radicals (Nelson & Cox, 2005). The high energy phosphate compound ATP, which is a coenzyme used as the main energy storage and transfer molecule in the cells of all known organisms, is further metabolised to adenosine diphosphate (ADP) then to adenosine monophosphate (AMP) and finally to hypoxanthine before conversion to xanthine and ending with uric acid (Furst & Hallstrom, 1992).

NADH plays a central role in the energy homeostasis of a cell. NADH carries electrons derived from catabolic reaction to their entry into the respiratory chain leading to the synthesis of ATP. This electron transfer results in the formation of NAD^+. Almost all of the cardiac ATP is regenerated by respiratory chain-linked phosphorylation, whereby the

reduction potential for the respiratory chain is mainly supplied as the reduced coenzyme NADH, which is oxidised by complex I of the respiratory chain. The cellular NADH content can be influenced by extracellular supply of metabolic substrates (Pelzmann *et al.*, 2003). The simultaneous measurement of these nucleotides provides a measure of overall cellular metabolic activity.

Cells usually need a constant supply of oxygen and nutrients to produce energy in the form of ATP. An insufficient supply of oxygen and nutrients results in ATP depletion, which leads to impaired cell function and cell death (Leppänen *et al.*, 2006). Compromised energy supply during hypoxia can be mitigated by ATP which is rapidly regenerated from ADP by creatine phosphate, via the creatine kinase pathway, and/or by anaerobic glycolysis (Hochachka & Guppy, 1987). ATP-demanding pathways are down-regulated, which often involves an inhibition of glycolysis, which generally results in a decrease in the rate of oxygen consumption (VO_2) (Hochachka *et al.*, 1996). Macrophages however function within sites in the body of low oxygen levels such as within an atherosclerotic plaque. The cells therefore should be able to reduce oxygen consumption and therefore generate more lactate. Bone marrow macrophages and human peripheral blood monocytes have increased survival under hypoxia in the presence of colony stimulating factor-1 (CSF-1), which is the primary growth factor for macrophages (Roiniotis *et al.*, 2009). Hypoxia actual stimulates the cells to generate their own CSF-1 which enhances the survival. Hypoxia caused these cells to have increased glycolytic activity, measured as increased glucose uptake, LDH enzyme activity and lactate production. Hypoxia also made the macrophages less adherent and show reduced spreading on tissue culture surface (Roiniotis *et al.*, 2009).

Studies on aortas removed from male albino New Zealand White rabbits, showed the tissue oxygen consumption decreased as the degree of atherosclerosis increased. In the advanced lesions, the ratio of foam cells increased, which lead to a thickening of the arterial wall and the rate of oxygen consumption decreased. Overall the cell viability decreased and the metabolic activity reduced (Bjornheden & Bondjers, 1987). Increased oxygen consumption is also a consequence of inflammation and activation of phagocytic cells. Zymasan activation of the murine macrophages-like cell line J774 causes increased oxygen consumption via activation of the membrane-bond NADPH-oxidase (NOX) which generates superoxide ($O_2^{\bullet -}$) and hydrogen peroxide (H_2O_2) (James *et al.*, 1998). OxLDL may also activate NOX activity so increasing macrophage oxygen consumption (Shatrov *et al.*, 2003).

Glutathione (GSH) is a key component of the cellular defense mechanism against oxidative and nitrosative stresses and plays important roles in the detoxification of free radicals (Ballatori *et al.*, 2009). Previous studies in our laboratory found that intracellular GSH is the main protective antioxidant against hypochlorite (HOCl) in HMDM cells. Interestingly, GSH is out competed for HOCl by 7,8-dihydroneopterin when added extracellularly to the cells (Yang, 2009). Removal of GSH from human monocyte-like cell line THP-1 cells with buthionine sulfoximine (BSO) demonstrated that GSH is the major antioxidant protecting cells from peroxyl radicals (Kappler *et al.*, 2007). Once GSH is lost from the cells, peroxyl radicals cause protein oxidation and cell death.

As discussed in the previous chapters, γ–interferon released from T-cells stimulates macrophages to synthesise 7,8-dihydroneopterin (Gieseg *et al.*, 2008). In *vitro* studies

have shown, 7,8-dihydroneopterin is a potent antioxidant that can protect a range of biomolecules and cells from various oxidants, including hydroxyl and peroxyl radicals (Gieseg *et al.*, 2008). It appears that the cells during oxidative stress need more protection than that provided by GSH suggesting the role of 7,8-dihydroneopterin is to give the cells added protection. Whether 7,8-dihydroneopterin addition can protect cellular metabolism from oxLDL will be examined in U937 cells as part of the research described in this chapter.

4.2 Results

4.2.1 Effect of oxLDL on lactate concentration released to U937 cell culture medium

The effect of oxLDL on the metabolic energy of U937 cells was studied by examining the lactate concentration released into the cell culture medium over 24 hours. A time-course study was carried out by incubating U937 cells in serum-free RPMI-1640 media without phenol red, with and without 0.5 mg/ml oxLDL over 24 hours. Untreated control cells were counted at each time point for comparison. There were no changes in the cell concentration with time (Table 4.1), but there was continuous production of lactate into the cell culture medium by the cells (Figure 4.1). During the initial 3 hours, there was a significant lactate production in oxLDL-treated cells, measured as lactate-release into the media, but after 3 hours lactate release completely stopped, with no significant increase in lactate levels at 6, 10 and 24 hours compared to the 0 hour control. In comparison to the respective controls of each time point, oxLDL-treated cells showed a rapid decrease in rate of lactate release into the cell culture medium (Figure 4.1).

Table 4.1 Time course of lactate production experiment showing control U937 cells concentration and treated cells.

Control cells were counted at various time points and treated cells with 0.5 mg/ml oxLDL were counted at 0 hours in the determination of lactate production experiment. U937 cells at 0.5 x10^6 cells/ml were incubated in media over a 24 hour period.

Time (hours)	0	3	6	10	24
Control cell conc. (x10^6 cells/ml)	0.5	0.5	0.49	0.48	0.49
Treated cell conc. (x10^6 cells/ml)	0.5				

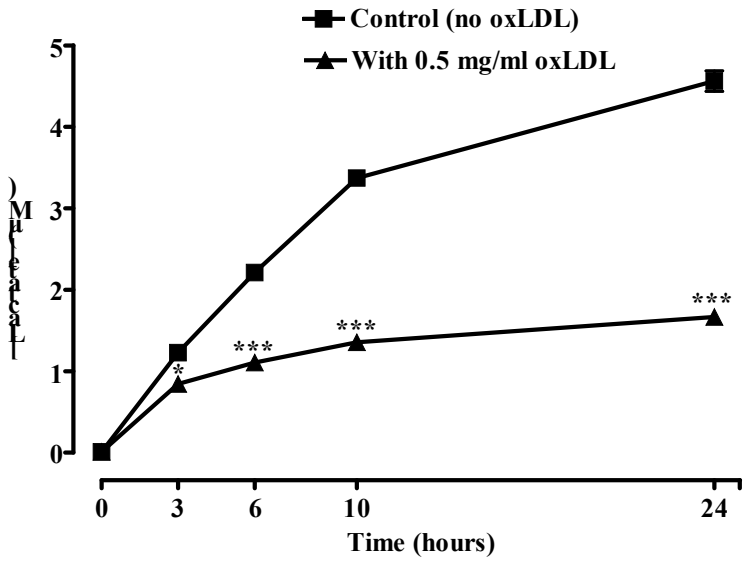

Figure 4.1 Time course showing the effect of oxLDL effect on lactate production in U937 cells.

U937 cells at 0.5 x10^6 cells/ml were incubated with 0.5 mg/ml oxLDL over a 24 hour period. The lactate released to the culture media was measured at various time points. Mean protein content was 50 mg/10^6 cells. Significance is indicated as *P < 0.05, ***P < 0.001 vs respective control of each time point containing cells alone. Results shown are the mean ± SEM of triplicate samples.

After 3, 6, 10 and 24 hours, lactate production was 32%, 50%, 60% and 64% lower than the respective controls at each time point (Figure 4.1). Therefore, oxLDL causes a dramatic decrease in the lactate production and release to the cell culture media from the initial 3 hours in U937 cells.

4.2.2 Effect of oxLDL on LDH activity in U937 cells

The effect of oxLDL on metabolic energy in U937 cells was studied by treating the cells with oxLDL and measuring the LDH activity both intracellularly and in cell culture media over 24 hours. U937 cells were incubated in serum-free RPMI-1640 media with 0.5 mg/ml oxLDL for 24 hours and the LDH activity measured at set time points. There was a loss of LDH activity inside the cells and an increase in LDH activity in the cell culture medium, after the initial 3 hour period (Figure 4.2a). The loss of LDH activity, as measured in cell pellets, was likely caused by the release of LDH through holes in plasma membrane. The observed release of LDH and corresponding cell lysis are caused by prolonged exposure to oxLDL. However, the total LDH activity remained stable over the course of the study (Figure 4.2b). This does not explain why within U937 cells, the oxLDL caused a drop in lactate production following the initial 3 hours, while the LDH enzyme release to the cell culture media did not occur after 3 hours. That indicating metabolism slowed before cell lysis took place and LDH was lost from the cells.

(a)

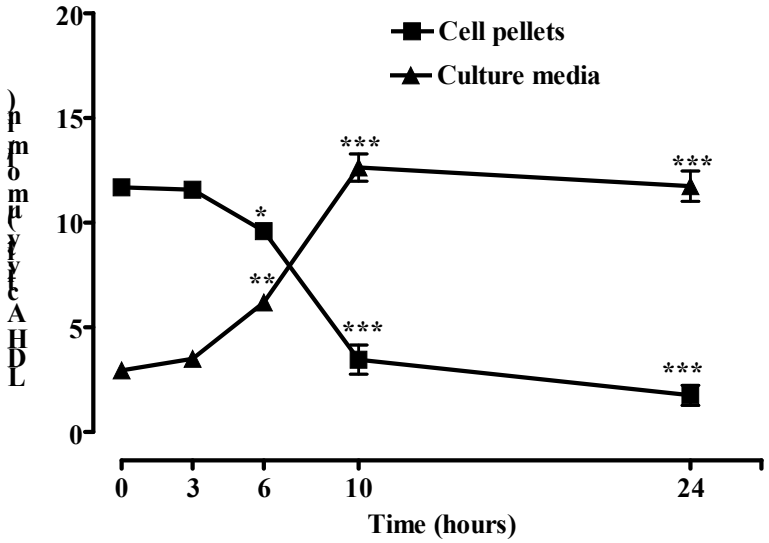

(b)

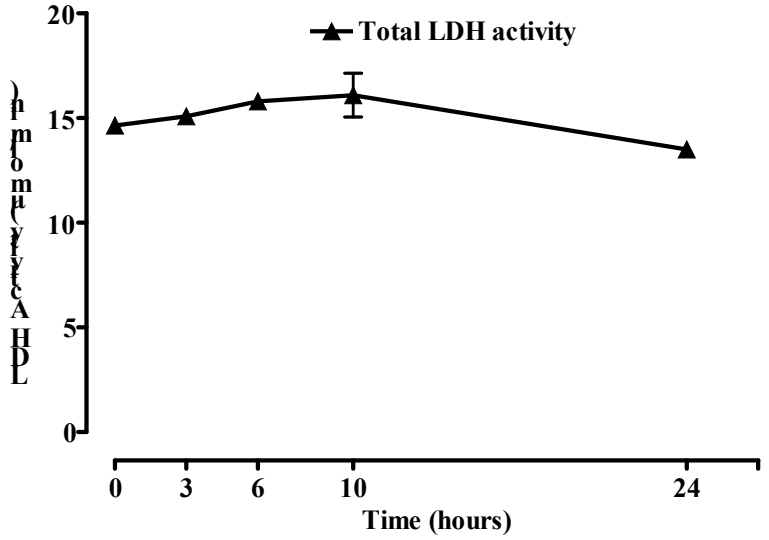

Figure 4.2 Time course showing the effect of oxLDL on the LDH activity in U937 cells.

U937 cells at 0.5 x10^6 cells/ml were incubated with 0.5 mg/ml oxLDL over a 24 hour period. (a) The LDH activity was measured in the cell culture media and in the cell pellets at various time points. (b) The total LDH activity was measured at various time points. Mean protein content was 50 mg/10^6 cells. Significance is indicated as * $P < 0.05$, ** $P < 0.01$, *** $P < 0.001$ vs respective 0 hr control. Results shown are the mean ± SEM of triplicate samples.

4.2.3 GAPDH activity in U937 cells

The loss of GAPDH activity was examined to explain the difference in timing between loss of LDH activity and lactate production in U937 cells treated with oxLDL. Initial studies examined the most suitable cell and oxLDL concentrations for the measurement of changes in GAPDH activity.

The GAPDH activity was measured in U937 cells using a range of different cell concentrations (0.3, 0.6, 1.2, 2.4 and 4.8 $x10^6$ cells/ml) to determine the best concentration to measure GAPDH activity changes. There was a concentration-dependent increase in GAPDH activity with increasing cell concentration (Figure 4.3). All cell concentrations between 0.3 and 4.8 $x10^6$ cells/ml gave sufficient signal to detect the GAPDH activity changes, even with low activity changes. In subsequent experiments, U937 cells were used at 0.5 $x10^6$ cells/ml to measure the GAPDH activity changes.

U937 cells were incubated in serum-free RPMI-1640 media for 48 and 24 hours with a range of oxLDL concentrations to determine a suitable concentration of oxLDL to examine changes in GAPDH activity. OxLDL caused a dramatic loss in GAPDH activity after 48 hours incubation with all oxLDL concentrations (Figure 4.4a). Incubation of U937 cells with 0.5 mg/ml oxLDL for 48 hours caused a 92% loss in GAPDH activity, 1.5 mg/ml oxLDL caused a 94% loss in GAPDH activity and 95% loss of GAPDH activity occurred with 3.0 mg/ml oxLDL. However, 48 hours appeared to be a relatively long time to expose the cells to such a toxic agent.

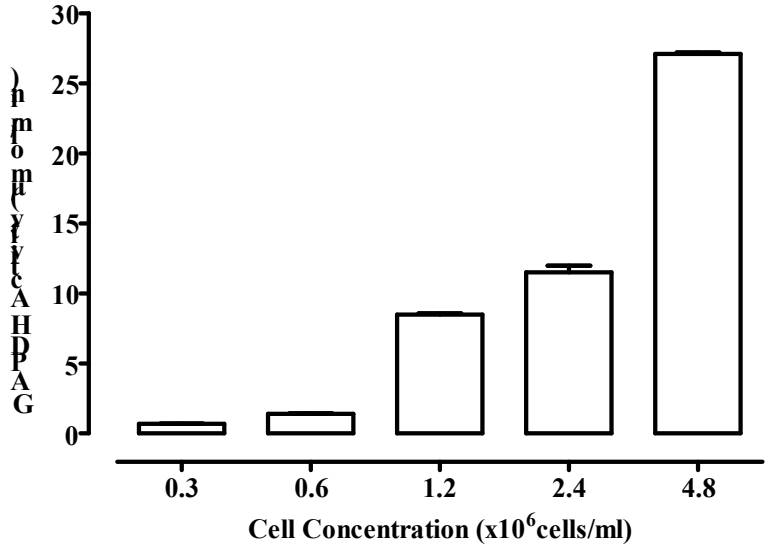

Figure 4.3 Effect of cell concentration of U937 cell GAPDH activity.
GAPDH activity (µmol/min) was measured in different concentrations of U937 cells ($x10^6$ cells/ml). Results shown are the mean ± SEM of triplicate samples.

(a)

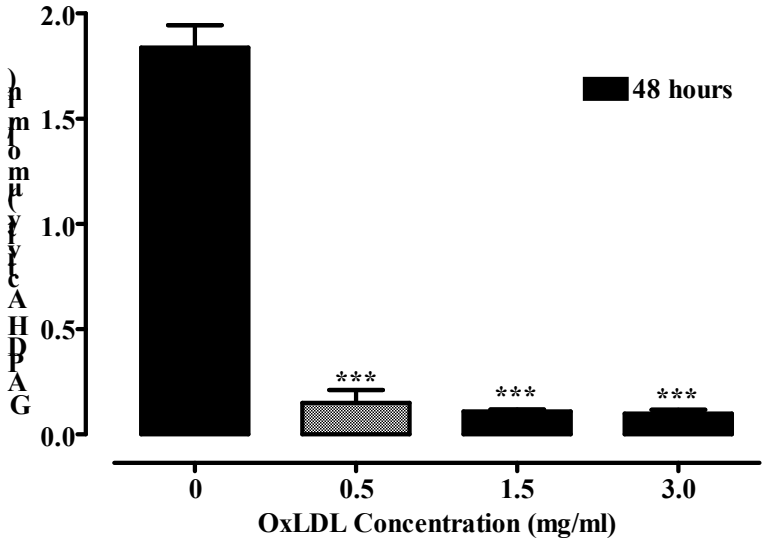

(b)

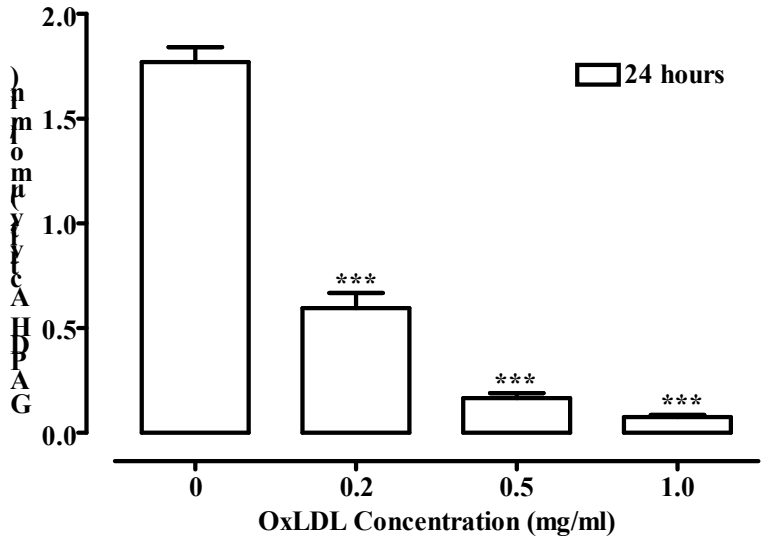

Figure 4.4 Effect of oxLDL concentration on GAPDH activity in U937 cells.
U937 cells at 0.5 x10^6 cells/ml were incubated with different oxLDL concentrations before GAPDH activity was measured: (a) (0, 0.5, 1.5 and 3.0 mg/ml) at 48 hours. (b) (0, 0.2, 0.5 and 1.0 mg/ml) at 24 hours. Mean protein content was 50 mg/10^6 cells. Significance is indicated as *** $P < 0.001$ vs 0.0 mg/ml oxLDL control. Results shown are the mean ± SEM of triplicate samples.

Using lower oxLDL concentrations and only incubating for 24 hours, oxLDL was shown to cause a concentration-dependent loss in U937 GAPDH activity after 24 hours (Figure 4.4b). Incubation of U937 cells for 24 hours with 0.2 mg/ml oxLDL caused a loss in GAPDH activity of 66%, with 0.5 mg/ml oxLDL a 91% loss in GAPDH activity was observed and a 96% loss in GAPDH activity with 1.0 mg/ml oxLDL. Therefore, in the time course experiments, U937 cells were incubated with 0.5 mg/ml oxLDL for no longer than 24 hours to determine the rate of GAPDH activity loss.

4.2.3.1 Rate of GAPDH loss by oxLDL in U937 cells

A time course study of the effect of oxLDL on GAPDH activity was conducted by incubating U937 cells in serum-free RPMI-1640 media with 0.5 mg/ml oxLDL for 24 hours. The GAPDH activity dropped dramatically, reaching a level 64% less than the control after 3 hours. The GAPDH activity decreased by 75% after 6 hours, followed by 90% loss after 10 and 24 hours (Figure 4.5). Therefore, GAPDH activity in U937 cells is very sensitive to the effect of oxLDL, which showed a rapid decrease between 0 and 3 hours of incubation. The rate of GAPDH loss appears to follow that observed with the timing of oxLDL-induced loss in lactate production.

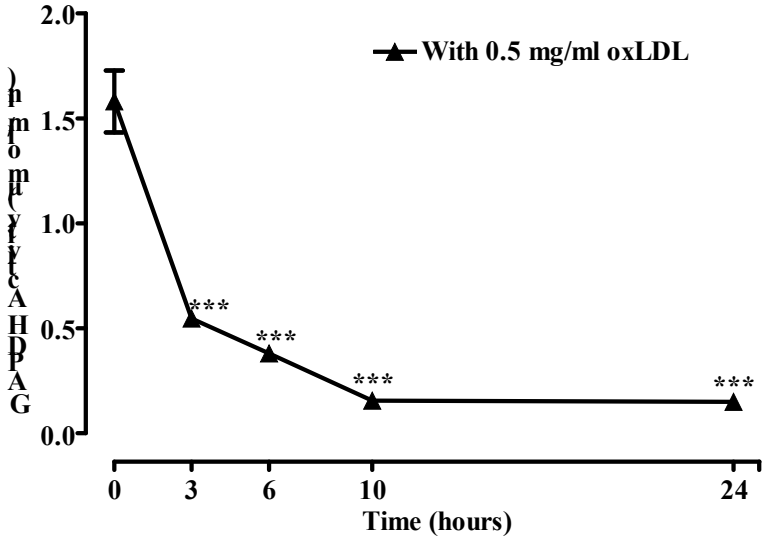

Figure 4.5 Time course showing the effect of oxLDL on GAPDH activity in U937 cells.

U937 cells at 0.5 x10^6 cells/ml were incubated with 0.5 mg/ml oxLDL over a 24 hour period. The GAPDH activity was measured at various time points. Mean protein content was 50 mg/10^6 cells. Significance is indicated as *** $P < 0.001$ vs 0 hr control. Results shown are the mean ± SEM of triplicate samples.

4.2.3.2 Effect of foetal calf serum on oxLDL induced loss of GAPDH activity in U937 cell.

The rate of GAPDH activity in the presence of heat-inactivated foetal calf serum (HI-FCS) was studied by incubating U937 cells in RPMI-1640 with 10% HI-FCS and 0.5 mg/ml oxLDL for 24 hours (Figure 4.6). There was no significant change in GAPDH activity in the presence of 10% HI-FCS and 0.5 mg/ml oxLDL during 24 hours incubation (Figure 4.6). Therefore, HI-FCS had a protective effect against the toxic effects of oxLDL on GAPDH enzyme activity in U937 cells.

4.2.4 Effect of oxLDL on GAPDH protein thiol in U937 cells

The most likely cause of the loss of GAPDH activity is the oxidation of the free thiol in the active site. This was measured by fluorescence labeling of the reduced thiol using 5-iodacetamidoflurescein (5-IAF) and separation of the cellular proteins by sodium dodecyl sulfate polyacrylamide gel electrophoresis (SDS-PAGE). This method has been used to previously show that GAPDH is one of the main cellular proteins whose thiol are oxidised during oxidative stress (Sukhanov *et al.*, 2006). Using this technique the effect of oxLDL on GAPDH free thiol levels was examined. Lysates were prepared by incubating U937 cells in serum-free RPMI-1640 media with 0.5 mg/ml oxLDL for 12 hours and reduced protein thiol were labeled with 5-IAF (Figure 4.7). Following 5-IAF staining, a series of intense bands were observed (Figure 4.7a). Lane 1 corresponds to control cells (without oxLDL added) and is indicative of the large number of reduced thiol proteins present in the cells. Lanes 2, 3 and 4 represent the incubation of U937 cells

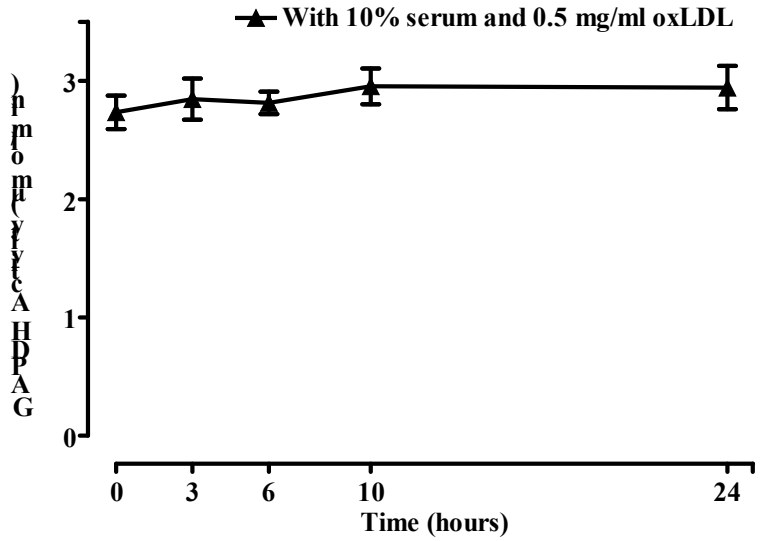

Figure 4.6 Time course showing the effect of oxLDL on GAPDH activity in U937 cells in the presence of HI-FCS.
U937 cells at 0.5 x10^6 cells/ml were incubated with 0.5 mg/ml oxLDL and 10 % HI-FCS over a 24 hour period. The GAPDH activity was measured at various time points. Mean protein content was 50 mg/10^6 cells. Results are compared to the 0 hr control and are the mean ± SEM of triplicate samples.

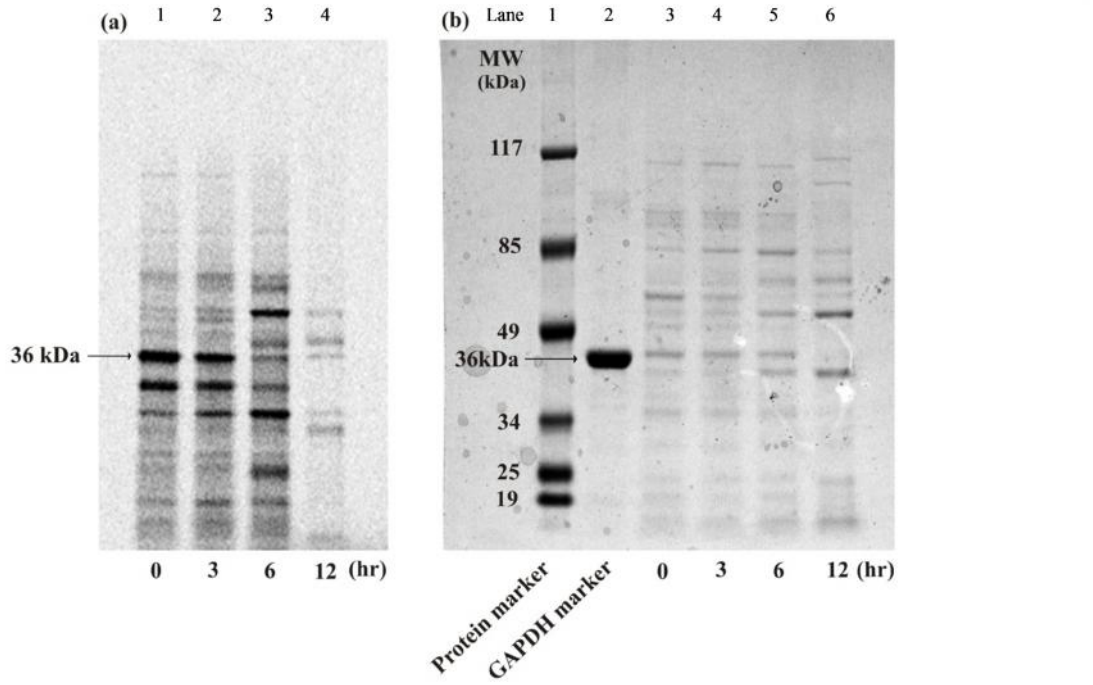

Figure 4.7 The effect of oxLDL on the reduction of thiol groups in GAPDH in U937 cells using SDS-PAGE.
U937 cells at 5.0 x10^6 were incubated with 0.5 mg/ml oxLDL over a 12 hour period. (a) Reduced thiol following IAF stain. Lane 1: Control U937 cells without oxLDL added; Lane 2: 3 hr; Lane 3: 6 hr; Lane 4: 12 hr. (b) Reduced thiol following coomassie blue stain. Lane 1: protein marker; Lane 2: GAPDH marker; Lane 3: Control U937 cells without oxLDL added; Lane 4: 3 hr; Lane 5: 6 hr; Lane 6: 12 hr. Protein content was 25 μg/20 μl of sample/gel well.

with oxLDL for 3, 6 and 12 hours, respectively. Over the 12 hours of incubation there was many changes in the thiol pattern with some proteins become more reduced (36 kDa band at 6 hours) while all others before 6 hours were less. Authentic pure GAPDH runs as a single 36 kDa band (line 2, Figure 4.7b) which aligns to a strongly fluorescing 5-IAF staining band in the zero time samples. This 36 kDa bands 5-IAF staining decreases with increasing time showing there is less free thiol associated with this protein.

The coomassie staining showed that the protein associated with the 5-IAF thiol staining was relatively stable but then was significantly lost at 12 hours suggesting the protein had been degraded. The 12 hours coomassie staining still shows many other proteins with no significant change in staining intensity which suggests the loss of this possible GAPDH coomassie staining protein band was a lost due to selective degradation as has been previously described in endothelial cells (Sukhanov *et al.*, 2006).

To gain a better understanding of the staining of the hypothesised GAPDH band, the staining intensity was digitised and plotted against coomassie staining and the GAPDH activity. The loss in 5-IAF staining intensity is faster than the loss detected by coomassie staining (Figure 4.8a). There was no significant loss in 5-IAF staining over the first 3 hours during which there was a major loss in enzyme activity (Figure 4.8b). However after 3 hours there was a linear relation between the 5-IAF staining intensity of the 36 kDa band and the GAPDH activity (Figure 4.8b). The intensity of fluorescing 5-IAF staining protein band decreased as the GAPDH activity decreased.

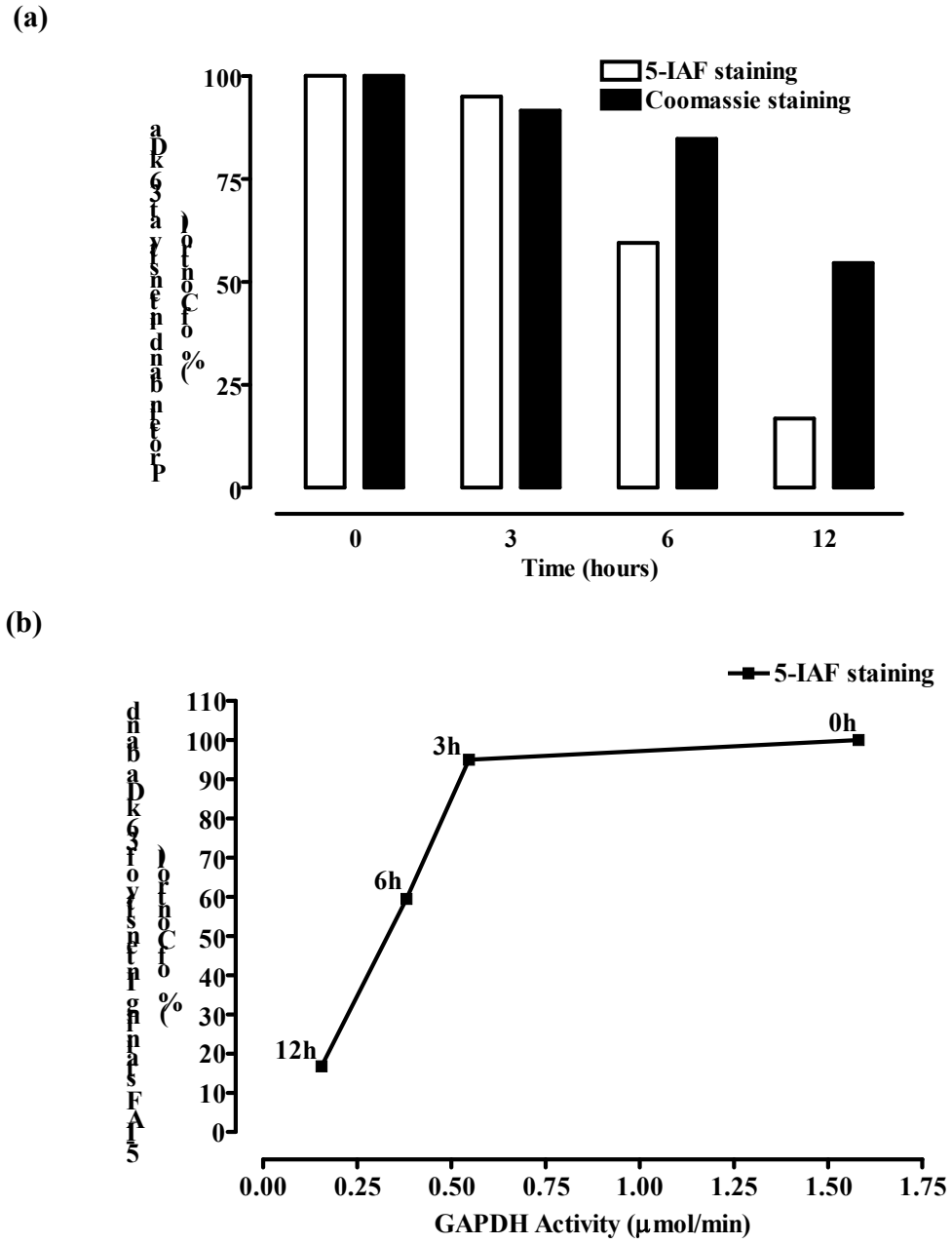

Figure 4.8 Measurement of 36 kDa protein band 5-IAF staining intensity.
The staining intensity of 5-IAF and coomassie of the 36 kDa band in Figure 4.7 was digitised using Image J software and the data was plotted for each time point to show (a) difference in coomassie and 5-IAF staining and (b) 5-IAF staining against GAPDH activity in U937 cells at 5.0 x10^6 were incubated with 0.5 mg/ml oxLDL over a 12 hour period.

This data shows that loss of reduced thiol in the 36 kDa proposed to be the GAPDH protein band is associated with the loss in GAPDH enzyme activity. The data supports the hypothesis that GAPDH activity loss is due to the oxidation of the free thiol in the GADPH activity site.

4.2.5 Effect of oxLDL on GSH concentration in U937 cells

Cellular GSH is a potent antioxidant and can efficiently neutralise reactive oxygen species (ROS) (Bilzer & Lauterburg, 1991). It is also one of the key redox agents maintain the reducing environment, and therefore the stability of the thiol status of proteins such as GAPDH. The potential effect of oxLDL on GSH has been previously documented by this laboratory (Gieseg *et al.*, 2009b) but the exact timing of the GSH loss in relationship to the GAPDH loss had not been examined.

U937 cells were incubated in serum-free RPMI-1640 media with and without 0.5 mg/ml oxLDL for 24 hours and the GSH levels determined at various time points. The number of control (no oxLDL) cells did not change with the time (Table 4.2), but there was a steady increase in the intracellular GSH concentration with increasing time (Figure 4.9). In contrast, in the oxLDL-treated cells, the intracellular GSH concentration decreased over time. Over the first 3 hours the GSH level did not change and was 36% less than that of the corresponding control cells. This difference between the control and oxLDL treated cell increased with time as the oxLDL treated GSH levels actual decreased. OxLDL caused a loss in intracellular GSH in the U937 cells and prevented the increase in

Table 4.2 Time course of GSH concentration experiment showing control U937 cells concentration and treated cells.

Control cells were counted over time and treated cells with 0.5 mg/ml oxLDL were counted at 0 hours in the determination of GSH concentration experiment. U937 cells at 0.5 x10^6 cells/ml were incubated in media over a 24 hour period.

Time (hours)	0	3	6	10	24
Control cell conc. (x10^6 cells/ml)	0.5	0.49	0.48	0.48	0.5
Treated cell conc. (x10^6 cells/ml)	0.5				

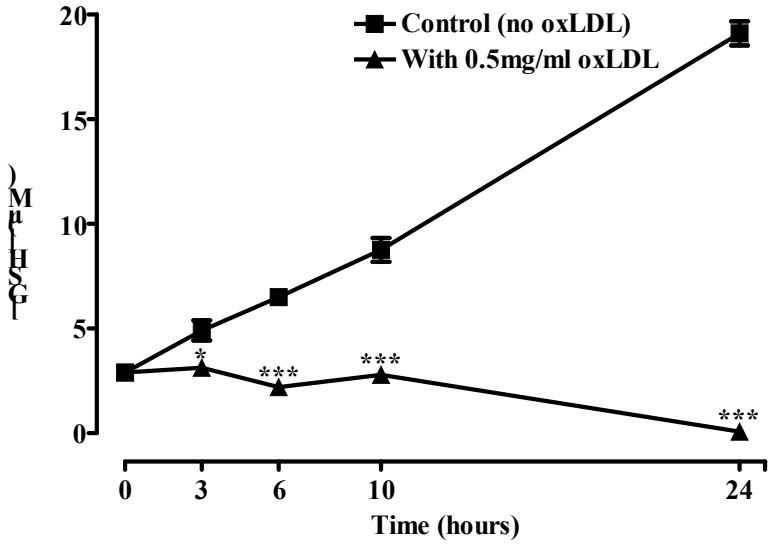

Figure 4.9 Time course showing the effect of oxLDL on GSH concentration in U937 cells.

U937 cells at 0.5 x10^6 cells/ml were incubated with or without 0.5 mg/ml oxLDL over a 24 hour period. The intracellular GSH concentration was determined by HPLC analysis. Mean protein content was 50 mg/10^6 cells. Significance is indicated as * $P < 0.05$, *** $P < 0.001$ vs respective control at each time point containing cells alone. Results shown are the mean ± SEM of triplicate samples.

GSH levels observed in the control cells. It is uncertain from this data whether oxLDL is preventing GSH formation or driving the oxidation of the GSH present in the cell.

4.2.6 Effect of oxLDL on intracellular purine nucleotides ATP, ADP, AMP, NAD^+ and $NADP^+$ levels in U937 cells

The importance of intracellular purine nucleotides, ATP, ADP and AMP, lie in the continuance of cellular homeostasis, modification of energy loads and play a key role in mitochondrial metabolic control (Hochachka & Mcclelland, 1997). The importance of NAD^+ is for the formation of NADH, which acts to transfer electrons between both the citric acid cycle and glycolysis and electron transport chain (Alberts *et al.*, 2002). The ratio of NAD^+ and NADH are markers of metabolic state and intracellular redox potential (Lin & Guarente, 2003). Although the NAD^+: NADH ratio may be a good indicator of metabolic state, in practice it is very labile and measurement is difficult (Caruso *et al.*, 2004). The effect of oxLDL on total metabolic energy of U937 cells was studied by treating cells with oxLDL and examining intracellular purine nucleotides, ATP, ADP, AMP, NAD^+ and $NADP^+$ at various time points. Initial studies were focused on developing the method for use with U937 cells using HPLC analysis. The retention times and the areas under chromatogram peaks for the purine nucleotides standards are shown in Table 4.3. The chromatograms of standards purine nucleotides and purine nucleotides levels (ATP, ADP, AMP, NAD^+ and $NADP^+$) and their levels in U937 cells incubated with 0.5 mg/ml oxLDL over the 12 hour time period are shown in Figure 4.10.

Table 4.3 HPLC characterisation of purine nucleotides ATP, ADP, AMP, NAD^+ and $NADP^+$ standards.

The HPLC analysis shows the retention times and the areas under chromatogram peaks of the purine nucleotides standards with 25 µM concentration.

Standard (25 µM)					
Purine nucleotides	**NAD^+**	**AMP**	**$NADP^+$**	**ADP**	**ATP**
Retention Time	14.666	17.605	21.904	25.090	33.216
Area	1080447	840132	904460	580779	559045

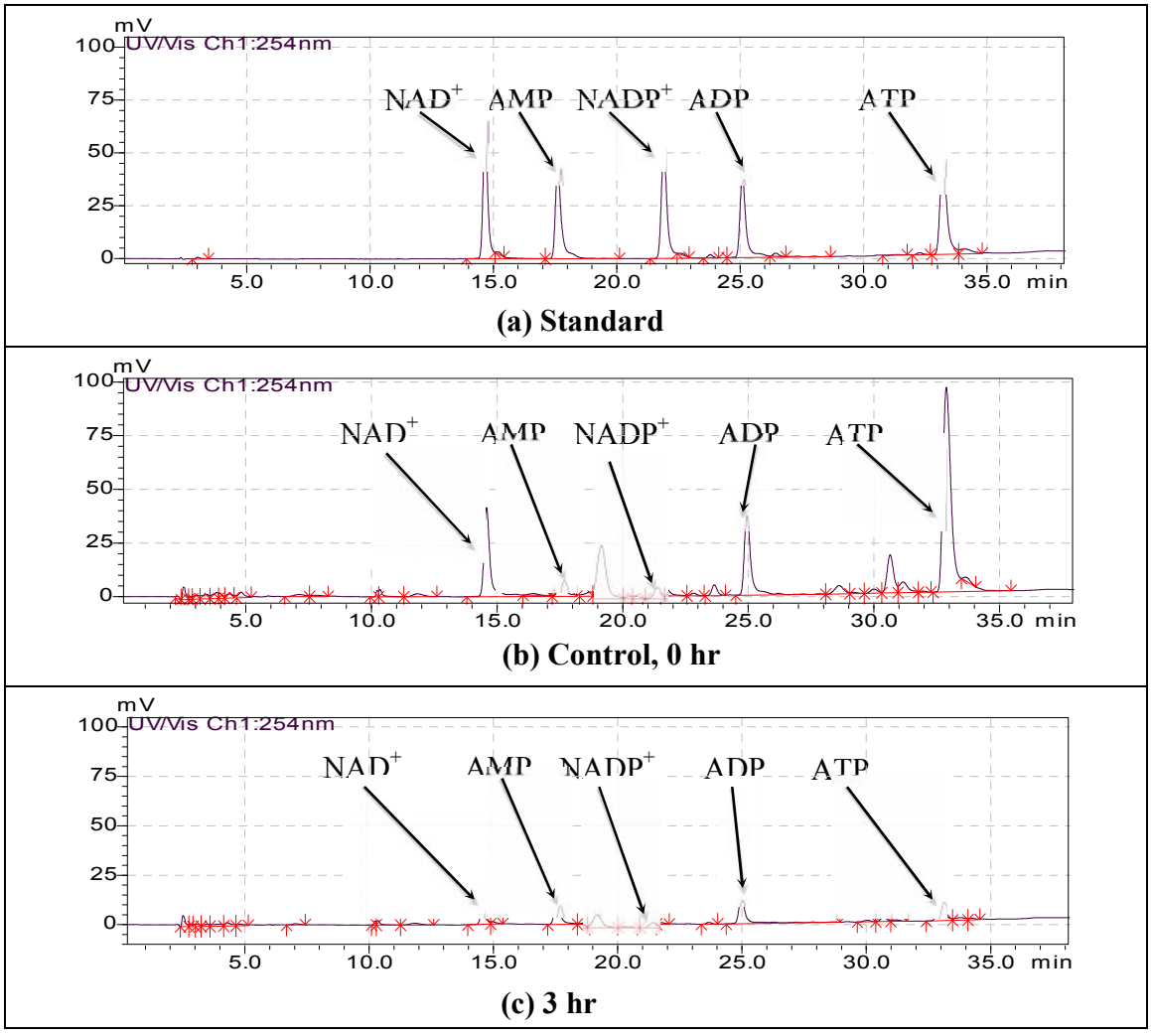

(a) Standard

(b) Control, 0 hr

(c) 3 hr

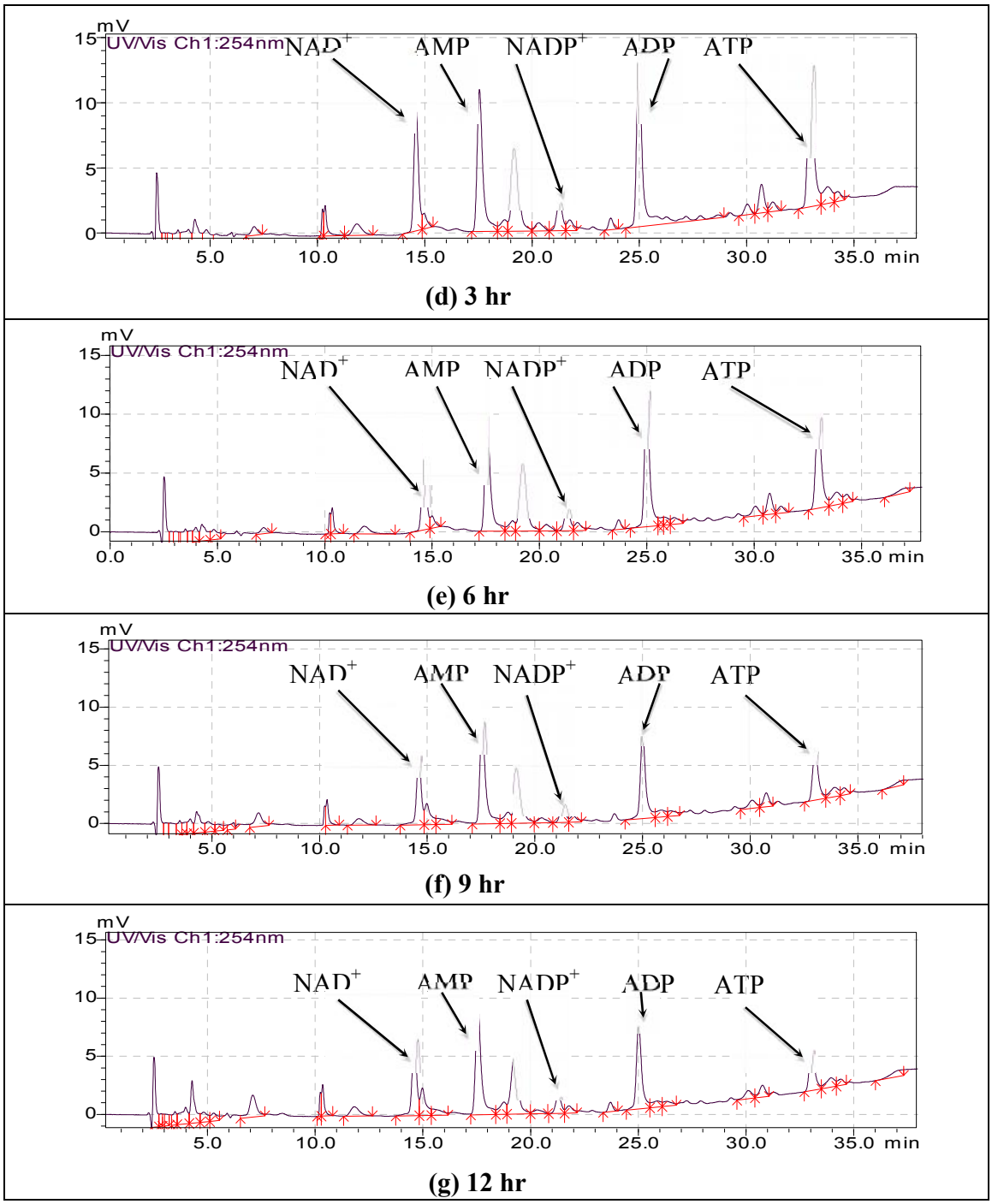

Figure 4.10 Chromatograms showing the effect of oxLDL on purine nucleotides ATP, ADP, AMP, NAD^+ and $NADP^+$ levels in U937 cells over time.
5.0 x10^6 of U937 cells were incubated with 0.5 mg/ml oxLDL over a 12 hour period. (a) purine nucleotides standards; (b) Control U937 cells without oxLDL added; (c) U937 cells with oxLDL after 3 hr; and at scale 0-15 mV (d) U937 cells with oxLDL after 3 hr; (e) 6 hr; (f) 9 hr; (g) 12 hr.

A time course study was conducted to investigate the effect of oxLDL on purine nucleotides levels by incubating U937 cells in serum-free RPMI-1640 media with 0.5 mg/ml oxLDL over a 12 hour period (Figure 4.11 and Figure 4.12).

There was an increase in the ATP level of control cells during the first 3 hours, after which time the ATP level then remained stable until 12 hours (Figure 4.11a). In oxLDL-treated cells, the ATP level dropped dramatically after 3 hours to 70% of the respective control values at 3 hours. The ATP level continued to decline, reaching a 75, 87 and 83% decrease compared to the corresponding control data, after 6, 9 and 12 hours, respectively (Figure 4.11a).

There was a slight increase in the ADP level of control cells during the initial 3 hours, and then the ADP level remained stable for the duration of the incubation (Figure 4.11b). In oxLDL-treated cells, the ADP level decreased by 49% during the first 3 hours. The ADP level continued to decline, reaching a level that was 65%, 79% and 85 % less than that of the corresponding control data, after 6, 9 and 12 hours, respectively (Figure 4.11b).

In comparison, there was no change in AMP level in control cells and in treated cells over the incubation period (Figure 4.11c).

The combined data for AMP, ADP and ATP levels over the 12 hours incubation are shown together in Figure 4.11d to clearly show the changes in concentration. OxLDL caused a decrease in ATP and ADP levels from initial 3 hours.

(a)

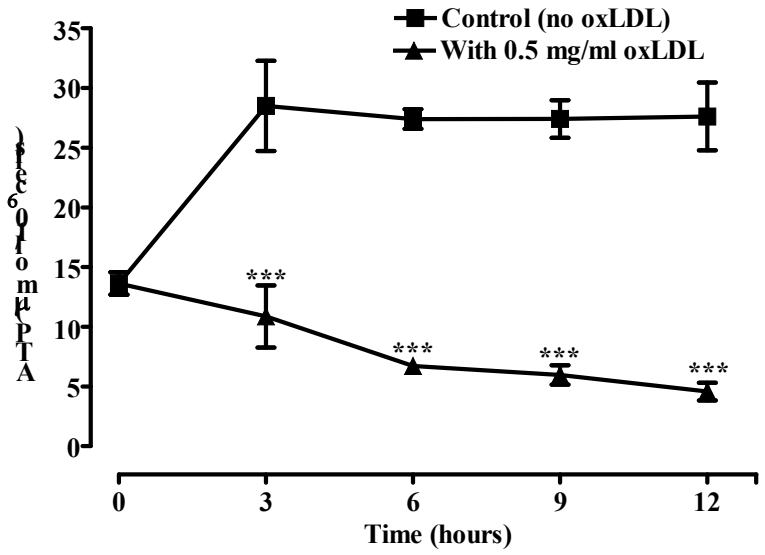
Control (no oxLDL)
With 0.5 mg/ml oxLDL
35
30
25
20
15
10
5
0
***
***
***
***
0
3
6
9
12
Time (hours)

(b)

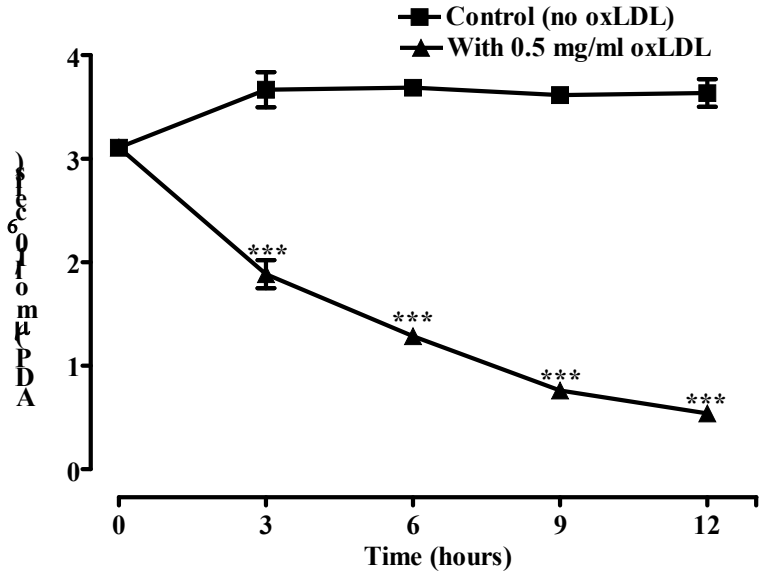
Control (no oxLDL)
With 0.5 mg/ml oxLDL
4
3
2
1
0
***
***
***
***
0
3
6
9
12
Time (hours)

(c)

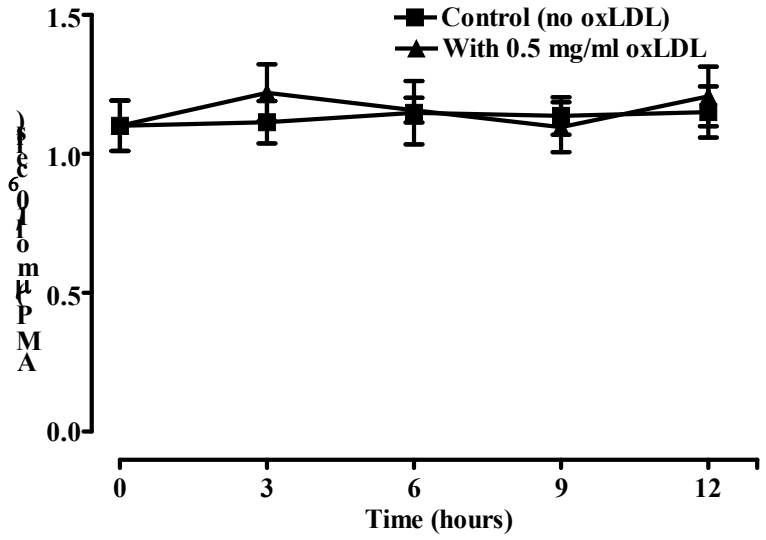

(d)

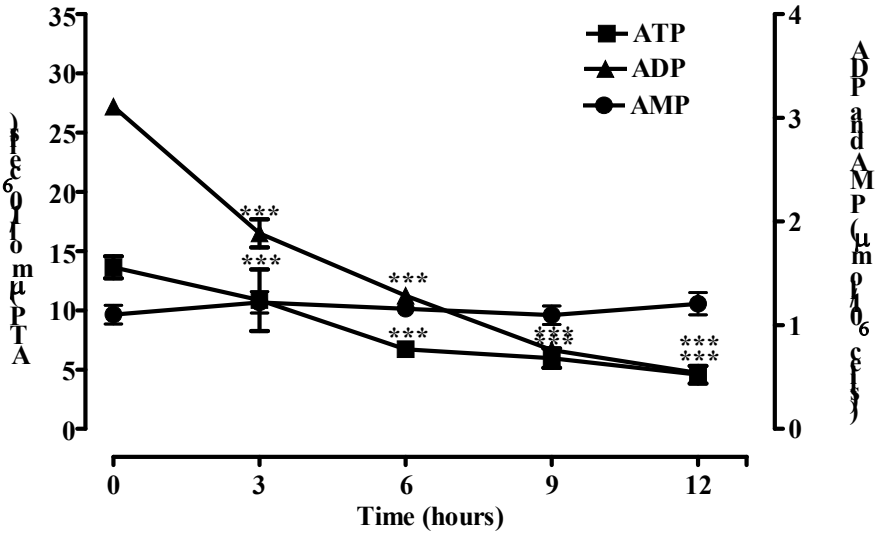

Figure 4.11 Time course showing the effect of oxLDL on ATP, ADP and AMP levels in U937 cells.

5.0 x10^6 of U937 cells were incubated with 0.5 mg/ml oxLDL over a 12 hour period. (a) ATP; (b) ADP; (c) AMP; (d) All ATP, ADP and AMP. All concentrations were determined by HPLC analysis. Mean protein content was 50 mg/10^6 cells. Significance is indicated as *** $P < 0.001$ vs respective control at each time point containing cells alone. Results shown are the mean ± SEM of triplicate samples.

This finding is in parallel to the loss in lactate, GSH levels and GAPDH activity that were measured. Subsequently, the metabolic energy appears to slow down before cell lysis occurs.

There was a decrease in the NAD^+ level in control cells during the initial 3 hours, then the NAD^+ level remained stable over the following 9 hours (Figure 4.12a). In oxLDL-treated cells the NAD^+ level had dropped dramatically, by 54% after 3 hours. The NAD^+ level continued to decline, reaching a level 68% lower than the corresponding control after 6 hours, and 73% lower after 9 and 12 hours (Figure 4.12a).

There was a decrease in the $NADP^+$ level in control cells during the initial 3 hours, before the $NADP^+$ level stabilised for the remaining length of the incubation (Figure 4.12b). In comparison, in oxLDL-treated cells, the $NADP^+$ level dropped by 46% during the initial 3 hours. The $NADP^+$ level continued to decline and reached levels that were 60 and 70% lower than their corresponding controls after 6 and 9 hours, respectively. There was no further change in $NADP^+$ levels after 9 hours incubation (Figure 4.12b).

Unfortunately NADH and NADPH were found to be too labile to measure using this technique in U937 cells.

(a)

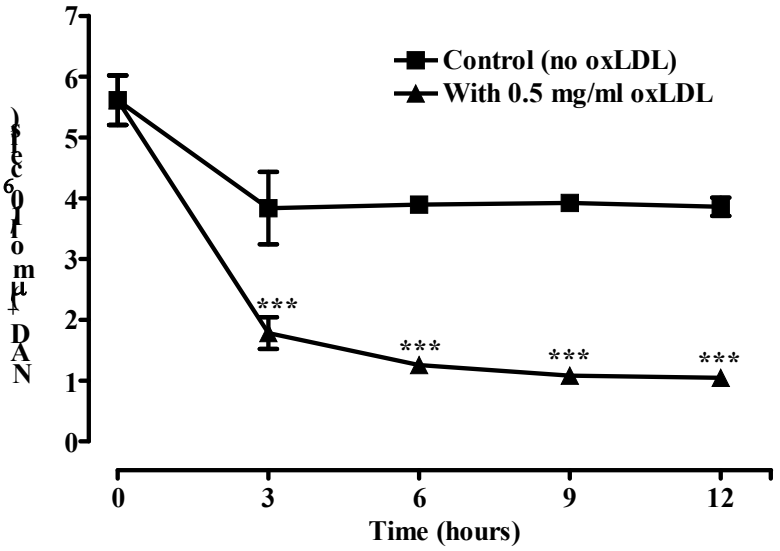

(b)

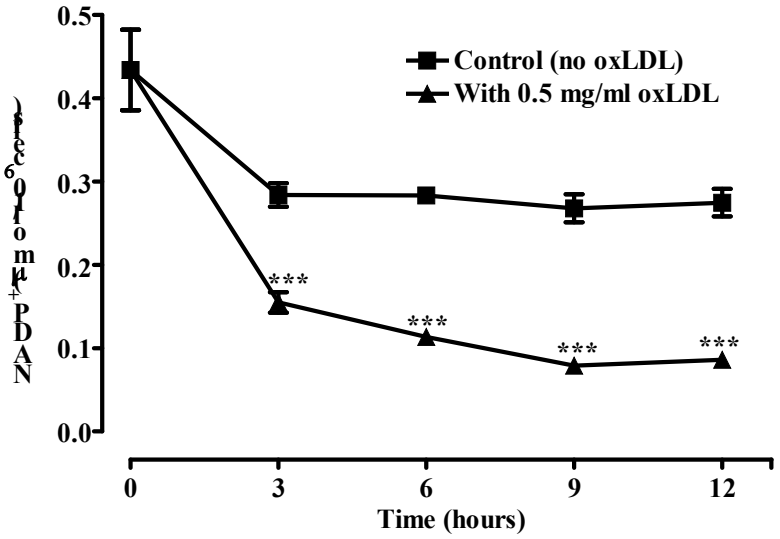

Figure 4.12 Time course showing the effect of oxLDL on NAD^+ and $NADP^+$ levels in U937 cells.

5.0 x10^6 of U937 cells were incubated with 0.5 mg/ml oxLDL over a 12 hour period. (a) NAD^+; (b) $NADP^+$. All concentrations were determined by HPLC analysis. Mean protein content was 50 mg/10^6 cells. Significance is indicated as *** $P < 0.001$ vs respective control at each time point containing cells alone. Results shown are the mean ± SEM of triplicate samples.

4.2.7 Effect of 7,8-dihydroneopterin concentration on lactate production in the cell culture media of oxLDL-treated U937 cells

All previous studies in U937 cells have shown 7,8-dihydroneopterin prevents the destructive effects of oxLDL on cells. The antioxidant effect of 7,8-dihydroneopterin on lactate production in cell culture media was studied by pre-incubated U937 cells for 10 minutes with various concentrations of 7,8-dihydroneopterin in serum-free RPMI-1640 (no phenol red) media before incubation with and without 0.5 mg/ml oxLDL for 12 hours (Figure 4.13).

The presence of 7,8-dihydroneopterin alone, up to a concentration of 200 μM did not affect the lactate level in U937 cells (Figure 4.13), while the presence of 0.5 mg/ml oxLDL alone caused a 50% decrease in the lactate concentration of the cell culture media (Figure 4.13). The presence of 7,8-dihydroneopterin caused a significant concentration dependent protection against oxLDL-induced loss of lactate production but only at 7,8-dihydroneopterin concentrations above 50 μM. In the presence of 100 and 150 μM 7,8-dihydroneopterin the lactate production increased by approximately 35% and 41% compared to the oxLDL only control, respectively (Figure 4.13).

A maximum protective effect was established with 200 μM 7,8-dihydroneopterin. The results show that 7,8-dihydroneopterin has a protective effect against oxLDL-induced damage to the overall glycolytic activity of the U937 cells as measured as lactate production.

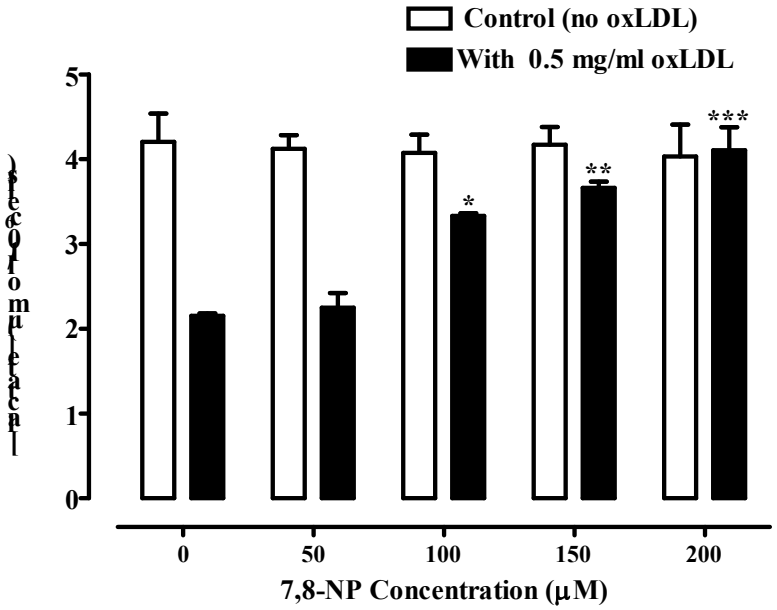

Figure 4.13 Effect of 7,8-NP concentration on lactate production in the cell culture media of oxLDL-treated U937 cells.
U937 cells at 0.5 x10^6 cells/ml were incubated with different concentrations of 7,8-NP (0, 50, 100, 150 and 200 μM) before incubation with or without 0.5 mg/ml oxLDL for 12 hours. The lactate released to the culture media was measured. Results shown are the mean ± SEM of triplicate samples. Mean protein content was 50 mg/10^6 cells. Significance of results was examined by comparing the lactate concentration with each 7,8-NP concentration with the positive control containing cells with oxLDL alone; * $P < 0.05$, ** $P < 0.01$, *** $P < 0.001$.

4.2.8 Effect of 7,8-dihydroneopterin on GAPDH activity in oxLDL-treated U937 cells

We had shown that GAPDH loss is a key event in oxLDL induced U937 cell death and lactate production was maintained in the presence of oxLDL if 7,8-dihydroneopterin was present. We therefore examined whether 7,8-dihydroneopterin was protecting the GAPDH activity.

As previously described U937 cells were pre-incubated for 10 minutes with 200 μM 7,8-dihydroneopterin in serum-free RPMI-1640 media with and without 0.5 mg/ml oxLDL for 12 hours. In the presence of 0.5 mg/ml oxLDL alone the GAPDH activity dropped dramatically; by 65% during the initial 3 hours (Figure 4.14). The GAPDH activity continued to decline, dropping to a level 76% less than the control after 6 hours. After 9 hours the GAPDH activity dropped by 88% and by 94% after 12 hours.

In the of presence of 200 μM 7,8-dihydroneopterin and 0.5 mg/ml oxLDL, the GAPDH activity remained the same over the incubation period compared to the corresponding control of each time point that contained oxLDL alone. 7,8-Dihydroneopterin has a protective effect against oxLDL-induced loss of GAPDH activity in U937 cells.

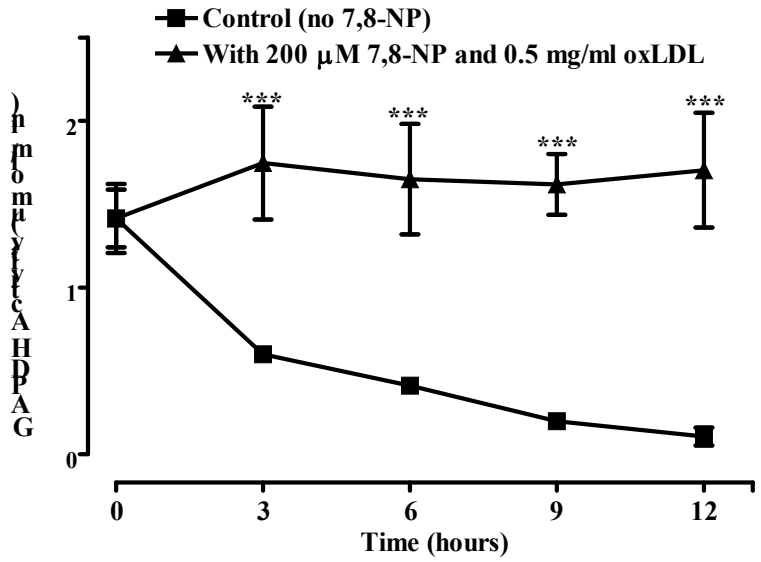

Figure 4.14 Time course showing the effect of 7,8-NP on GAPDH activity in oxLDL-treated U937 cells.

U937 cells at 0.5 x10^6 cells/ml were incubated with or without 200 μM 7,8-NP before incubation with 0.5 mg/ml oxLDL over a 12 hour period. The GAPDH activity was measured at various time points. Mean protein content was 50 mg/10^6 cells. Significance is indicated as *** $P < 0.001$ vs respective control at each time point containing cells with oxLDL alone. Results shown are the mean ± SEM of triplicate samples.

4.2.9 The VO_2 in U937 cells

Mitochondrial NADH metabolism is dependent on the VO_2. NOX activity also requires oxygen. The investigation has centred on glycolysis and shown that oxLDL has a major effect on GAPDH and overall glycolytic function as measured by lactate generation. OxLDL could be expected to either cause a large burst in the rate of VO_2 through NOX or the possible loss of mitochondrial function would appear as a decrease in the VO_2. We investigated these possibilities and examined the effect of oxygen tension on U937 cells VO_2.

4.2.9.1 Effect of 7,8-dihydroneopterin on the VO_2 of U937 cells

The effect of 7,8-dihydroneopterin on the VO_2 over time was examined by pre-incubated U937 cells in a stirred temperature controlled (37ºC) respirometers for 10 minutes with or without 200 μM 7,8-dihydroneopterin in serum-free RPMI-1640 media (without oxLDL) then sealing the ringer of the chamber and measuring the VO_2 of cells every 10 minutes over 7 hours as described in the methods chapter (section 2.2.10). There was no difference between the VO_2 of control cells (incubated with RPMI-1640 alone; without 7,8-dihydroneopterin and without oxLDL) and treated cells (incubated with RPMI-1640 and with 7,8-dihydroneopterin alone) over the incubation period (Figure 4.15a). However, both treatments showed that there was a decrease in the VO_2, by 20% during the first 30 minutes before a steady state was reached. The control cells showed that the VO_2 was dependent on the partial pressure of oxygen (PO_2) (Figure 4.15b). There was no difference between control cells and 7,8-dihydroneopterin treated cells in the VO_2 with

(a)

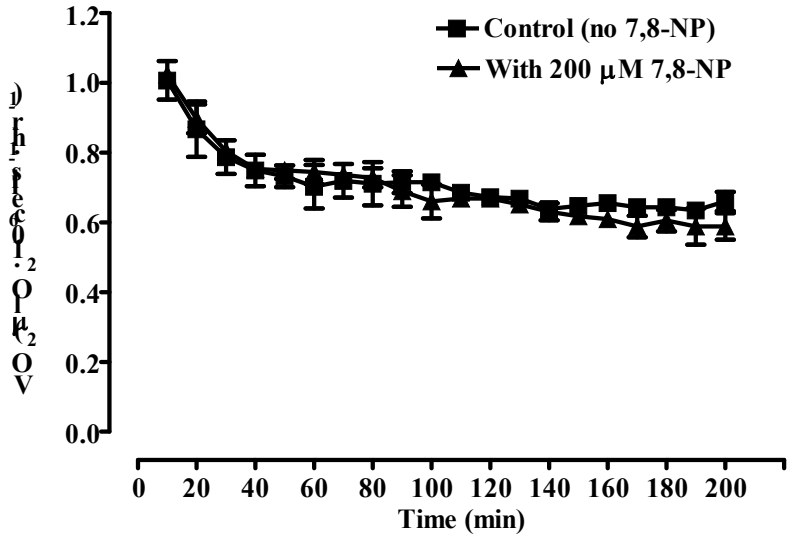

(b)

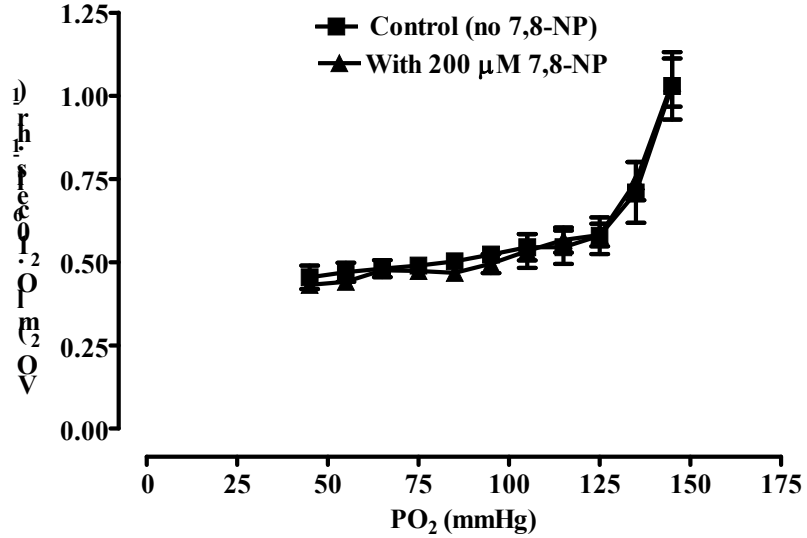

Figure 4.15 Time course showing the effect of 7,8-NP on oxygen consumption in U937 cells.

U937 cells at 2.0 x10^6 cells/ml were incubated with or without 200 μM 7,8-NP (without oxLDL) over a 7 hour period. (a) VO_2 vs time. (b) VO_2 vs PO_2. Mean protein content was 50 mg/10^6 cells. Results shown are the mean ± SEM of triplicate samples.

respect to the change in the PO_2 (Figure 4.15b). Therefore, 7,8-dihydroneopterin alone has no effect on the VO_2 of U937 cells.

4.2.9.2 Effect of oxLDL on the VO_2 in U937 cells

The effect of 0.5 mg/ml oxLDL on the VO_2 over time was performed by incubating U937 cells in serum-free RPMI-1640 media with or without 0.5 mg/ml oxLDL over 7 hours in a closed respirometers at 37ºC (methods chapter, section 2.2.10). In control cells (without oxLDL) there was decrease in the VO_2 of 20% during the first 30 minutes before steady state was reached as previously described (Figure 4.16a). The addition of oxLDL caused the VO_2 to decrease by 36% during the first 30 minutes before a slow phase of decreasing the VO_2 for the next 6.5 hours where a further decrease of 28% occurred. The total decrease in the VO_2 over the 7 hours was 64% with oxLDL. The PO_2 in the control cells remained stable over the course of the experiment, but in the oxLDL-treated cells there was a constant decrease in the VO_2 as the PO_2 decreased (Figure 4.16b). OxLDL appear to have removed the cells ability to regulate the rate of the VO_2 and removed the ability to maintain the VO_2 in decreasing oxygen concentrations.

4.2.9.3 Effect of 7,8-dihydroneopterin on the VO_2 of oxLDL-treated U937 cells

The ability of 7,8-dihydroneopterin to protect the cells VO_2 regulation in the presence of oxLDL was examined by pre-incubated U937 cells for 10 minutes with or without 200 μM 7,8-dihydroneopterin in serum-free RPMI-1640 media before incubation with 0.5 mg/ml oxLDL over 7 hours in a closed respirometers at 37ºC (methods chapter, section 2.2.10).

(a)

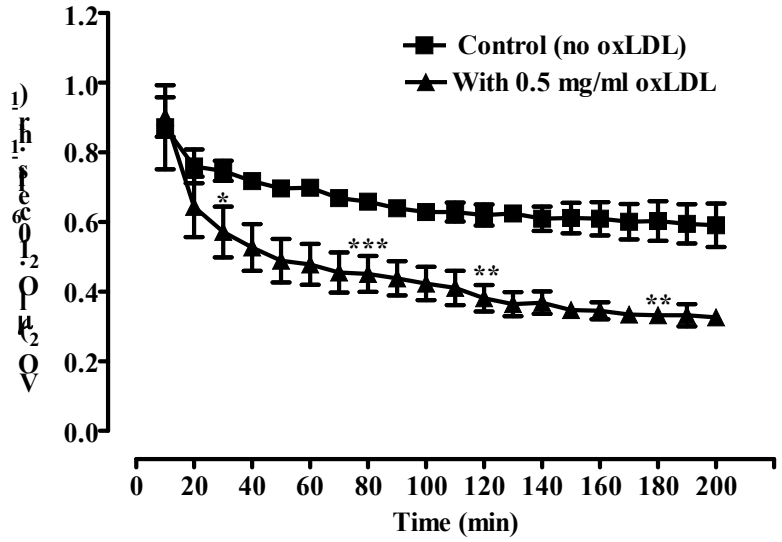

(b)

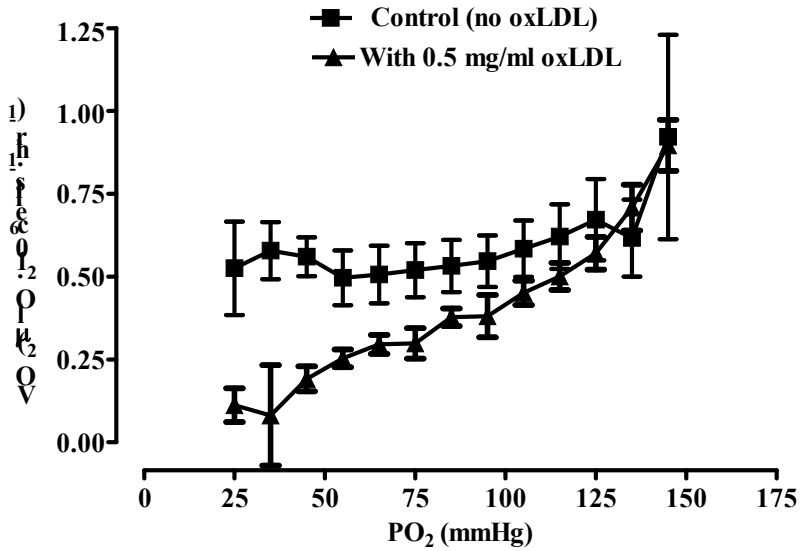

Figure 4.16 Time course showing the effect of oxLDL on oxygen consumption in U937 cells.

U937 cells at 2.0 x10^6 cells/ml were incubated with or without 0.5 mg/ml oxLDL over a 7 hour period. (a) VO2 vs time. (b) VO2 vs PO2. Mean protein content was 50 mg/10^6 cells. Significance is indicated as * $P < 0.05$, ** $P < 0.01$, *** $P < 0.001$ vs respective control at each time point containing cells alone. Results shown are the mean ± SEM of triplicate samples.

There was no difference in the VO_2 between the cells incubated with oxLDL alone and the cells incubated with 7,8-dihydroneopterin and oxLDL over the course of the experiment (Figure 4.17). In both treatments, there was a decrease in the VO_2, by 40% during the first 30 minutes, before steady state was reached. This suggested that 7,8-dihydroneopterin was unable to prevent the loss of the VO_2 by oxLDL. This result was different to the previously observed antioxidant effect of 7,8-dihydroneopterin. The most likely explanation for this result was the 7,8-dihydroneopterin was being oxidised to neopterin in the ringer of the chamber very quickly during the first 30 minutes of the experiment. It is possible that this reaction was being enhanced at the oxygen electrode so the 7,8-dihydroneopterin levels fell faster than normally observed in solution. This led to modification of the method to measure the possible protective effect of 7,8-dihydroneopterin on oxygen consumption. The experiments to date have measured the VO_2 in sealed respirometers chambers where the oxygen is consumed by the cells and the PO_2 (amount) decreases.

The experiment was changed so the U937 cells were incubated in the tissue flasks with oxLDL or oxLDL plus 7,8-dihydroneopterin or without additives. At set time points the cells were collected and placed in the respirometers and the initial VO_2 recorded over 30 minutes. With control cells (incubated with RPMI-1640 alone, without 7,8-dihydroneopterin and without oxLDL) there was a significant 3.8 fold increase in the VO_2 over the 7 hours of the experiment (Figure 4.18). The addition of 0.5 mg/ml oxLDL cut the increase in U937 cells VO_2 to only 1.7 fold after 7 hours. Relative to the control cells, the oxLDL treated U937 cells VO_2, had decreased by 25% at 3 hours, 42% at 5 hours and by 50% at 7 hours compared to the corresponding control cells at each time

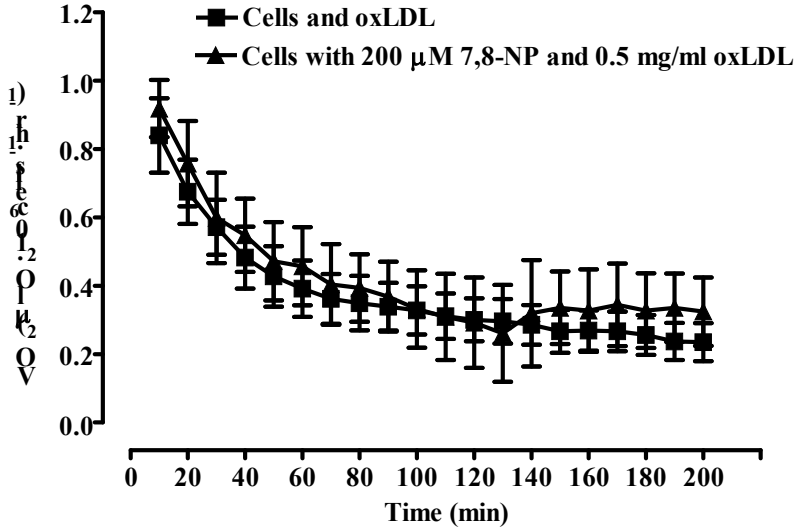

Figure 4.17 Time course showing the effect of 7,8-NP on oxygen consumption of U937 cells.

U937 cells at 2.0 x10^6 cells/ml were incubated with or without 200 μM 7,8-NP before incubation with 0.5 mg/ml oxLDL over a 7 hour period. Mean protein content was 50 mg/10^6 cells. Results shown are the mean ± SEM of triplicate samples.

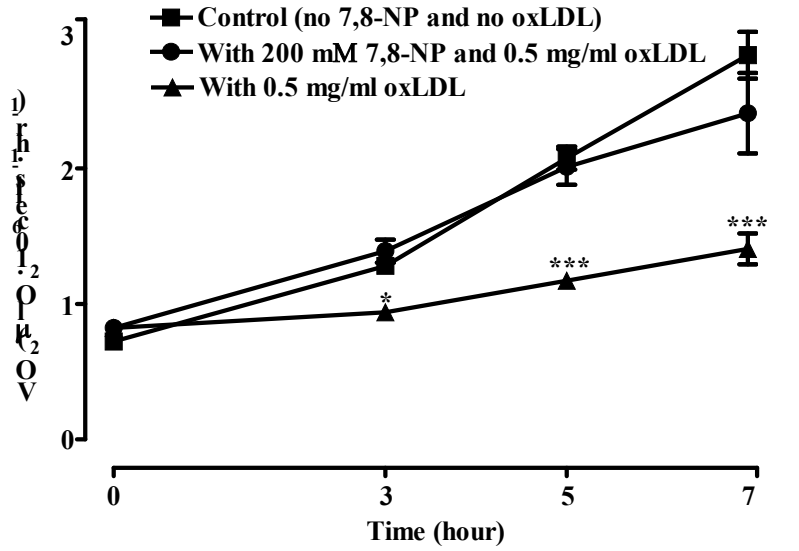

Figure 4.18 Time course showing the effect of 7,8-NP on oxygen consumption in U937 cells.

U937 cells at 2.0 x10^6 cells/ml were incubated with or without 200 μM 7,8-NP before incubation with 0.5 mg/ml oxLDL over a 7 hour period. Mean protein content was 50 mg/10^6 cells. Significance is indicated as * $P < 0.05$, *** $P < 0.001$ vs respective control at each time point containing cells without 7,8-NP and without oxLDL. Results shown are the mean ± SEM of triplicate samples.

point. The addition of 7,8-dihydroneopterin prevented this loss in the VO_2 caused by the presence of the oxLDL. There was no significant difference in the VO_2 between the control cells and the 7,8-dihydroneopterin plus oxLDL treated cells. Therefore, 7,8-dihydroneopterin is able to protect U937 cells VO_2 in the presence of oxLDL. It appears that using this approach of incubating the cells in flasks then measuring the initial VO_2 at normoxic levels allows the protective effect of 7,8-dihydroneopterin to be observed.

4.3 Discussion

4.3.1 Metabolic activity

In this chapter the cytotoxicity of oxLDL on U937 cell metabolism has been examined as well as the protective effect of 7,8-dihydroneopterin on the cell metabolism. One of the markers of the cytotoxic effect of oxLDL on metabolic functions in U937 cells was the change in concentration of lact released into cell culture medium and the LDH activity. Untreated U937 cells had a steady output of lactate into the media as part of their normal metabolism in cell culture media. U937 cells being cancer cells derived from the monocytes lineage were expected to be highly reliant on anaerobic glycolysis with high lactate production. Inefficient mitochondrial function is thought to cause cancer cells to produce excessive lactate (John, 2001). Other studies have demonstrated a large production of lactate by macrophages in atherosclerotic lesions, which transform the environment to an acidic one (Leppänen *et al.*, 2006, Loike *et al.*, 1993). This expected reliance on anaerobic glycolytic activity by U937 cells, with its associated lactate production, allowed the overall metabolism of the cells to be measured.

The time course studies with oxLDL-treated U937 cells indicated that the decrease in lactate concentration caused by incubation with oxLDL occurred rapidly; within 3 hours. This rapid progression in the decrease of the lactate concentration was very closely correlated with loss of cell viability, which was illustrated in the previous chapter.

In U937 cells, time course studies indicated that the loss of intracellular LDH activity and the rise in LDH activity in the cell culture media both occur after the initial 3 hours incubation with oxLDL and appears to be due to the lysis of the cells. There appeared to no change in the total amount of LDH activity indicating that LDH was not inactivated by the oxLDL-induced oxidative stress.

The loss of lactate and overall metabolism was therefore clearly due to changes in enzyme activity before the loss of LDH enzyme. We and others have repeatedly shown the oxLDL causes a string of oxidative stress in the cells. This was further shown here by the loss of GSH (to be discussed later). GAPDH is an essential enzyme in glycolysis that is one of several enzymes in the metabolic pathway converting glucose to pyruvate with a net production of 2 ATP and 2 NADH molecules. It catalyses the conversion of glyceraldehyde-3-phosphate to 1,3-bis-phosphoglycerate with the generation of 2 NADH (Mathews & Van Holde, 1996). It is also highly susceptible to oxidative loss of activity (Ralser *et al.*, 2007). The incubation of U937 cells with oxLDL caused a concentration- and time-dependent decrease in GAPDH activity (Figure 4.4b and Figure 4.5). This loss occurred rapidly, within 3 hours of oxLDL addition and before the loss in U937 cell viability.

GAPDH has two domains; one end binds NAD^+ and the second one binds GAP (Yamaguchi *et al.*, 2003). The loss of GAPDH activity could be partly attributed to the loss of NAD^+, a cofactor required for the activity of GAPDH (Schraufstatter *et al.*, 1990). OxLDL can react with NAD^+ within the cells. However, this was less likely to be the major cause of GAPDH inactivation in U937 cells, because GAPDH activity was measured in this research by supplementing the oxLDL-treated cell samples with required substrates including NAD^+, after which GAPDH activity was still not recovered. A more likely explanation for GAPDH inactivation in oxLDL-treated U937 cells was that oxLDL induced oxidation to the GAPDH active site. The GAPDH active site contains an essential cysteine thiol group (Cys^{149}) which can be oxidised by oxidants to a disulfide, sulfenic acid, or other high oxidation product(s) (Albina *et al.*, 1999, Pullar *et al.*, 2000). There is increasing evidence to suggest that GAPDH is a preferential target for oxidative stress. The inactivation of GAPDH indicates oxidative stress (Ralser *et al.*, 2007). NO and ROS-mediated oxidation of GAPDH thiol and GAPDH inactivation was found in inflamed mucosa in colon epithelial cells of patients with inflammatory bowel disease (Mckenzie *et al.*, 1996). OxLDL has been shown to cause increased ROS formation, including rapid elevation of H_2O_2. OxLDL has been shown to induce the down-regulation of GAPDH via a H_2O_2-dependent decrease in protein stability, resulting in inhibition of glycolysis and marked depletion of cellular ATP levels in human aortic smooth muscle cells (HASMCs) (Sukhanov *et al.*, 2006). OxLDL down-regulated GAPDH appears to play an important role in the mechanisms of atherogenesis (Sukhanov *et al.*, 2006). The inactivation of the GAPDH enzyme has been the subject of much research. Under conditions where glucose uptake is inhibited, GAPDH is inactivated and ATP formation

is halted (Schraufstatter *et al.*, 1990). In addition, GAPDH inactivation by another oxidant, acetylleucine chloromethyl ketone (ALCK), has also been reported in U937 cells (Yamaguchi *et al.*, 2003). NO has been reported to reduce GAPDH activity and ATP content in macrophages (Albina *et al.*, 1999). NO caused the thiol at the active site of GAPDH enzyme to form sulfenic acid, resulting in activity loss (Ishii *et al.*, 1999). The reactive aldehydes, 4-hydroxy-2-nonenal (HNE) and 4-hydroxy-2-hexenal (HHE) both primary products of LDL oxidation inhibit GAPDH (Tsuchiya *et al.*, 2005) though this is an unlikely mechanism in our experiments as these aldehydes are too reactive to be present in the highly oxidised LDL. GAPDH inactivation by HOCl oxidation has been demonstrated in colon epithelial cells (Mckenzie *et al.*, 1999), human endothelial cells (ECs) (Pullar *et al.*, 1999) and human mononuclear leukocytes (Smit & Anderson, 1992).

These observations of GAPDH activity are supported by direct observation of the thiol content of GAPDH by thiol staining of the U937 cell proteins on SDS-PAGE. This method allowed the cells proteins to be rapidly separated and stained for thiol (Baty *et al.*, 2002). As expected GAPDH appeared to be extremely sensitive to thiol modification most likely due to a cysteine residue (Cys^{149}) located in the active site of the enzyme (Schuppe-Koistinen *et al.*, 1994). The human GAPDH molecular mass is 36 kDa (Torchinsky, 1981). As commented in chapter 1, Cysteine is an ideal redox sensor due to its sulfhydryl group (-SH) being easily oxidised. The presence of positively charged residues in the local protein environment can stabilise the thiolate anion ($-S^-$), providing a mechanism for increasing the reactivity of selective cysteine residues. The $-S^-$ is a strong nucleophile that can be oxidised to sulfenic (-SOH), sulfinic ($-SO_2H$) and sulfonic (-

SO_3H) acids, S-nitrosothiols (-SNO) and disulfides (R-S-S-R) (Cuddihy *et al.*, 2009a, Sukhanov *et al.*, 2006).

In this study, the detection of the GAPDH protein thiol reduction state was conducted using the iodoacetyl group of 5-IAF that reacts specifically with reduced thiol and provides a fluorescent label at the cysteine residue (Cys^{149}) located in the active site of the GAPDH enzyme with molecular size 36 kDa as well as with other thiol groups in the cell. Reduced GAPDH protein thiol were labelled with 5-IAF while still within the cell, so preventing the oxidation of the GAPDH during sample processing. This analysis shows a large number of reduced thiol proteins in untreated U937 cells. SDS-PAGE analysis of the 5-IAF stained cell lysates showed a number of proteins that lost thiol staining. One of these bands had the same mobility as authentic GAPDH with a molecular weight of 36 kDa suggesting that this band was GAPDH. This corresponded to a coomaasie staining band also which showed increased levels of degradation after 12 hours of incubation. This suggests that there was increased degradation of the oxidised GAPDH as was reported in smooth muscle cells (Sukhanov *et al.*, 2006). Further analysis of the data showed a relationship between decrease in 5-IAF staining 36 kDa band and the loss of GAPDH activity upon exposure to oxLDL in U937 cells. This is consistent with the hypothesis that the loss of GAPDH activity is primarily due to the oxidation of the active site cysteine by oxLDL which cause proteolysis of the GAPDH at 12 hours.

These observations of GAPDH in U937 cells treated with oxLDL were similar to those reported with HASMCs after exposure to oxLDL or H_2O_2. GAPDH-labelling efficiency with the thiol-sensitive dye, fluorescein-5-maleimide, was dramatically decreased

following treatment with oxLDL or H_2O_2 (Sukhanov *et al.*, 2006). OxLDL and exogenous H_2O_2 oxidised GAPDH thiol, decreasing GAPDH protein half-life and increasing GAPDH sensitivity to proteasome-mediated protein degradation in *vitro* (Sukhanov *et al.*, 2006). Also, there was a decrease in the intensity of reduced GAPDH protein thiol of Jurkat T-lymphoma cells which were labelled with 5-IAF after treatment with H_2O_2 (Cuddihy *et al.*, 2009a). Exposure of Jurkat T-lymphoma cells to diamide for 10 minutes led to a dramatic increase in thiol protein oxidation after labelling with 5-IAF (Baty *et al.*, 2002).

Surprisingly, the inhibition of GAPDH activity by oxLDL was prevented by the presence of 10% HI-FCS in the U937 cell culture medium. It is possible that the HI-FCS prevented the saturation of scavenger receptors with oxLDL, so that free oxLDL could not exert its toxic effect, as measured in the absence of HI-FCS. This would prevent a decrease in both GAPDH activity and cell viability from occurring. The major component of serum is serum albumin which is considered to be a type of antioxidant as it can scavenge radicals through reactions of the amino acid side changes (Stocker *et al.*, 1987). Albumin binds fatty acids protecting them from oxidation; binds copper and keeps it from participating in oxidation reactions; binds cysteine and glutathione protecting them from oxidation and binds bilirubin and pyridoxal-5'-phosphate preventing oxidation (Kouoh *et al.*, 1999, Roche *et al.*, 2008).

4.3.2 Intracellular GSH concentration

OxLDL clearly causes an oxidative stress within the U937 cells resulting in the loss of GAPDH. GSH is a key antioxidant within the cells and has previously been shown in this

laboratory to be critical in the prevention of oxidative damage in the related THP-1 cell line (Kappler *et al.*, 2007). GSH loss also provides a direct measure of the cellular antioxidant status and it has been established previously that cellular GSH loss results in a further increased susceptibility to oxidative stress (Ballatori *et al.*, 2009, Kappler *et al.*, 2007). Intracellular GSH levels must be maintained for cells to function properly. GSH can act as an antioxidant by directly reacting with a range of oxidants such as hydroxyl radical ($HO^{\bullet}$), HOCl, peroxynitrite ($ONOO^{-}$), alkoxyl radical ($RO^{\bullet}$), nitric dioxide ($NO_2^{\bullet}$) and less efficiently with $O_2^{\bullet -}$ (Halliwell & Gutteridge, 2007). The GSH/GSSG couple is a major contributor to the redox state of the cell, with most cells having this couple at a ratio of 100:1 (Akerboom *et al.*, 1982). Changes in this couple appear to correlate with cell proliferation, differentiation, or apoptosis (Boggs *et al.*, 1998, Ballatori *et al.*, 2009).

Time course studies with U937 cells showed that there was an increase in intracellular GSH concentration in the control sample of cells. The increase in GSH concentration was actually an increase in intracellular GSH concentration as there was no increase in cell number. It appears that in the serum free condition of the experiment, the cells have taken up cysteine to make more GSH suggesting that they are under some oxidative stress even in the absence of oxLDL. The increase in cellular GSH appears to be the cells adapting and reducing the oxidative stress. The lack of cell growth is most likely due to the known effect of the serum free media inhibiting mitosis in cell lines (Freshney, 2000).

The time course studies conducted on oxLDL-treated U937 cells showed the decrease in intracellular GSH concentration was very rapidly occurring within hours of the oxLDL

addition. The loss of GSH appears to occur at the same time as the loss of the cell viability. OxLDL clearly induces an oxidative stress in U937 cells, causing loss of intracellular GSH concentration and cell death. The loss of GSH means the cells can no longer protect and maintain the reduced state of the essential thiol in GAPDH leading to the loss in glycolytic activity and therefore cell viability as measured by the cell ability to reduce MTT. The leakage of LDH from the cells is the failure of the cell to maintain its integrity. This study is consistent with previous studies of this laboratory showing oxLDL caused a dramatic loss of cellular GSH and caspase-independent cell death in U937 cells (Baird *et al.*, 2004). This previous study did not explain what drove the death mechanism in U937 cells as the loss of GSH alone does not necessary cause cell to die (Kappler *et al.*, 2007). The loss of metabolic function, particularly the loss of GAPDH appears to be a key event causing the cells to die.

4.3.3 Intracellular purine nucleotides ATP, ADP, AMP, NAD^+ and $NADP^+$ production

The relationship between intracellular ATP, ADP and AMP is particularly important for maintenance of cellular homeostasis and adaptation to changing energy demands. Although ATP represents the primary source of energy, ADP, AMP and inorganic phosphate are substrates that are not only required for generation of ATP, but are thought to play a key role in mitochondrial metabolic control (Hochachka & Mcclelland, 1997). AMP in particular, acting through the cAMP-activated protein kinase cascade, has been implicated in the control of a number of factors important to metabolic state in

mammalian cardiac and skeletal muscle and allosterically activates the glycolytic enzyme phosphofructokinase (Hardie, 2000, Lee *et al.*, 2006).

NAD^+ is the substrate for the formation of NADH, which serves to transfer electrons between both the citric acid cycle and glycolysis and electron transport chain (Alberts *et al.*, 2002). NAD^+ also functions as a coenzyme for hydride-transfer enzymes and as a substrate for NAD^+ consuming enzyme (Belenky *et al.*, 2007).

The effect of oxLDL on metabolic energies was further investigated by examining the ATP, ADP, AMP, NAD^+ and $NADP^+$ loss in oxLDL-treated U937 cells. Time course studies showed that ATP and ADP levels increased in control cells during the initial 3 hours then remained stable, reaching equilibrium. OxLDL treatment induced ATP and ADP depletion that occurred within 3 hours of the treatment and decreased further over time. Interestingly, there was no change in the AMP level during incubation with oxLDL. The time course studies of NAD^+ and $NADP^+$ showed a decrease in their levels in control cells during the initial 3 hours, before stabilisation. In oxLDL-treated cells, NAD^+ and $NADP^+$ dropped significantly within 3 hours of the treatment.

These results suggest that, relative to controls, oxLDL-treated U937 cells showed a rapid decrease, in intracellular ATP, ADP, NAD^+ and $NADP^+$ levels 3 hours before cell lysis (measured as LDH loss after 6 hours). This ATP loss is consistent with the loss in the GAPDH activity, loss in lactate production and loss of the cells ability to protect itself from oxidative stress with intracellular GSH. Loss of ATP is critical to the loss of cell viability as measured by the MTT assay was observed to occur at the same time as ATP loss.

These results may model some of the process occurring in the plaque as low oxygen and nutrients levels are thought to cause ATP depletion, and macrophage death in the atherosclerotic lesions of rabbits leading to necrotic core formation (Leppänen *et al.*, 2006). The toxic effect of oxLDL on GAPDH would further enhance this failure of ATP generation. Other oxidants have also been reported to inhibit ATP levels causing cell death. In neuronal cells peroxynitrite and S-nitrosothiols inhibit GAPDH and glycolytic ATP production, which causes necrosis via failure of the ATP-driven calcium and sodium pumps resulting in osmotic rupture of the plasma membrane (Brown, 2010). In contrast, peroxynitrite induced death in U937 and THP-1 cells is not dependent on the loss of ATP and appears to be a regulated process (Cantoni *et al.*, 2005). ATP loss also features in the hydrogen peroxide mediated death of murine macrophages-like P388D1 cells where there was a 83% loss of ATP reported within minutes of H_2O_2 treatment (Spragg *et al.*, 1985). ATP loss has been cited as the switch between apoptosis and necrosis where the loss of ATP triggers necrosis (Eguchi *et al.*, 1997).

In this study, AMP levels in oxLDL-treated U937 cells did not significantly differ from the controls. Previous studies have suggested that ATP may not always be degraded to AMP. Supplementation of guinea-pig ventricular cardiomyocytes with NADH causes a significant reduction of pinacidil-primed ($I_{K(ATP)}$) and elevation in intracellular ATP levels whereas no difference was detected in ADP and AMP levels (Pelzmann *et al.*, 2003). Using a bioluminescent enzymatic cycling assay for ATP and AMP, it was found that ATP was not degraded to AMP in a number of food samples including milk (Sakakibara *et al.*, 1999). In addition, under hypoxic conditions AMP-activated protein kinase (AMPK) activation is not associated with an increase in AMP/ATP ratio, but is

dependent on the generation of mitochondrial reactive oxygen species (mtROS) (Emerling *et al.*, 2009).

As the cycling of NAD^+ and NADH is a redox reaction, their relative ratios are indicators of metabolic state and intracellular redox potential (Lin & Guarente, 2003). The NAD^+:NADH ratio can be increased by the addition of glutamate and other metabolic substrates like pyruvate (Williams *et al.*, 2001, White & Wittenberg, 2000). Although the NAD^+: NADH ratio may be a good indicator of metabolic state, in practice it is very labile and measurement is difficult (Caruso *et al.*, 2004). This finding is consistent with our study, which found NADH and NADPH levels in U937 cells to be very labile to measure by our HPLC method.

4.3.4 7,8-Dihydroneopterin protection to metabolic function

This study examined the protective effect of 7,8-dihydronepterin on U937 cells metabolism. 7,8-Dihydroneopterin protected the U937 cells against oxLDL-induced GAPDH activity loss in U937 and allowed the cells to maintain glycolytic metabolism as measured as lactate production in cell culture media. The maximum protection of the metabolic parameters measured was observed with 200 μM 7,8-dihydronepterin. Therefore, 7,8-dihydronepterin has a protective effect against oxLDL-induced damage by maintaining U937 cellular metabolic activity. 7,8-dihydroneopterin appears to be able to scavenge the ROS generated in response to the oxLDL. Previous studies have shown 7,8-dihydroneopterin protects the intracellular GSH levels (Amit, 2008). Since 7,8-dihydroneopterin was unable to reduce the oxidised protein thiol, it is unlikely that 7,8-dihydroneopterin can regenerate or increase the intracellular GSH levels (Duggan *et al.*,

2002). Therefore, it is very likely that with U937 cells, 7,8-dihydroneopterin protects the intracellular thiol pool by scavenging ROS generated in the presence of oxLDL. With THP-1 cells this does not occur and the reason still unknown (Baird *et al.*, 2005). In macrophages and U937 cells, the maintenance or protection of the cell GSH levels via increasing the intracellular thiol pool (Kinscherf *et al.*, 1998, Lizard *et al.*, 2000) will ensure the functioning of the GAPDH enzyme and overall metabolic function.

4.3.5 The VO_2 and 7,8-dihydronepterin

A lack of oxygen leads to depletion of ATP which is generated by oxidative phosphorylation and subsequently the ATP is supplied by an anaerobic pathway (Hochachka *et al.*, 1996). In *vivo*, there was a balance between oxygen supply by the cardiovascular system for tissues respiration and oxygen demand. When the recovery from exercise are included, the metabolic rate of working muscle are significantly increased (Turner *et al.*, 2006). Oxygen may play a regulatory role in aerobic metabolism, particularly in skeletal muscle (Hochachka, 2003). Supplying oxygen in excess of requirements could result in the formation of free radicals and facilitate damage in the tissues (Tuckey *et al.*, 2009, Gnaiger, 2003). Thus, balance must be maintained to ensure that PO_2 in the tissue is retained with the optimal range to prevent tissue damage while ensuring oxygen demand is met under a range of conditions (Forgan & Forster, 2009).

The effect of oxLDL on metabolic energies and the antioxidant effect of 7,8-dihydronepterin were studied by examining the effect of oxLDL on the VO_2 of U937 cells using two methods. The first method involved, calculation of the VO_2 for every 10

minutes period over the course of the experiment for the same sample incubated in a closed chamber while the other method involved calculating the VO_2 every 10 minutes period for 30 minutes for a new sample placed into the oxygen measuring chamber at each time point during the course of the experiment. The first method examined the VO_2 with decreasing oxygen levels while the latter method measured the VO_2 at normoxic levels. This showed that U937 cells could very effectively maintain their VO_2 as the oxygen levels decreased, which was abolished with the addition of oxLDL. This data also showed that the VO_2 is PO_2-dependent. Diffusion down the partial pressure gradient is unlikely to limit the VO_2 in isolated cells. There are numerous cases where a similar dependency of the VO_2 on PO_2 has been shown (Schumacker *et al.*, 1993, Budinger *et al.*, 1996).

Surprisingly, 7,8-dihydroneopterin was found to be very labile in the chambers via the first method suggesting it was being oxidised at the oxygen electrode. By separating the 7,8-dihydroneopterin plus oxLDL incubation from the oxygen measurement using the second method it was shown that 7,8-dihydroneopterin did preserve the VO_2 of the U937 cells. Surprisingly, the data did not show a significant burst on the VO_2 with the addition of oxLDL suggesting the oxidant production in the cells is less than that reported for classical respiratory burst (Fischer *et al.*, 2002). It is possible that the oxidant production causing the reported GSH loss and GAPDH inhibition observed in this research is very localised and intracellular. So although the oxygen up take for the oxidant production is small, it has a very destructive effect within the cell. As commented on above, the U937 cells showed remarkable alteration to their VO_2 with falling oxygen levels. The regulation of ATP supply-demand pathways by the reduction of blood flow and therefore oxygen

availability, could serve as an extremely important trait for species survival and adaptation when oxygen supply is inadequate (Forgan & Forster, 2010).

In this experiment the U937 cells VO_2 related to PO_2 between 0 and 155 mmHg. Blood vessel VO_2 displayed varying degrees of independence in a PO_2 range of 15-95 mmHg, while VO_2 by striated muscle tissue slices from all species related linearly to PO_2 between 0 and 125 mmHg, despite VO_2 rates varying greatly between species and muscle type (Forgan & Forster, 2010). The reduction in the $VO_2$with falling partial pressure results in a decrease in ATP demand, suggesting that the hypoxic signal is sensed and cellular changes effected (Forgan & Forster, 2010). Once oxygen delivery satisfies the metabolic requirement of skeletal muscle, the VO_2 is delivery independent. During increasing aerobic muscle work and while recovering from anaerobic activity the oxygen requirement of muscle increases. Furthermore, basal metabolic rate and aerobic scope of muscle is related to the fibers that constitute it (Forgan & Forster, 2009). Patients with chronic heart failure (CHF) have lower peak oxygen consumption (pVO_2) than normal subjects, and for a given quantity of work, have lower total VO_2 than controls. This apparent increase in biomechanical efficiency (BE) might be due to a higher proportion of anaerobic metabolism which, although leading to lower VO_2 during steady state exercise, must be compensated for during recovery (Witte *et al.*, 2007). Thus, lack of oxygen and nutrients may cause ATP depletion in the core of atherosclerotic plaques. ATP depletion, in turn, may promote cell death and the formation of a necrotic core (Geiringer, 1951).

Macrophages can efficiently adapt to hypoxic conditions via a compensatory increase in anaerobic ATP production (Cramer *et al.*, 2003). It is thus possible that macrophages could maintain adequate ATP concentrations in the hypoxic plaque core. Anaerobic glycolysis is inefficient, consuming 15 times more glucose per ATP molecule produced than oxidative phosphorylation. This strains the glucose supply and may deplete available glycogen stores. In addition, it causes lactate to accumulate in the tissue which may decrease tissue pH (Leppänen *et al.*, 2006). Indeed, lactate concentrations in plaque were high, indicating that extensive anaerobic glycolysis consumes glucose, reducing its availability to cells in the core. The combined lack of both oxygen and glucose may, in turn, cause ATP depletion in macrophages which contributes to cell death and the subsequent formation of a necrotic core (Leppänen *et al.*, 2006).

5 Effect of oxLDL and 7,8-dihydroneopterin on the metabolic function of HMDM cells

5.1 Introduction

In this chapter the effect of oxidised low-density lipoprotein (oxLDL) on human monocyte-derived macrophage (HMDM) cells is examined and compared to that observed with U937 cells as described in chapter 4. In chapter 3, oxLDL was observed to have the similar effect on cell viability as that observed with U937 cells but it was not examined whether the mechanism also involved damage to the HMDM cells metabolic systems. As with the U937 cells, here we examine the effect of oxLDL on lactate dehydrogenase (LDH) and glyceraldehyde-3-phosphate dehydrogenase (GAPDH) activity, lactate production and purine nucleotide levels (ATP, ADP, AMP, NAD^+ and $NADP^+$). If U937 cells are a good model of oxLDL induced HMDM cell death, we expect that 7,8-dihydroneopterin (7,8-NP) will prevent the loss of HMDM cell metabolic activity. These experiments also explore whether 7,8-dihydroneopterin may have an effect on oxLDL uptake.

Macrophages derive a significant amount of their metabolic energy from glycolysis which is why in tissue culture they generate a considerable amount of lactate. During inflammation, macrophage glucose levels decrease and the level of lactate production increase, which in turn lowers the pH of the environment. Interestingly macrophages possess stereospecific transporters for lactate that allows them to take up lactate preferentially in an acidic environment which they can further metabolise. As a result, macrophages can as a result accumulate extracellular lactate and utilise it as a source of

energy if required (Loike *et al.*, 1993). As seen in chapter 4 with U937 cells, cell membrane rupture releases lactate dehydrogenase into the media increasing the extracellular activity of the enzyme during oxidative stress (Jovanovic *et al.*, 2010).

In human aortic smooth muscle cells (HASMCs), oxLDL was reported to down-regulate GAPDH, causing a decrease in glycolytic activity and ATP levels (Sukhanov et al., 2006). The death of macrophages in atherosclerotic lesions and the formation of a necrotic core is associated with a reduction in ATP levels resulting from a lack of oxygen and nutrition (Leppänen et al., 2006). As previously discussed, the loss of GAPDH activity appears to be due to enzyme oxidative damage (Ralser et al., 2007). As seen with the U937 cells, the antioxidant 7,8-dihydroneopterin should have a similar protective role on HMDM cell metabolism, as demonstrated in this chapter. This study expects to see 7,8-dihydroneopterin addition preventing the loss of the various metabolic markers such as lactate levels and GAPDH activity.

5.2 Results

5.2.1 Effect of oxLDL on HMDM cell lactate generation

The effect of oxLDL on the metabolic energy of HMDM cells was studied by examining the lactate released into the cell culture medium during 12 hours incubation. The time course study was performed by incubating HMDM cells in RPMI-1640 media without phenol red containing 10% HIHS with and without 2.0 mg/ml oxLDL over 12 hours (Figure 5.1). In control cells there was a continuous production of lactate which was released into the cell culture medium over time (Figure 5.1). In oxLDL-treated cells, lactate production was identical to the controls until 6 hours.

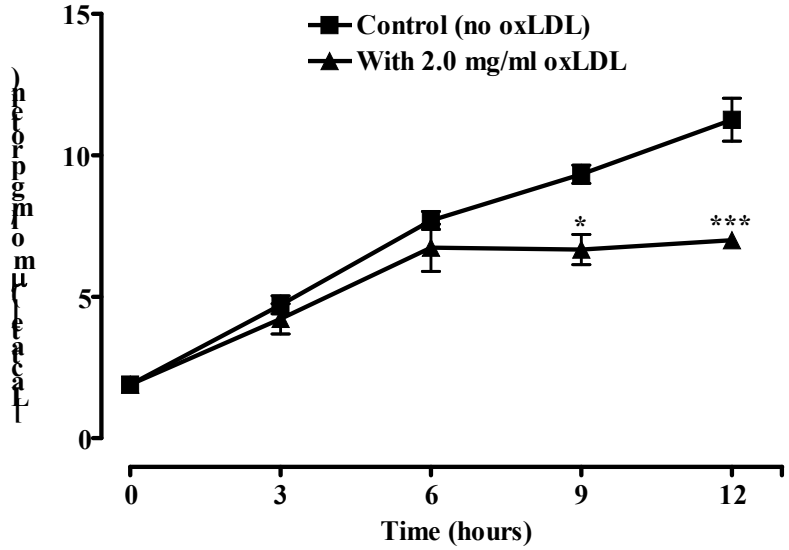

Figure 5.1 Time course showing the effect of oxLDL on lactate production in HMDM cells.
HMDM cells at 5.0 x10^6 cells/ml were incubated with 2.0 mg/ml oxLDL over a 12 hour period. The lactate released to the culture media was measured at various time points. Mean protein content was 0.5 mg/well. Significance is indicated as * $P < 0.05$, *** $P < 0.001$ vs respective control of each time point. Results shown are the mean ± SEM of triplicate samples.

Lactate release into the media completely stopped after this point with no significant increase in lactate levels at 9 and 12 hours compared to 0 hour control. The lactate levels in the oxLDL treated cells were reduced by 29% at 9 hours, and 38% at 12 hours incubation, compared to the respective controls of each time point (Figure 5.1). Therefore, with HMDM cells, oxLDL causes a large and dramatic decrease in the lactate release after 6 hours.

5.2.2 Effect of oxLDL on LDH activity in HMDM cells

The LDH activity is a marker of the metabolic energy of cells. We measured both intracellular and in cell culture media LDH activity to study the effect of oxLDL on the metabolic energy of HMDM cells. The LDH activity of HMDM cells over time was studied by incubating HMDM cells in RPMI-1640 media without phenol red containing 10% HIHS with 2.0 mg/ml oxLDL for 12 hours (Figure 5.2). There was a loss of LDH activity inside the cells and an increase in LDH activity in the cell culture media, although this was not significant until the 9 hour time point (Figure 5.2a). The loss of intracellular LDH activity, as measured in cell pellets, was likely to be caused by the release of LDH through plasma membrane lysis into the cell culture media. The observed release of LDH and corresponding cell lysis are caused by prolonged exposure to oxLDL. However, the total LDH activity remained stable over the course of the study showing lactate dehydrogenase is not inhibited by the level of oxidative stress (Figure 5.2b). Lactate production dropped after 6 hours. Significant LDH enzyme release into the cell culture media did not occur until approximately 9 hours. It appears that oxLDL was slowing the cells metabolism before cell lysis occurred in HMDM cells.

(a)

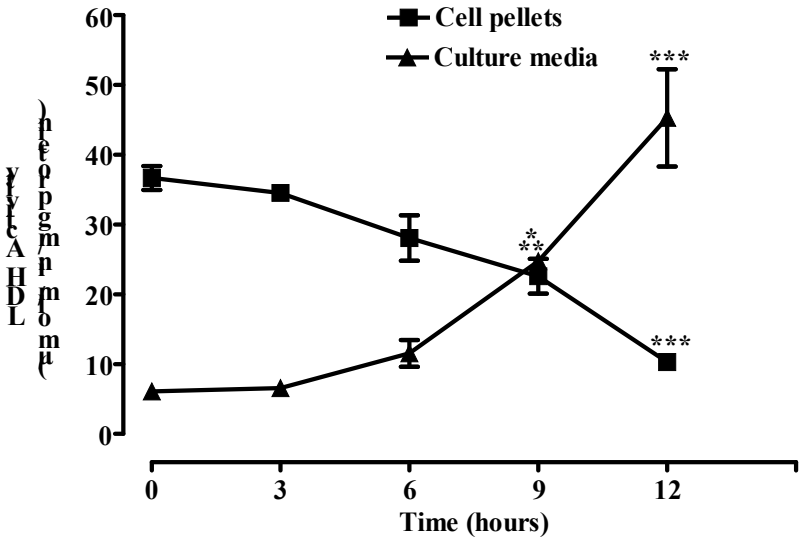

(b)

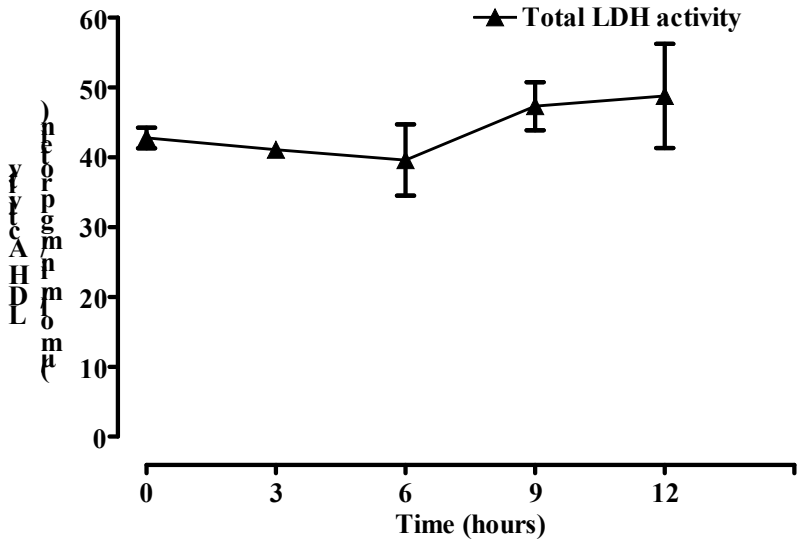

Figure 5.2 Time course showing the effect of oxLDL on the LDH activity in HMDM cells.

HMDM cells at 5.0 x10^6 cells/ml were incubated with 2.0 mg/ml oxLDL over a 12 hour period. (a) The LDH activity was measured in the cell culture media and in the cell pellets at various time points. (b) The total LDH activity was measured at various time points. Mean protein content was 0.5 mg/well. Significance is indicated as * $P < 0.05$, ** $P < 0.01$, *** $P < 0.001$ vs respective 0 hr control. Results shown are the mean ± SEM of triplicate samples.

5.2.3 Effect of oxLDL on GAPDH activity in HMDM cells

A time course study of the effect of oxLDL on GAPDH activity was conducted by incubating HMDM cells in RPMI-1640 media containing 10% HIHS with 2.0 mg/ml oxLDL for 24 hours (Figure 5.3). The GAPDH activity dropped rapidly, reaching a level 39% less than the control after 3 hours and continued to decline to 53% after 6 hours. Then it reached 69% after 10 hours and 91% after 24 hours incubation compared to the control (Figure 5.3). Though not as dramatic as the loss of GAPDH activity with U937 cells (Figure 4.5) this loss of activity is very significant (Figure 5.3). Therefore, GAPDH activity in HMDM cells is very sensitive to the oxidative stress induced by the oxLDL, but was occurring 6 hours before cell lysis was observed as measured by LDH release. The GAPDH loss though is occurring faster than the loss in lactate level.

5.2.4 Effect of oxLDL on intracellular purine nucleotides ATP, ADP, AMP, NAD^+ and $NADP^+$ levels in HMDM cells

The effect of oxLDL on total metabolic energy of HMDM cells was studied by treating cells with oxLDL and examining intracellular purine nucleotide levels at various time points as described with U937 cells in Chapter 4. These purine nucleotides were adenosine triphosphate (ATP), adenosine diphosphate (ADP), adenosine monophosphate (AMP), nicotinamide adenine dinucleotide (NAD^+) and nicotinamide adenine dinucleotide phosphate ($NADP^+$).

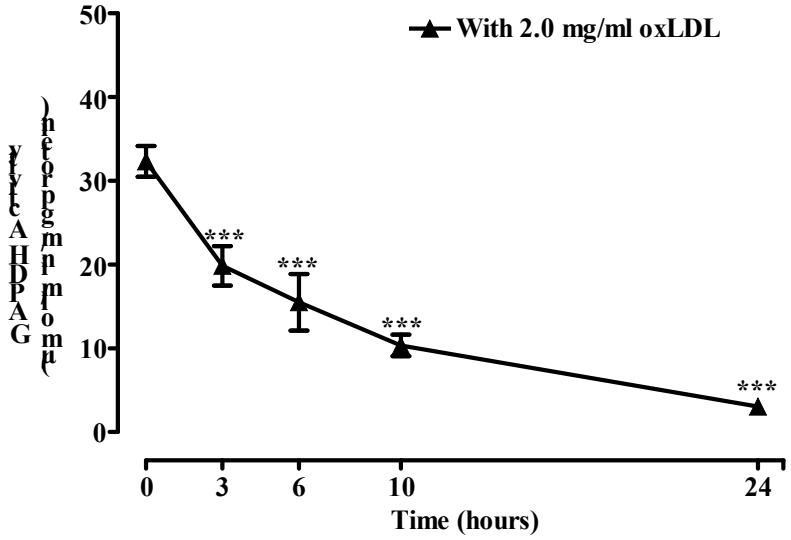

Figure 5.3 Time course showing the effect of oxLDL on GAPDH activity of HMDM cells.

HMDM cells at 5.0 x10^6 cells/ml were incubated with 2.0 mg/ml oxLDL over a 24 hour period. The GAPDH activity was measured at various time points. Mean protein content was 0.5 mg/well. Significance is indicated as *** $P < 0.001$ vs 0 hr control. Results shown are the mean ± SEM of triplicate samples.

The chromatograms of standard purine nucleotides and purine nucleotide levels (ATP, ADP, AMP, NAD^+ and $NADP^+$) in HMDM cells incubated with 2.0 mg/ml oxLDL over the 12 hour time period are shown in Figure 5.4. The changes in the individual purine levels identified over the 12 hours of incubation are shown graphically Figure 5.5 and Figure 5.6.

In control cells, the ATP level remained stable for 12 hours (Figure 5.5a). In oxLDL-treated cells, the ATP level dropped gradually, by 40%, 42% and 48% after 3, 6 and 9 hours, respectively, compared to the corresponding control data. The ATP level continued to decline, until 61% decrease had occurred after 12 hours, compared to the respective control (Figure 5.5a).

The ADP level remained stable in control cells for the entire duration of the incubation (Figure 5.5b). While in oxLDL-treated cells, the ADP level dropped by 27% during the first 3 hours. The ADP level continued to decline, reaching a level that was 33%, 45% and 51% less than that of the corresponding control data, after 6, 9 and 12 hours, respectively (Figure 5.5b).

In comparison, there was no change in the AMP level within control cells and in treated cells during the incubation period (Figure 5.5c).

The data for AMP, ADP and ATP levels over the 12 hour incubation period are shown together in Figure 5.5d.

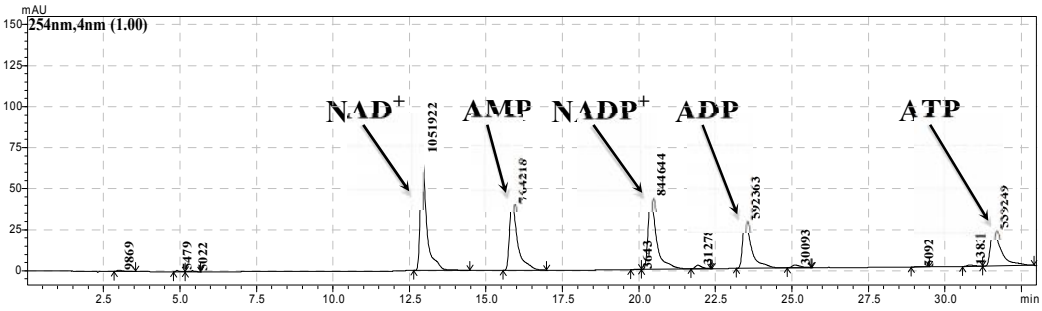

(a) Standard

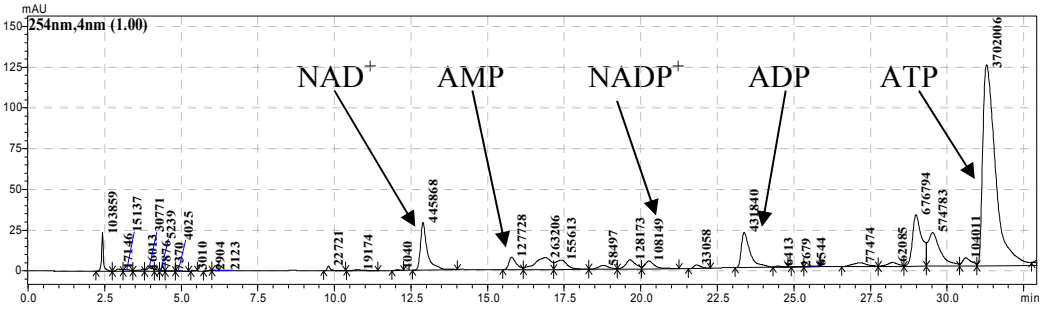

(b) Control, 0 hr

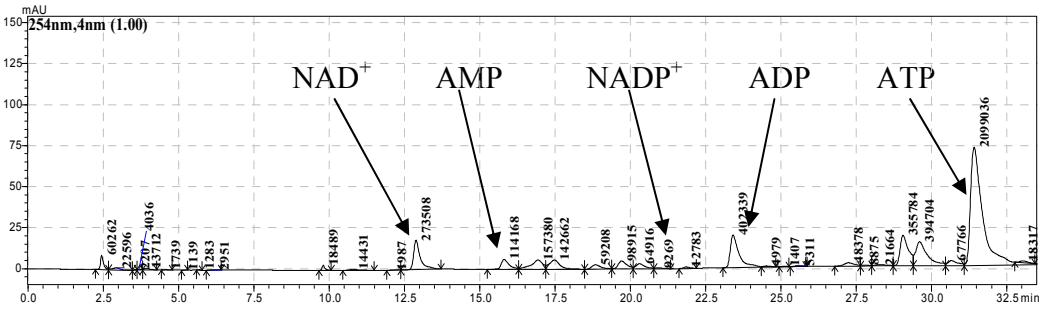

(c) 3 hr

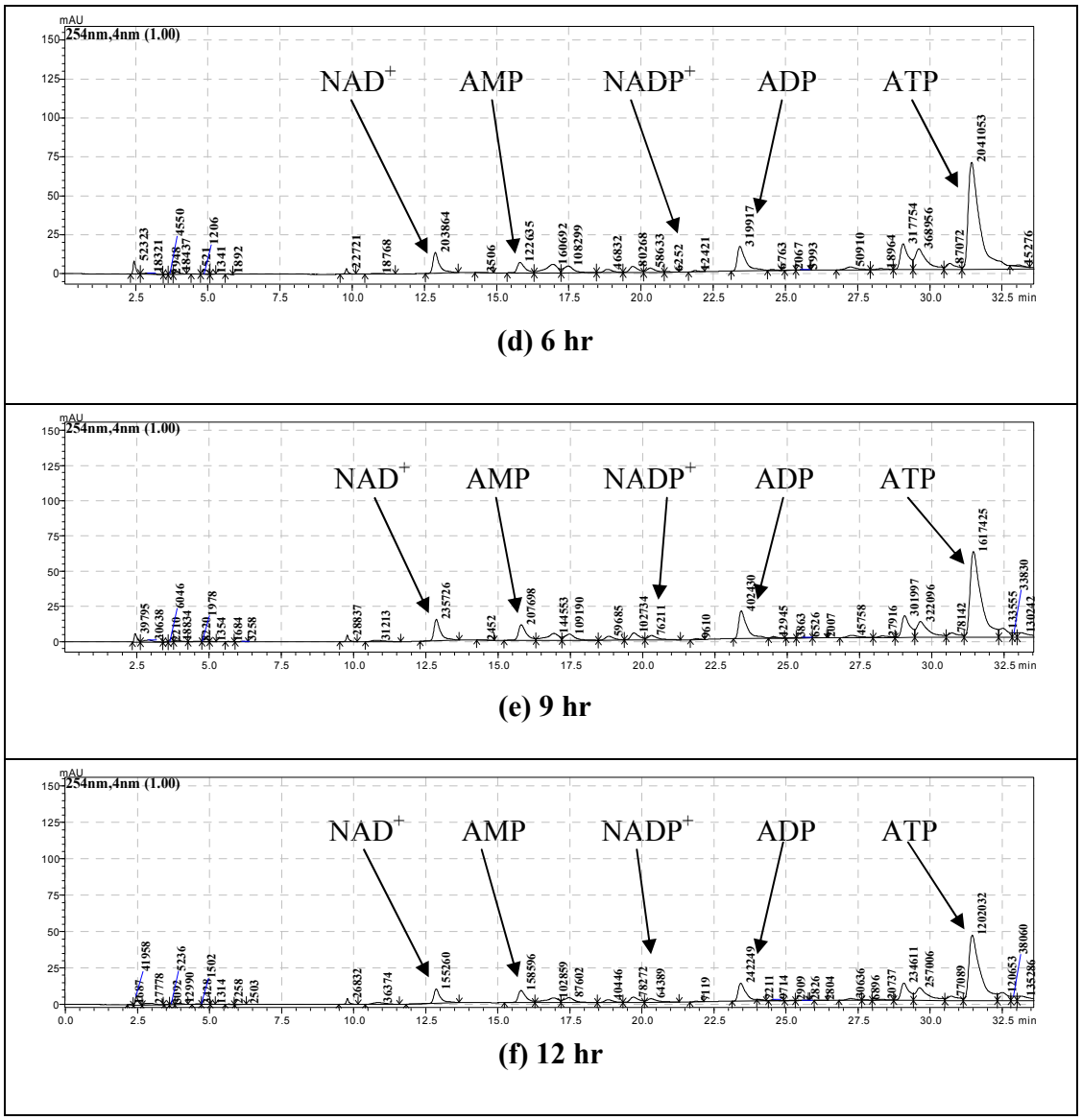

Figure 5.4 Chromatograms showing the effect of oxLDL on purine nucleotides ATP, ADP, AMP, NAD^+ and $NADP^+$ levels in HMDM cells over time.

15.0 x10^6 of HMDM cells at were incubated with 2.0 mg/ml oxLDL over a 12 hour period. (a) Standard; (b) Control HMDM cells without oxLDL added; (c) 3 hr; (d) 6 hr; (e) 9 hr; (f) 12 hr.

(a)

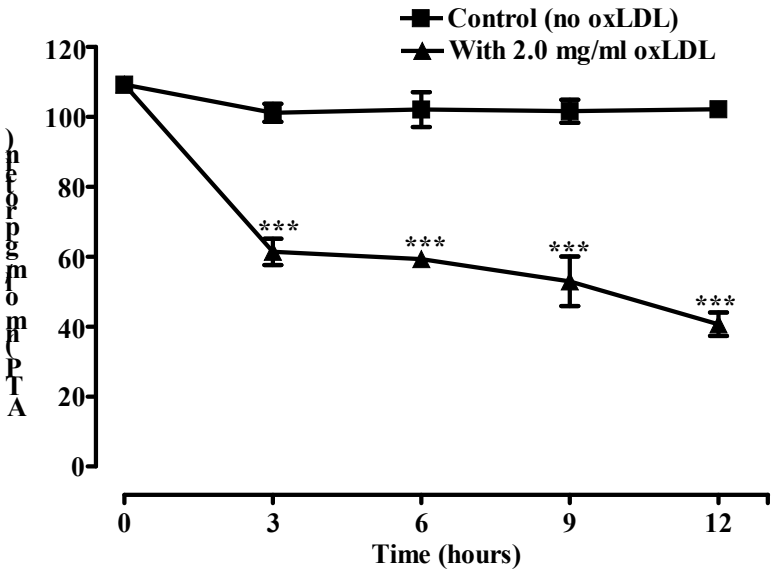
Control (no oxLDL)
With 2.0 mg/ml oxLDL
120
100
80
60
40
20
0
***
***
***
***
0
3
6
9
12
Time (hours)

(b)

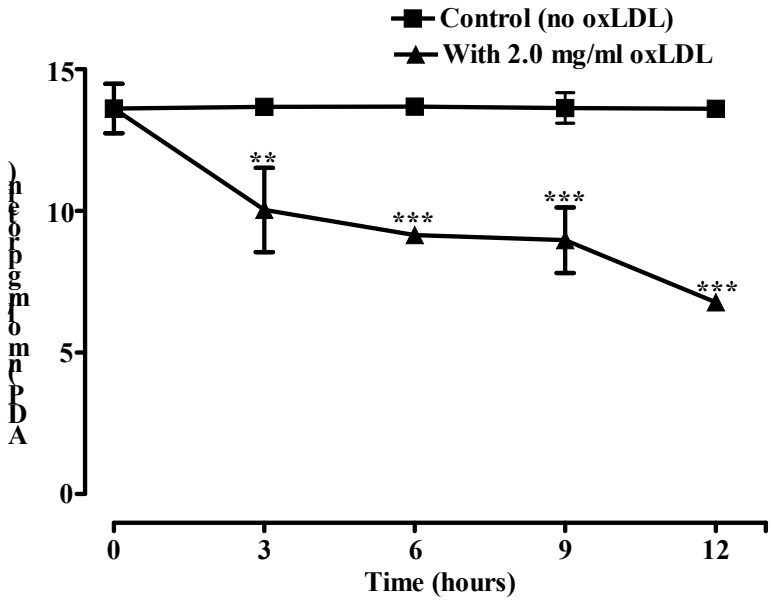
Control (no oxLDL)
With 2.0 mg/ml oxLDL
15
10
5
0
**
***
***
***
0
3
6
9
12
Time (hours)

(c)

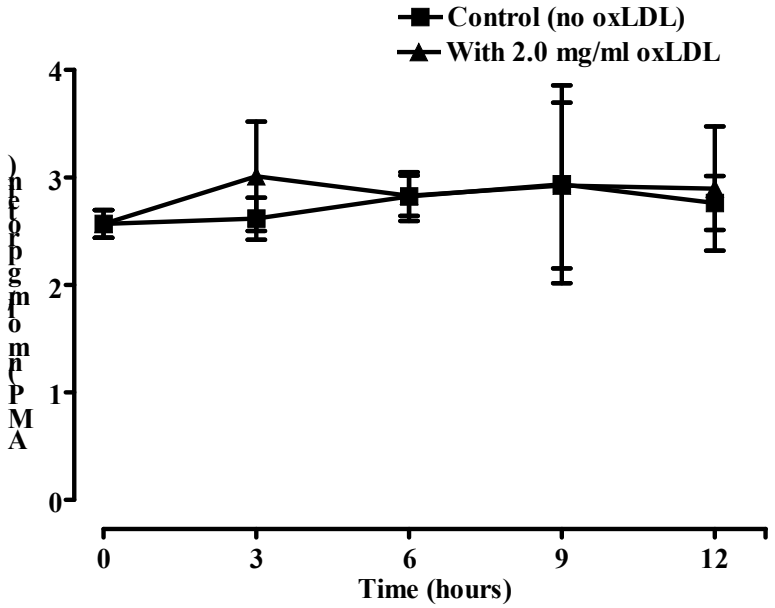

(d)

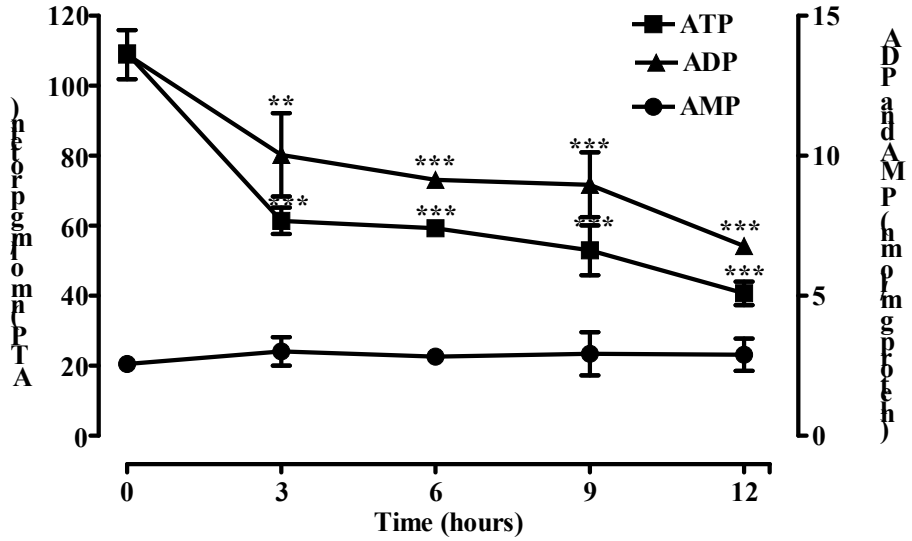

Figure 5.5 Time course showing the effect of oxLDL on ATP, ADP and AMP levels in HMDM cells.

15.0 x10^6 HMDM cells were incubated with 2.0 mg/ml oxLDL over a 12 hour period. (a) ATP; (b) ADP; (c) AMP; (d) All ATP, ADP and AMP. All concentrations were determined by HPLC analysis. Mean protein content was 0.5 mg/well. Significance is indicated as ** $P < 0.01$, *** $P < 0.001$ vs respective control of each time point. Results shown are the mean ± SEM of triplicate samples.

In HMDM cells, oxLDL caused a decrease in ATP and ADP levels, which began during the initial 3 hours. This loss of ADP and ATP levels is faster than the previously measured loss in lactate but is similar to the loss in GAPDH activity. Therefore, the cells' metabolic energy appears to slow down before cell lysis occurs; after 9 hours incubation, as measured by LDH release.

The NAD^+ level in control cells remained stable over the 12 hours (Figure 5.6a). In oxLDL-treated cells the NAD^+ level had dropped by 52% after 3 hours. The NAD^+ level continued to decline, reaching a level 57% lower than the corresponding control after 6 hours, 63% lower after 9 hours and 65% lower after 12 hours (Figure 5.6a).

The $NADP^+$ level in control cells remained stable during the incubation time (Figure 5.6b). In comparison, in oxLDL-treated cells, the $NADP^+$ level dropped by 34% during the initial 3 hours. The $NADP^+$ level continued to decline and reached levels that were 37%, 40% and 46% lower than their corresponding controls after 6, 9 and 12 hours, respectively (Figure 5.6b).

Therefore, oxLDL caused a decrease in the NAD^+ and $NADP^+$ levels in the first 3 hours, before cell lysis occurred. Cell lysis was after 9 hours, as measured by LDH release. This data was very similar to that observed with U937 cells described in chapter 4. Unfortunately we were unable to measure NADH and NADPH as they were found to be highly labile in the mobile phase used in this analysis.

(a)

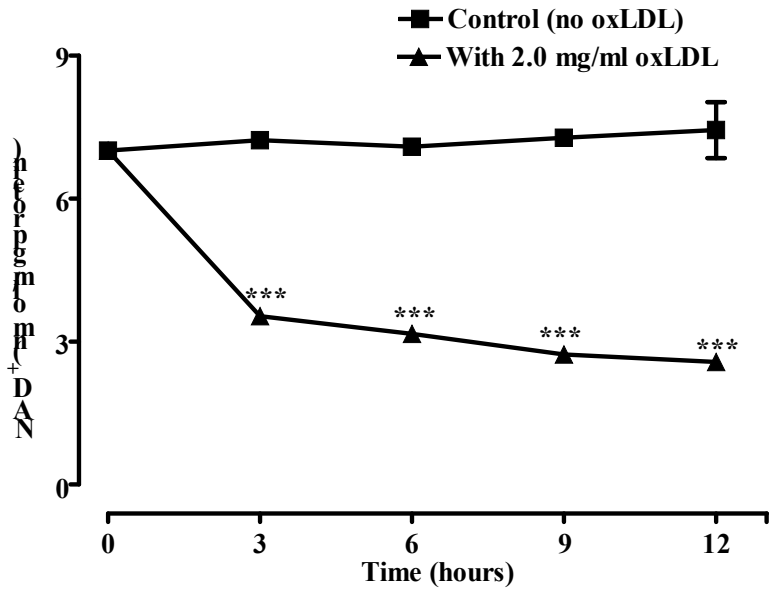

(b)

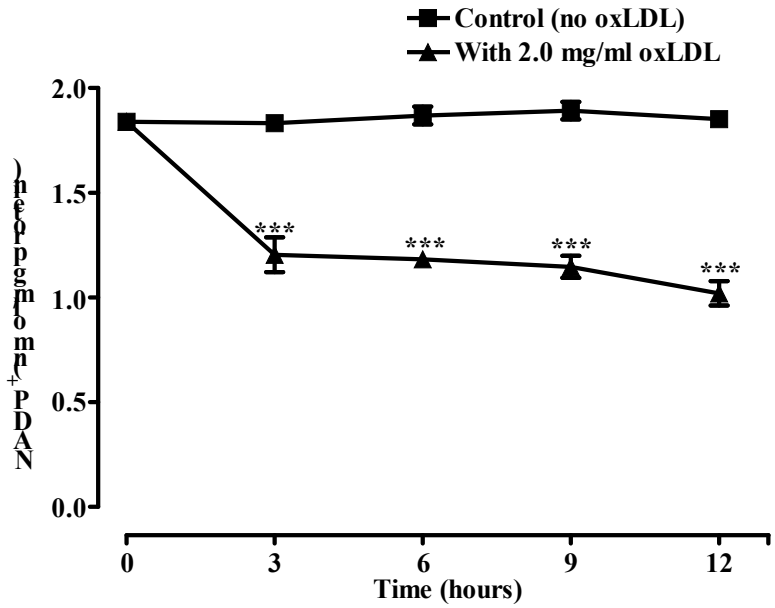

Figure 5.6 Time course showing the effect of oxLDL on NAD^+ and $NADP^+$ levels in HMDM cells.

15.0 x10^6 HMDM cells were incubated with 2.0 mg/ml oxLDL over a 12 hour period. (a) NAD^+; (b) $NADP^+$. All concentrations were determined by HPLC analysis. Mean protein content was 0.5 mg/well. Significance is indicated as *** $P < 0.001$ vs respective control of each time point. Results shown are the mean ± SEM of triplicate samples.

5.2.5 Effect of different concentration of 7,8-dihydroneopterin on lactate production in cell culture media of oxLDL-treated HMDM cells

The antioxidant effect of 7,8-dihydroneopterin on lactate production in cell culture media was studied by pre-incubated HMDM cells for 10 minutes with increasing concentrations of 7,8-dihydroneopterin (0, 50, 100, 150 and 200 μM) in RPMI-1640 (no phenol red) media containing 10% HIHS before incubation with and without 2.0 mg/ml oxLDL for 12 hours (Figure 5.7).

The presence of 7,8-dihydroneopterin alone, up to a concentration of 200 μM did not affect the lactate level in HMDM cells (Figure 5.7), while the presence of 2.0 mg/ml oxLDL alone caused a 44% decrease in the lactate level of the cell culture media (Figure 5.7). The presence of 7,8-dihydroneopterin caused a significant concentration dependent protection against oxLDL-induced loss of lactate production. This only occurred at 7,8-dihydroneopterin concentrations above 50 μM. At 100 μM 7,8-dihydroneopterin the lactate production increased by approximately 20% compared to the oxLDL only control. With 200 μM 7,8-dihydroneopterin the lactate output by the cells was fully protected such there was no significant effect due to the presence of oxLDL (Figure 5.7). The data shows 7,8-dihydroneopterin has a protective effect against oxLDL-induced damage to HMDM cells glycolytic activity, as measured by the lactate levels measured in the cell culture media.

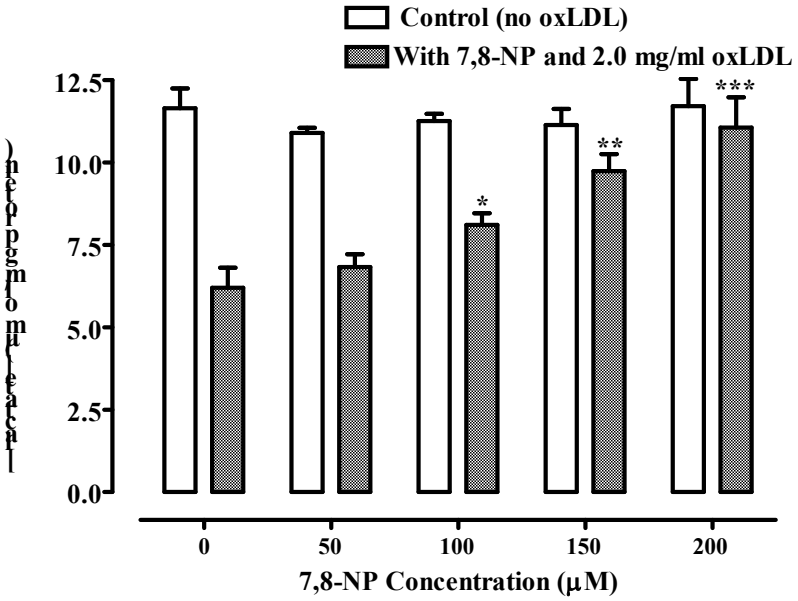

Figure 5.7 Effect of 7,8-NP concentration on lactate production in cell culture media of oxLDL-treated HMDM cells.

HMDM cells at 5.0 x10^6 cells/ml were incubated with different concentrations of 7,8-dihydroneopterin (0, 50, 100, 150 and 200 μM) before incubation with or without 2.0 mg/ml oxLDL for 12 hours. The lactate released to culture media was measured. Mean protein content was 0.5 mg/well. Results shown are the mean ± SEM of triplicate samples. Significant of results was examined by comparing the lactate concentration with each 7,8-dihydroneopterin concentration with the positive control containing cells with just oxLDL; Significance is indicated as * $P < 0.05$, ** $P < 0.01$, *** $P < 0.001$.

5.2.6 Effect of 7,8-dihydroneopterin concentration on GAPDH activity in oxLDL-treated HMDM cells

The antioxidant effect of 7,8-dihydroneopterin on GAPDH activity was studied by pre-incubated HMDM cells for 10 minutes with various concentrations of 7,8-dihydroneopterin (0, 25, 50, 100, 150 and 200 μM) in RPMI-1640 (no phenol red) media containing 10% HIHS before incubation with and without 2.0 mg/ml oxLDL for 24 hours (Figure 5.8).

The presence of 7,8-dihydroneopterin alone, up to a concentration of 200 μM, did not affect the GAPDH activity in HMDM cells (Figure 5.8), while the presence of 2.0 mg/ml oxLDL alone caused a 72% decrease in the GAPDH activity (Figure 5.8). In the presence of 25 and 50 μM 7,8-dihydroneopterin, there was an increased GAPDH activity from the oxLDL alone controls but this increase was not significant until 100 μM 7,8-dihydroneopterin or greater was added to the media. In the presence of 150 and 200 μM 7,8-dihydroneopterin, GAPDH activity 50% and 70% greater than the oxLDL only control, respectively (Figure 5.8). This shows that at concentrations of 100 μM and greater, 7,8-dihydroneopterin protects GAPDH from the oxidative stress induced by oxLDL.

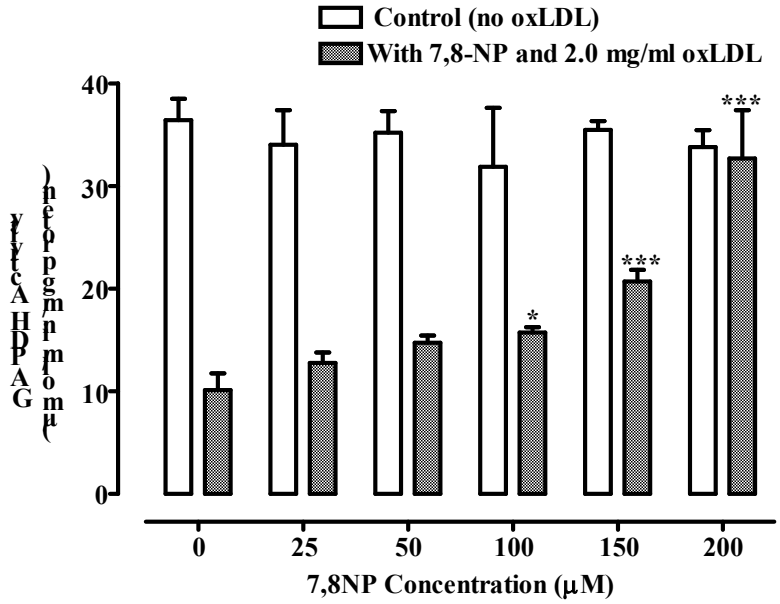

Figure 5.8 Effect of 7,8-NP concentration on GAPDH activity of oxLDL-treated HMDM cells.

HMDM cells at 5.0 x10^6 cells/ml were incubated with different concentrations of 7,8-dihydroneopterin (0, 25, 50, 100, 150 and 200 μM) before incubation with or without 2.0 mg/ml oxLDL for 24 hours. The GAPDH activity was measured. Mean protein content was 0.5 mg/well. Results shown are the mean ± SEM of triplicate samples and significant was tested between the positive control of cells with just oxLDL and cells with 7,8-dihydroneopterin and oxLDL. Significance is indicated as * $P < 0.05$, *** $P < 0.001$.

5.2.7 Effect of 7,8-dihydroneopterin on GAPDH activity in oxLDL-treated HMDM cells

A time course study of the antioxidant effect of 7,8-dihydroneopterin on HMDM cell GAPDH activity was conducted by pre-incubated HMDM cells for 10 minutes with 200 μM 7,8-dihydroneopterin in RPMI-1640 media containing 10% HIHS with and without 2.0 mg/ml oxLDL for 24 hours (Figure 5.9). In the presence of 2.0 mg/ml oxLDL alone, the GAPDH activity dropped by 28% during the initial 3 hours and 53% less than the control after 6 hours. Only 9% of the original HMDM GAPDH activity remained after 24 hours with oxLDL (Figure 5.9). In the presence of 200 μM 7,8-dihydroneopterin and 2.0 mg/ml oxLDL, the GAPDH activity remained the same over time compared to the corresponding control of each time point (with oxLDL alone) (Figure 5.9).

5.2.8 Effect of 7,8-dihydroneopterin on oxLDL uptake by HMDM cells

It was possible that the observed protective effect of 7,8-dihydroneopterin was simply due to this compound affecting the uptake of oxLDL and therefore preventing the oxLDL having a toxic effect on the cells. This was examined by measuring the uptake of labelled oxLDL. DiI was chosen because we were concerned about possible protein oxidation effects with other labelling systems and the stability of the label. DiI is a fluorescent lipophilic dye which is rapidly absorbed into the lipid layer of the oxLDL and becomes trapped within the cells once the oxLDL is taken up (Stephan & Yurachek, 1993).

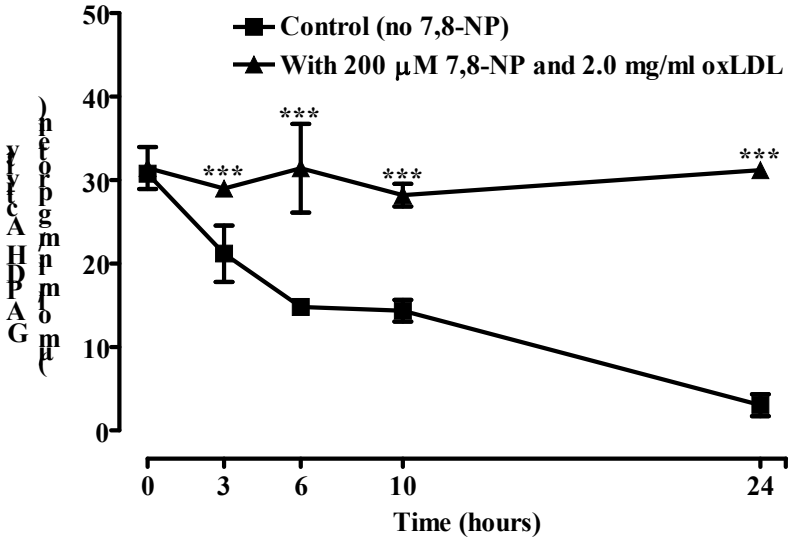

Figure 5.9 Time course showing the effect of 7,8-NP on GAPDH activity in oxLDL-treated HMDM cells.

HMDM cells at 5.0 x10^6 cells/ml were incubated with or without 200 μM 7,8-dihydroneopterin before incubation with 2.0 mg/ml oxLDL over a 24 hour period. The GAPDH activity was measured at various time points. Mean protein content was 0.5 mg/well. Significance is indicated as *** $P < 0.001$ vs respective control at each time point. Results shown are the mean ± SEM of triplicate samples.

5.2.8.1 Standardisation of fluorescence for DiI and DiI-oxLDL concentrations

The main fluorescence intensity (MFI) of DiI and DiI-oxLDL (oxLDL which had been labelled with fluorescent DiI at 37°C) was measured at different concentrations in order to generate a standard curve and measure the range of linearity of both free and bound label. With free DiI in isopropanol there was a direct liner relationship between the DiI concentration and fluorescence intensity between 1 to 10 μg/ml (Figure 5.10a). Above 10 μg/ml the fluorescence intensity reached a maximal level. When absorbed into oxLDL there was some change in the fluorescent intensity. The concentration-dependent fluorescence of DiI-oxLDL is shown in Figure 5.10b. There was a linear correlation between DiI-oxLDL concentration and fluorescence between 0.05 and 200 μg/ml; above this concentration the fluorescence intensity reached a maximal level. Therefore, DiI and DiI-oxLDL up to a concentration of 10 and 200 μg/ml, respectively, must be used in order to obtain a true reading of fluorescence intensity. Any fluorescence intensities above this concentration may give an inaccurate result.

5.2.8.2 Effect of DiI-oxLDL and 7,8-dihydroneopterin on HMDM cell viability and morphology

The effect of DiI-oxLDL with and without 7,8-dihydroneopterin, on HMDM cell viability and morphology were studied by pre-incubated HMDM cells for 10 minutes with or without 200 μM 7,8-dihydroneopterin in RPMI-1640 media plus 10% HIHS for 12 hours (Figure 5.11 and Figure 5.12). However, preliminary studies suggested that the DiI was acting as an antioxidant and so was affecting the oxLDL cytotoxicity. This was

(a)

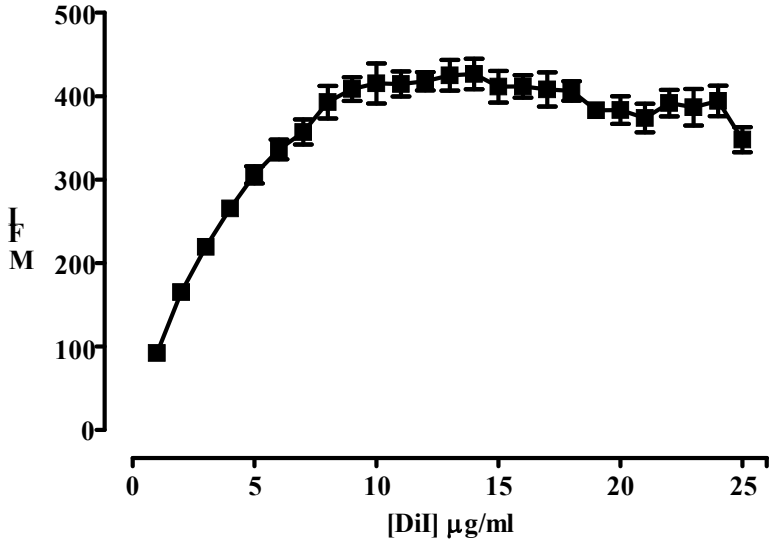

(b)

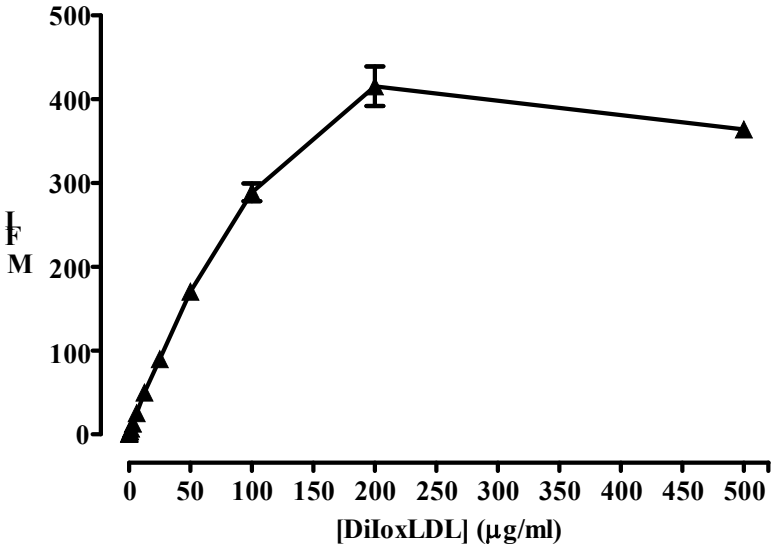

Figure 5.10 Concentration-dependent fluorescence of DiI and DiI-oxLDL.
(a) Free DiI concentration range from 1 to 25 µg/ml. The correlation remained linear up to a concentration of 10 µg/ml. (b) DiI-oxLDL concentration range from 0.5 to 500 µg/ml. The correlation remained linear up to a concentration of 200 µg/ml.

confirmed when it was shown that 2.0 mg/ml DiI-oxLDL was not cytotoxic (bar e, Figure 5.11) while oxLDL (bar b, Figure 5.11) was cytotoxic and only 49% of cells were still viable. The addition of 0.2 mg/ml DiI-oxLDL did not reduce the toxicity of the 2.0 mg/ml oxLDL on the HMDM cells (bar c, Figure 5.11). The DiI-oxLDL at 0.2 mg/ml as expected was also not cytotoxic (bar d, Figure 5.11). The addition of 7,8-dihydroneopterin to the DiI combination still prevented the loss of cell viability showing that the DiI did not interfere with the action of the 7,8-dihydroneopterin (bars f-i, Figure 5.11). HMDM cell morphology was photographed before the MTT viability assay after 12 hour incubation (Figure 5.12).

Control cells showed a typical, round shape (Figure 5.12a) but in the presence of 2.0 mg/ml oxLDL (Figure 5.12b) and 0.2 mg/ml DiI-oxLDL with 2.0 mg/ml oxLDL (Figure 5.12c), there appeared to be more cell lysis compared to the control cells but the presence of 200 μM 7,8-dihydroneopterin prevented the loss of normal cell morphology (Figure 5.12f & g). There was no change in cell morphology in the presence of the 0.2 mg/ml DiI-OxLDL (Figure 5.12d) or 2.0 mg/ml DiI-oxLDL (Figure 5.12e) or in the presence of 200 μM 7,8-dihydroneopterin (Figure 5.12h & i) compared to the control cells. The cell morphology was in agreement with that measured by the MTT viability reduction assay. Therefore, the presence of the DiI was not masking changes measured by the MTT reduction.

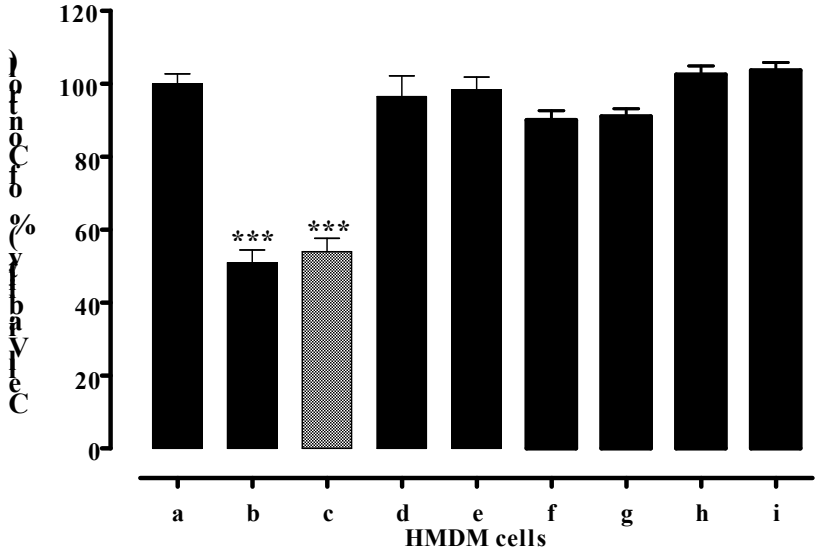

Figure 5.11 Effect of DiI-oxLDL and 7,8-NP on HMDM cell viability.
HMDM cells (5.0 x10^6 cells/ml) were incubated for 12 hours before cell viability measurement by MTT reduction. The figure shows cells alone (a), cells with 2.0 mg/ml oxLDL (b), cells with 0.2 mg/ml DiI-oxLDL and 2.0 mg/ml oxLDL (c), cells with 0.2 mg/ml DiI-oxLDL (d), cells with 2.0 mg/ml DiI-oxLDL (e), cells with 200 µM 7,8-dihydroneopterin and 2.0 mg/ml oxLDL (f), cells with 200 µM 7,8-dihydroneopterin, 0.2 mg/ml DiI-oxLDL and 2.0 mg/ml oxLDL (g), cells with 200 µM 7,8-dihydroneopterin and 0.2 mg/ml DiI-oxLDL (h), cells with 200 µM 7,8-dihydroneopterin and 2.0 mg/ml DiI-oxLDL (i). Results shown are the mean ± SEM of triplicate samples. Significance was determined between the control of cell without oxLDL (a) and the other conditions and shown as *** $P < 0.001$.

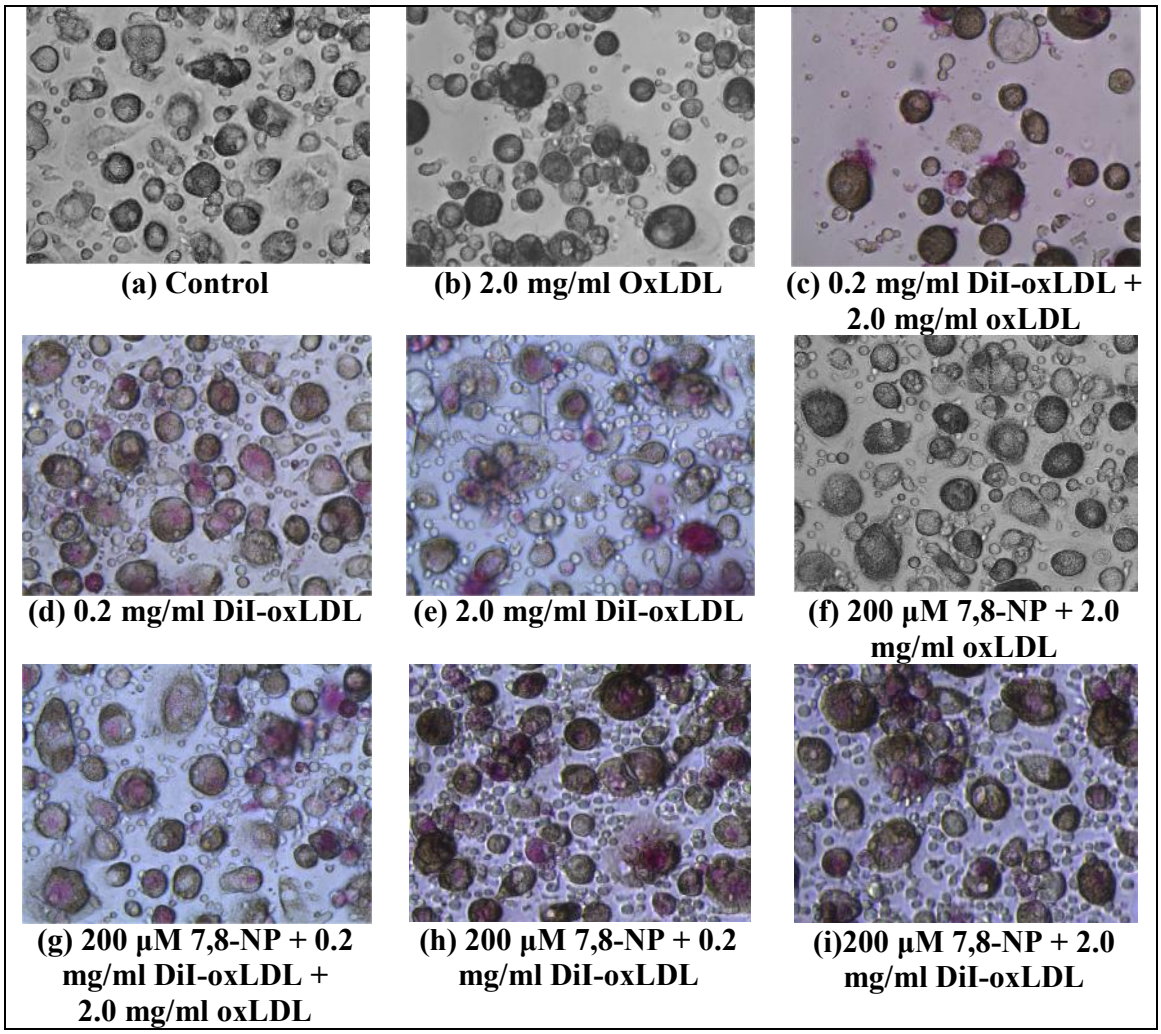

Figure 5.12 HMDM cell morphology during incubation with DiI-oxLDL.
HMDM cells at 5.0 x10^6 cells/ml were incubated with 2.0 mg/ml oxLDL, or 0.2 mg/ml DiI-oxLDL, or 0.2 mg/ml DiI-oxLDL, or 2.0 mg/ml DiI-oxLDL without or with 200 µM 7,8-dihydroneopterin for a 12 hours. (a) HMDM cells; (b) 2.0 mg/ml oxLDL; (f) 7,8-dihydroneopterin and 2.0 mg/ml oxLDL; (d) 0.2 mg/ml DiI-oxLDL; (c) 0.2 mg/ml DiI-oxLDL and 2.0 mg/ml oxLDL; (e) 2.0 mg/ml DiI-oxLDL; (h) 200 µM 7,8-dihydroneopterin and 0.2 mg/ml DiI-oxLDL (g) 7,8-dihydroneopterin, 0.2 mg/ml DiI-oxLDL and 2.0 mg/ml oxLDL; (i) 200 µM 7,8-dihydroneopterin and 2.0 mg/ml DiI-oxLDL.

Overall the data shows that 0.2 mg/ml DiI-oxLDL can be used to measure oxLDL uptake under non-cytotoxic conditions. In cytotoxic conditions, a mixture of 0.2 mg/ml DiI-oxLDL with non-labelled 2.0 mg/ml oxLDL can be used to measure the oxLDL uptake also, because both are taken up equally by the same mechanism. The 2.0 mg/ml DiI-oxLDL cannot be used for the uptake studies because it is not cytotoxic.

5.2.8.3 Effect of 7,8-dihydroneopterin on HMDM cell uptake of DiI-oxLDL at non-cytotoxic levels

The death of the HMDM cells with cytotoxic levels of oxLDL makes the uptake data difficult to interpret. As a result, the first uptake studies were conducted with the 0.2 mg/ml DiI oxLDL. HMDM cells were then pre-incubated for 10 minutes with or without 200 μM 7,8-dihydroneopterin in RPMI-1640 media containing 10% HIHS with 0.2 DiI-oxLDL (non-cytotoxic level) at 37°C (to measure cell association) over a 10 hour period (Figure 5.13). In control cells, the uptake of DiI-oxLDL by HMDM cells increased during the initial 3 hours, before it slowed and uptake stopped at 6 hours. The presence of 200 μM 7,8-dihydroneopterin significantly slowed the rate of uptake. The final concentration of DiI in the cells was 35% of the control cells without 7,8-dihydroneopterin (Figure 5.13). Therefore, 7,8-dihydroneopterin decreased the uptake of oxLDL when a non-toxic concentration of DiI-oxLDL was used.

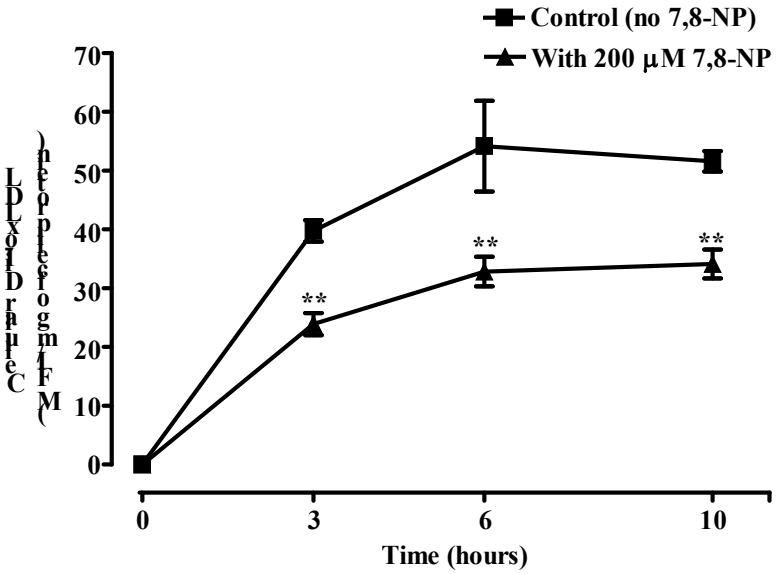

Figure 5.13 Time course showing the effect of 7,8-NP on the uptake of non-cytotoxic level of DiI-oxLDL by HMDM cells.

HMDM cells at 5.0 x10^6 cells/ml were incubated with or without 200 μM 7,8-dihydroneopterin before incubation with 0.2 mg/ml DiI-oxLDL at 37°C (to measure cell association) over a 10 hour period. Mean protein content was 0.5 mg/well. Significance is indicated as ** $P < 0.01$ vs respective control at each time point. Results shown are the mean ± SEM of triplicate samples.

5.2.8.4 Effect of 7,8-dihydroneopterin on HMDM cell uptake of a non-cytotoxic level of DiI-oxLDL mixed with cytotoxic level of oxLDL

There was the possibility that oxLDL and DiI-oxLDL might be treated differently by the cell. Though difficult to explore this was examined by mixing 50 ug/ml DiI-oxLDL with non-labelled oxLDL at 2.0 mg/ml and giving this to the HMDM cells. HMDM cells were pre-incubated for 10 minutes with or without 200 μM 7,8-dihydroneopterin in RPMI-1640 containing 10% HIHS with 0.05 mg/ml DiI-oxLDL mixed with 2.0 mg/ml oxLDL (cytotoxic level) at 37°C over a 10 hour period (Figure 5.14). There was a time dependent uptake of DiI-oxLDL by HMDM cells. In control cells, the uptake of DiI-oxLDL by HMDM cells increased during the initial 3 hours, and then the rate decreased during the following 6 hours before stopping after 6 hours. The same trend was recorded in 7,8-dihydroneopterin treated cells, but the DiI-oxLDL uptake in the presence of 7,8-dihydroneopterin was reduced by 22%, 42% and 40% after 3, 6 and 10 hours, respectively, as compared to the respective control at each time point (Figure 5.14). Therefore, 7,8-dihydroneopterin was able to slow uptake of Di-oxLDL into the cell in the presence of a toxic oxLDL concentration. Examination of the cells at 12 hours (Figure 5.12) shows that in the absence of 7,8-dihydroneopterin there was considerable cell damage which may explain the lack of DiI-oxLDL uptake after 6 hours. In contrast the 7,8-dihydroneopterin appears to have stopped the oxLDL uptake after 3 hours and the cells have remained healthy.

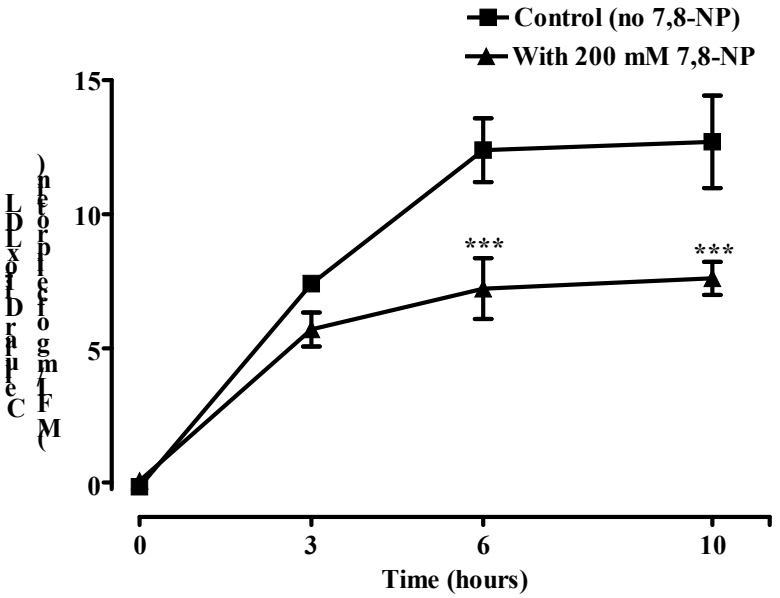

Figure 5.14 Time course showing the effect of 7,8-NP on the uptake of non-cytotoxic level of DiI-oxLDL mixed with cytotoxic level of oxLDL by HMDM cells.
HMDM cells at 5.0 x10^6 cells/ml were incubated with or without 200 μM 7,8-dihydroneopterin before incubation with 0.05 mg/ml DiI-oxLDL and 2.0 mg/ml oxLDL at 37°C (to measure cell association) over a 10 hour period. Mean protein content was 0.5 mg/well. Significance is indicated as ***P < 0.001 vs respective control at each time point. Results shown are the mean ± SEM of triplicate samples.

5.3 Discussion

5.3.1 Lactate release and metabolic activity

The cytotoxicity of oxLDL in HMDM cells has been clearly demonstrated in chapter 3; as a loss in cell viability after 6 hours, measured using MTT reduction, which concluded with extensive cell lysis. In this chapter 5, the cytotoxicity of oxLDL to HMDM cells has been further shown by measuring lactate and purine nucleotide concentrations in addition to measuring lactate dehydrogenase and GAPDH activity. As discussed in chapter 4, the effects on U937 cells and on HMDM, in this chapter, are very similar to what has previously been described for smooth muscle cells (SMCs) in *vitro* (Sukhanov *et al.*, 2006).

Lactate is the end product of anaerobic glycolysis, which is one of the major metabolic pathways in macrophage cells (Loike *et al.*, 1993, Nelson & Cox, 2005). As was observed with the U937 cells in chapter 4, there was no overall loss in LDH activity. When cell lysis started to occur, the LDH enzyme began to leak from the intracellular space into the cell culture media. The changes in lactate levels are therefore a consequence in the change in metabolism of the HMDM cells. In HMDM cells, time course studies indicated that lactate production and release-into the cell culture media dropped after 6 hours yet significant LDH loss from the cell did not occur till 9 hours showing that cell metabolism slowed before cell lysis occurred in HMDM cells.

As previously described, GAPDH is a critical enzyme in glycolysis as it contains oxidatively sensitive thiol. Net ATP production in glycolytic cells, such as macrophages, results mainly from substrate level phosphorylation reactions catalysed by enzymes

below GAPDH in glycolysis (phosphoglycerate kinase and pyruvate kinase). In HMDM cells, oxLDL caused a decrease in GAPDH activity and in ATP, ADP, NAD^+ and $NADP^+$ levels from the initial 3 hours. This occurred faster than the loss in cell viability and in lactate levels, which happened after 6 hours. Therefore, in HMDM cells the metabolic energy production slowed down before cell lysis occurred, which was after 9 hours as measured by LDH release. In HMDM cells, the reduction in GAPDH activity and in ATP, ADP, NAD^+ and $NADP^+$ levels happened at the same time as in U937 cells, as discussed in a previous chapter 4 of this study.

This delay in time between LDH enzyme loss to the cytoplasm and lactate production suggests that the LDH enzyme was still active after the shutdown of glycolysis but pyruvate synthesis from glycolysis and pentose phosphate had decreased. The loss of GAPDH will have decreased glycolysis production of pyruvate. The decrease in $NADP^+$ (Figure 5.6b) before cell lysis suggests that much of the lost $NADP^+$ was converted to NADPH. Pentose phosphate activity is controlled by the enzyme glucose-6-phosphate dehydrogenase which is inhibited by NADPH. The drop in lactate production after treatment with oxLDL dose suggests both glycolysis and the pentose phosphate pathway were inhibited at 6 hours. Unfortunately, with our high performance liquid chromatography (HPLC) method NADPH and NADH were extremely labile and therefore cannot be measured so we are unable to confirm this hypothesis. The same finding was found in U937 cells in this study and in other study (Caruso *et al.*, 2004) as discussed in a previous chapter 4.

Interestingly, inflammation plays an important role in the elevation of lactate concentration by macrophages (Leppänen *et al.*, 2006, Loike *et al.*, 1993, Samuvel *et al.*, 2009). Increased lactate concentration affects gene expression and cell function (Hunt *et al.*, 1978). Lactate enhances lipopolysaccharide (LPS)-induced inflammation by stimulating cytokine expression by macrophages (Samuvel *et al.*, 2009, Nareika *et al.*, 2005). As discussed in detail in the previous chapter 4, macrophages transported lactate to the extracellular space and utilised it as source of energy (Loike *et al.*, 1993, Drake *et al.*, 1980). The extracellular activity of the LDH enzyme increases under the condition of oxidative stress (Jovanovic *et al.*, 2010). This is very different to what we have observed; we have measured a cell death process rather than an activation or inflammation process.

The results of oxidative stress are lipid peroxidation of the cell membrane, enzyme inactivation through sulfydryl groups (-SH), protein aggregation, polysaccharide polymerisation and the damage of nucleic acids. It occurs in the chain of acute processes, such as in some inflammatory reactions (Ames *et al.*, 1993). With HMDM cells, oxLDL triggered a large oxidative stress, causing the rapid loss of cellular glutathione (GSH), GAPDH inhibition and eventual loss of viability, without caspase-3 activation (Gieseg *et al.*, 2010). As discussed in detail in chapter 4, many studies have shown that inactivation of GAPDH is a marker of oxidative stress, which results in a decrease in intracellular ATP levels (Ralser *et al.*, 2007, Mckenzie *et al.*, 1996, Schraufstatter *et al.*, 1990). OxLDL has been shown to decrease GAPDH activity, which causes inhibition of glycolysis and decreases ATP levels in HASMCs, which in turn plays an important role in the mechanisms of atherogenesis (Sukhanov *et al.*, 2006). In addition, GAPDH inactivation by another oxidant, nitric oxide (NO) has been shown to reduce GAPDH

activity and ATP content in macrophages (Albina *et al.*, 1999). In a previous study in our laboratory, hypochlorite (HOCl)-treated HMDM cells showed a concentration-dependent decrease in intracellular ATP when a concentration above 50 μM of HOCl was used. The time course study showed that 100 μM HOCl induced a rapid decrease in intracellular ATP. HOCl mediated intracellular ATP loss in HMDM cells, which contributes to necrotic cell death (Yang, 2009).

Surprisingly, the AMP levels in HMDM cells did not significantly differ from the controls over time (Figure 5.5c). This was also found with U937 cells in this study and in other studies (Pelzmann *et al.*, 2003, Emerling *et al.*, 2009) as discussed in chapter 4. We would have expected the cellular AMP levels to increase as cells can regenerate ATP by substrate level phosphorylation of ADP by adenylate-kinase, producing ATP and AMP (Solaroli *et al.*, 2009). This reaction does not appear to have been significant within the oxLDL treated macrophages.

5.3.2 7,8-Dihydroneopterin protection of metabolic function

In this study, the potential antioxidant effect of 7,8-dihydroneopterin against the damage caused by oxLDL was investigated in HMDM cells. The influence of 7,8-dihydroneopterin was assessed by measuring the lactate level and the activity of the GAPDH enzyme in the presence of 7,8-dihydroneopterin and oxLDL. In the previous chapters, 7,8-dihydroneopterin was shown to be very effective at preventing the loss of metabolic function in U937 cells. In this chapter, we examine if HMDM cells, which unlike U937 cells, are found in the artery wall, will respond in the same way. With the

related THP-1 cell line, 7,8-dihydroneopterin had no protective effect against oxLDL or peroxyl-radicals. The reason behind this difference remains unresolved.

In HMDM cells, there was a concentration-dependent protection by 7,8-dihydroneopterin against oxLDL-induced loss of lactate production and in the loss of GAPDH activity. A maximum protective effect was established with 200 μM 7,8-dihydroneopterin. Therefore, 7,8-dihydroneopterin has a protective effect against oxLDL-induced damage by maintaining metabolic activity as measured by lactate levels in the cell culture media of HMDM cells and glycolytic GAPDH activity. In HMDM cells, time course studies indicated that 7,8-dihydroneopterin protects GAPDH activity loss against oxLDL-induced damage in HMDM cells from the initial 3 hours. The protective effect of 7,8-dihydroneopterin against the damage caused by oxLDL in HMDM cells occurred with the same timing as that measured in U937 cells in this study (as discussed in a previous chapter).

7,8-Dihydroneopterin appears to decrease the cytotoxicity of oxLDL in HMDM cells and protects the cellular GSH and GAPDH activity by scavenging oxidants generated in response to oxLDL (Gieseg *et al.*, 2010). Previous studies found that during inflammation, 7,8-dihydroneopterin has a protective effect against oxidants (Gieseg *et al.*, 1995, Gieseg *et al.*, 2000, Gieseg *et al.*, 2001b, Duggan *et al.*, 2002, Firth *et al.*, 2008b) as discussed in detail before in Chapters 3 and 4.

5.3.3 OxLDL uptake

There is a possibility that the protective effect of 7,8-dihydroneopterin-against oxLDL-induced damage is established by influencing the uptake of oxLDL. In the present study, it was found that 7,8-dihydroneopterin was able to inhibit oxLDL uptake when used at a non-cytotoxic level of DiI-oxLDL alone or mixed with cytotoxic level of oxLDL. The non-cytotoxic concentration of DiI-oxLDL did not affect cell viability, while mixed with a cytotoxic level of oxLDL did cause cell viability loss. Although, the high concentration of DiI-oxLDL (2.0 mg/ml), which is supposed to be cytotoxic, did not affect the cell viability and so appeared to have acted as protectant.

This finding is consistent with previous studies in this laboratory, which have shown a time-dependent uptake of Di-oxLDL by HMDM cells, and a significant inhibitory effect of 7,8-dihydroneopterin on the uptake of oxLDL when non-toxic oxLDL concentrations were used (Amit, 2008). Later studies have now shown a down regulation of HMDM cell plasma membrane CD36 receptor by 7,8-dihydroneopterin which may cause a decrease in oxLDL uptake by HMDM cells (Gieseg *et al.*, 2010). The ability of 7,8-dihydroneopterin to protect HMDM cells from oxLDL-induced death provides further evidence that this antioxidant may be secreted by HMDM cells to provide protection against oxidative damage in the highly oxidative environment of atherosclerotic plaque.

6 General discussion and conclusion

6.1 Hypothesis

The primary hypothesis of this research was that oxidised low density lipoprotein (oxLDL) causes human monocyte-like cell line U937 and human monocyte-derived macrophage (HMDM) cells to undergo necrotic cell death, via oxidative loss of key metabolic enzymes causing the loss of glycolytic activity and the shutdown of metabolism. This was tested by examining the effect of oxLDL on the U937 and HMDM cells glycolytic activity through measuring glyceraldehyde-3-phosphate dehydrogenase (GAPDH) and lactate dehydrogenase (LDH) enzyme activity, lactate production, the rate of oxygen consumption (VO_2) and intracellular adenosine triphosphate (ATP) levels. The study showed that oxLDL caused a progressive, time-dependent shutdown of glycolytic metabolism. Study of the GAPDH enzyme showed that the loss of this enzyme activity was due to oxidative inactivation. It was also hypothesised that the antioxidant 7,8-dihydroneopterin (7,8-NP) would protect cells from this oxidative stress. The addition of 7,8-dihydroneopterin did prevent the loss of intracellular glutathione (GSH) and the various enzyme markers studied.

The findings of this PhD research are summarised in Figure 6.1. OxLDL interacts with the cell via an as yet, undetermined mechanism to produce an intracellular oxidative stress. This oxidative stress is thought to be in the initial form of superoxide ($O_2^{\bullet -}$) generated via NADPH-oxidase (NOX) (Selemidis *et al.*, 2007). The resulting reactive oxygen species (ROS) generated within the cell cause the loss of GSH. In the absence of

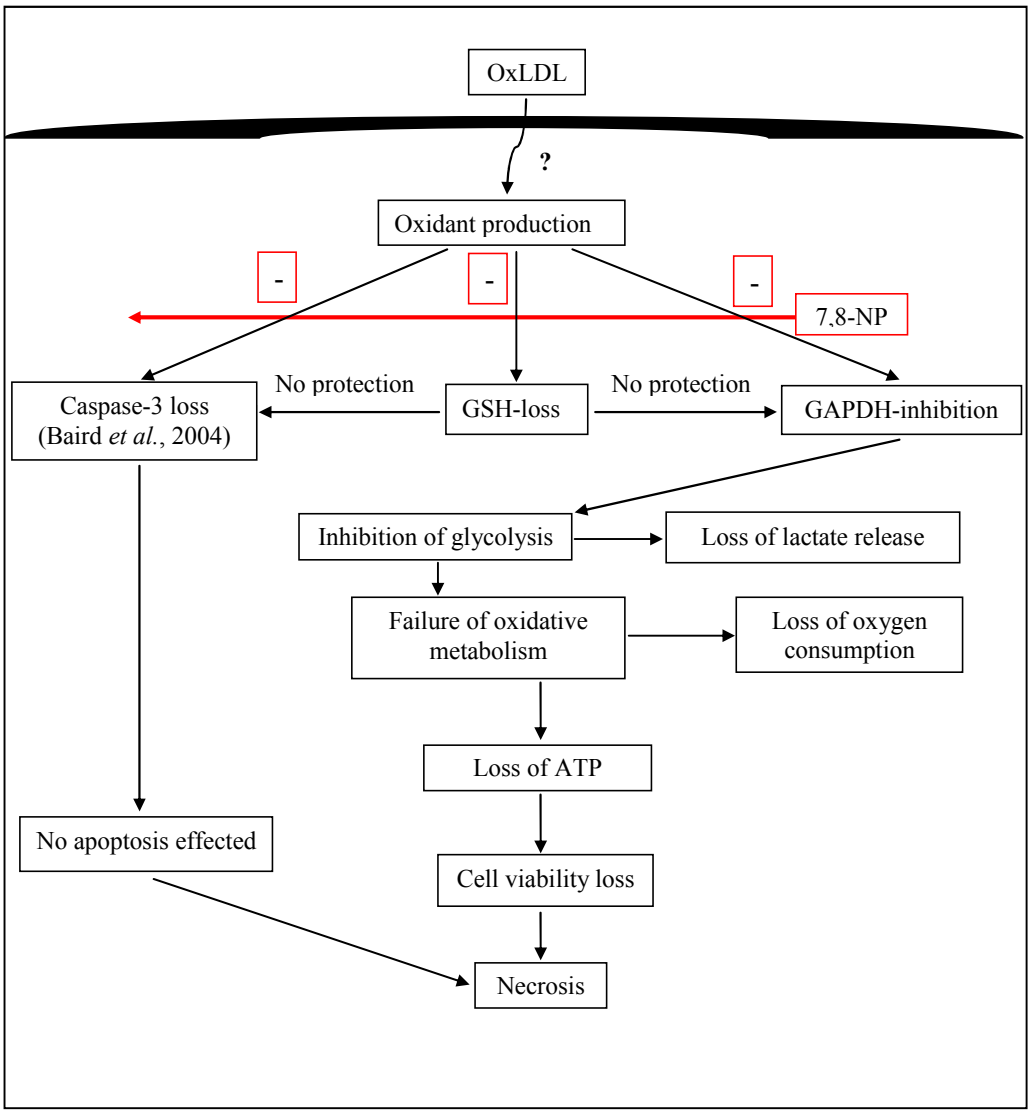

Figure 6.1 Events lead to metabolic activity loss, GSH loss and necrotic cell death in oxLDL-treated U937 and HMDM cells.
The addition of oxLDL to the cells triggers a series of events starting with the loss of GSH. The loss of GSH allows the oxidative loss of caspase and GAPDH activity. 7,8-Dihydroneopterin protecting U937 and HMDM cells' metabolic activity by preventing the loss of GSH so preventing cell death.

the GSH, the oxidative stress then is able to oxidise and inactivate the GAPDH, so causing the glycolysis pathway to fail, resulting in decreased lactate production and loss of oxygen consumption. The lack of ATP production means the cell can no longer maintain normal function and goes into cell death. The oxidative stress also causes the inactivation of the caspase enzymes, causing the failure of the apoptosis system and the cell defaults to a necrotic cell death. 7,8-Dihydroneopterin protecting U937 and HMDM cells' metabolic activity by preventing the loss of GSH so preventing cell death.

6.2 Effect of oxLDL on the cells' metabolic functions in U937 cells and HMDM cells

OxLDL caused a rapid decrease in GAPDH activity during the first 3 hours of incubation in both U937 and HMDM cells. This suggests that GAPDH, which is the key enzyme in glycolysis, shows similar susceptibility towards oxLDL toxicity in both cell types. It is known that GAPDH is extremely sensitive to thiol modification because of the oxidation of cysteinyl sulfydryl (Cys^{149}) located in the active site of the enzyme. This oxidation is responsible for the loss of GAPDH activity during oxidative stress (Schuppe-Koistinen *et al.*, 1994, Cuddihy *et al.*, 2009a). The sodium dodecyl sulfate polyacrylamide gel electrophoresis (SDS-PAGE) results of U937 cells in this study showed that a number of proteins had lost their thiol groups within 3 hours of oxLDL addition. This finding is consistent with reported data from human aortic smooth muscle cells (HASMCs) where oxLDL, after 3 hours of exposure, caused the down regulation of GAPDH expression and a decrease in GAPDH thiol (Sukhanov *et al.*, 2006). This GAPDH activity results

supported the theory of the importance of GAPDH to sustain glycolysis and provide substrates for the Krebs cycle and electron transport chain (ETC) (Nelson & Cox, 2005).

In both cell types, the loss of GAPDH by the oxLDL occurred when there was a decrease in ATP and adenosine diphosphate (ADP). The oxLDL also caused a decrease in the VO_2 in U937 cells during this time period. These finding are consistent with studies on rabbit macrophages (Leppänen *et al.*, 2006), where an impaired supply of oxygen and nutrients resulted in ATP depletion and lead to the shutdown of cell function and ultimately cell death. In HASMCs (Sukhanov *et al.*, 2006), oxLDL caused the down regulation of GAPDH, inhibition of glycolysis and ATP depletion. Inhibition of glucose uptake caused inactivation of GAPDH and suppression of ATP levels (Schraufstatter *et al.*, 1990). ATP is important in the maintenance of cell membrane integrity (Halliwell & Gutteridge, 2007). Inhibition of GAPDH and ATP productions by peroxynitrite and S-nitrosothiols caused necrotic cell death and rupture of the plasma membrane (Brown, 2010). As macrophage foam cells, with high oxygen and glucose consumption, accumulate within the intima, the metabolic demands increase. During the later stages of the development of the lesions, the VO_2 of a proportion in the cells of the arterial wall becomes reduced. This might eventually cause ischemia in the arterial wall, which in turn might lead to decreased viability and reduced metabolic activity (Bjornheden & Bondjers, 1987).

In cells where glucose metabolism is the main source of energy, the glycolytic pathway is a primary source of carbon (as pyruvate) for the Krebs cycle. In tissue culture, U937 and HMDM cells also generate large amounts of lactate suggesting either an impaired Krebs cycle or ETC, or simply an oversupply of pyruvate by both glycolysis and the pentose

phosphate pathway. This pyruvate is converted to lactate for removal from the cells. In oxLDL treated U937 cells, the lactate production decrease occurred at the same time as GAPDH loss, but in the HMDM cells there was a significant lag of 3 hours where lactate was still generated. The source of this pyruvate most likely was the pentose phosphate pathway which is not affected by oxidative stress (Kruger & Von Schaewen, 2003). NADH generated in the Krebs cycle is a possible source of the reducing equivalents required for the lactate production. This NAD^+ regeneration via LDH would have allowed the Krebs cycle and pentose phosphate pathway to continue for some time, even with the loss of mitochondrial activity. Why this was different to the U937 cells is uncertain but it mainly reflects the level of oxidative stress and the possible oxidative inhibition of aconitase in the U937 cells (Gumieniczek *et al.*, 2011, Gupta *et al.*, 2012). Also, the U937 cell lysis followed soon after GADPH loss so the loss of the LDH enzyme from the cells may also explain the loss of lactate generation in the U937 cells. LDH was released to the cell culture media after 3 hours in U937 cells and after 6 hours in HMDM cells. The experimental data supports the proposal that the observed lag time in decreased metabolic function could be a reflection on the HMDM cells ability to maintain membrane function and hold onto the LDH within the cytoplasm. The loss of ATP in the U937 cells was faster than the HMDM cells so the loss of membrane function could be expected to be faster as ATP is required to maintain the various ion channels within the membrane.

This correlated to cell viability loss, which occurred from the initial 3 hours in U937 cells and after 6 hours in HMDM cells. Overall, there is a slowing of cell metabolism before cell lysis occurred in HMDM cells while the processes were very rapid in the U937 cells.

6.3 GSH and oxidative stress

Oxidative stress caused by oxLDL in U937 cells, resulted in loss of GSH level within the first 3 hours. Cellular GSH is a very potent antioxidant and can efficiently neutralise ROS such as nitric oxide (NO), $O_2^{\bullet-}$, and hydrogen peroxide (H_2O_2), and hypochlorite (HOCl). Previous studies in this laboratory have shown that oxLDL induces intracellular GSH loss in HMDM cells immediately from the initial 3 hours. This GSH loss was faster than the loss of cell viability at all time points, which showed 20% reduction after 3 hours and by 60% after 24 hours (Amit, 2008). This could indicate that the gradual collapse of the GSH level induced by oxLDL preceded macrophage death. This could also suggest that GSH depletion was required for oxLDL-induced macrophage toxicity (Amit, 2008, Gieseg *et al.*, 2009b). These observations are in agreement with results demonstrating that depletion of reduced GSH enhances oxLDL cytotoxicity in human macrophages (Darley-Usmar *et al.*, 1991, Gotoh *et al.*, 1993, Wang *et al.*, 2006). The most likely explanation for this is that the depletion of reduced GSH by oxLDL (Wang *et al.*, 2006) alters the GSH thiol redox state (GSH/GSSG ratio). Since GSH/GSSG ratio is one of the principal determinants of the cellular redox environment, any alteration in the redox environment can lead to cellular dysfunction and cell death (Schafer & Buettner, 2001). Loss of glutathione may exacerbate the oxidative stress effect of the oxLDL on HMDM cells.

6.4 OxLDL uptake and Cytotoxicity

OxLDL appears to cause U937 and HMDM cells to undergo a rapid necrotic cell death due to failure of metabolism and loss of cell membrane integrity after 6 and 12 hours,

respectively. The cell death with oxLDL occurred with the loss of GSH but no caspase-3 activation. All morphological characteristics were of necrosis in the presence of oxLDL. The rapid loss of the enzyme GADPH was not unexpected as previous studies (Baird *et al.*, 2004) had shown the oxidative stress induced by oxLDL was sufficient to inhibit capsase-3 which blocks the apoptotic process leaving necrosis as the default.

Caspases have been shown to be inactivated through the oxidative loss of the key catalytic thiol within the active site (Hampton *et al.*, 2002b). This inactivation has been demonstrated with hydrogen peroxide (H_2O_2), a key ROS within cells during oxidative stress, and protein hydroperoxides of Trp and Tyr, hypothesised products of the ROS (Hampton *et al.*, 2002a). These studies suggest that oxidative stress can inactivate caspases so driving dying cells into necrosis rather than apoptosis. OxLDL causes ROS generation by cells, leading to oxidative stress, shutdown of metabolism and breakdown of mitochondrial ETC and escape of its components such as cytochrome c through mitochondrial membrane pores. OxLDL induced cytochrome c released from mitochondria into the cytosol and causes caspase-3-inactivation leading to cell death by necrosis (Gieseg *et al.*, 2009a). Examination of plaque necrotic core does show a considerable amount of extra cellular debris (Stocker & Keaney, 2004) suggesting that necrosis is a major process occurring with the plaque.

6.5 Protective effect of 7,8-dihydroneopterin on cell viability and metabolic function

In some plaques there are regions of high 7,8-dihydroneopterin level, the average is 55.59±5.19 nM (Gieseg *et al.*, 2008, Firth *et al.*, 2008a, Genet, 2010) and up to 18 μM

(personal communication in our laboratory). 7,8-Dihydroneopterin is hypothesised to be synthesised to protect macrophages and other cells formed in the plaque from the oxidants such as HOCl, NO and peroxyl radicals released during inflammation (Gieseg *et al.*, 2008, Gieseg *et al.*, 1995). This research clearly shows 7,8-dihydroneopterin, in *vitro*, effectively protects human monocyte-like U937 and HMDM cells from oxLDL-induced loss of glycolytic function and cell death. 7,8-Dihydroneopterin also appears to slow the uptake of oxLDL suggesting it may also be able to modulate or slow foam cell formation if produced at micromolar levels.

It is possible that if 7,8-dihydroneopterin is generated in the intracellular spaces at concentrations exceeding 100 μM then there would be a considerable stabilising of the macrophage cells viability. It is possible that necrotic core regions may be associated with regions of low 7,8-dihydroneopterin level. This is however very difficult to demonstrate for a number of fundamental reasons. The production of 7,8-dihydroneopterin and neopterin is likely to be a transitory processes, triggered by specific inflammatory events within the plaque. As the neopterin and 7,8-dihydroneopterin appear to readily diffuse out of the plaque, what is measured in advanced plaque, removed during surgery, is a snap shot of the plaque state at the time of removal. Also, only advanced human plaques are available for study, so it is not possible to study early stage plaques. Classical animal models cannot give any information of this process as mice, rats and rabbit macrophages do not make 7,8-dihydroneopterin.

This argument also assumes that cell death is bad as it promotes further inflammation. However 7,8-dihydroneopterin, destabilising the cell metabolism may allow foam cells to

reach a level of stability which promotes further plaque grow. It is difficult to determine where the balance is, especially as there is a strong correlation between plasma neopterin, atherosclerosis and poor clinical outcomes (Gieseg *et al.*, 2008, Adachi *et al.*, 2007). This correlation shows that atherosclerosis is an inflammatory disease. What is missing from the data is a measure of 7,8-dihydroneopterin vs neopterin in atherosclerotic patients which may indicate the level of oxidative inflammation occurring within the plaques.

6.6 Further studies

This study focused on only one enzyme, glycolytic enzyme GAPDH due to its reported susceptibility to oxidative stress. The loss of this enzyme would effectively knock out glycolysis and the flow of carbon into the mitochondria from sugar metabolism, the almost complete loss of ATP production was observed. OxLDL also caused a major loss in the VO_2 suggesting that other enzymes within mitochondria were affected by the oxidative stress. The protection of the VO_2 by 7,8-dihydroneopterin supports this hypothesis. The Krebs cycle enzyme aconitase is found both in the cytoplasm and mitochondria and is known to be oxidised by ROS. Loss of this enzyme would also be a key event in oxLDL-mediated cell death.

The source of the oxidative stress has not been fully confirmed and most studies have focused on endothelium cells. Macrophages generate superoxide ($O_2^{\bullet -}$) during inflammation via the membrane-bounded NADPH-oxidase enzyme (NOX). It is possible that over stimulation of NOX is the source of the oxidative stress causing GAPDH inactivation and cell death. In addition to measuring the timing of NOX activation, measuring whether it is cytoplasmic or mitochondrial aconitase which is inactivated may

show where the ROS is generated. Isolating the location of the ROS generation using ROS scavenging dyes such as dihydroethidium (DHE) and red mitochondrial superoxide indicator (MitoSox) would be a key investigation.

Assuming NOX is activated, the role of calcium in activating this enzyme would be of interest. Previous work in this laboratory using HOCl has shown the opening of Ca^{+2} channels is important to the cell death process, so should be examined. Whether 7,8-dihydroneopterin can prevent a calcium influx into the cytoplasm would need to be examined. The down regulation of the scavenger receptor CD36 and lipid uptake by 7,8-dihydroneopterin does not appear to affect the ROS production (Gieseg *et al.*, 2010). 7,8-Dihydroneopterin is likely to affect foam cell formation needs to be explored by measuring cholesterol ester accumulation in macrophages by high performance liquid chromatography (HPLC) analysis.

In this project, the VO_2 was measured using suspension cell line U937 cells but not the adherent HMDM cells. It was assumed that U937 cells would responded the same as HMDM cells but this is only an assumption. There is very little data on HMDM cells VO_2 or how these cells metabolise different substrates, especially triglycerides vs glucose. The establishment of protocols to measure adherent, or at least human blood derived monocytes, VO_2 would provide valuable information on these cells metabolism, especially in the oxygen and possibly nutrient restricted environment of the atherosclerotic plaque.

REFERENCES

Acton, S., Rigotti, A., Landschulz, K. T., Xu, S., Hobbs, H. H. and Krieger, M. (1996). Identification of scavenger receptor SR-BI as a high density lipoprotein receptor. *Science,* 271**,** 518-520.

Acton, S. L., Scherer, P. E., Lodish, H. F. and Krieger, M. (1994). Expression cloning of SR-B1, a CD36-related class B scavenger receptor. *Journal of Biological Chemistry,* 269**,** 21003-21009.

Adachi, T., Naruko, T., Itoh, A., Komatsu, R., Abe, Y., Shirai, N., Yamashita, H., Ehara, S., Nakagawa, M., Kitabayashi, C., Ikura, Y., Ohsawa, M., Yoshiyama, M., Haze, K. and M., U. (2007). Neopterin is associated with plaque inflammation and destabilisation in human coronary atherosclerotic lesions. *Heart,* 93**,** 1537-1541.

Akerboom, T. P., Bilzer, M. and Sies, H. (1982). The relationship of biliary glutathione disulfide efflux and intracellular glutathione disulfide content in perfused rat liver. *Journal of Biological Chemistry,* 257**,** 4248-4252.

Alberts, B., Johnson, A., Lewis, J., Raff, M., Roberts, K. and Walter, P. (2002). Molecular Biology of the Cell. *Fourth Edition.* Garland Science.

Albina, J. E., Mastrofrancesco, B. and Reichner, J. S. (1999). Acyl phosphatase activity of NO-inhibited glyceraldehyde-3-phosphate dehydrogenase (GAPDH): a potential mechanism for uncoupling glycolysis from ATP generation in NO-producing cells. *Biochemical Journal,* 341**,** 5-9.

Ames, B. N., Shigenaga, M. K. and Hagen, T. M. (1993). Oxidants, antioxidants, and the degenerative diseases of aging. *Proceedings of the National Academy of Sciences,* 90**,** 7915-7922.

Amit, Z. (2008). A modle of complex plaque formation: 7,8-dihydroneopterin protects human monocyte-derived macrophages from oxidised low density lipoprotein-induced death. Ph.D.thesis, Biological Sciences. University of Canterbury. Christchurch, New Zealand.

Anraku, M., Kitamura, K., Shinohara, A., Adachi, M., Suenaga, A., Maruyama, T., Miyanaka, K., Miyoshi, T., Shiraishi, N., Nonoguchi, H., Otagiri, M. and Tomita, K. (2004). Intravenous iron administration induces oxidation of serum albumin in hemodialysis patients. *Kidney International,* 66**,** 841-848.

Asmis, R. and Begley, J. G. (2003). Oxidized LDL promotes peroxide-mediated mitochondrial dysfunction and cell death in human macrophages: a caspase-3-independent pathway. *Circulation Research,* 92**,** e20-e29.

Asmis, R., Begley, J. G., Jelk, J. and Everson, W. V. (2005). Lipoprotein Aggregation Protects Human Monocyte-Derived Macrophages From OxLDL-Induced Cytotoxicity. *Journal of Lipid Research,* 46**,** 1124-1132.

Asmis, R. and Jelk, J. (2000a). Large variations in human foam cell formation in individuals: a fully autologous in vitro assay based on the quantitative analysis of cellular neutral lipids. *Atherosclerosis,* 148**,** 243-253.

Asmis, R. and Jelk, J. (2000b). Vitamin E supplementation of human macrophages prevents neither foam cell formation nor increased susceptibility of foam cells to lysis by oxidized LDL. *Arteriosclerosis Thrombosis and Vascular Biology,* 20**,** 2078-2086.

Asmis, R. and Wintergerst, E. S. (1998). Dehydroascorbic acid prevents apoptosis induced by oxidized low-density lipoprotein in human monocyte-derived macrophages. *European Journal of Biochemistry,* 255**,** 147-155.

Baier-Bitterlich, G., Fuchs, D., Murr, C., Reibnegger, G., Werner-Felmayer, G., Sgonc, R., Böck, G., Dierich, M. P. and Wachter, H. (1995). Effect of neopterin and 7,8-dihydroneopterin on tumor necrosis factor-α induced programmed cell death. *FEBS Letters,* 364**,** 234-238.

Baird, S. (2003). 7,8-Dihydroneopterin inhibition oxidised low density lipoproten-induced cellular death. Ph.D.thesis, University of Canterbury. Christchurch, New Zealand.

Baird, S. K., Hampton, M. B. and Gieseg, S. P. (2004). Oxidized LDL triggers phosphatidylserine exposure in human monocyte cell lines by both caspase-dependent and -independent mechanisms. *FEBS Letters,* 578**,** 169-174.

Baird, S. K., Reid, L., Hampton, M. B. and Gieseg, S. P. (2005). OxLDL induced cell death is inhibited by the macrophage synthesised pterin, 7,8-dihydroneopterin, in U937 cells but not THP-1 cells. *Biochimica et Biophysica Acta (BBA) - Molecular Cell Research,* 1745**,** 361-369.

Bakker, J., Coffernils, M., Leon, M., Gris, P. and Vincent, J. L. (1991). Blood lactate levels are superior to oxygen-derived variables in predicting outcome in human septic shock. *Chest,* 99**,** 956-962.

Balcerczyk, A. and Bartosz, G. (2003). Thiols are main determinants of total antioxidant capacity of cellular homogenates. *Free Radical Research,* 37**,** 537-541.

Ballatori, N., Krance, S. M., Notenboom, S., Shi, S., Tieu, K. and Hammond, C. L. (2009). Glutathione dysregulation and the etiology and progression of human diseases. *Biological Chemistry,* 390**,** 191-214.

Bansal, S. K. and Kaw, J. L. (1981). Lactate dehydrogenase isoenzymes in macrophages and serum during the development of pulmonary silicosis in the rat. *Toxicology Letters,* 7**,** 279-283.

Barrett, R. J., Harleman, J. H. and Joseph, E. C. (1988). The evaluation of HBDH and LDH isoenzymes in cardiac cell necrosis of the rat. *Journal of Applied Toxicology,* 8**,** 233-238.

Baty, J. W., Hampton, M. B. and Winterbourn, C. C. (2002). Detection of oxidant sensitive thiol proteins by fluorescence labeling and two-dimensional electrophoresis. *Proteomics,* 2**,** 1261-1266.

Bea, F., Hudson, F. N., Chait, A., Kavanagh, T. J. and Rosenfeld, M. E. (2003). Induction of glutathione synthesis in macrophages by oxidized low-density lipoproteins is mediated by consensus antioxidant response elements. *Circulation Research,* 92**,** 386-393.

Beckert, S., Farrahi, F., Aslam, R. S., Scheuenstuhl, H., Königsrainer, A., Hussain, M. Z. and Hunt, T. K. (2006). Lactate stimulates endothelial cell migration. *Wound Repair and Regeneration,* 14**,** 321-324.

Belenky, P., Bogan, K. L. and Brenner, C. (2007). NAD^+ metabolism in health and disease. *Trends in Biochemical Sciences,* 32**,** 12-19.

Berthier, A., Lemaire-Ewing, S., Prunet, C., Monier, S., Athias, A., Bessede, G., De Barros, J. P. P., Laubriet, A., Gambert, P., Lizard, G. and Neel, D. (2004). Involvement of a calcium-dependent dephosphorylation of BAD associated with the localization of TRPC-1 within lipid rafts in 7-ketocholesterol-induced THP-1 cell apoptosis. *Cell Death and Differentiation,* 11**,** 897-905.

Bilzer, M. and Lauterburg, B. H. (1991). Glutathione metabolism in activated human neutrophils: stimulation of glutathione synthesis and consumption of glutathione by reactive oxygen species. *European Journal of Clinical Investigation,* 21**,** 316-322.

Binder, C. J., Hartvigsen, K. and Witztum, J. L. (2007). Promise of immune modulation to inhibit atherogenesis. *Journal of the American College of Cardiology,* 50**,** 547-550.

Bjornheden, T. and Bondjers, G. (1987). Oxygen consumption in aortic tissue from rabbits with diet-induced atherosclerosis. *Arteriosclerosis Thrombosis and Vascular Biology,* 7**,** 238-247.

Blasi, C. (2008). The autoimmune origin of atherosclerosis. *Atherosclerosis,* 201**,** 17-32.

Boggs, S. E., Mccormick, T. S. and Lapetina, E. G. (1998). Glutathione levels determine apoptosis in macrophages. *Biochemical and Biophysical Research Communications,* 247**,** 229-233.

Boullier, A., Bird, D. A., Chang, M.-K., Dennis, E. A., Friedman, P., Gillotte-Taylor, K., Hörkkö, S., Palinski, W., Quehenberger, O., Shaw, P., Steinberg, D., Terpstra, V. and Witztum, J. L. (2001). Scavenger receptors, oxidized LDL and atherosclerosis. *Annals of the New York Academy of Sciences,* 947**,** 214-223.

Bowry, V. W., Ingold, K. U. and Stocker, R. (1992). Vitamin E in human low-density lipoprotein. When and how this antioxidant becomes a pro-oxidant. *Biochemical Journal,* 288**,** 341-344.

Braun, A., Trigatti, B. L., Post, M. J., Sato, K., Simons, M., Edelberg, J. M., Rosenberg, R. D., Schrenzel, M. and Krieger, M. (2002). Loss of SR-B1 expression leads to the early onset of occlusive atherosclerotic coronary artery disease, spontaneous myocardial infarctions, severe cardiac dysfunction, and premature death in apolipoprotein E, in deficient Mice. *Circulation Research,* 90**,** 270-276.

Brown, A. J., Leong, S. L., Dean, R. T. and Jessup, W. (1997). 7-Hydroperoxycholesterol and its products in oxidized low density lipoprotein and human atherosclerotic plaque. *Journal of Lipid Research,* 38**,** 1730-1745.

Brown, A. J., Mander, E. L., Gelissen, I. C., Kritharides, L., Dean, R. T. and Jessup, W. (2000). Cholesterol and oxysterol metabolism and subcellular distribution in macrophage foam cells. Accumulation of oxidized esters in lysosomes. *Journal of Lipid Research,* 41**,** 226-237.

Brown, G. C. (2010). Nitric oxide and neuronal death. *Nitric Oxide,* 23**,** 153-165.

Brown, M. S. and Goldstein, J. L. (1986). A receptor-mediated pathway for cholesterol homeostasis. *Science,* 232**,** 34-47.

Budinger, G. R., Chandel, N., Shao, Z. H., Li, C. Q., Melmed, A., Becker, L. B. and Schumacker, P. T. (1996). Cellular energy utilization and supply during hypoxia in embryonic cardiac myocytes. *American Journal of Physiology - Lung Cellular and Molecular Physiology,* 270**,** L44-L53.

Cantoni, O., Guidarelli, A., Palomba, L. and Fiorani, M. (2005). U937 cell necrosis mediated by peroxynitrite is not caused by depletion of ATP and is prevented by arachidonate via an ATP-dependent mechanism. *Molecular Pharmacology,* 67**,** 1399-1405.

Carpenter, K. L., Brabbs, C. E. and Mitchinson, M. J. (1991). Oxygen radicals and atherosclerosis. *Klin Wochenschr,* 69**,** 1039-1045.

Carpenter, K. L., Challis, I. R. and Arends, M. J. (2003). Mildly oxidised LDL induces more macrophage death than moderately oxidised LDL: roles of peroxidation, lipoprotein-associated phospholipase A2 and PPAR-γ. *FEBS Letters,* 553**,** 145-150.

Caruso, R., Campolo, J., Dellanoce, C., Mariele, R., Parodi, O. and Accinni, R. (2004). Critical study of preanalytical and analytical phases of adenine and pyridine nucleotide assay in human whole blood. *Analytical Biochemistry,* 330**,** 43-51.

Cassatella, M. A., Dellabianca, V., Berton, G. and Rossi, F. (1985). Activation by γ-interferon of human macrophage capability to produce toxic oxygen molecules is accompanied by decreased Km of the superoxide-generating NADPH oxidase. *Biochemical and Biophysical Research Communications,* 132**,** 908-914.

Chen, W., Silver, D. L., Smith, J. D. and Tall, A. R. (2000). Scavenger receptor-B1 inhibits ATP-binding cassette transporter 1- mediated cholesterol efflux in macrophages. *Journal of Biological Chemistry,* 275**,** 30794-30800.

Chisolm, G. M. and Chai, Y. (2000). Regulation of cell growth by oxidized LDL. *Free Radical Biology and Medicine,* 28**,** 1697-1707.

Christen, S., Thomas, S. R., Garner, B. and Stocker, R. (1994). Inhibition by γ-interferon of human mononuclear cell-mediated low density lipoprotein oxidation. Participation of tryptophan metabolism along the kynurenine pathway. *Journal of Clinical Investigation,* 93**,** 2149-2158.

Chung, B. H., Segrest, J. P., Ray, M. J., Brunzell, J. D., Hokanson, J. E., Krauss, R. M., Beaudrie, K. and Cone, J. T. (1986). Single vertical spin density gradient centrifugation. *Methods in Enzymology,* 128**,** 181-209.

Clare, K., Hardwick, S. J., Carpenter, K. L., Weeratunge, N. and Mitchinson, M. J. (1995). Toxicity of oxysterols to human monocyte-macrophages. *Atherosclerosis,* 118**,** 67-75.

Coffey, M. D., Cole, R. A., Colles, S. M. and Chisolm, G. M. (1995). In vitro cell injury by oxidized low density lipoprotein involves lipid hydroperoxide-induced formation of alkoxyl, lipid and peroxyl radicals. *Journal of Clinical Investigation,* 96**,** 1866-1873.

Colussi, C., Albertini, M. C., Coppola, S., Rovidati, S., Galli, F. and Ghibelli, L. (2000). H_2O_2-Induced Block of Glycolysis as an Active ADP-Ribosylation Reaction Protecting Cells From Apoptosis. *FASEB Journal,* 14**,** 2266-2276.

Cotgreave, I. A. and Moldeus, P. (1986). Methodologies for the application of monobromobimane to the simultaneous analysis of soluble and protein thiol components of biological systems. *Journal of Biochemical and Biophysical Methods,* 13**,** 231-249.

Cramer, T., Yamanishi, Y., Clausen, B. R. E., FRster, I., Pawlinski, R., Mackman, N., Haase, V. H., Jaenisch, R., Corr, M., Nizet, V., Firestein, G. S., Gerber, H.-P., Ferrara, N. and Johnson, R. S. (2003). HIF-1[alpha] Is Essential for Myeloid Cell-Mediated Inflammation. *Cell,* 112**,** 645-657.

Cuddihy, S. L., Baty, J. W., Brown, K. K., Winterbourn, C. C. and Hampton, M. B. (2009a). Proteomic detection of oxidized and reduced thiol proteins in cultured cells. *Two-Dimensional Electrophoresis Protocols.*Chapter 23:363-375.

Cuddihy, S. L., Baty, J. W., Brown, K. K., Winterbourn, C. C. and Hampton, M. B. (2009b). Proteomic Detection of Oxidized and Reduced Thiol Proteins in Cultured Cells. *Two-Dimensional Electrophoresis Protocols.* 363-375.

Darley-Usmar, V. M., Severn, A., O'leary, V. J. and Rogers, M. (1991). Treatment of macrophages with oxidized low-density lipoprotein increases their intracellular glutathione content. *Biochemical Journal,* 278 (Pt 2)**,** 429-434.

Decker, T. and Lohmann-Matthes, M. (1988). A quick and simple method for the quantification of lactate dehydrogenase release in the measurements of cellular cytotoxicity and tumor necrosis factor (TNF) activity. *Journal of Immunological Methods,* 15**,** 61-69.

Devaraj, S., Hugou, I. and Jialal, I. (2001). Alpha-Tocopherol decreases CD36 expression in human monocyte-derived macrophages. *Journal of Lipid Research,* 42**,** 521-527.

Dietl, K., Renner, K., Dettmer, K., Timischl, B., Eberhart, K., Dorn, C., Hellerbrand, C., Kastenberger, M., Kunz-Schughart, L. A., Oefner, P. J., Andreesen, R., Gottfried, E. and Kreutz, M. P. (2010). Lactic Acid and Acidification Inhibit TNF Secretion and Glycolysis of Human Monocytes. *The Journal of Immunology,* 184**,** 1200-1209.

Digirolamo, M., Newby, F. D. and Lovejoy, J. (1992). Lactate production in adipose tissue: a regulated function with extra- adipose implications. *The FASEB Journal,* 6**,** 2405-2412.

Dimmeler, S., Haendeler, J., Galle, J. and Zeiher, A. M. (1997). Oxidized low-density lipoprotein induces apoptosis of human endothelial cells by activation of CPP32-like proteases - A mechanistic clue to the 'response to injury' hypothesis. *Circulation,* 95**,** 1760-1763.

Douvdevani, A., Rapoport, J., Konforti, A., Zlotnik, M. and Chaimovitz, C. (1993). The effect of peritoneal dialysis fluid on the release of IL-1β and TNF-α by macrophages/monocytes. *Peritoneal Dialysis International,* 13**,** 112-117.

Drake, A. J., Haines, J. R. and Noble, M. I. M. (1980). Preferential uptake of lactate by the normal myocardium in dogs. *Cardiovascular Research,* 14**,** 65-72.

Draper, H. H., Squires, E. J., Mahmoodi, H., Wu, J., Agarwal, S. and Hadley, M. (1993). A comparative evaluation of thiobarbituric acid methods for the determination of malondialdehyde in biological materials. *Free Radical Biology and Medicine,* 15**,** 353-363.

Duggan, S., Rait, C., Gebicki, J. M. and Gieseg, S. P. (2001). Inhibition of protein oxidation by the macrophage-synthesised antioxidant 7,8-dihydroneopterin. *Redox Report,* 6**,** 188-190.

Duggan, S., Rait, C., Platt, A. and Gieseg, S. P. (2002). Protein and thiol oxidation in cells exposed to peroxyl radicals is inhibited by the macrophage synthesised pterin 7,8-dihydroneopterin. *Biochimica et Biophysica Acta (BBA) - Molecular Cell Research,* 1591**,** 139-145.

Eguchi, Y., Shimizu, S. and Tsujimoto, Y. (1997). Intracellular ATP levels determine cell death fate by apoptosis or necrosis. *Cancer Research,* 57**,** 1835-1840.

Ehrenwald, E. and Fox, P. L. (1996). Role of endogenous ceruloplasmin in low density lipoprotein oxidation by human U937 monocytic cells. *Journal of Clinical Investigation,* 97**,** 884-890.

Emerling, B. M., Weinberg, F., Snyder, C., Burgess, Z., Mutlu, G. K. M., Viollet, B., Budinger, G. R. S. and Chandel, N. S. (2009). Hypoxic activation of AMPK is dependent on mitochondrial ROS but independent of an increase in AMP/ATP ratio. *Free Radical Biology and Medicine,* 46**,** 1386-1391.

Esterbauer, H., Dieber-Rotheneder, M., Striegl, G. and Waeg, G. (1991). Role of vitamin E in preventing the oxidation of low-density-lipoprotein. *American Journal of Clinical Nutrition,* 53**,** 314-321.

Esterbauer, H., Dieber-Rotheneder, M., Waeg, G., Striegl, G. and Juergens, G. (1990). Biochemical structural and functional properties of oxidized low-density lipoprotein. *Chemical Research in Toxicology,* 3**,** 77-92.

Esterbauer, H., Gebicki, J., Puhl, H. and Jurgens, G. (1992). The role of lipid peroxidation and antioxidants in oxidative modification of LDL. *Free Radical Biology and Medicine,* 13**,** 341-390.

Esterbauer, H., Striegl, G., Puhl, H. and Rotheneder, M. (1989). Continuous monitoring of in vitro oxidation of human low density lipoprotein. *Free Radical Research Communications,* 6**,** 67-75.

Febbraio, M., Hajjar, D. P. and Silverstein, R. L. (2001). CD36: a class B scavenger receptor involved in angiogenesis, atherosclerosis, inflammation and lipid metabolism. *Journal of Clinical Investigation,* 108**,** 785-791.

Febbraio, M., Podrez, E. A., Smith, J. D., Hajjar, D. P., Hazen, S. L., Hoff, H. F., Sharma, K. and Silverstein, R. L. (2000). Targeted disruption of the class B scavenger receptor CD36 protects against atherosclerotic lesion development in mice. *Journal of Clinical Investigation,* 105**,** 1049-1056.

Firth, C. A., Crone, E. M., Flavall, E. A., Roake, J. A. and Gieseg, S. P. (2008a). Macrophage mediated protein hydroperoxide formation and lipid oxidation in low density lipoprotein are inhibited by the inflammation marker 7,8-dihydroneopterin. *Biochimica et Biophysica Acta (BBA) - Molecular Cell Research,* 1783**,** 1095-1101.

Firth, C. A., Laing, A. D., Baird, S. K., Pearson, J. and Gieseg, S. P. (2008b). Inflammatory sites as a source of plasma neopterin: measurement of high levels of neopterin and markers of oxidative stress in pus drained from human abscesses. *Clinical Biochemistry,* 41**,** 1078-1083.

Firth, C. A., Yang, Y. and Gieseg, S. P. (2007a). Lipid oxidation predominates over protein hydroperoxide formation in human monocyte-derived macrophages exposed to aqueous peroxyl radicals. *Free Radical Research,* 41**,** 839-848.

Firth, C. A., Yang, Y. T. and Gieseg, S. P. (2007b). Lipid oxidation predominates over protein hydroperoxide formation in human monocyte-derived macrophages exposed to aqueous peroxyl radicals. *Free Radical Research,* 41**,** 839-848.

Fischer, B., Von Knethen, A. and Brune, B. (2002). Dualism of oxidized lipoproteins in provoking and attenuating the oxidative burst in macrophages: role of peroxisome proliferator-activated receptor-γ. *Journal of Immunology,* 168**,** 2828-2834.

Fischer, K., Hoffmann, P., Voelkl, S., Meidenbauer, N., Ammer, J., Edinger, M., Gottfried, E., Schwarz, S., Rothe, G., Hoves, S., Renner, K., Timischl, B., Mackensen, A., Kunz-Schughart, L., Andreesen, R., Krause, S. W. and Kreutz, M. (2007). Inhibitory effect of tumor cell¬ñderived lactic acid on human T cells. *Blood,* 109**,** 3812-3819.

Forgan, L. and Forster, M. (2009). Oxygen consumption and blood flow distribution in perfused skeletal muscle of chinook salmon. *Journal of Comparative Physiology B: Biochemical, Systemic and Environmental Physiology,* 179**,** 359-368.

Forgan, L. and Forster, M. (2010). Oxygen-dependence of metabolic rate in the muscles of craniates. *Journal of Comparative Physiology B: Biochemical, Systemic and Environmental Physiology,* 180**,** 715-729.

Freeman, N. E., Rusinol, A. E., Linton, M., Hachey, D. L., Fazio, S., Sinensky, M. S. and Thewke, D. (2005). Acyl-coenzyme A:cholesterol acyltransferase promotes oxidized LDL/oxysterol-induced apoptosis in macrophages. *J Lipid Res,* 46**,** 1933-1943.

Freshney, R. I. (2000). Culture of animal cells: a manual of basic technique. *Fourth Edition.* Wiley-Liss Inc., New York.

Fuhrman, B., Volkova, N. and Aviram, M. (2005). Pomegranate juice inhibits oxidized LDL uptake and cholesterol biosynthesis in macrophages. *Journal of Nutritional Biochemistry,* 16**,** 570-576.

Furst, W. and Hallstrom, S. (1992). Simultaneous determination of myocardial nucleotides, nucleosides, purine-bases and creatine-phosphate by ion-pair high-performance liquid-chromatography. *Journal of Chromatography-Biomedical Applications,* 578**,** 39-44.

Gatenby, R. A. and Gillies, R. J. (2004). Why do cancers have high aerobic glycolysis? *Nature Reviews Cancer,* 4**,** 891-899.

Gebicki, J. M., Collins, J., Gay, C., Duggan, S. and Gieseg, S. (2000). The dissection of oxidative changes in human blood serum and U937 cells exposed to free radicals. *Redox Report,* 5**,** 55-56.

Geiringer, E. (1951). Intimal vascularisation and atherosclerosis. *Journal of Pathology and Bacteriology,* 63**,** 201-211.

Geisbuhler, T. P. and Rovetto, M. J. (1990). Lactate does not enhance anoxia/reoxygenation damage in adult rat cardiac myocytes. *Journal of Molecular and Cellular Cardiology,* 22**,** 1325-1335.

Genet, R. M. (2010). A study of oxidation and inflammation using plaque and plasma of vascular disease patients. Master thesis, Biological Sciences. University of Canterbury. Christchurch, New Zealand.

Gerry, A. B. and Leake, D. S. (2008). A moderate reduction in extracellular pH protects macrophages against apoptosis induced by oxidized low density lipoprotein. *Journal of Lipid Research,* 49**,** 782-789.

Gerry, A. B., Satchella, L. and Leake, D. S. (2007). A novel method for production of lipid hydroperoxide- or oxysterol-rich low-density lipoprotein. *Athersoclerosis,* 197**,** 579-587.

Gey, K. F., Puska, P., Jordan, P. and Moser, U. K. (1991). Inverse correlation between plasma vitamin E and mortality from ischemic heart disease in cross-cultural epidemiology. *American Journal of Clinical Nutrition,* 53**,** 326S-334S.

Gieseg, S. P., Amit, Z., Yang, Y.-T., Shchepetkina, A. and Katouah, H. (2010). Oxidant production, oxLDL Uptake, and CD36 levels in human monocyte–derived macrophages are downregulated by the macrophage-generated antioxidant 7,8-dihydroneopterin. *Antioxidants and Redox Signaling,* 13**,** 1525-1534.

Gieseg, S. P. and Cato, S. (2003). Inhibition of THP-1 cell-mediated low-density lipoprotein oxidation by the macrophage-synthesised pterin, 7,8-dihydroneopterin *Redox Report,* 8**,** 113-119.

Gieseg, S. P., Crone, E. and Amit, Z. (2009a). Oxidised low density lipoprotein cytotoxicity and vascular disease. *Endogenous Toxins: Diet, Genetics, Disease*

and Treatment.O'brien, P. J. and Bruce, R. W. Weinheim, Wiley-VCH.Chapter 25:620-645.

Gieseg, S. P., Crone, E. M., Flavall, E. and Amit, Z. (2008). Potential to inhibit growth of atherosclerotic plaque development through modulation of macrophage neopterin/7,8-dihydroneopterin synthesis. *British Journal of Pharmacololgy,* 153**,** 627-635.

Gieseg, S. P. and Esterbauer, H. (1994). Low density lipoprotein is saturable by pro-oxidant copper. *FEBS Letters,* 343**,** 188-194.

Gieseg, S. P., G., M. and Glubb, D. (2000). Inhibition of haemolysis by the macrophage synthesized antioxidant, 7,8-dihydroneopterin. *Redox Report,* 5**,** 97-100.

Gieseg, S. P., Leake, D. S., Flavall, E. M., Amit, Z., Reid, L. and Yang, Y. T. (2009b). Macrophage antioxidant protection within atherosclerotic plaques. *Frontiers in Bioscience,* 14**,** 1230-1246.

Gieseg, S. P., Maghzal, G. and Glubb, D. (2001a). Protection of erythrocytes by the macrophage synthesized antioxidant 7,8 dihydroneopterin. *Free Radical Biology and Medicine,* 34**,** 123-136.

Gieseg, S. P., Pearson, J. and Firth, C. A. (2003). Protein hydroperoxides are a major product of low density lipoprotein oxidation during copper, peroxyl radical and macrophage-mediated oxidation. *Free Radical Biology and Medicine,* 37**,** 983-991.

Gieseg, S. P., Reibnegger, G., Wachter, H. and Esterbauer, H. (1995). 7,8 Dihydroneopterin inhibits low density lipoprotein oxidation in vitro. Evidence that this macrophage secreted pteridine is an anti-oxidant. *Free Radical Research,* 23**,** 123-136.

Gieseg, S. P., Whybrow, J., Glubb, D. and Rait, C. (2001b). Protection of U937 cells from free radical damage by the macrophage synthesized antioxidant 7,8-dihydroneopterin. *Free Radical Research,* 35**,** 311-318.

Gnaiger, E. (2003). Oxygen conformance of cellular respiration. A perspective of mitochondrial physiology. *Advances in Experimental Medicine and Biology,* 543**,** 39-55.

Gotoh, N., Graham, A., Nikl, E. and Darley-Usmar, V. M. (1993). Inhibition of glutathione synthesis increases the toxicity of oxidized low-density lipoprotein to human monocytes and macrophages. *Biochemical Journal,* 296**,** 151-154.

Gottfried, E., Kunz-Schughart, L. A., Ebner, S., Mueller-Klieser, W., Hoves, S., Andreesen, R., Mackensen, A. and Kreutz, M. (2006). Tumor-derived lactic acid modulates dendritic cell activation and antigen expression. *Blood,* 107**,** 2013-2021.

Griffith, O. W. (1999). Biologic and pharmacologic regulation of mammalian glutathione synthesis. *Free Radical Biology and Medicine,* 27**,** 922-935.

Gumieniczek, A., Komsta, Å. U. and Chehab, M. R. (2011). Effects of two oral antidiabetics, pioglitazone and repaglinide, on aconitase inactivation, inflammation and oxidative/nitrosative stress in tissues under alloxan-induced hyperglycemia. *European Journal of Pharmacology,* 659**,** 89-93.

Gupta, K. J., Shah, J. K., Brotman, Y., Jahnke, K., Willmitzer, L., Kaiser, W. M., Bauwe, H. and Igamberdiev, A. U. (2012). Inhibition of aconitase by nitric oxide leads to induction of the alternative oxidase and to a shift of metabolism towards biosynthesis of amino acids. *Journal of Experimental Botany,* 63**,** 1773-1784.

Guyton, J. R., Lenz, M. L., Mathews, B., Hughes, H., Karsan, D., Selinger, E. and Smith, C. V. (1995). Toxicity of oxidized low density lipoproteins for vascular smooth muscle cells and partial protection by antioxidants. *Atherosclerosis,* 118**,** 237-249.

Halliwell, B. (2003). Oxidative stress in cell culture: an under-appreciated problem? *FEBS Letters,* 540**,** 3-6.

Halliwell, B. and Gutteridge, J. M. C. (2007). Free radicals in biology and medicine. *Fourth Edition.* Oxford Univeristy Press, Oxford.

Halliwell, B. and Whiteman, M. (2004). Measuring reactive species and oxidative damage in vivo and in cell culture: how should you do it and what do the results mean? *British Journal of Pharmacology,* 142**,** 231-255.

Hampton, M. B., Morgan, P. E. and Davies, M. J. (2002a). Inactivation of cellular caspases by peptide-derived tryptophan and tyrosine peroxides. *FEBS Letters,* 527**,** 289-292.

Hampton, M. B., Stamenkovic, I. and Winterbourn, C. C. (2002b). Interaction with substrate sensitises caspase-3 to inactivation by hydrogen peroxide. *FEBS Letters,* 517**,** 229-232.

Hansson, G. K. (2005). Mechanisms of disease: inflammation atherosclerosis and coronary artery disease. *New England Journal of Medicine,* 352**,** 1685-1695.

Hansson, G. K., Robertson, A. K. and Söderberg-Nauclér, C. (2006). Inflammation and atherosclerosis. *Annual Review of Pathology,* 1**,** 297-329.

Hara, M. R., Cascio, M. B. and Sawa, A. (2006). GAPDH as a sensor of NO stress. *Biochimica et Biophysica Acta (BBA) - Molecular Basis of Disease,* 1762**,** 502-509.

Harada-Shiba, M., Kinoshita, M., Kamido, H. and Shimokado, K. (1998). Oxidized low density lipoprotein induces apoptosis in cultured human umbilical vein endothelial cells by common and unique mechanisms. *Journal of Biological Chemistry,* 273**,** 9681-9687.

Hardie, D. G. (2000). Metabolic control: A new solution to an old problem. *Current Biology,* 10**,** R757-R759.

Hardwick, S. J., Hegyi, L., Clare, K., Law, N. S., Carpenter, K. L., Mitchinson, M. J. and Skepper, J. N. (1996). Apoptosis in human monocyte-macrophages exposed to oxidized low density lipoprotein. *Journal of Pathology,* 179**,** 294-302.

Harris, L. K., Mann, G. E., Ruiz, E., Mushtaq, S. and Leake, D. S. (2006). Ascorbate does not protect macrophages against apoptosis induced by oxidised low density lipoprotein. *Archives of Biochemistry and Biophysics,* 455**,** 68-76.

Hashimoto, T., Hussien, R., Oommen, S., Gohil, K. and Brooks, G. A. (2007). Lactate sensitive transcription factor network in L6 cells: activation of MCT1 and mitochondrial biogenesis. *FASEB Journal,* 21**,** 2602-2612.

Haunstetter, A. and Izumo, S. (1998). Apoptosis: basic mechanisms and implications for cardiovascular disease. *Circulation Research,* 82**,** 1111-1129.

Hazell, L. J., Van Den Berg, J. J. and Stocker, R. (1994). Oxidation of low-density lipoprotein by hypochlorite causes aggregation that is mediated by modification of lysine residues rather than lipid oxidation. *Biochemical Journal,* 302**,** 297-304.

Hazen, S. L. and Heinecke, J. W. (1997). 3-Chlorotyrosine, a specific marker of myeloperoxidase-catalyzed oxidation, is markedly elevated in low density lipoprotein isolated from human atherosclerotic intima. *Journal of Clinical Investigation,* 99**,** 2075-2081.

Hegyi, L., Skepper, J. N., Cary, N. R. and Mitchinson, M. J. (1996). Foam cell apoptosis and the development of the lipid core of human atherosclerosis. *Journal of Pathology,* 180**,** 423-429.

Henriksen, T., Evensen, S. A. and Carlander, B. (1979). Injury to human-endothelial cells in culture induced by low-density lipoproteins. *Scandinavian Journal of Clinical and Laboratory Investigation,* 39**,** 361-368.

Hessler, J. R., Robertson, A. L. and Chisolm, G. M. (1979). LDL-induced cytotoxicity and its inhibition by HDL in human vascular smooth-muscle and endothelial-cells in culture. *Atherosclerosis,* 32**,** 213-229.

Hochachka, P., Bucke, L., Doll, C. and Land, S. (1996). Unifying theory of hypoxia tolerance: molecular/metabolic defense and rescue mechanisms for surviving oxygen lack. *Proceedings of the National Academy of Sciences in USA,* 93**,** 9493-9498.

Hochachka, P. and Mcclelland, G. (1997). Cellular metabolic homeostasis during large-scale change in ATP turnover rates in muscles. *Journal of Experimental Biology,* 200**,** 381-386.

Hochachka, P. W. (2003). Intracellular convection, homeostasis and metabolic regulation. *Journal of Experimental Biology,* 206**,** 2001-2009.

Hochachka, P. W. and Guppy, M. (1987). Metabolic arrest and the control of biological time. Harvard University Press, Cambridge.

Hoff, F., O'neil, J., Chisolm, G. M., Cole, T. B., Quehenberger, O., Esterbauer, H. and Jurgens, G. (1989). Modification of low density lipoproteins with 4-hydroxylnonenal induces uptake by macrophges. *Atherosclerosis,* 9**,** 538-549.

Horton, R. A., Ceppi, E. D., Knowles, R. G. and Titheradge, M. A. (1994). Inhibition of hepatic gluconeogenesis by nitric oxide: a comparison with endotoxic shock. *Biochemical Journal,* 299**,** 735-739.

Hsieh , C. C., Yen, M. H., Yen , C. H. and Lau, Y. T. (2001). Oxidized low density lipoprotein induces apoptosis via generation of reactive oxygen species in vascular smooth muscle cells. *Cardiovascular Research,* 49**,** 135-145.

Hunt, T. K., Conolly, W. B., Aronson, S. B. and Goldstein, P. (1978). Anaerobic metabolism and wound healing: an hypothesis for the initiation and cessation of collagen synthesis in wounds. *American Journal of Surgery,* 135**,** 328-332.

Inoue, M., Itoh, H., Tanaka, T., Chun, T. H., Doi, K., Fukunaga, Y., Sawada, N., Yamshita, J., Masatsugu, K., Saito, T., Sakaguchi, S., Sone, M., Yamahara, K., Yurugi, T. and Nakao, K. (2001). Oxidized LDL regulates vascular endothelial growth factor expression in human macrophages and endothelial cells through activation of peroxisome proliferator-activated receptor-γ. *Arteriosclerosis Thrombosis and Vascular Biology,* 21**,** 560-566.

Iscra, F., Gullo, A. and Biolo, G. (2002). Bench-to-bedside review: lactate and the lung. *Critical Care,* 6**,** 327 - 329.

Ishii, T., Sunami, O., Nakajima, H., Nishio, H., Takeuchi, T. and Hata, F. (1999). Critical role of sulfenic acid formation of thiols in the inactivation of glyceraldehyde-3-phosphate dehydrogenase by nitric oxide. *Biochemical Pharmacology,* 58**,** 133-143.

James, P., Grinberg, O. and Swartz, H. (1998). Superoxide production by phagocytosing macrophages in relation to the intracellular distribution of oxygen. *Journal of Leukocyte Biology,* 64**,** 78-84.

Jenner, A. M., Ruiz, J. E., Dunster, C., Halliwell, B., Mann, G. E. and Siow, R. C. (2002). Vitamin C protects against hypochlorous acid-induced glutathione depletion and DNA base and protein damage in human vascular smooth muscle cells. *Arteriosclerosis Thrombosis and Vascular Biology,* 22**,** 574-580.

Jensen, J., Buresh, C. and Norton, J. (1990). Lactic acidosis increases tumor necrosis factor secretion and transcription *in vitro*. *Journal of Surgical Research,* 49**,** 350-353.

Jessup, W. and Kritharides, L. (2000). Metabolism of oxidized LDL by macrophages. *Current Opinion in Lipidology,* 11**,** 473-481.

Jessup, W., Rankin, S. M., De Whalley, C. V., Hoult, R. S. and Scott, J. (1990). Alpha-tocopherol consumption during low density lipoprotein oxidation. *Biochemical Journal,* 265**,** 399-405.

John, A. P. (2001). Dysfunctional mitochondria, not oxygen insufficiency, cause cancer cells to produce inordinate amounts of lactic acid: the impact of this on the treatment of cancer. *Medical hypotheses,* 57**,** 429-431.

Johs, A., Hammel, M., Waldner, I., May, R. P., Laggner, P. and Prassl, R. (2006). Modular Structure of Solubilized Human Apolipoprotein B-100 - Low Resolution Model Revealed by Small Angle Neutron Scattering. *Journal of Biological Chemistry,* 281**,** 19732-19739.

Jovanovic, P., Zoric, L., Stefanovic, I., Dzunic, B., Djordjevic-Jocic, J., Radenkovic, M. and Jovanovic, M. (2010). Lactate dehydrogenase and oxidative stress activity in primary open-angle glaucoma aqueous humour. *Bosnian Journal of Basic Medical Sciences,* 10**,** 83-88.

Kappler, M., Gerry, A. J., Brown, E., Reid, L., Leake, D. S. and Gieseg, S. P. (2007). Aqueous peroxyl radical exposure to THP-1 cells causes glutathione loss followed by protein oxidation and cell death without increased caspase-3 activity. *Biochemica et Biophysica Acta,* 1773**,** 945-953.

Khoo, J. C., Miller, E., Mcloughlin, P. and Steinberg, D. (1988). Enhanced macrophage uptake of low density lipoprotein after self-aggregation. *Arteriosclerosis,* 8**,** 348-358.

Kikuchi, H., Fujinawa, T., Kuribayashi, F., Nakanishi, A., Imajohohmi, S., Goto, M. and Kanegasaki, S. (1994). Induction of essential components of the superoxide generating-system in human monoblastic leukemia U937 cells. *Journal of Biochemistry,* 116**,** 742-746.

Kim, J. M., Kim, H., Kwon, S. B., Lee, S. Y., Chung, S. C., Jeong, D. W. and Min, B. M. (2004). Intracellular glutathione status regulates mouse bone marrow monocyte-derived macrophage differentiation and phagocytic activity. *Biochemical and Biophysical Research Communications,* 325**,** 101-108.

Kinscherf, R., Claus, R., Wagner, M., Gehrke, C., Kamencic, H., Hou, D., Nauen, O., Schmiedt, W., Kovacs, G., Pill, J., Metz, J. and Deigner, H. P. (1998). Apoptosis caused by oxidized LDL is manganese superoxide dismutase and p53 dependent. *FASEB Journal,* 12**,** 461-467.

Kouoh, F., Gressier, B., Luyckx, M., Brunet, C., Dine, T., Cazin, M. and Cazin, J. C. (1999). Antioxidant properties of albumin: effect on oxidative metabolism of human neutrophil granulocytes. *II Farmaco,* 54**,** 695-699.

Kritharides, L., Jessup, W., Gifford, J. and Dean, R. T. (1993). A method for defining the stages of low-density lipoprotein oxidation by the separation of cholesterol and cholesterol ester-oxidation products using HPLC. *Analytical Biochemistry,* 213**,** 79-89.

Kritharides, L., Jessup, W., Mander, E. L. and Dean, R. T. (1995). Apolipoprotein A1 mediated efflux of sterols from oxidised LDL load macrophages
Arteriosclerosis, Thrombosis, and Vascular Biology, 15**,** 276-289.

Kruger, N. J. and Von Schaewen, A. (2003). The oxidative pentose phosphate pathway: structure and organisation. *Current Opinion in Plant Biology,* 6**,** 236-246.

Lamb, D. J. and Leake, D. S. (1994). Iron released from transferrin at acidic pH can catalyse the oxidation of low density lipoprotein. *FEBS Letters,* 352**,** 15-18.

Lau, B. H. S. (2006). Suppression of LDL oxidation by garlic compounds is a possible mechanism of cardiovascular health benefit. *Journal of Nutrition,* 136**,** 765S-768S.

Leake, D. S. and Rankin, S. M. (1990). The oxidative modification of low-density lipoproteins by macrophages. *Biochemical Journal,* 270**,** 741-748.

Lee, W. J., Kim, M., Park, H. S., Kim, H. S., Jeon, M. J., Oh, K. S., Koh, E. H., Won, J. C., Kim, M. S., Oh, G. T., Yoon, M., Lee, K. U. and Park, J. Y. (2006). AMPK activation increases fatty acid oxidation in skeletal muscle by activating PPAR-α and PGC-1. *Biochemical and Biophysical Research Communications,* 340**,** 291-295.

Legrand, C. (1992). Lactate dehydrogenase (LDH) activity of the number of dead cells in the medium of cultured eukaryotic cells as marker. *Journal of biotechnology,* 25**,** 231-243.

Lenz, M. L., Hughes, H., Mitchell, J. R., Via, D. P., Guyton, J. R., Taylor, A. A., Gotto, A. M. and Smith, C. (1990). Lipid hydroperoxy and hydroxy derivatives in copper-catalyzed oxidation of low density lipoprotein. *Journal of Lipid Research,* 31**,** 1043-1050.

Leonarduzzi, G., Vizio, B., Sottero, B., Verde, V., Gamba, P., Mascia, C., Chiarpotto, E., Poli, G. and Biasi, F. (2006). Early involvement of ROS overproduction in apoptosis induced by 7-ketocholesterol. *Antioxidants and Redox Signaling,* 8**,** 375-380.

Leppänen, O., Björnheden, T., Evaldsson, M., Borén, J., Wiklund, O. and Levin, M. (2006). ATP depletion in macrophages in the core of advanced rabbit atherosclerotic plaques in vivo. *Atherosclerosis,* 188**,** 323-330.

Leverve, X. and Mustafa, I. (2002). Lactate: a key metabolite in the intercellular metabolic interplay. *Critical Care,* 6**,** 284-285.

Li, A. C. and Glass, C. K. (2002). The macrophage foam cell as a target for therapeutic intervention. *Nature Medicine,* 8**,** 1235-1242.

Li, D., Saldeen, T. and Mehta, J. L. (1999). γ-Tocopherol decreases ox-LDL-mediated activation of nuclear factor-kB and apoptosis in human coronary artery endothelial cells. *Biochemical and Biophysical Research Communications,* 259**,** 157-161.

Liao, H. S., Kodama, T. and Geng, Y. J. (2000). Expression of class A scavenger receptor inhibits apoptosis of macrophages triggered by oxidized low density lipoprotein and oxysterol. *Arteriosclerosis Thrombosis and Vascular Biology,* 8**,** 1968-1975.

Libby, P., Ridker, P. M. and Maseri, A. (2002). Inflammation and Atherosclerosis. *Circulation,* 105**,** 1135-1143.

Lin, S.-J. and Guarente, L. (2003). Nicotinamide adenine dinucleotide, a metabolic regulator of transcription, longevity and disease. *Current Opinion in Cell Biology,* 15**,** 241-246.

Linton, M. F. and Fazio, S. (2001). Class A scavenger receptors, macrophages and atherosclerosis. *Current Opinion in Lipidology,* 12**,** 489-495.

Liu, W. L., Guo, X. and Guo, Z. G. (1998). Oxidized low-density lipoproteins induce apoptosis in vascular smooth muscle cells. *Acta Pharmacologica Sinica,* 19**,** 245-247.

Lizard, G., Gueldry, S., Sordet, O., Monier, S., Athias, A., Miguet, C., Bessede, G., Lemaire, S., Solary, E. and Gambert, P. (1998). Glutathione is implied in the control of 7-ketocholesterol-induced apoptosis, which is associated with radical oxygen species production. *FASEB Journal,* 12**,** 1651-1663.

Lizard, G., Miguet, C., Bessede, G., Monier, S., Gueldry, S., Neel, D. and Gambert, P. (2000). Impairment with various antioxidants of the loss of mitochondrial transmembrane potential and of the cytosolic release of cytochrome c occuring

during 7-ketocholesterol-induced apoptosis. *Free Radical Biology and Medicine,* 28**,** 743-753.

Loike, J. D., Kaback, E., Silverstein, S. C. and Steinberg, T. H. (1993). Lactate transport in macrophages. *Journal of Immunology,* 150**,** 1951-1958.

Lougheed, M. and Steinbrecher, U. P. (1996). Mechanism of uptake of copper-oxidized low density lipoprotein in macrophages is dependent on its extent of oxidation. *Journal of Biological Chemistry,* 271**,** 11798-11805.

Lusis, A. J. (2000). Atherosclerosis. *Nature,* 407**,** 233-241.

Mandal, K., Jahangiri, M. and Xu, Q. (2004). Autoimmunity to heat shock proteins in atherosclerosis. *Autoimmunity Reviews,* 3**,** 31-37.

Maor, I. and Aviram, M. (1994). Oxidised low density lipoprotein leads to macrophage accumulation of unesterified cholesterol as a result of lyosomal trapping of the lipoprotein hydrolysed cholesterol ester. *Journal of Lipid Research,* 35**,** 803-819.

Marecaux, G., Pinsky, M. R., Dupont, E., Kahn, R. J. and Vincent, J. L. (1996). Blood lactate levels are better prognostic indicators than TNF and IL-6 levels in patients with septic shock. *Intensive Care Medicine,* 22**,** 404-408.

Massaeli, H., Austria, J. A. and Pierce, G. N. (1999). Chronic exposure of smooth muscle cells to minimally oxidized LDL results in depressed inositol 1,4,5-trisphosphate receptor density and Ca^{2+} transients. *Circulation Research,* 85**,** 515-523.

Mathews, C. K. and Van Holde, K. E. (1996). Biochemistry. The Benjamin/Cummings Publishing Company, Inc., Redwood City, California.

Maxeiner, H., Husemann, J., Thomas, C. A., Loike, J. D., El Khoury, J. and Silverstein, S. C. (1998). Complementary roles for scavenger receptor a and CD36 of human monocyte-derived macrophages in adhesion to surfaces coated with oxidized low-density lipoproteins and in secretion of H_2O_2. *Journal of Experimental Medicine,* 188**,** 2257-2265.

Mcdonald, L. J. and Moss, J. (1993). Stimulation by nitric oxide of an NAD linkage to glyceraldehyde-3-phosphate dehydrogenase. *Proceedings of the National Academy of Sciences,* 90**,** 6238-6241.

Mckenzie, S. J., Baker, M. S., Buffinton, G. D. and Doe, W. F. (1996). Evidence of oxidant-induced injury to epithelial cells during inflammatory bowel disease. *Journal of Clinical Investigation,* 98**,** 136-141.

Mckenzie, S. M., Doe, W. F. and Buffinton, G. D. (1999). 5-Aminosalicylic acid prevents oxidant mediated damage of glyceraldehyde-3-phosphate dehydrogenase in colon epithelial cells. *Gut,* 44**,** 180-185.

Meister, A. (1988). Glutathione metabolism and its selective modification. *Journal of Biological Chemistry,* 263**,** 17205-17208.

Mendis, S., Nordet, P., Fernandez-Britto, J. E. and Sternby, N. (2005). Atherosclerosis in children and young adults: an overview of the world health organization and international society and federation of cardiology study on pathobiological determinants of atherosclerosis in youth study (1985-1995). *Prevention and Control,* 1**,** 3-15.

Messmer, U. K., Reed, J. C. and Brune, B. (1996). Bcl-2 Protects macrophages from nitric oxide-induced apoptosis. *Journal of Biological Chemistry,* 271**,** 20192-20197.

Miller, A. M., Nolan, M. J., Choi, J., Koga, T., Shen, X., Yue, B. Y. J. T. and Knepper, P. A. (2007). Lactate treatment causes NF-kB activation and CD44 shedding in cultured trabecular meshwork cells. *Investigative Ophthalmology and Visual Science,* 48**,** 1615-1621.

Minetti, M., Pietraforte, D., Di Stasi, A. M. and Mallozzi, C. (1996). Nitric oxide-dependent NAD linkage to glyceraldehyde-3-phosphate dehydrogenase: possible involvement of a cysteine thiyl radical intermediate. *Biochemical Journal,* 319**,** 369-375.

Mohr, S., Stamler, J. S. and Brune, B. (1996). Posttranslational modification of glyceraldehyde-3-phosphate dehydrogenase by S-nitrosylation and subsequent NADH attachment. *Journal of Biological Chemistry,* 271**,** 4209-4214.

Molina Y Vedia, L., Mcdonald, B., Reep, B., Brune, B., Di Silvio, M., Billiar, T. R. and Lapetina, E. G. (1992). Nitric oxide-induced S-nitrosylation of glyceraldehyde-3-phosphate dehydrogenase inhibits enzymatic activity and increases endogenous ADP-ribosylation. *Journal of Biological Chemistry,* 267**,** 24929-24932.

Moore, Kathrynâ j. and Tabas, I. (2011). Macrophages in the pathogenesis of atherosclerosis. *Cell,* 145**,** 341-355.

Morel, D. W., Hessler, J. R. and Chisolm, G. M. (1983). Low-density lipoprotein cytotoxicity induced by free-radical peroxidation of lipid. *Journal of Lipid Research,* 24**,** 1070-1076.

Mosmann, T. (1983a). Rapid colorimetric assay for cellular growth and survival: Application to proliferation and cytotoxicity assays. *Journal Immunological Methods,* 65**,** 55-63.

Mosmann, T. (1983b). Rapid colorimetric assay for cellular growth and survival: application to proliferation and cytotoxicity assays. *Journal of Immunological Methods,* 65**,** 55-63.

Mustafa, I. and Leverve, X. (2002). Metabolic and hemodynamic effects of hypertonic solutions: sodium lactate versus sodium chloride infusion in postoperative patients. *Shock***,** 306-310.

Nakajima, H., Amano, W., Fujita, A., Fukuhara, A., Azuma, Y.-T., Hata, F., Inui, T. and Takeuchi, T. (2007). The active site cysteine of the proapoptotic protein glyceraldehyde-3-phosphate dehydrogenase is essential in oxidative stress-induced aggregation and cell death. *Journal of Biological Chemistry,* 282**,** 26562-26574.

Nareika, A., He, L., Game, B. A., Slate, E. H., Sanders, J. J., London, S. D., Lopes-Virella, M. F. and Huang, Y. (2005). Sodium lactate increases LPS-stimulated MMP and cytokine expression in U937 histiocytes by enhancing AP-1 and NF-kB transcriptional activities. *American Journal of Physiology and Endocrinology and Metabolism,* 289**,** E534-E542.

Nelson, D. L. and Cox, M. M. (2005). Lehninger's Principles of Biochemistry. *Fourth Edition.*

Newby, A. C. and Zaltsman, A. B. (1999). Fibrous cap formation or destruction - the critical importance of vascular smooth muscle cell proliferation, migration and matrix formation. *Cardiovascular Research,* 41**,** 345-360.

Nguyen-Khoa, T., Massy, Z. A., Witko-Sarsat, V., Canteloup, S., Kebede, M., Lacour, B., Drueke, T. and Descamps-Latscha, B. (1999). Oxidized low-density lipoprotein induces macrophage respiratory burst via its protein moiety: a novel pathway in atherogenesis? *Biochemical and Biophysical Research Communications,* 263**,** 804-809.

Nhan, T. Q., Liles, W. C., Chait, A., Fallon, J. T. and Schwartz, S. M. (2003). The P17 cleaved form of caspase-3 is present within viable macrophages *in vitro* and in

therosclerotic plaque. *Arteriosclerosis Thrombosis and Vascular Biology,* 23**,** 1276-1282.

Niki, E. (2009). Lipid peroxidation: physiological levels and dual biological effects. *Free Radical Biology and Medicine,* 47**,** 469-484.

Niu, X. L., Zhang, X. W. and Guo, Z. G. (1996). Oxidized low-density lipoproteins induce apoptosis in macrophages. *Acta Pharmacologica Sinica,* 17 467-470

Niu, X. W., Zammit, V., Upston, J. M., Dean, R. T. and Stocker, R. (1999). Coexistence of oxidized lipids and α-tocopherol in all lipoprotein density fractions isolated from advanced human atherosclerotic plaques. *Arteriosclerosis Thrombosis and Vascular Biology,* 19**,** 1708-1718.

Obama, T., Kato, R., Masuda, Y., Takahashi, K., Aiuchi, T. and Itabe, H. (2007). Analysis of modified apolipoprotein B-100 structures formed in oxidized low-density lipoprotein using LC-MS/MS. *Proteomics,* 7**,** 2132-2141.

Oettl, K., Dikalov, S., Freisleben, H. J., Mlekusch, W. and Reibnegger, G. (1997). Spin trapping study of antioxidant properties of neopterin and 7,8-dihydroneopterin. *Biochemical and Biophysical Research Communications,* 234**,** 774-778.

Ouimet, M. and Marcel, Y. L. (2011). Regulation of lipid droplet cholesterol efflux from macrophage foam cells. *Arteriosclerosis, Thrombosis and Vascular Biology,* 32**,** 575-581.

Palinski, W., Tangirala, R. K., Miller, E., Young, S. G. and Witztum, J. L. (1995). Increased autoantibody titers against epitopes of oxidized LDL in LDL receptor–deficient mice with increased atherosclerosis. *Arteriosclerosis, Thrombosis and Vascular Biology,* 15**,** 1569-1576.

Parthasarathy, S., Khoo, J. C., Miller, E., Barnett, J., Witztum, J. L. and Steinberg, D. (1990). Low density lipoprotein rich in oleic acid is protected against oxidative modification: implications for dietary prevention of atherosclerosis. *Proceedings of the National Academy of Sciences in USA,* 87**,** 3894-3898.

Pelzmann, B., Hallstrom, S., Schaffer, P., Lang, P., Nadlinger, K., Birkmayer, G. D., Vrecko, K., Reibnegger, G. and Koidl, B. (2003). NADH supplementation decreases pinacidil-Primed $I_{K(ATP)}$ in ventricular cardiomyocytes by increasing intracellular ATP. *British Journal of Pharmacology,* 139**,** 749-754.

Plüddemanna, A., Neyena, C. and Gordon, S. (2007). Macrophage scavenger receptors and host-derived ligands. *Methods,* 43**,** 207-217.

Prohaszka, Z. and Fust, G. (2004). Immunological aspects of heat-shock proteins-the optimum stress of life. *Molecular immunology,* 41**,** 29-44.

Pullar, J. M., Vissers, M. C. and Winterbourn, C. C. (2000). Living with a killer: the effects of hypochlorous acid on mammalian cells. *IUBMB Life,* 50**,** 259-266.

Pullar, J. M., Winterbourn, C. C. and Vissers, M. C. (1999). Loss of GSH and thiol enzymes in endothelial cells exposed to sublethal concentrations of hypochlorous acid. *American Journal of Physiology,* 277**,** H1505-H1512.

Quinlan, G. J., Martin, G. S. and Evans, T. W. (2005). Albumin: biochemical properties and therapeutic potential. *Hepatology,* 41**,** 1211-1219.

Ralser, M., Wamelink, M. M., Kowald, A., Gerisch, B., Heeren, G., Struys, E. A., Klipp, E., Jakobs, C., Breitenbach, M., Lehrach, H. and Krobitsch, S. (2007). Dynamic rerouting of the carbohydrate flux is key to counteracting oxidative stress. *Journal of Biology,* 6**,** 10.

Ray, K. K., Morrow, D. A., Sabatine, M. S., Shui, A., Rifai, N., Cannon, C. P. and Braunwald, E. (2007). Long-term prognostic value of neopterin a novel marker of monocyte activation in patients with acute coronary syndrome. *Circulation Journal,* 115**,** 3071-3078.

Reid, V. C., Mitchinson, M. J. and Skeper, J. N. (1993). Cytotoxicity of oxidised low density lipoprotein towards mouse peritoneal macrophages: An ultrastructural study. *Journal of Pathology,* 171**,** 321-328.

Rekhter, M. D. and Gordon, D. (1995). Active proliferation of different cell types, including lymphocytes, in human atherosclerotic plaques. *American journal of pathology,* 147**,** 668-677.

Retsky, K. L., Chen, K., Zeind, J. and Frei, B. (1999). Inhibition of copper-induced LDL oxidation by vitamin C is associated with decreased copper-binding to LDL and 2-oxo-histidine formation. *Free Radical Biology and Medicine,* 26**,** 90-98.

Roche, M., Rondeau, P., Singh, N. R., Tarnus, E. and Bourdon, E. (2008). The antioxidant properties of serum albumin. *FEBS Letters,* 582**,** 1783-1787.

Roiniotis, J., Dinh, H., Masendycz, P., Turner, A., Elsegood, C. L., Scholz, G. M. and Hamilton, J. A. (2009). Hypoxia prolongs monocyte/macrophage survival and enhanced glycolysis is associated with their maturation under aerobic conditions. *Journal of Immunology,* 182**,** 7974-7981.

Rosenson-Schloss, R. S., Chnari, E., Brieva, T. A., Dang, A. and Moghe, P. V. (2005). Glutathione preconditioning attenuates ac-LDL-induced macrophage apoptosis via protein kinase c-dependent Ac-LDL trafficking. *Experimental Biology and Medicine,* 230**,** 40-48.

Ross, R. (1993). The pathogenesis of atherosclerosis: a perspective for the 1990s. *Nature,* 362**,** 801-809.

Rutherford, L. and Gieseg, S. (2011). 7-Ketocholesterol is not cytotoxic to U937 cells when incorporated into acetylated low density lipoprotein. *Lipids,* 47**,** 239-247.

Sakakibara, T., Murakami, S., Eisaki, N., Nakajima, M.-O. and Imai, K. (1999). An enzymatic cycling method using pyruvate orthophosphate dikinase and firefly luciferase for the simultaneous determination of ATP and AMP (RNA). *Analytical Biochemistry,* 268**,** 94-101.

Salonen, J. T., Yla-Herttuala, S., Yamamoto, R., Butler, S., Korpela, H., Salonen, R., Nyyssonen, K., Palinski, W. and Witztum, J. L. (1992). Autoantibody against oxidised LDL and progression of carotid atherosclerosis. *Lancet,* 339**,** 883-887.

Salvayre, R., Auge, N., Benoist, H. and Negre-Salvayre, A. (2002). Oxidized low-density lipoprotein-induced apoptosis. *Biochim et Biophys Acta,* 1585**,** 213-221.

Samuvel, D. J., Sundararaj, K. P., Nareika, A., Lopes-Virella, M. F. and Huang, Y. (2009). Lactate boosts TLR4 signaling and NF-kB pathway-mediated gene transcription in macrophages via monocarboxylate transporters and MD-2 up-regulation. *Journal of Immunology,* 182**,** 2476-2484.

Schafer, F. Q. and Buettner, G. R. (2001). Redox environment of the cell as viewed through the redox state of the glutathione disulfide/glutathione couple. *Free Radical Biology and Medicine,* 30**,** 1191-1212.

Schraufstatter, I. U., Browne, K., Harris, A., Hyslop, P. A., Jackson, J. H., Quehenberger, O. and Cochrane, C. G. (1990). Mechanisms of hypochlorite injury of target cells. *Journal of Clinical Investigation,* 85**,** 554-562.

Schumacker, P. T., Chandel, N. and Agusti, A. G. (1993). Oxygen conformance of cellular respiration in hepatocytes. *American Journal of Physiology - Lung Cellular and Molecular Physiology,* 265**,** L395-L402.

Schuppe-Koistinen, I., Moldéus, P., Bergman, T. and Cotgreave, I. A. (1994). S-Thiolation of human endothelial cell glyceraldehyde-3-phosphate dehydrogenase after hydrogen peroxide treatment. *European Journal of Biochemistry,* 221**,** 1033-1037.

Schuster, B., Prassl, R., Nigon, F., Chapman, M. J. and Laggner, P. (1995). Core lipid structure is a major determinant of the oxidative resistance of low density lipoprotein. *Proceedings of the National Academy of Sciences,* 92 2509-2513.

Seimon, T. and Tabas, I. (2009). Mechanisms and consequences of macrophage apoptosis in atherosclerosis. *Journal of Lipid Research,* 50**,** S382-S387.

Selemidis, S., Dusting, G. J., Peshavariya, H., Kemp-Harper, B. K. and Drummond, G. R. (2007). Nitric oxide suppresses NADPH oxidase-dependent superoxide production by S-nitrosylation in human endothelial cells. *Cardiovascular Research,* 75**,** 349-358.

Shatrov, V. A., Sumbayev, V. V., Zhou, J. and Brune, B. (2003). Oxidized low-density lipoprotein (oxLDL) triggers hypoxia-inducible factor-1α (HIF-1α) accumulation via redox-dependent mechanisms. *Blood,* 101**,** 4847-4849.

Shaw, P. X., Horkko, S., Chang, M.-K., Curtiss, L. K., Palinski, W., Silverman, G. J. and Witztum, J. L. (2000). Natural antibodies with the T15 idiotype may act in atherosclerosis, apoptotic clearance and protective immunity. *Journal of Clinical Investigation,* 105**,** 1731-1740.

Shaw, P. X., Horkko, S., Tsimikas, S., Chang, M. K., Palinski, W., Silverman, G. J., Chen, P. P. and Witztum, J. L. (2001). Human-derived anti-oxidized LDL autoantibody blocks uptake of oxidized LDL by macrophages and localizes to atherosclerotic lesions in vivo. *Arteriosclerosis Thrombosis and Vascular Biology,* 21**,** 1333-1339.

Shen, L. and Sevanian, A. (2001). OxLDL induces macrophage γ-GCS-HS protein expression: a role for oxLDL-associated lipid hydroperoxide in GSH synthesis. *Journal of Lipid Research,* 42**,** 813-823.

Shimada, K. (2009). Immune system and atherosclerotic disease. *Circulation Journal,* 73**,** 994-1001.

Shime, H., Yabu, M., Akazawa, T., Kodama, K., Matsumoto, M., Seya, T. and Inoue, N. (2008). Tumor-secreted lactic acid promotes IL-23/IL-17 proinflammatory pathway. *Journal of Immunology,* 180**,** 7175-7183.

Shoenfeld, Y., Wu, R., Dearing, L. D. and Matsuura, E. (2004). Are anti–oxidized low-density lipoprotein antibodies pathogenic or protective? *Circulation Journal,* 110**,** 2552-2558.

Sies, H. (1991). Oxidative stress: from basic research to clinical application. *American journal of medicine,* 91**,** S31-S38.

Siow, R. C. M., Richards, J. P., Pedley, K. C., Leake, D. S. and Mann, G. E. (1999). Vitamin C protects human vascular smooth muscle cells against apoptosis induced by moderately oxidized LDL containing high levels of lipid hydroperoxides. *Arteriosclerosis Thrombosis and Vascular Biology,* 19**,** 2387-2394.

Siow, R. C. M., Sato, H., Leake, D. S., Pearson, J. D., Bannai, S. and Mann, G. E. (1998). Vitamin C protects human arterial smooth muscle cells against atherogenic lipoproteins. Effects of antioxidant vitamins C and E on oxidized LDL-induced adaptive increases in cystine transport and glutathione *Arteriosclerosis, Thrombosis and Vascular Biology,* 18**,** 1662-1670.

Smit, M. J. and Anderson, R. (1992). Biochemical mechanisms of hydrogen peroxide- and hypochlorous acid-mediated inhibition of human mononuclear leukocyte functions in vitro: protection and reversal by anti-oxidants. *Agents Actions,* 36**,** 58-65.

Solaroli, N., Panayiotou, C., Johansson, M. and Karlsson, A. (2009). Identification of two active functional domains of human adenylate kinase 5. *FEBS Letters,* 583**,** 2872-2876.

Soto, Y., Acosta, E., Delgado, L., Pérez, A., Falcón, V., Bécquer, M. A., Fraga, Á., Brito, V., Álvarez, I., Griñán, T., Fernández-Marrero, Y., López-Requena, A., Noa, M., Fernández, E. and Vázquez, A. M. (2012). Antiatherosclerotic effect of an antibody that binds to extracellular matrix glycosaminoglycans. *Arteriosclerosis, Thrombosis and Vascular Biology,* 32**,** 595-604.

Sparrow, C. P., Parthasarathy, S. and Steinberg, D. (1988). Enzymatic modification of low-density lipoprotein by purified lipoxygenase plus phospholipase-A2 mimics cell-mediated oxidative modification. *Journal of Lipid Research,* 29**,** 745-753.

Spragg, R. G., Hinshaw, D. B., Hyslop, P. A., Schraufstätter, I. U. and Cochrane, C. G. (1985). Alterations in adenosine triphosphate and energy charge in cultured endothelial and P388D1 cells after oxidant injury. *Journal of Clinical Investigation,* 76**,** 1471-1476.

Steck, T. L. and Kant, J. A. (1974). Preparation of impermeable ghosts and inside out vesicles from human erythrocyte membranes. *Methods in Enzymology,* 31**,** 172-180.

Steinberg, D. (1997). Lewis A. conner memorial lecture: oxidative modification of LDL and atherogenesis. *Circulation Journal,* 95**,** 1062-1071.

Steinberg, D. (2002). Atherogenesis in perspective: hypercholesterolemia and inflammation as partners in crime. *Nature Medicine,* 8**,** 1211-1217.

Steinberg, D. (2009). The LDL modification hypothesis of atherogenesis: an update. *Journal of Lipid Research,* 50**,** S376-S381.

Steinberg, D., Parthasarathy, S., Carew, T. E., Khoo, J. C. and Witztum, J. L. (1989). Beyond cholesterol: modifications of low-density lipoprotein that increase its atherogenicity. *New England Journal of Medicine,* 320**,** 915-924.

Steinbrecher, U. P. and Lougheed, M. (1992). Scavenger receptor-inpendent stimulation of cholesterol esterification in macrophages by low density lipoprotein extracted from human aortic intima. *Atherosclerosis,* 12**,** 608-625.

Steinbrecher, U. P., Parthasarathy, S., Leake, D. S., Witztum, J. L. and Steinberg, D. (1984). Modification of low density lipoprotein by endothelial cells involves lipid peroxidation and degradation of low density lipoprotein phospholipids. *Proceedings of the National Academy of Sciences,* 81**,** 3883-3887.

Stephan, Z. F. and Yurachek, E. C. (1993). Rapid fluorometric assay of LDL receptor activity by DiI-labeled LDL. *Journal of Lipid Research,* 34**,** 325-330.

Stocker, R., Glazer, A. N. and Ames, B. N. (1987). Antioxidant activity of albumin-bound bilirubin (reactive oxygen species/ plasma antioxidants/ biliverdin/ evolution). *Proceedings of the National Academy of Sciences in USA,* 84**,** 5918-5922.

Stocker, R. and Keaney, J. F. J. (2004). Role of oxidative modifications in atherosclerosis. *Physiological Reviews,* 84**,** 1381-1478.

Sukhanov, S., Higashi, Y., Shai, S.-Y., Itabe, H., Ono, K., Parthasarathy, S. and Delafontaine, P. (2006). Novel effect of oxidized low-density lipoprotein: cellular ATP depletion via downregulation of glyceraldehyde-3-phosphate dehydrogenase. *Circulation Research,* 99**,** 191-200.

Sundstrom, C. and Nilsson, K. (1976). Establishment and characterization of a human histiocytic lymphoma cell line (U-937). *International Journal of Cancer,* 17**,** 565-577.

Szabo, S. J., Sullivan, B. M., Peng, S. L. and Glimcher, L. H. (2003). Molecular mechanisms regulating Th1 immune responses *Annual Review of Immunology,* 21**,** 713-758.

Tabas, I. (2005). Consequences and therapeutic implications of macrophage apoptosis in atherosclerosis - the importance of lesion stage and phagocytic efficiency. *Arteriosclerosis Thrombosis and Vascular Biology,* 25**,** 2255-2264.

Takahashi, K., Takeya, M. and Sakashita, N. (2002). Multifunctional roles of macrophages in the development and progression of atherosclerosis in humans and experimental animals. *Medical Electron Microscopy,* 35**,** 179-203.

Tashiro, K., Makita, Y., Shike, T., Shirato, I., Sato, T., Cynshi, O. and Tomino, Y. (1999). Detection of cell death of cultured mouse mesangial cells induced by oxidized low-density lipoprotein. *Nephron,* 82 51-58.

Terasaka, N., Wang, N., Yvan-Charvet, L. and Tall, A. R. (2007). High-density lipoprotein protects macrophages from oxidized low-density lipoprotein-induced apoptosis by promoting efflux of 7-ketocholesterol via ABCG1. *Proceedings of the National Academy of Sciences,* 104**,** 15093-15098.

Thomas, M. J., Thornburg, T., Manning, J., Hooper, K. and Rudel, L. L. (1994). Fatty acid composition of low-density lipoprotein influences its susceptibility to autoxidation. *Biochemistry,* 33**,** 1828-1834.

Torchinsky, Y. M. (1981). The role of SH group in enzymes in sulfur in proteins. *Pergamon Press, Oxford,* pp**,** 154-179.

Toshima, S.-I., Hasegawa, A., Kurabayashi, M., Itabe, H., Takano, T., Sugano, J., Shimamura, K., Kimura, J., Michishita, I., Suzuki, T. and Nagai, R. (2000). Circulating oxidized low density lipoprotein levels : a biochemical risk marker for coronary heart disease. *Arteriosclerosis, Thrombosis and Vascular Biology,* 20**,** 2243-2247.

Trabold, O., Wagner, S., Wicke, C., Scheuenstuhl, H., Hussain, M. Z., Rosen, N., Seremetiev, A., Becker, H. D. and Hunt, T. K. (2003). Lactate and oxygen constitute a fundamental regulatory mechanism in wound healing. *Wound Repair and Regeneration,* 11**,** 504-509.

Tsai, M.-J., Shyue, S.-K., Weng, C.-F., Chung, Y., Liou, D.-Y., Huang, C.-T., Kuo, H.-S., Lee, M.-J., Chang, P.-T., Huang, M.-C., Huang, W.-C., Liou, K. D. and Cheng, H. (2005). Effect of enhanced prostacyclin synthesis by adenovirus-mediated transfer on lipopolysaccharide stimulation in neuron-glia cultures. *Annals of the New York Academy of Sciences,* 1042**,** 338-348.

Tsimikas, S., Brilakis, E. S., Miller, E. R., Mcconnell, J. P., Lennon, R. J., Kornman, K. S., Witztum, J. L. and Berger, P. B. (2005). Oxidized phospholipids, Lp(a) lipoprotein and coronary artery disease. *New England Journal of Medicine,* 353**,** 46-57.

Tsuchiya, Y., Yamaguchi, M., Chikuma, T. and Hojo, H. (2005). Degradation of glyceraldehyde-3-phosphate dehydrogenase triggered by 4-hydroxy-2-nonenal and 4-hydroxy-2-hexenal. *Archives of Biochemistry and Biophysics,* 438**,** 217-222.

Tuckey, N. P., Forster, M. E. and Gieseg, S. P. (2009). Lipid oxidation is inhibited by isoeugenol exposure in chinook salmon (oncorhynchus tshawytscha) fillets during storage at 15°C. *Journal of Food Science,* 74**,** 333-338.

Tuckey, N. P. L., Forster, M. E. and Gieseg, S. P. (2010). Effects of rested harvesting on muscle metabolite concentrations and K-values in chinook salmon (oncorhynchus tshawytscha) fillets during storage at 15 °C. *Journal of Food Science,* 75**,** C459-C464.

Turner, N., Hulbert, A. and Else, P. L. (2006). Limits to physical performance and metabolism across species. *Current Opinion in Clinical Nutrition and Metabolic Care,* 9**,** 691-696

Van Engeland, M., Nieland, L. J. W., Ramaekers, F. C. S., Schutte, B. and Reutelingsperger, C. P. M. (1998). Annexin V-affinity assay: a review on an apoptosis detection system based on phosphatidylserine exposure. *Cytometry,* 31**,** 1-9.

Van Reyk, D. M. and Jessup, W. (1999). The macrophage in atherosclerosis: modulation of cell function by sterols. *Journal of Leukocyte Biology,* 66**,** 557-561.

Vicca, S., Hennequin, C., Nguyen-Khoa, T., Massy, Z. A., Descamps-Latscha, B., Drueke, T. B. and Lacour, B. (2000). Caspase-dependent apoptosis in THP-1 cells exposed to oxidized low-density lipoproteins. *Biochemical and Biophysical Research Communications,* 273**,** 948-954.

Vicca, S., Massy, Z. A., Hennequin, C., Rihane, D., Drueke, T. B. and Lacour, B. (2003). Apoptotic pathways involved in U937 cells exposed to LDL oxidized by hypochlorous acid. *Free Radical Biology and Medicine,* 35**,** 603-615.

Wachter, H., Fuchs, D., Hausen, A., Reibnegger, G. and Werner, E. R. (1989). Neopterin as marker for activation of cellular immunity: immunologic basis and clinical application. *Advances in Clinical Chemistry,* 27**,** 81-141.

Wang, Y., Qiao, M., Mieyal, J. J., Asmis, L. M. and Asmis, R. (2006). Molecular mechanism of glutathione-mediated protection from oxidized low-density lipoprotein-induced cell injury in human macrophages: role of glutathione reductase and glutaredoxin. *Free Radical Biology and Medicine,* 41**,** 775-785.

Warner, G. J., Stoudt, G., Bamberger, M., Johnson, W. J. and Rothblat, G. H. (1995). Cell toxicity induced by inhibition of acyl coenzyme A:cholesterol acyltransferase and accumulation of unesterified cholesterol. *Journal of Biological Chemistry,* 270**,** 5772-5778.

White, R. L. and Wittenberg, B. A. (2000). Mitochondrial NAD(P)H, ADP, oxidative phosphorylation and contraction in isolated heart cells. *American Journal of Physiology - Heart Circulatory Physiology,* 279**,** H1849-H1857.

Williams, H., King, N., Griffiths, E. J. and Suleiman, M. S. (2001). Glutamate-loading stimulates metabolic flux and improves cell recovery following chemical hypoxia in isolated cardiomyocyte. *Journal of Molecular and Cellular Cardiology,* 33**,** 2109-2119.

Wintergerst, E. S., Jelk, J., Rahner, C. and Asmis, R. (2000). Apoptosis induced by oxidized low density lipoprotein in human monocyte-derived macrophages involves CD36 and activation of caspase-3. *European Journal of Biochemistry,* 267**,** 6050-6059.

Witte, K. K., Levy, W. C., Lindsay, K. A. and Clark, A. L. (2007). Biomechanical efficiency is impaired in patients with chronic heart failure. *European Journal of Heart Failure,* 9**,** 834-838.

Yamaguchi, M., Tsuchiya, Y., Hishinuma, K., Chikuma, T. and Hojo, H. (2003). Conformational change of glyceraldehyde-3-phosphate dehydrogenase induced

by acetylleucine chloromethyl ketone is followed by unique enzymatic degradation. *Biological and Pharmaceutical Bulletin,* 26**,** 1648-1651.

Yang, Y.-T. (2009). Mechanism and inhibition of hypochlorous acid-mediated cell death in human monocyte-derived macrophages. Ph.D.thesis, Biological Sciences. University of Canterbury. Christchurch, New Zealand.

Yuan, X. M., Li, W., Brunk, U. T., Dalen, H., Chang, Y. H. and Sevanian, A. (2000). Lysosomal destabilization during macrophage damage induced by cholesterol oxidation products. *Free Radical Biology and Medicine,* 28**,** 208-218.

Ziouzenkova, O., Sevanian, A., Abuja, P. M., Ramos, P. and Esterbauer, H. (1998). Copper can promote oxidation of LDL by markedly different mechanisms. *Free Radical Biology and Medicine,* 24**,** 607-623.

Zmijewski, J. W., Moellering, D. R., Goffe, C. L., Landar, A., Ramachandran, A. and Darley-Usmar, V. M. (2005). Oxidized LDL induces mitochondrially associated reactive oxygen/nitrogen species formation in endothelial cells. *American Journal of Physiology - Heart Circulatory Physiology,* 289**,** H852-H861.